

Ferdigstilling og testing av mekanisk struktur for NUTS CubeSat

Anders Håland

Produktutvikling og produksjon

Innlevert: juni 2014

Hovedveileder: Jan Magnus Granheim Farstad, IPM

Norges teknisk-naturvitenskapelige universitet
Institutt for produktutvikling og materialer

NORGES TEKNISK-
NATURVITENSKAPELIGE UNIVERSITET
INSTITUTT FOR PRODUKTUTVIKLING
OG MATERIALER

MASTEROPPGAVE VÅR 2014
FOR
STUD.TECHN. ANDERS HÅLAND

Ferdigstilling og testing av mekanisk struktur for NUTS CubeSat
Completion and testing of mechanical structure for NUTS CubeSat

NUTS (NTNU Test Satellite) er ett tverrfaglig prosjekt-samarbeid ved NTNU. Ved IPM er det identifisert flere fokusområder knyttet til mekaniske system på satellitten, deriblant utvikling av komposittrammen, mekanismer for solcellepanel og antenner, fullskala dynamisk testing, tribologi, slitasje og nedbrytning, kvalifikasjon i henhold til eksisterende regelverk samt overordnet PLM for prosjektet. I prosjektoppgaven i høstsemesteret er den mekaniske strukturen videreutviklet spesielt med tanke på produksjonsvennlighet, samt et utkast til ny antennemodul er utviklet.

Kandidaten skal ferdigstille/komplementere tidligere løsninger for NUTS-rammen, og slutføre design og produksjonsprosessen. Målet med arbeidet er å få ferdig en engineeringmodell av rammen som kan brukes til engineeringmodell av satellitten. Kandidaten skal også bistå NUTS med annen mekanisk design, hvor antennemodulen er en spesielt viktig del.

Senest 3 uker etter oppgavestart skal et A3 ark som illustrerer arbeidet leveres inn. En mal for dette arket finnes på instituttets hjemmeside under menyen masteroppgave (<http://www.ntnu.no/ipm/masteroppgave>). Arket skal også oppdateres en uke før innlevering av masteroppgaven.

Arbeidet i masteroppgaven skal risikovurderes. Hovedaktiviteter som er kjent/planlagt skal risikovurderes ved oppstart og skjema skal leveres innen 3 uker etter utlevering av oppgavetekst. Alle prosjekt skal vurderes, også de som kun er teoretiske og virtuelle. Skjemaet må signeres av veileder. Risikovurdering er en løpende dokumentasjon og skal gjøres før oppstart av enhver aktivitet som KAN være forbundet med risiko. Kopi av signert risikovurdering skal være inkludert i vedlegg ved levering av rapport

Besvarelsen skal ha med signert oppgavetekst, og redigeres mest mulig som en forskningsrapport med et sammendrag på norsk og engelsk, konklusjon, litteraturliste, innholdsfortegnelse, etc. Ved utarbeidelse av teksten skal kandidaten legge vekt på å gjøre teksten oversiktlig og velskrevet. Med henblikk på lesning av besvarelsen er det viktig at de nødvendige henvisninger for korresponderende steder i tekst, tabeller og figurer anføres på


begge steder. Ved bedømmelse legges det stor vekt på at resultater er grundig bearbeidet, at de oppstilles tabellarisk og/eller grafisk på en oversiktlig måte og diskuteres utførlig.

Som et vedlegg til rapporten skal det leveres en PU-journal. Denne skal være uredigert og inneholde alle de notater og idéer man har vært inne på undervegs i arbeidet. Fortrinnsvis skal den være i instituttets A3-format.

Besvarelsen skal leveres i elektronisk format via DAIM, NTNUs system for Digital arkivering og innlevering av masteroppgaver.

Kontaktpersoner:

Ved instituttet: Nils Petter Vedvik
Prosjektleder: Roger Birkeland, IET
Teknisk koordinator: Amund Gjersvik, IET


Torgeir Welo
Instituttleder


Jan Magnus Granheim Farstad
Faglærer

 NTNU
Norges teknisk-
naturvitenskapelige universitet
Institutt for produktutvikling
og materialer

ABSTRACT

The focus in this master thesis has been on development and manufacturing of the mechanical design of the NUTS CubeSat. The aim has been to take the NUTS project one step closer to launch. This implies completing parts and components for the entire satellite with a special focus on the primary structure and the antenna module assembly.

The primary structure is the satellites skeleton and is a square cylinder consisting of aluminium rails and carbon fibre panels. The structure has strict demands regarding dimensions, surface roughness and coating. The work processes used to solve the manufacturing challenges is duly discussed and described. A mechanical model was made as verification of production methods.

The antenna module assembly has encapsulated antenna elements for two dipole radios. The antenna module has been developed in parallel with the production of antenna elements made of beryllium copper alloy. To unfold the antenna elements when the satellite is in orbit an electrical release mechanism is developed. The prototype of the entire antenna module has been tested with success.

To develop certain components a close collaboration with other disciplines within the NUTS project is required. This is the case with the development of magnetic coils for the positioning system, the internal structure and the antenna module. The issue is discussed further, later in the report.

The main outcome of the work is that NUTS has taken a major and important step forward towards being finalized. The prototypes were so promising that production of parts and components now can be made in space grade material. The basis for this conclusion lies in the test of adhesive used between carbon fibre and aluminium, functional tests of antenna module and release mechanism, control of production parameters of the primary structure and machine drawings of remaining components of the satellite. The production of mechanical components can therefore commence and the assembly begin. Only then can mandatory tests required of CubeSat's be completed and succeeded by manufacturing a flight model.

SAMMENDRAG

Arbeidet i denne oppgaven har bestått av å utvikle og produsere den mekaniske konstruksjonen til NUTS CubeSat. Målet har vært å ta prosjektet NUTS et steg nærmere oppskytning. Dette innebærer å ferdigstille deler og komponenter for hele satellitten med et spesielt fokus på primærstrukturen og antennemodulen.

Primærstrukturen er satellittens skjellett som er en firkantet sylinder med aluminiumshjørner og karbonfiberplater. Strukturen har strenge krav til dimensjon og overflate. Løsningen av strukturens produksjonstekniske utfordringer er behørig beskrevet og diskutert. Det er også laget en mekanisk modell for å verifisere produksjonsmetodene.

Antenne-modulen er en sammenstilling som har innkapslede antennelementer for to dipol radioer. Antennemodulen er utviklet parallelt med produksjon av antenneelementer laget av berylliumkopperlegering. For å folde ut antenneelementene når satellitten er i bane er det utviklet elektriske frigjøringsmekanismer. Prototypen av antennemodulen er testet i sin helhet med suksess.

Enkelte komponenter krever et tett samarbeid med andre fagdisipliner innad i NUTS prosjektet for å utvikles. Dette har vært tilfellet med utviklingen av magnetpoler til posisjoneringssystemet, den indre strukturen og antennemodulen. Dette er omtalt senere i rapporten.

Det viktigste resultatet fra arbeidet med oppgaven er at NUTS har kommet et stort og viktig steg videre. Prototypene var så gode at produksjon av komponenter og deler nå kan lages i materialer som er godkjent for verdensrommet. Denne konklusjonen baseres på tester av limet som er brukt til sammenføyning mellom karbonfiber og aluminium, funksjonelle tester av antennemodul og frigjøringsmekanismer, kontroll over produksjonsmetoder av primærstruktur og maskintegninger av resterende komponenter til satellitten. Produksjonen av de mekaniske komponentene kan derfor starte og sammenstillingen begynne. Da kan de obligatoriske testene som kreves av en CubeSat bli gjennomført og en flight modell kan produseres.

PREFACE

This master thesis is written on behalf of the NTNU test satellite project, NUTS, in the spring of 2014 at the Norwegian University of Science and Technology, NTNU. NUTS is an ongoing student based project with the goal of developing a pico satellite. The Department of Electronics and Telecommunication, IET, is responsible for the project and have requested participants from the Department of Engineering Design and Materials, IPM, for the design and manufacturing of the mechanical structure of the satellite. The master thesis will complete a two year master program at NTNU. The last year has been dedicated to the NUTS project. In the fall of 2013 a pilot project on NUTS was completed which gave 15 out of 30 study points. The master thesis gave 30 study points, a full semester. This thesis will make use of the findings in the pilot project. Three master theses and four pilot projects on the mechanical structure have previously been completed, as a part of the development.

This project was a part of a cluster of project assignments called Building Complex Products presented by IPM. Building complex products implies multi-disciplinary development and manufacturing. This direction was chosen as it provided the opportunity to work with other disciplines at NTNU and the assurance of practical work with development and manufacturing. This thesis is focused on the completion and manufacturing of parts and components for the CubeSats.

Big thanks are given to Roger Birkeland and Amund Gjersvik who have helped with everything during the last year. Special thanks to Tore Landsem who has helped with manufacturing of parts and discussions regarding the parts and design. I would also like to thank my subject teacher Jan Magnus G. Farstad.



Trondheim, 10/06-2014

TABLE OF CONTENTS

ABSTRACT.....	i
SAMMENDRAG.....	ii
PREFACE.....	iii
Table of Contents	iv
List of Figures.....	viii
List of Tables.....	xi
List of Abbreviations.....	xii
Nomenclature.....	xiii
1 Introduction.....	1
1.1. Scope.....	2
1.2. Relevant information	3
1.2.1. Design requirements.....	3
1.2.2. Previous work.....	5
1.2.3. Design philosophy.....	6
1.2.4. Introduction to parts.....	6
1.2.5. Primary structure.....	7
1.2.6. Antenna module assembly.....	8
2 Design and development.....	11
2.1. Orientation of the satellite	11
2.2. Secondary structure	14
2.3. Backplane.....	17
2.4. ADCS.....	20
2.5. Solar cell panels.....	21
3 Primary structure.....	25
3.1. Design of rail and standoff	25

3.2.	Design of CFRP-panels.....	30
3.3.	Design of adhesive jig.....	30
3.4.	Prototyping primary structure.....	35
3.4.1.	Materials	35
3.4.2.	Manufacturing CFRP.....	37
3.4.3.	Assembly procedure.....	41
3.4.4.	Evaluation of the Primary structure	44
4	Antenna module assembly.....	46
4.1.	Design of antenna module.....	46
4.2.	Design of antenna module release mechanism	53
4.3.	Antenna element.....	58
4.4.	Prototyping electrical release mechanism	69
4.5.	Prototyping the mechanical release mechanism	74
4.6.	Redesign of antenna module.....	79
4.7.	Testing the antenna module.....	82
4.8.	Evaluation of antenna module.....	85
5	Testing.....	87
5.1.	Lap shear test	87
5.1.1.	Test procedure	88
5.2.	Surface roughness measurements.....	93
6	Discussion.....	98
6.1.	Further work.....	99
7	Conclusion	102
8	Reference	103
1	Appendix 1.....	1
1.1.	Antenna Element Length	1

1.2.	Pre-preg density.....	2
1.3.	Burn off points redundancy.....	3
1.4.	Static hand calculation on truss in secondary structure.....	7
1.5.	CTE and fatigue.....	8
1.6.	Measurements of satellite	9
2	Appendix 2.....	19
2.1.	Primary structure.....	19
2.1.1.	Rail.....	20
2.1.2.	Standoff top.....	21
2.1.3.	Standoff separation spring	22
2.2.1.	CFRP-Panel.....	25
2.3.	Secondary structure	26
2.3.1.	Truss	27
2.3.2.	Brace	28
2.3.3.	Brace mirrored	29
2.3.4.	Insert	30
2.4.	Antenna module assembly.....	31
2.4.1.	Antenna module.....	31
2.4.2.	Gate	32
2.4.3.	Bushing.....	33
2.4.4.	PCB bottom	34
2.5.	Solar cell	35
2.5.1.	PCB solar cell interface.....	35
2.5.2.	Solar cell interface assembly.....	37
2.5.3.	PCB solar cell side	38
2.5.4.	Solar cell side assembly	39

2.5.5.	PCB solar cell top	40
2.5.6.	Solar cell top assembly	41
2.6.	Adhesive jig	42
2.6.1.	Bottom plate	42
2.6.2.	Top plate	43
2.6.3.	Wall	44
2.6.4.	Endplate	45
2.7.	ADCS.....	46
2.7.1.	ADCS top.....	47
2.7.2.	ADCS left side	48
2.7.3.	ADCS right side	49
3	Appendix 3.....	50
3.1.	Lap shear test thickness.....	50
3.2.	Adhesive	51
3.3.	CDS.....	55
3.4.	PEEK.....	92
3.5.	Pre-Preg.....	93
3.6.	ISIS.....	97
3.7.	BeCU.....	100
4	Appendix 4.....	109
4.1.	HMS	109

LIST OF FIGURES

Figure 1: CDS, 2U.....	4
Figure 2: NUTS CAD-model.....	7
Figure 3: Description of satellite.....	7
Figure 4: Primary structure.....	7
Figure 5: Antenna module assembly.....	9
Figure 6: Access ports in CDS.....	12
Figure 7: Orientation of satellite and interface.....	13
Figure 8: Secondary structure.....	15
Figure 9: Secondary structure and ADCS prototype.....	16
Figure 10: Assembly of secondary structure and backplane.....	17
Figure 11: Backplane and secondary structure.....	18
Figure 12: ADCS prototype module card.....	18
Figure 13: Flush alignment.....	19
Figure 14: ADCS design.....	21
Figure 15: Solar cell interface module.....	22
Figure 16: Assembly of solar cell panels.....	23
Figure 17: P-POD.....	26
Figure 18: Crack due to anodizing layer.....	27
Figure 19: Rail and standoff.....	29
Figure 20: Complex geometry.....	29
Figure 21: Rail profile v01.....	29
Figure 22: Rail profile v02.....	29
Figure 23: CFRP-Panel cut outs.....	30
Figure 24: 45° Adhesive jig.....	32
Figure 25: 0° Adhesive jig.....	32
Figure 26: Adhesion sequence.....	33
Figure 27: Adhesive jig with different configurations.....	34
Figure 28: Cutting pre-preg.....	38
Figure 29: Pre-preg layup.....	38
Figure 30: Debulking schematic.....	38
Figure 31: Debulking.....	38

Figure 32: Compression mould and mould	40
Figure 33: Machining CFRP-panel.....	41
Figure 34: Abrasive pre-treatment.....	42
Figure 35: 10 g of resin.....	43
Figure 36: 4 g of hardener	43
Figure 37: Applying adhesive.....	43
Figure 38: Jig assembled for 1 side.....	43
Figure 39: Antenna module assembly	46
Figure 40: Antenna configurations	47
Figure 41: X-Y plane configuration	48
Figure 42: Standoff piece wrapping around Z-axis	49
Figure 43: Antenna module fastened to secondary structure	52
Figure 44: Antenna module v09 prototype	53
Figure 45: Burn off points.....	54
Figure 46: Probability of earth contact vs. burn off success rate.....	55
Figure 47: Burn of contact.....	55
Figure 48: burn off mechanism	57
Figure 49: Heat treatment of BeCu, tensile strength	59
Figure 50: Heat treatment of BeCu, yield strength.....	59
Figure 51: Buckling load in the different directions of the antenna element.....	60
Figure 52: Inertia of an ellipse.....	61
Figure 53: Antenna press machine drawing.....	63
Figure 54: Milling antenna element press.....	64
Figure 55: Forming tool.....	65
Figure 56: Antenna element	66
Figure 57: Change in radius under manufacturing	67
Figure 58: The radius effect on stiffness.....	67
Figure 59: Coiled up with a radius of 1-2 mm.....	67
Figure 60: R5.....	68
Figure 61: R2.....	68
Figure 62: R1.5.....	68
Figure 63: R0.75	68

Figure 64: No visible plastic deformation	68
Figure 65: No visible plastic deformation	68
Figure 66: Plastic deformation	68
Figure 67: Plastic deformation	68
Figure 68: Burn of thread test jig 1.....	70
Figure 69: Temperature vs. time, prototype 1	71
Figure 70: Burn of thread test jig 2	72
Figure 71: Temperature vs time, prototype 2	73
Figure 72: No configuration.....	75
Figure 73: 60x60x60 configuration	75
Figure 74: Sharp angle configuration	76
Figure 75: Wide angle configuration.....	76
Figure 76: Medium angle configuration.....	76
Figure 77: Direction of force in relationship to bending angle.....	77
Figure 78: Antenna element end.....	77
Figure 79: UHF element release mechanism configuration.....	79
Figure 80: Hinge mechanism opposite sides	80
Figure 81: Antenna module v.01.....	81
Figure 82: Antenna module v.05.....	81
Figure 83: Antenna element start end position	81
Figure 84: Antenna module assembly 1.....	82
Figure 85: Assembly connected to bread board.....	83
Figure 86: Signal processor.....	83
Figure 87: Antenna module release mechanism	84
Figure 88: Single lap shear	88
Figure 89: Lap shear test specimens.....	89
Figure 90: Test specimen #2 in the machine	90
Figure 91: Standoff measured.....	94
Figure 92: Rail measured in centre side 1.....	94
Figure 93: Rail measured in end side 2	94
Figure 94: Left side milled from top, right side milled from side	95
Figure 95: Difference between the two production series.....	95

Figure 96: Measurement 1 and 2.....	96
Figure 97: Measurement 1	96
Figure 98: Measurement 2	96
Figure 99: Measurement 3	97
Figure 100: Measurement 4.....	97

LIST OF TABLES

Table 1: X-Y dimensions.....	44
Table 2: Z dimensions	44
Table 3: Antenna module.....	50
Table 4: Evaluation of burn off mechanisms.....	56
Table 5: Material properties	58
Table 6: Resistance wires	70
Table 7: Shear stress and elongation at break	91
Table 8: Sorted by adhesive layer thickness.....	91
Table 9: Sorted by shear stress values	91
Table 10: Result of surface roughness test.....	94
Table 11: Measurement of side in milling master thesis rail	96
Table 12: Measurement of top down milling on master thesis rail.....	97

LIST OF ABBREVIATIONS

ABS	-	Acrylonitrile Butadiene Styrene
ADCS	-	Altitude Determination and Control System
1U	-	1 Unit
2U	-	2 Unit
BeCu	-	Beryllium Copper
CAC	-	CubeSat Acceptance Checklist
CAD	-	Computer Aided Design
CDS	-	CubeSat Design Specification
CFRP	-	Carbon Fibre Reinforced Polymer
CNC	-	Computer Numerical Control
COG	-	Centre of Gravity
CTE	-	Coefficient of Thermal Expansion
DAR	-	Deviation Waiver Approval Request
EPS	-	Electronic Power Supply
FEA	-	Finite Element Analysis
IET	-	Department of Electronics and Telecommunication
IPM	-	Department of Engineering Design and Materials
ISIPOD	-	ISIS Picosatellite Orbital Deployer
ISIS	-	Innovative Solutions In Space
LEO	-	Low Earth Orbit
LSS	-	Lap Shear Strength
LV	-	Launch Vehicle
NASA	-	National Aeronautics And Space Administration
NUTS	-	NTNU Test Satellite
NTNU	-	Norwegian University of Science and Technology
OBC	-	On Board Computer
PCB	-	Printed Circuit Board
PEEK	-	Polyether Ether Ketone
POD	-	Picosatellite Orbital Deployer
P-POD	-	Poly Picosatellite Orbital Deployer
Pre-preg	-	Pre Impregnated Epoxy Composite Material
RBF	-	Remove Before Flight
UHF	-	Ultra High Frequency
USB	-	Universal Service Bus
VHF	-	Very High Frequency

NOMENCLATURE

P	-	Power
V	-	Volt
A	-	Ampere
R	-	Resistance
mA	-	Milli Ampere
g	-	Earths gravitation
MPa	-	Mega Pascal
E1/E2/E3	-	Young's modulus
kN	-	kilo Newton
m	-	Milli
m	-	Metre
K	-	Kelvin
mm	-	Millimetre
C	-	Celsius
Sigma uts	-	Ultimate tensile strength
GPa	-	Giga Pascal
μ	-	Micro

Chapter 1

1 INTRODUCTION

NUTS is student satellite project run by the Department of Electronics and Telecommunication. The goal is to develop a fully functional student designed satellite. It implies development and manufacturing of satellite structure, hardware and software.

The satellite is designed according to CubeSat design specification, CDS. The CDS was written with the purpose of having a standard to reduce development cost and time, thus increasing access to space with frequent launches. It was made as collaboration between California Polytechnic State University, Cal Poly, and Stanford University's Space Systems Development Laboratory.

A CubeSat is a 10 cm cube with mass of 1.33 kg and is called a 1 Unit, 1U. CubeSat's come in different shapes and sizes but common for all is the basis of 1U. There is 1, 1.5, 2, 3 and 6U CubeSat's. NUTS is building 2U CubeSat. When built, CubeSat's are put into a deployer called POD, Picosatellite Orbital Deployer. The deployer is then attached inside a launch vehicle, LV. The LV is the carrier rocket which brings the satellites into orbit and the deployer deploys the satellite. NUTS will be "piggy backing" into space which means a commercial party buys the LV and sell excessive space. They will then be primary payload, and most likely there will be a secondary payload and CubeSat's will be tertiary payload. NUTS will orbit in low earth orbit, LEO, and is expected to be in an orbit approximately 350 km from earth. The orbit is chosen by the primary pay load.

Introduction

In order to purchase a space for a POD it needs to go through a broker. Innovative solutions in space, ISIS, is among else a launch broker and is engaged by NUTS. The launch is the largest budget post for a student satellite. Therefore NUTS is sponsored with a funding guarantee from Norwegian Space Centre. The access to space is limited due to low availability in LV providers. But the Norwegian Space Centre is also funding CubeStar, which is a satellite built by The University of Oslo, and they are delayed. Therefore a possible position has opened up for NUTS to launch in 2015. The launch is scheduled to be in June but rumoured to be in September.

ISIS is a spinoff company from a satellite project from Delft University of Technology. They specialize in engineering solutions and services for space and provide a variety of off the shelf products. From NUTS' perspective the most important services is being launch broker, providing ISIS picosatellite orbital deployer, ISIPOD, and guidance towards launch. ISIPOD is for all reasons the same as the original P-POD which is developed by Cal Poly. Both PODs are designed for deploying CubeSat's with a preloaded spring. The difference lies in the available space between the contact surfaces and the accessibility of the satellite ones inserted into the PODs. Regardless of which POD used, all CubeSat's are designed according to the CDS. In addition to the CDS there are requirements from the LV provider. Since they are not known through the whole design process they are difficult to account for.

Commercially built CubeSat structures are available to buy off the shelf and this is common practice. NUTS however is building its own structure and producing all structural components on campus. Commercially structures mainly consist of aluminium and NUTS are aiming for a lighter structure consisting of advanced materials. The design philosophy is to build it in light weight composite and polymer. Due to constraint in the CDS aluminium interfaces will be used.

1.1. Scope

Complete and complement solutions for NUTS frame and finalize the design and production process. The aim is to finish an engineering model of the primary structure that can be used as engineering model of the satellite. Further development of the antenna module and assist NUTS in mechanical design.

1.2. Relevant information

1.2.1. Design requirements

The CDS is the CubeSat design manual. It includes general, mechanical, electrical, operational and test requirements. The essentials from the CDS will be mentioned here in order to improve the understanding of the main parts of the report.

General requirements

- CubeSat's materials shall have a Total Mass Loss, TML < 1.0 %.
- CubeSat materials shall have a Collected Volatile Condensable Material, CVCN, < 0.1%
- CubeSats which incorporate any deviation from the CDS will submit a deviation waiver approval request, DAR, and adhere to the waiver process

Mechanical requirements

- The CubeSat shall use the coordinate system as defined in Figure 1 for the appropriate size. The CubeSat coordinate system will match the P-POD coordinate system while integrated into the P-POD. The origin of the CubeSat coordinate system is located at the geometric centre of the CubeSat
- The -Z face of the CubeSat will be inserted first into the P-POD.
- Rails shall have a minimum width of 8.5mm
- Rails will have a surface roughness less than 1.6 µm.
- The edges of the rails will be rounded to a radius of at least 1 mm
- The ends of the rails on the +/- Z face shall have a minimum surface area of 6.5 mm x 6.5 mm contact area for neighbouring CubeSat rails
- The maximum mass of a 2U CubeSat shall be 2.66 kg.
- The CubeSat centre of gravity shall be located within 2 cm from its geometric centre in the X and Y direction.
- The 2U CubeSat centre of gravity shall be located within 4.5 cm from its geometric centre in the Z direction.
- Aluminium 7075, 6061, 5005, and/or 5052 will be used for both the main CubeSat structure and the rails.
- The CubeSat rails and standoff, which contact the P-POD rails and adjacent CubeSat standoffs, shall be hard anodized aluminium to prevent any cold welding within the P-POD.

Introduction

- The 1U, 1.5U, and 2U CubeSat separation spring will be centred on the end of the standoff on the CubeSat's -Z face

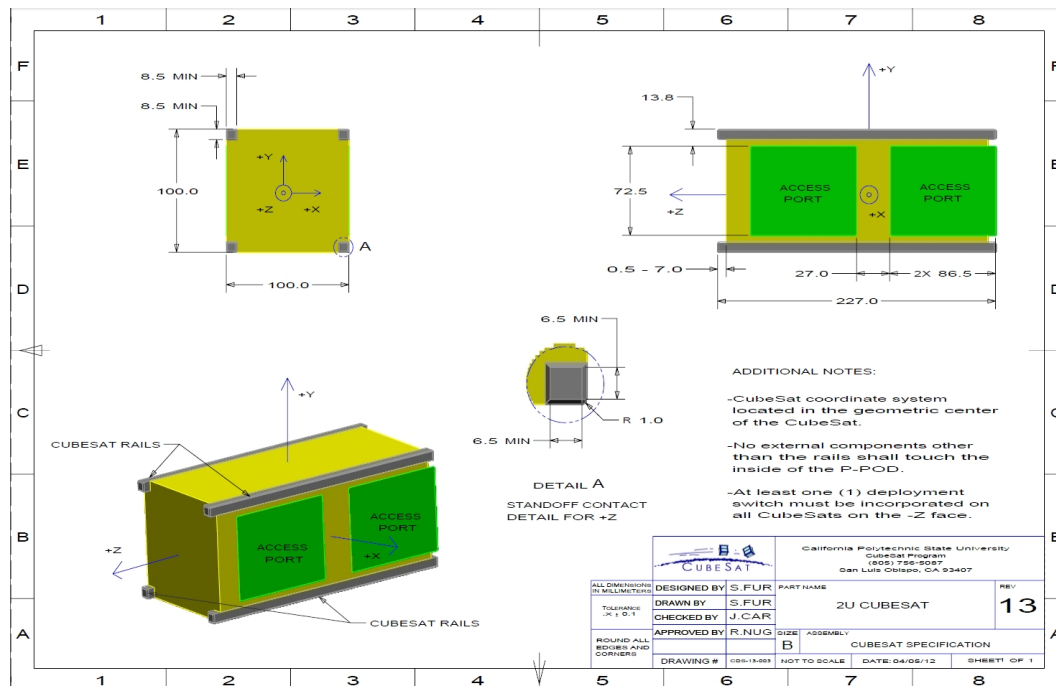


Figure 1: CDS, 2U

Electrical requirements

- The CubeSat shall have, at a minimum, one deployment switch on a rail standoff
- In the actuated state, the CubeSat deployment switch shall electrically disconnect the power system from the powered functions
- The CubeSat shall include a remove before flight pin, RBF-pin
- The RBF-pin shall be removed from the CubeSat after integration into the P-POD

Operational requirements

- All deployables such as booms, antennas, and solar panels shall wait to deploy a minimum of 30 minutes after the CubeSat's deployment switch(es) are activated from P-POD ejection.

Test requirements

- Testing will be performed to meet all launch provider requirements as well as any additional testing requirements deemed necessary to ensure the safety of the CubeSats, P-POD, and the primary mission.
- Random vibration testing shall be performed as defined by the launch provider.
- Thermal vacuum bakeout shall be performed to ensure proper outgassing of components. The test specification will be outlined by the launch provider.
- Shock testing shall be performed as defined by the launch provider.
- Visual inspection of the CubeSat and measurement of critical areas will be performed per the appropriate CubeSat Acceptance Checklist

Comments

According to the general requirements a DAR should be written for any deviation from the CDS. The NUTS satellite is using carbon fibre reinforced polymer panels, CFRP, which deviate from the mechanical requirements, thus a DAR should be written. This has not yet been completed. There is an uncertainty regarding if it is necessary since ISIS is used, also this is mainly affected by requirements by the launch provider, LP.

In the electrical requirements it is written *“The CubeSat shall have, at a minimum, one deployment switch on a rail standoff”*. NUTS will use two. The reason is that these switches need to withstand the total amount of current the batteries can deliver.

1.2.2. Previous work

Christian Nomme was the previous student writing a thesis on the mechanical system for NUTS. His thesis *“Mechanical design of CubeSat structure using composites and polymers”* were almost written as an introduction in how to design and build a CubeSat. The thesis does describe the space environment and how it affects materials. This thesis is based on conclusion presented in Nomme’s work.

1.2.3. Design philosophy

The design philosophy is based on modular design. This implies components can be changed without conflict with the remaining components, also the basic components can easily be configured into other applications. This can be seen throughout the design as the secondary structure, solar cell panels, primary structure etc.

The satellite is designed with respect to launch. The satellite will be subjected to acceleration and vibrational loads during launch. The design acceleration is 10.5 g [1]. For a static load case on the most exposed area in satellite this yields less than 2 MPa, see Appendix 1. This illustrates that the vibrational loads are the designing factor. Therefore measures have been taken to ensure that all load bearing component is in direct contact with another and thus supported. Thus preventing translation and increased effects of acceleration.

The rails in the satellite will be in contact with the rail within the POD, and the standoffs will be in contact with the POD or a neighbouring CubeSat, in either case it will be geometrically fixed. The force induced on the weight of internal components will have to be taken up by the secondary structure.

The centre of gravity, COG, has to be within an ellipsoid around geometric centre of 2 cm in X- and Y-direction and 4.5 cm in Z-direction. This means object with largest mass will be located near geometric centre.

1.2.4. Introduction to parts

In this section a brief introduction to the main parts and components discussed in this thesis will be given. In Figure 2, an overview of the complete satellite can be seen and in Figure 3 an overview of the main internal components can be seen.

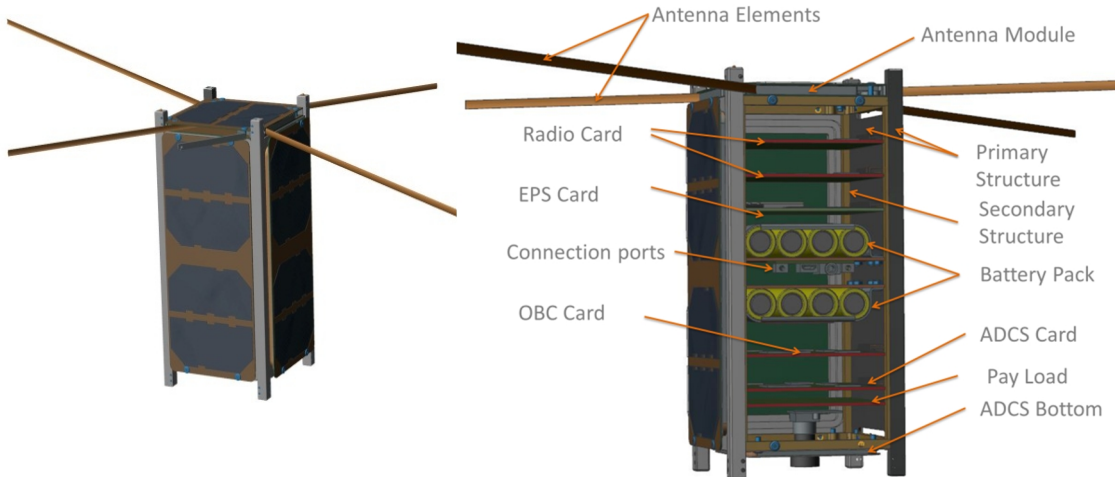


Figure 2: NUTS CAD-model

Figure 3: Description of satellite

1.2.5. Primary structure

The Primary Structure, see Figure 4, serves as the skeleton for the NUTS satellite. It is the main structural component and connects the external and internal parts. The structure consists of four CFRP-panels, four rails and eight standoff pieces. The rails and standoff pieces are made out of aluminium. This is a CDS requirement, and there are specific demands to surface and coating. The rails will be in contact with the deployer and the standoff pieces are in place to set a distance from the deployer and neighbouring satellite.

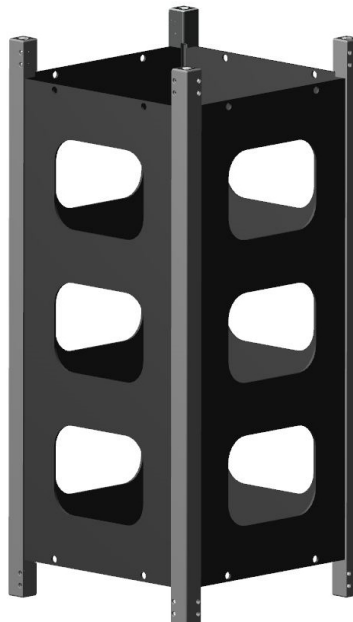


Figure 4: Primary structure

1.2.6. Antenna module assembly

The antenna module assembly is a sandwich construction. One printed circuit board card, PCB-card, is the bottom, and it includes two radio circuits, eight burn-off circuits which will be on the opposite side and twelve holes for mechanical purposes. On top of the bottom PCB-card the antenna module is placed. It is a mechanical structure designed to pocket the antenna elements, provide antenna elements attachment point and in combination with the electric, releases the antenna elements at the right time. On top of the antenna module is one of the solar panels. The solar panel is adhered to a PCB-card and this makes the top of the sandwich, see Figure 5. The radios are ultra-high frequency, UHF, and very high frequency, VHF, with the frequency of 437 MHz and 145 MHz respectively. The antennas are made to work as half wave antennas and there are two antennas for each frequency. The VHF antenna element length is approximately 171.5 mm, and the UHF is approximately 517.5 mm, ref Appendix 1. The antenna elements will be made of beryllium copper, BeCu. The antenna module assembly is a mission critical component since the communication can't work without it, thus the mission success cannot be confirmed.

From a mechanical perspective the most important part is the design of the antenna module, the release mechanism and to allow for an assembly procedure. The design involves the size and angles of the pockets for the antenna elements and how to enclose the pockets see Figure 5.

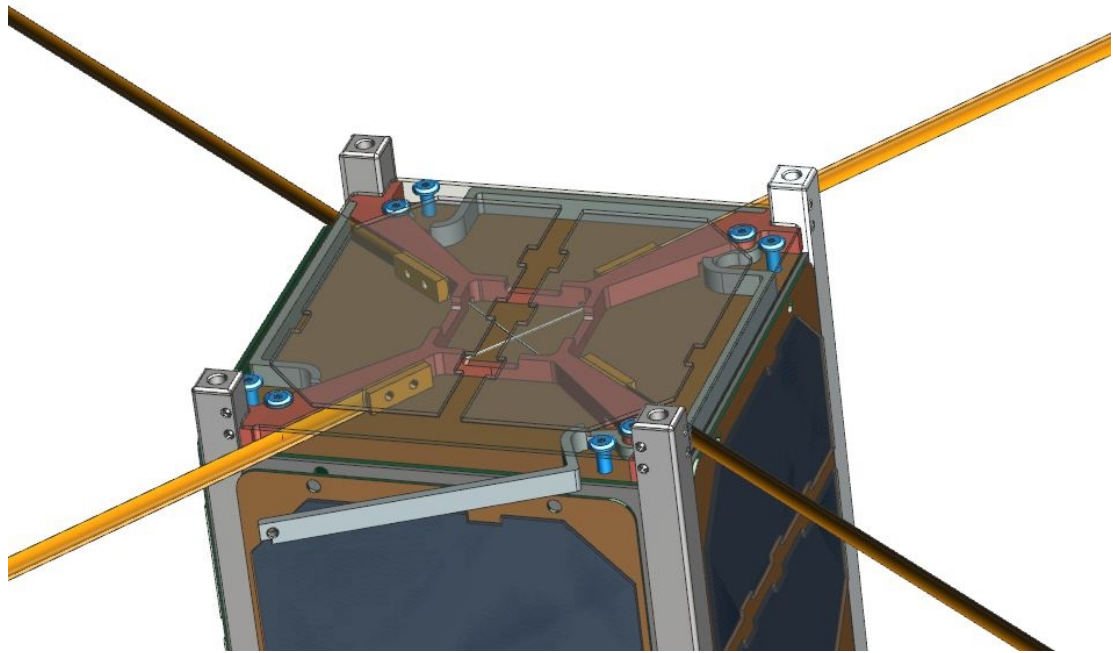


Figure 5: Antenna module assembly

Chapter 2

2 DESIGN AND DEVELOPMENT

The whole satellite is 3D modelled using the CAD program Siemens NX 8.5. The former master student Christian Nomme handed over a file with a complete model in 2013. In the NUTS project there are very few complex geometries, but the number of components and the dependency between them make it complex. As the project progressed it became evident that it was more convenient to build a new model rather than make the necessary changes to the existing. There are two main reasons for this decision: first each designer has a different way to build up components, thus it can be time consuming to adjust components, secondly some parts were easier to build new rather than making the required changes. The process of building a new model did inevitably take some time, and during this time the understanding of the design increases rapidly. Each line or feature must be thought through, and a lot of possibilities prove themselves while an ownership is acquired.

2.1. Orientation of the satellite

NUTS are designing the satellite according to CDS. The CDS have a predefined coordinate system for the P-POD and the CubeSat's. It states that the $-Z$ face of the CubeSat will be inserted first into the P-POD. This is important since the separation switches and springs are located on the $-Z$ face. These components are located inside the standoff pieces. Thus the standoff pieces in the opposite direction, $+Z$, should be solid to ensure contact between adjacent satellite's separation springs/switches. According to the CDS the P-POD has two access ports for a 2U and these are located on the $+X$ face, see Figure 6. Even though NUTS is designing ac-

Design and development

According to CDS it is not going to use its deployer, the P-POD, but ISIPOD from ISIS. The main difference between the PODs is the envelopes and access points. Envelope in this context is the space between the rails inside the POD. The rails of the satellite is the only contact area between the POD and the CubeSat, thus the envelope. In the P-POD there is 6.5 mm envelope contrary to the 9.0 mm envelope in the ISIPOD. The ISIPOD has a whole face which is accessible after the insertion. The reason why this is so important is that through that access face NUTS can access the satellites interface. This interface consists of RBF, power source and a USB-port. The interface was a catalyst for defining the orientation of the satellite. There have been a consensus for a long time of what is $-/+Z$ but not the orientation of X and Y. In order with the CDS requirements, the interface is placed on the $+X$ face and major parts are again located accordingly.

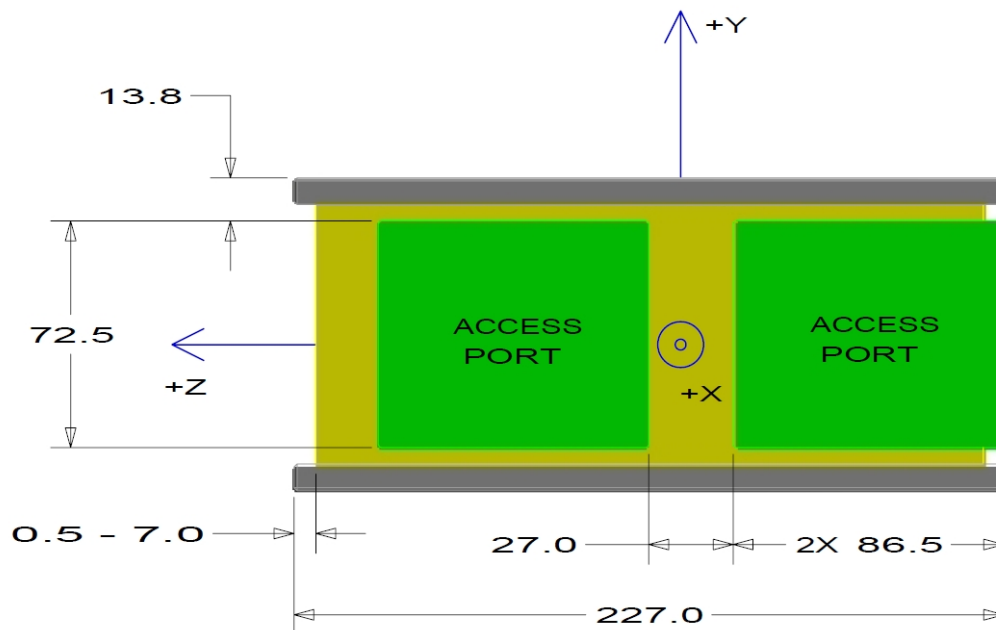


Figure 6: Access ports in CDS

The $+X$ face, as all other major faces are covered with solar panels. On two of the major faces there are also ADCD copper coils. These coils affect the COG due to its mass and distance from the COG. The backplane inside the structure will also be a COG-factor. Therefore it is important to avoid having the backplane and a copper coil on the same face. The interface needs an area of 10 x 40 mm on the $+X$ face, and it needs to be wired and fastened to something. There are basically three PCB-cards inside the satellite which can be used for this purpose. The payload-card and the

Design and development

two battery-cards are dead cards, meaning they only serve a mechanical function. It implies that the fastening and wiring of the interface can be done without affecting a circuit. The batteries are also important factors to the COG and it is desirable that they are placed as close as possible to COG. Two solutions support this principle. One is where both battery packs are fastened to the same PCB-card, the other is where they are fastened to separate PCB-cards. The latter is the better solution. A PCB-card with two battery pack would yield a higher stress concentration to the card and the secondary structure it is inserted in. Also placing the battery packs on two different cards would allow for the interface to be secured on the opposing side of the PCB-card. The fact that the location of the battery pack coincides with the most easily available space between the solar panels on the outside is convenient. The persons in charge of the solar panels have confirmed that if the wiring of the solar panels is made with the new design requirement it is possible to make space for the interface. Most of the available area is in middle of the section between the four solar cells, which means the interface will be located in the centre on the +X face, see Figure 7, between the battery packs. (X, Y, Z) is defined according to CDS and origin will be in the geometric centre. The backplane will be in the X-Z plane in positive direction. Z is defined as the height of the backplane with payload on the -Z face and antenna module assembly on +Z face.

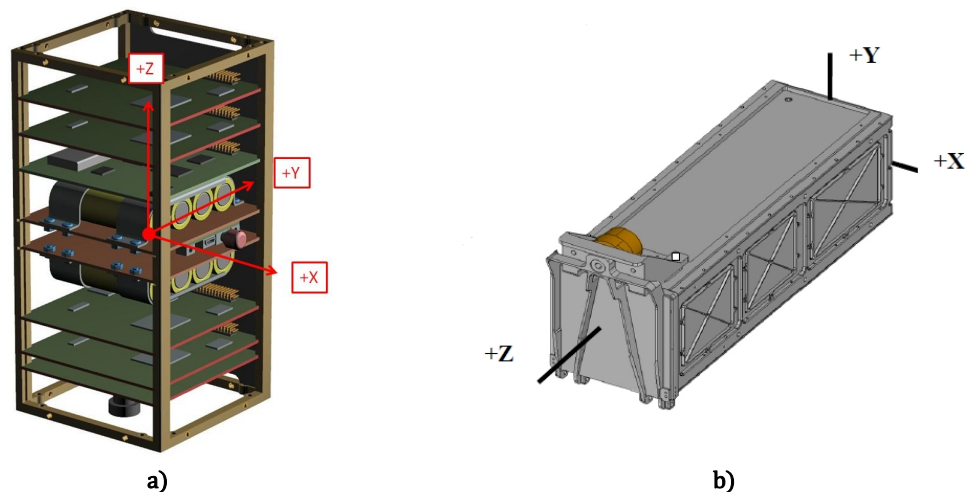


Figure 7: Orientation of satellite and interface.

2.2. Secondary structure

Purpose

The secondary structure is the structure within the primary structure. It incorporates the backplane and allows the backplane to be a modular design. This is due to its easy assembly process of inserting module cards into predefined slots. When the backplane is inside the secondary structure, it is then dropped down into the primary structure. This allows easy testing and fitting without compromising the structural integrity of the satellite. It also serves as the primary attachment point for altitude determination and control system, ADCS, solar cell panels, and antenna module assembly.

Design

The structure consists of four braces, two trusses and eight inserts. Each brace has eight cuts for module cards and a hole in each end for the inserts. The trusses are on each end and bind the structure together with inserts, see Figure 8. The ADCS, solar cell panels, and antenna module assembly is as mentioned fastened to the structure. They will be fastened by a screw joint, consisting of aluminium screws. Metal to plastic screw joints have very limited assembly/dismantle cycle. Therefore helicoil inserts will be used. Helicoil is a metal threaded insert which allows for higher assembly/dismantle cycle.

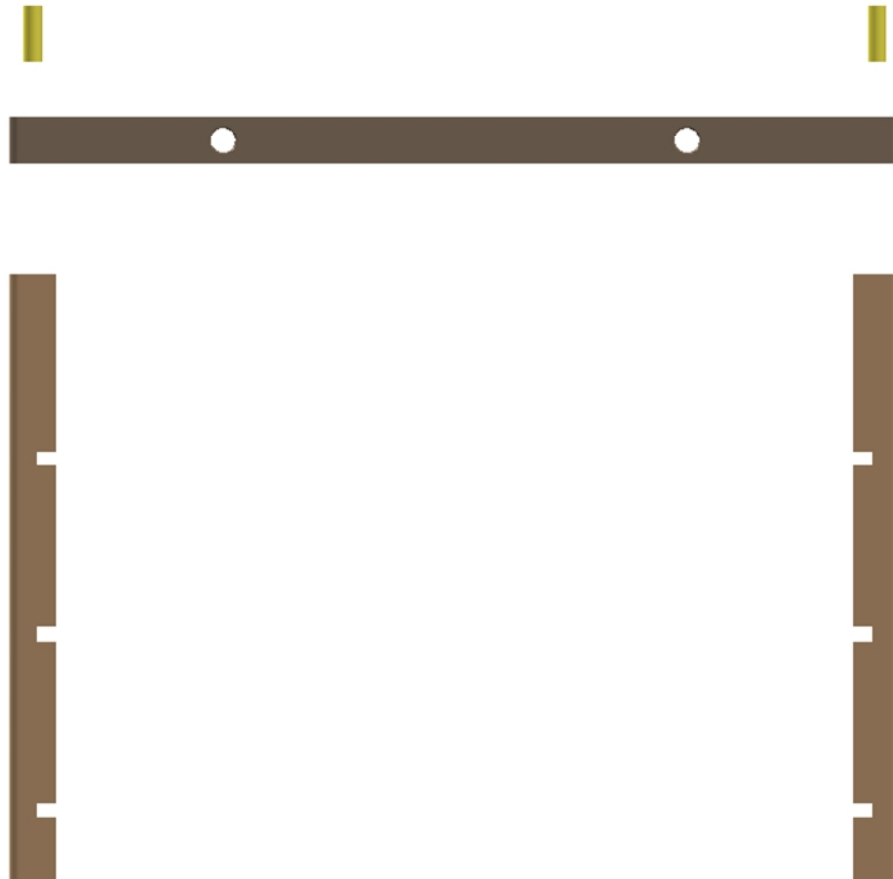


Figure 8: Secondary structure

Constraint

The braces are to be attached to trusses by insert. The reason behind using inserts is that a screw joint will result in removing material for chamfering. Due to the joints position in regard to stress it is not desired. An adhesive joint was considered to not be structural sound and difficult to position. The adhesive joint cannot be assembled and dismantled as easily as a friction based joint. This structure will only experience compressional stress and therefore inserts is sufficient.

Material and manufacturing

The components in this structure are going to be made out of polyether ether ketone, PEEK. This material has according to National aeronautics and space administration, NASA TLM of 0.2 % and CVCM of 0 %, which is less than the 1% and 0.1 % required [2]. The machinability, mechanical, thermal and outgassing properties

Design and development

makes it suitable for this application. It has not been manufactured in PEEK yet. This is due to design of the backplane, which is in revision. The backplane will govern the distance between the each module card. A recommendation for the layout of the backplane is presented in chapter 2.3. For prototyping purposes it has been 3D-printed, and has been used extensively for prototyping of the ADCS, see Figure 9. When manufactured, it will be milled out from a sheet of PEEK.

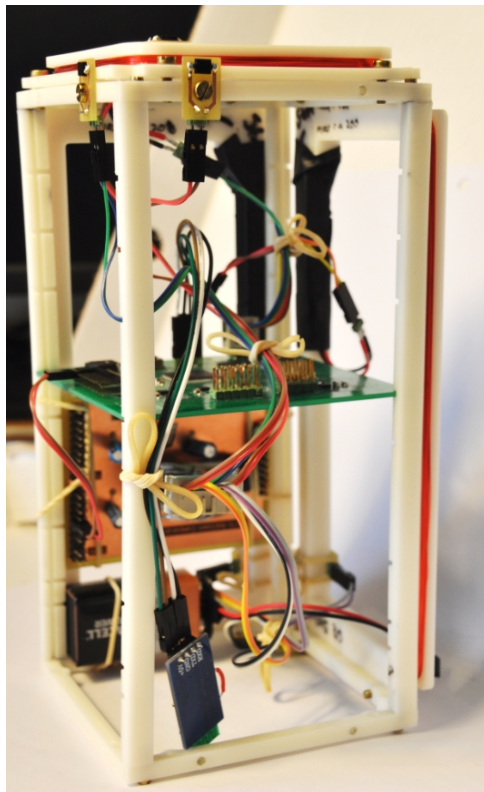


Figure 9: Secondary structure and ADCS prototype

Assembly

The complete assembly of the secondary structure can first be done when backplane is manufactured. The assembly procedure is illustrated in Figure 10. First one truss is assembled to the four braces with inserts, then the backplane is inserted, before the second truss is assembled with inserts. The trusses have holes on all sides. On the top of the satellite the antenna module assembly is going to be fastened to top truss, on the bottom the bottom ADCS module is going to be fastened, and on the sides ADCS and solar cell panels is going to be fastened to the secondary structure.

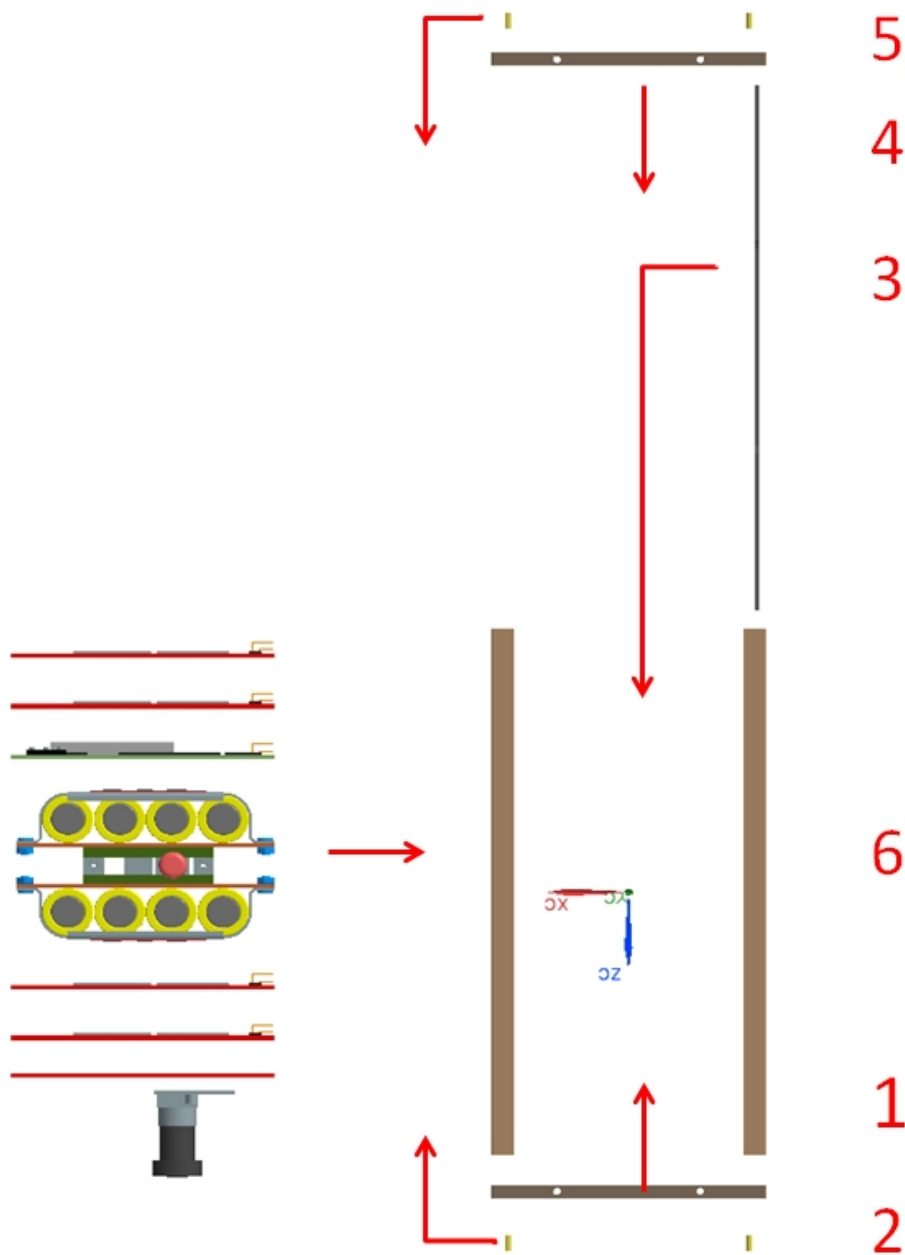


Figure 10: Assembly of secondary structure and backplane

2.3. Backplane

Purpose

The backplane is the connection between the different module cards. It has eight ports with two masters and four ports. It has ability for more ports but batteries have been chosen. The backplane inside the secondary structure can be seen in Fig-

Design and development

Figure 11, and the ADCS module card can be seen in Figure 12. The current stacking order for the backplane from top till bottom is as follow:

1	Master	-	Radio
2	Slave	-	Radio
3	Slave	-	Electric power supply, EPS
4	Battery pack		
5	Battery pack		
6	Master	-	On board computer, OBC
7	Slave	-	Empty
8	Slave	-	Payload

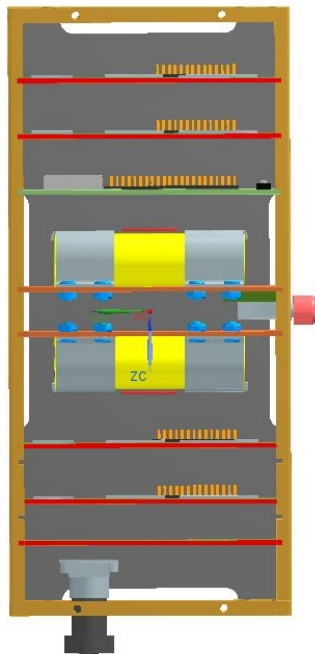


Figure 11: Backplane and secondary structure

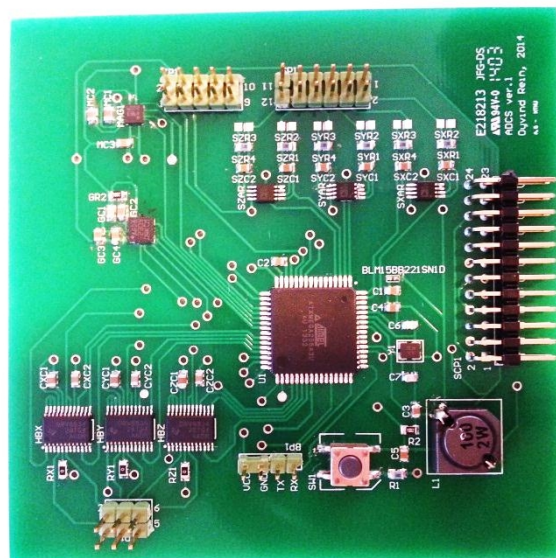


Figure 12: ADCS prototype module card

Design and constraint

The distances between each module card is of now 17.4 mm but this not certain since the component height on top of each module card can vary, also it not decided. But from a mechanical perspective the most important factors are the dimensions, sizing and the connection between the backplane and module cards. Each module cards are to be pushed into the secondary structure and it is constrained when it meet the backplane. It is important that each module is flush with the edge in the

Design and development

secondary structure. In Figure 13 the three upper cards are flush with this edge, see top arrow, and the battery pack is not flush for illustrational reasons, bottom arrow. When it is flush it will be constrained in all directions. This is important since the orientation of the POD inside the LV is unknown. Each module card has connection pins which will be soldered to the backside of backplane.

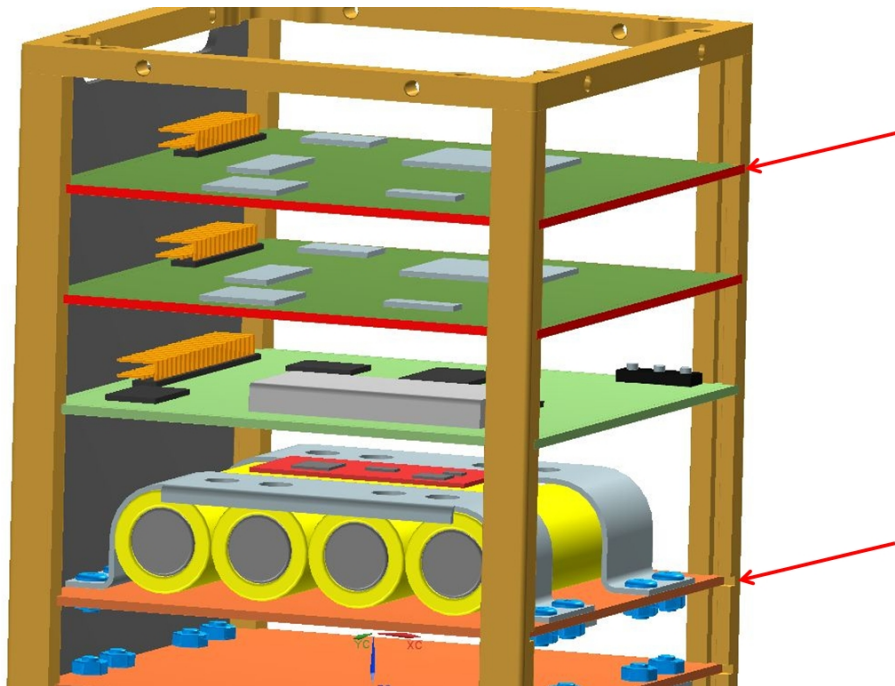


Figure 13: Flush alignment

The shape of the backplane is also important. It need to allow for wiring, therefore cuts are design into the four edges of the backplane, see Figure 11. Large radiuses are designed in to avoid large stress concentrations.

Material and manufacturing

The material for use is FR4 glass/epoxy. FF4 is sandwich structure of woven fiber-glass in epoxy resin with copper sheets on top and bottom. It is the most common PCB material for use in aerospace projects[1]. This material is approved for aerospace. Two different thicknesses will be used, 1.6 mm thickness for backplane and

PCBs for the backplane, and 0.8 mm for solar cell panels and in antenna module assembly.

2.4. ADCS

Purpose

After the deployment into orbit the satellite will most likely spin. In order to stop the spin, called detumbling, and orient the satellite it has the ADCS. It consists of three electro magnets which are located on three sides normal to each other. The ADCS has two sensor systems for input to calculations. The system for detumbling is based on measuring the magnetic field of the earth and then counteract according to it. This system will work even though the satellite is on the shadow side of the earth. The other system is for fine tuning and is based on sun sensors, see Figure 14, which will only work on the sun side. These will measure the angles relative to the sun and calculate the velocity, rotation and position. With this input it calculates the amount of current and the order to switch on the different ADCS modules. They can only work in pair to affect the orientation. Other than detumbling the satellite and fine tuning the satellite for the optical camera, it will also spin the satellite around the Z-axis in a controlled manner, called the barbeque effect, to prevent too elevated temperatures.

Design

The ADCS modules come in two sizes. There are the side modules on the X-Z and Y-Z face, and bottom module on the X-Y face. The ability of the magnets to create a magnetic field is governed by current, distance from rotation axis and number of windings. The ADCS modules on the sides are double in height compared to the bottom face, and the current available is the same. To compensate for reduces distance around rotation axis, the number of windings is greater on the bottom module. The number of windings has to be added inwards as there is no space to add outwards due to rails and CDS. The sides have 155 turns and the bottom has 238 turns. To growth inward reduced the effect and adds more turns and mass. The design requirements are to allow for enough turns for the copper coil, allow to coil the copper coils and constraining it, see Figure 14. Two pins will be placed in a corner and the coiling will start from there. Two access cuts are made from the pins. The connection between the copper coil and the pin is an electric conductive adhesive. Then the

coiling will be carried out and the end will be connected with the second pin. The principle is the same for both ADCS modules.

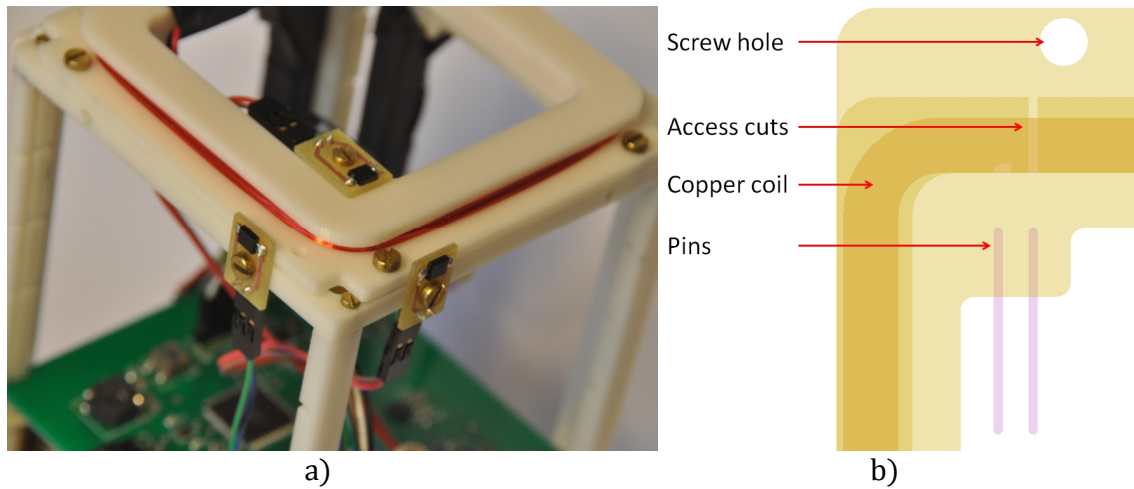


Figure 14: ADCS design

Constraint

The ADCS side modules will be covered by solar cell panels. The same screws will be used to constraint the solar cell panels as the ADCS. The bottom ADCS module will not be covered by solar panels since the optical camera will be located on the $-Z$ face. It will be constraint with screws.

Material and manufacturing

The module for where the copper is coiled will be milled in PEEK. The copper wire is isolated with solderable polyurethane with polyamide overcoat. The pins will be the same as for the connection between module cards and backplane.

2.5. Solar cell panels

Purpose

The solar cell panels are located on five of six sides. Its sole purpose is to recharge the batteries in the satellite. The reason to not have on all sides is due to optical camera on the $-Z$ face.

Design

The solar cell panel design on this satellite is designed to be between the rails of the primary structure, 83 mm and the height of the CFRP-panel, 196 mm. Therefore the

Design and development

PCB for the solar cells is 83 x 196 mm. The dimensions of the solar cells are 40 x 80 mm. This allows for four cells on the sides and two on top. One of the sides is affected by the interface. Therefore one side has a cut for the interface, see Figure 15.

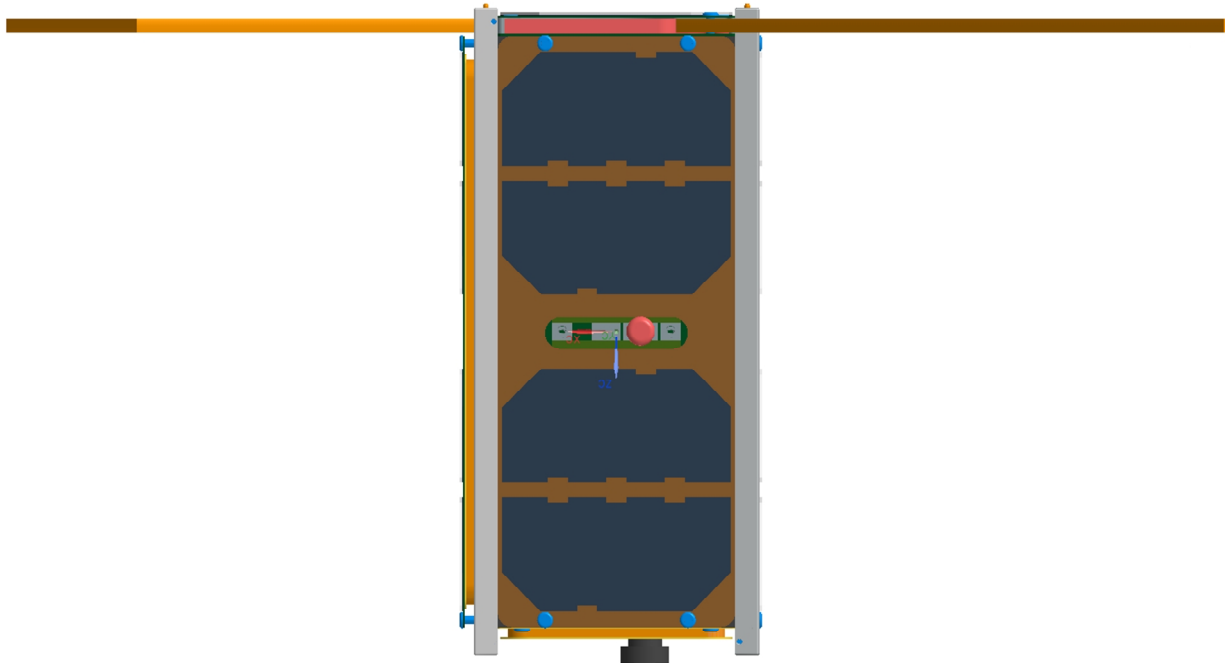


Figure 15: Solar cell interface module

Material and manufacturing

The cells are currently Azurspace TJ Solar Cell 3G30C – GaInP/GaAs/Ge, with an efficiency of 30%. The cells thickness is 0.15 mm with a 0.15 mm glass cover for protection. Due to its fragility and need for connections circuit it will be fastened to a 0.8 mm PCB-card. A double-sided adhesive tape consisting of polyimide film, with low volatility silicone adhesives it planned to be used. The tapes used are produced for space applications [1].

Constraint and assembly

The solar cells panels are going to be constrained by a screw joint. To constraint the top solar panel the antenna assembly needs to be placed on top of the secondary structure, then the top solar cell can be laid on top and fastened. Two of the side solar panels will be screwed directly on to the CFRP-panel, the other two will be screwed together with the ACDS modules, see Figure 16.

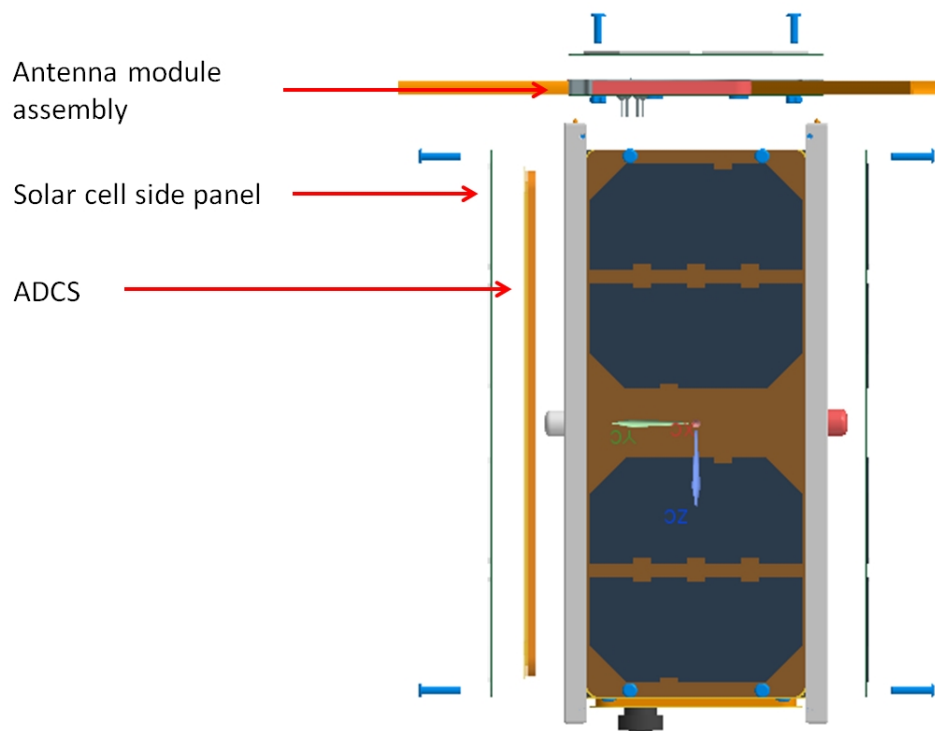


Figure 16: Assembly of solar cell panels

Chapter 3

3 PRIMARY STRUCTURE

The Primary Structure is as mentioned earlier the skeleton of the satellite. It consists of rails, CFRP-panels and standoff pieces. This section will describe the development, design and manufacturing of all components in the Primary Structure.

3.1. Design of rail and standoff

Design history

The design of the primary structure was changed in 2013. Originally the primary structure consisted of CFRP only. This made a rectangular tube and the holes were cut out to reduce mass. There were some obvious challenges with this design. To manufacture a square tube with the precision required can be solved, but the corners would be more challenging. The CDS states the corners need a width of minimum 8.5 mm. This is due to the protrusion in the POD, see Figure 17, which it needs to be in contact with during launch. It is simpler to mill out such a corner than produce it in CFRP.

If corners could be made with a sufficient quality regarding dimension and tolerance requirements, it would be required to be tested and verified for its durability and friction. That would require another master thesis. Therefore it was decided to change the structure to consist of four aluminium rails as corners separated by CFRP-panels. The panels are simpler to manufacture on campus with the equipment available, and the rails can be manufactured at campus. The current design is based on the dimensions defined in the CDS. The rails need an outer surface of 8.5 mm and

Primary structure

are separated with an outer dimension equal to 100.00 mm. The panels are designed to be 1 x 93 x 196 mm being, thickness, width and height.



Figure 17: P-POD

Current design

The CDS states that all faces in contact with the deployer and neighbouring satellites shall be hard anodized. Hard anodizing is demanded to prevent any cold welding or friction welding between the satellites and the deployer during launch. Cold welding is joining of materials without providing external heat, which can be the case in an environment exposed to vibration, like during a launch. For NUTS this means the rails and standoff need to be hard anodized, also called Type III anodizing. In the process of hard anodization 50 % of the layer thickness will grow into the material and the rest will add to its thickness [3]. The CDS does not specify a layer thickness, but a thickness of 50 μm is regarded as an industry standard for hard anodized applications. The anodization layer will have a different density compared to the base material. This change in density will lead to cracks in sharp corners[4]. This effect is worst in external corners where the increased volume will make it crack, see Figure 18. This is solved by introducing radiuses to all corners.

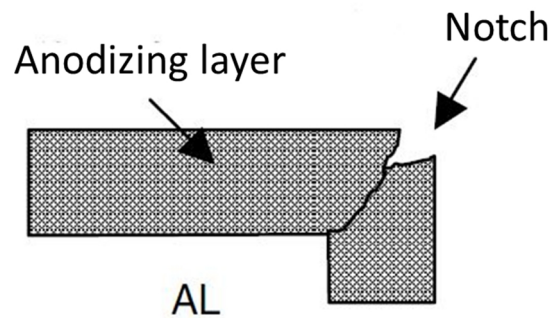


Figure 18: Crack due to anodizing layer

The rails in the satellite can be looked upon as an L with two steps on the inside, see Figure 21. It does have sharp edges in all but one, which is the outside corner. The thickness of the rail has been set to 0.925 mm with the steps to be approximately 1 mm. The reason for the steps, see Figure 21, are to have perpendicular surfaces for the CFRP-panel for support. This means the compressional forces will be transferred from one rail through the CFRP-panel by contact, and not with the adhesive. The loads on the adhesive in this design are bending of the CFRP-panel due to vibrational loads, and thermal loads. The whole satellite will undergo vibration test to verify the structure. The adhesive has been checked for thermal loads. With the CFRP-panel adhered to the rail, the inside of the primary structure will be completely square. The second step could have been on the secondary structure. But as one step was needed, it would be quicker and easier to have the cut in the rail rather than in the secondary structure.

The producer of anodizing layer recommends a minimum radius of 1.5 mm on a layer thickness of 50 μm . This is to avoid any cracks in the material [3]. Therefore the radius on the corner along the length has been changed from 1.0 mm to 1.5 mm. There has also been added a radius on the far edges, see Figure 21 and Figure 22. The radius is larger than the thickness of the rail. As the rail has a thickness of 0.925 mm it is impossible to obtain a full quarter circle. This means that there cannot be a smooth transition on both sides where the radius is applied, in contrast to the case of the corner in the middle of the "L". Since sharp edges are destructive, the smooth transition is chosen to be along the width of the rail. The other edge will inevitably be sharp with this thin structure. This meant the rail would have 7 sharp edges

Primary structure

where cracks would be initiated. This fact was reasons for concern. No obvious solution was found which wouldn't require significant redesign of many parts. A literature study was made in order to try to find out how large these cracks could be. But the size of the cracks largely depends on the operation condition like chemical solution, temperature and time, and these are kept secret for competitive reasons. Even if the cracks would be small it was still unsettling due to vibrations during launch. The fact that the satellite would primarily be under compressional loading, which does not initiate crack propagation, did not stop the search for a better solution. After a long time the idea of "masking" the inside of the "L" originated. That means the inside will not have an anodizing layer and therefore the problems with cracks on the inside would be solved. The anodizing producer was asked if they provided a service similar to "masking" and they did, at an additional cost. Still the edges at each end of the "L" would experience cracks. Therefore the width of the rail has been increased from 8.5 mm to 9.00 mm. After the anodization the rail will be trimmed down to the original 8.5 mm without anodizing cracks.

At each end in the length direction a standoff piece is placed. It is also required to be hard anodized. The standoff piece is only rounded at the top, see Figure 19, which is demanded by CDS [5]. This means there will be cracks on this part since the whole piece will be anodized. The standoff will not be a bearing structure and therefore extra action will not be put into effect to prevent this.

The radius of 1.5 mm does add complexity to the rail assembly. Since the radius is larger than the thickness small adjustments are needed on the standoff, see Figure 20. The radius on the rail will continue on to the standoff. Therefore the corners of the standoffs need to be grinded down. This will be done by hand before anodizing.

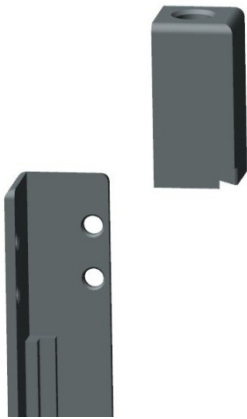


Figure 19: Rail and standoff

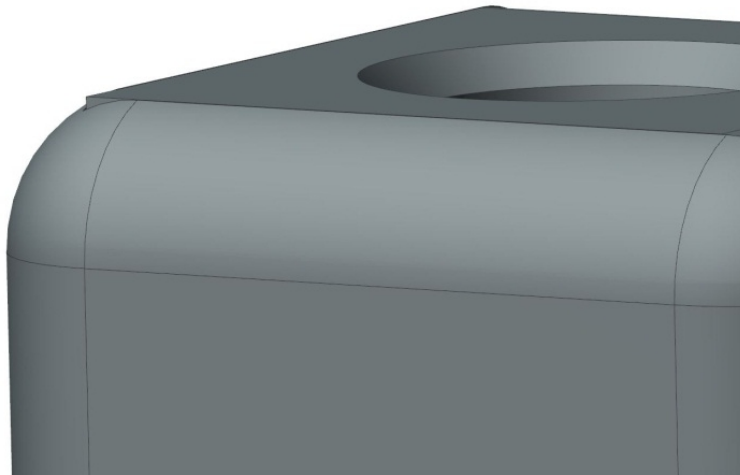


Figure 20: Complex geometry



Figure 21: Rail profile v01



Figure 22: Rail profile v02

On the $-Z$ face there shall be two separation springs and at least one deployment switch. The separation spring is a small spring where its intention is to separate satellites from each other. The LV has a larger spring that will plunge all satellites out of the LV and the springs are merely in place to separate the satellites. The deployment switch, also called a kill switch, is there to ensure that no current is on before deployment out of the POD. These components are going to be placed inside the standoff pieces. The standoff piece has the dimension $7.5 \times 7.5 \times 15$ mm. The original idea was to utilize a screw connection between the standoffs and the rails in order to be able to assemble and dismantle. But the separation switches generally have too large diameter to allow for threads in the standoff. Conveniently one side of the primary structure needs to have standoffs attached when inserting the secondary structure to constrain it. This will be on the $-Z$ face. Because then the standoff could have an adhesive connection. The adhesive connection on the face with sepa-

ration springs would eliminate the demand of threads in the standoff for screws, thus allowing larger diameter separation switches. The other face shall not have any separation springs or switches and there can easily accommodate room for threads.

3.2. Design of CFRP-panels

The panels in the Primary Structure been modified. The reason for this change is that the satellite has an interface which needs to be accessible after assembly, as described in section 2.1. Previous there has been two cut-outs. This has now been changed to three cut-outs, see Figure 23. The interface is going to be fastened under the battery PCB-card. The battery pack is placed in the centre of the satellite and a cut in the centre was necessary.



Figure 23: CFRP-Panel cut outs

3.3. Design of adhesive jig

In 2013 the first prototype utilizing rails and panels were made. This work was done during the master thesis by Christian Nomme [1]. The setup for aligning the components consisted of angle bars and clamps. This setup yielded a result which did not meet the requirements in the CDS. Despite the result, it gave a lot of experience and insight.

The primary structure consists of four CFRP-panels which are to be joined together with four aluminium rails. The result is a squared tube. The components are joined together with a NASA approved adhesive. The primary structure has to be within CDS specifications which also make out the design requirements for this jig.

Design requirements

Primary structure

- Outer dimensions:
 - X-Y direction: 100.0 ± 0.1 mm
 - Z direction: 227 ± 0.1 mm
- Ensure alignment in all directions in first and through last joining

With the results from Christian Nommes thesis at hand a jig design was started in the fall of 2013. The jig has been further developed in this thesis. In order to design a jig which fulfils the requirements of CDS, it is important to have a plan, and to think through the whole process. The most important factors which needed to be sorted out are listed below.

- Orientation of the jig
- Order of assembly
- How will the growth of the assembly make an affect
- Geometry effects
- Spillage
- Adhesive properties
 - Pot life
 - Mechanical properties
 - Curing time

In the start different orientations of the jig was considered. Sketches were made where the rail was in the centre and the CFRP-panels were placed in the jig with 45° angle relative to the horizontal plane, see Figure 24. This would make a steady and quick production jig. The primary structure could have been built in two sessions. At the time the possibility of adhesive spillage was held against this solution. But the adhesive later proved to be sluggish and did not show any tendency to spill. There was a clear disadvantage in regard to production. It is more demanding to mill in a 45° angle than in a horizontal plane and the idea was discarded. An idea making production easier was sought. A horizontal jig where the rails could be laid on each side with one CFRP-panel in between them was sketched, see Figure 25

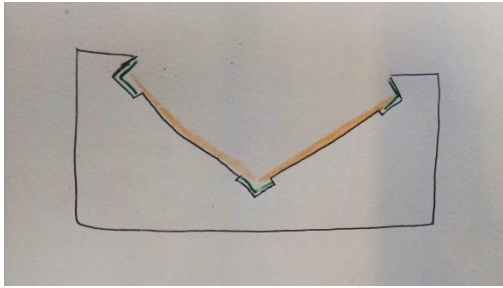


Figure 24: 45° Adhesive jig

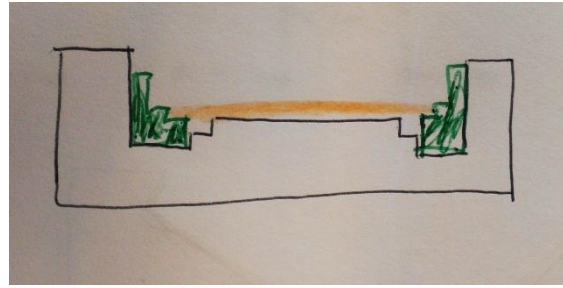


Figure 25: 0° Adhesive jig

The jig with 0° orientation cannot build the structure as fast as the other, but it is a small series production. Also the quality and precision required are considered to be more important than to save time two days. Below is a list describing the design features made to achieve the design requirements.

Ensuring dimensional requirements in X-Y direction.

To obtain the outer dimension of 100.0 mm two slots were milled. The width of the slot is equal to width of the rail. The depth was made to equal be the thickness of the rail. This means the jig has can imbed the rails and the CFRP-panel can be laid on top. In addition external pressure could be applied under the curing. Next to the rail slot a second slot were milled to prevent excessive adhesive to adhere the primary structure to the jig.

Ensuring dimensional requirements in Z direction.

The base plate in the jig is made equal to the length of CFRP-panel, 196 mm. Thus the CFRP-panel should be kept within base plate of the jig. The rails are 31 mm longer than the CFRP-panels and only 15.5 mm should protrude the jig in each end. The extra 15.5 mm are in place to attach the standoff pieces at each end. To keep the CFRP-panel within the base plate and the rail to only protrude 15.5 mm, a distance fixture was made. The fixture constrains the CFRP-panel to stay at the centre, and the rail 15.5 mm from the edge of the base plate, see Figure 27 a).

Adhesion procedure

The adhesion procedure is illustrated in Figure 26. The first step consists of two rails and one CFRP-panel, and this step is repeated a second time. Step three consists of joining the two previous with one CFRP-panel. Step four consists of adding the last of the four CFRP-panels.

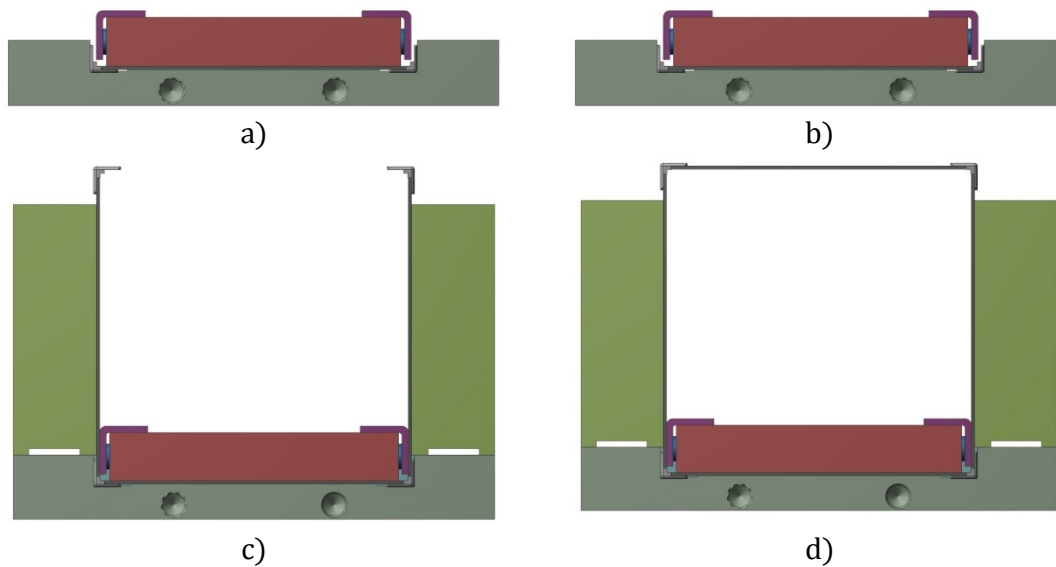


Figure 26: Adhesion sequence

Alignment

Alignment is essential in order to get all sides within the dimensional requirements. When the rails were laid in their slots, see Figure 27 c), a shadow was seen between the rail and the jig. This indicates incomplete contact. To rectify this, thin plates were laid between the top plate and the rail. In Figure 27 b) they can be seen laid on top of the jig. These plates were set with set screws to apply pressure on the thin plate to align the rail parallel with the base plate. That is sufficient for step 1 and 2, but in step 3 and 4 the CFRP-panels can incline due to the width of the panel. Therefore two support walls were made. The walls, light green in Figure 26, are made 1 mm wider than the base plate to allow for the thickness of the rail. To ensure the walls are aligned, two guiding pins per wall were used. The base plate has two holes which are broached to be 0.01 mm larger in diameter than the pins in the walls. To ensure that the walls were perpendicular to the baseplate they were milled with a nifty technique. First the centre of the wall was milled and one strip was left at each side. Then the strips was milled with a mill wider than the strip to ensure no exces-

Primary structure

sive material could unalign it. The white gap in Figure 26 c) illustrates this. When in use, it was planned to utilize clamps to avoid inclination towards centre.

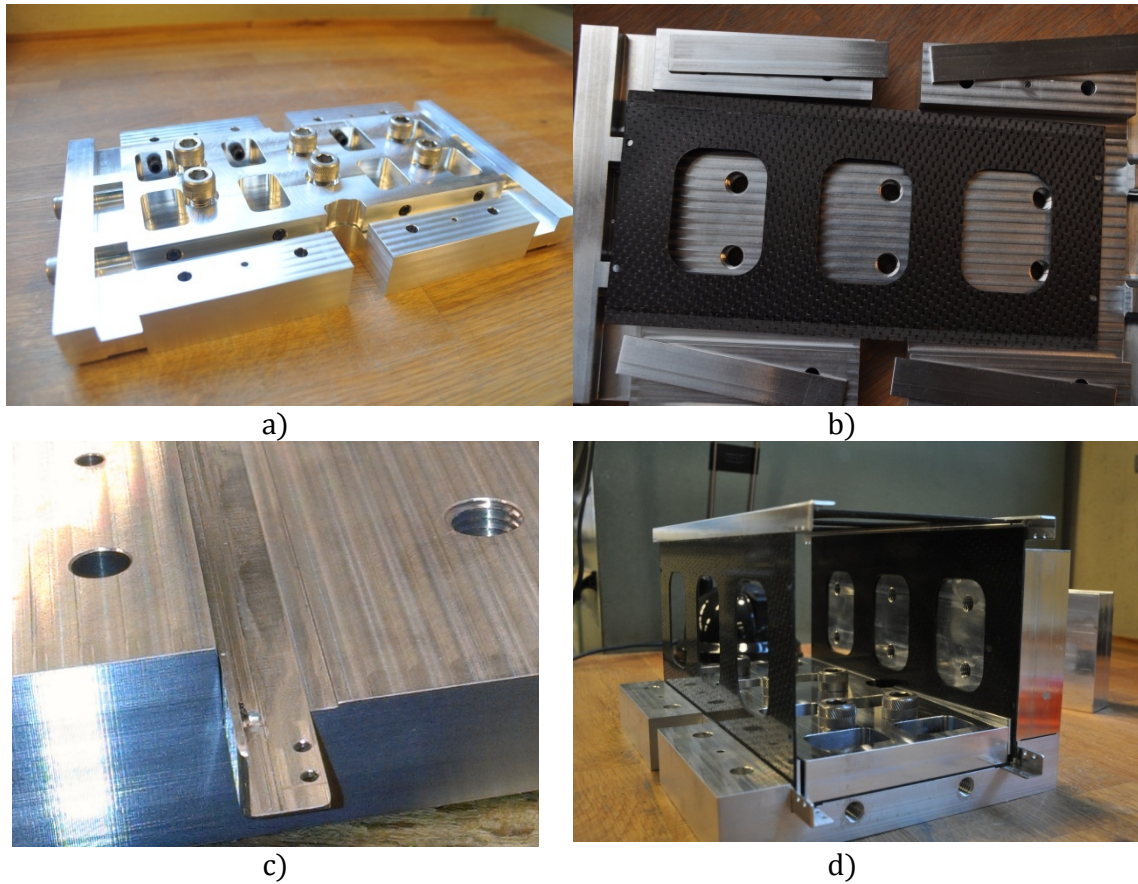


Figure 27: Adhesive jig with different configurations

Adhesive

There are several factors which are important in order to obtain the best mechanical properties of the adhesive. The adhesive layer thickness should be within the range of 0.05 – 0.10 mm, pressure should be applied while curing, and it should cure under elevated temperatures [6]. The fact that it should be under pressure while a certain layer thickness should be maintained is a paradox difficult to overcome. Therefore it was decided to focus on the layer thickness. There is a difference between the rail and the distance to the CFRP-panel in the jig of 0.10 mm. When the adhesive is applied on the rail, the volume of adhesive is larger than the volume acquired. The applied pressure evens out the adhesive with the top plate. There are 8 screws to keep the top plate in place. The mechanical strength of the adhesive varies

Primary structure

in relation to curing temperature. Higher temperature yields higher lap shear strength, LSS, values. Since the jig and rail is made out of aluminium with a large coefficient of thermal expansion, CTE and the CFRP-panel with a smaller CTE, it could not be placed in an oven for curing. For a tension load case it could be beneficial to cure aluminium to CFRP and gain residual compressive stress, but not for a compressive stress state. The jig would most likely need to be designed different in order to be put in an oven for curing. A complex finite element analysis, FEA, would have to be performed to design the jig. Another reason for not designing a jig to compensate for the CTE was the primary structure would not need the extra strength.

3.4. Prototyping primary structure

It is of interest to the NUTS project to have a mechanical model. A mechanical model will be used to see if everything that will be stored inside it will fit. It is made to see if the processes with producing the components are done with satisfying precision. This will be verified if the prototype will be within specifications given in the CDS.

Goals with prototype

- Gain experience with the adhesive
- Verify the adhesive jig
- Learn adhesive procedure
- Make a mechanical model
- Measure the dimensions of the mechanical model

3.4.1. Materials

Araldite AV 138M with hardener HV 998

Araldite AV138M with hardener HV 998 is a product from Huntsman. This two component epoxy adhesive has properties suitable for NUTS. It is thixotropic, gap filling paste, low out gassing, room temperature curing and good mechanical properties in the temperature range - 60° C to 100° C. The out gassing properties of the adhesive is below requirement given in CDS which is important to NUTS, also that it is gap filling, meaning that there will be few air bubbles which can expand in vacuum and ruin the bonding. This makes it suitable adhesive for this project [6].

Aluminium 6082 T6

Primary structure

In this prototype the aluminium rails were produced in the stock aluminium available at the workshop at IET. The stock aluminium is 6082. For the flight model, 7075 T6 will be used. The 7075 T6 has higher yield strength and is self-hardening in room temperature and is widely used in aerospace applications.

Anodizing theory

Anodizing is an oxidation process. Aluminium is the anode, and placed in an electrolyte. The electrolyte has a current running and an oxidation layer can occur. In the process two layers are formed. First an extremely thin layer is formed and then an outer thicker porous layer. The inner layer is called barrier layer. This layer will have a strong bond to aluminium and will practically be insoluble, moreover it will virtually be a non-conductive film on the anode. The barrier film will grow until the layer thickness prevents the current to reach the anode.

The outer porous layer is formed by local dissolution of the film. These small holes are the start of pores. These pores are wide enough for current to reach the anode and the reaction can continue. With continued growth of the film the resistance increases and the growth gradually slows down. The film growth ends when it's equal to the rate of dissolution of the film in the electrolyte. The barrier film thickness strongly depends on operating conditions and the electrolyte. To achieve maximum thickness it is important with high anodize current densities, low electrolyte temperature and low acid concentration. The film dissolution is favoured by low currents, high temperature and high acid concentration.

Hard anodization is a variant of anodization where the layer thickness is above 25 μm , and a general hard anodization is 50 μm . Hard anodization is generally achieved with temperatures below -5°C , high current densities and special electrolytes. This enables the layer to become up to 200 μm . The change in operation conditions affects the diameter of the pores and the density of them [4]. Horsens Hai in Denmark provides hard anodization.

HexPly® 6376C-905-36%

HexPly® 6376C-905-36% is a high strength woven carbon pre impregnated epoxy composite material, pre-preg, which was given as courtesy by Kongsberg Aerospace. The material original has a density of 1.612 g/cm^3 , but with the method used in

Primary structure

this project it has slightly higher density, 1656 g/cm^3 . This is due to the curing process which forces epoxy out of the composite yielding a higher fibre/epoxy ratio see Appendix 1.

HexPly datasheet gives a compressive strength of 920 MPa, a tensile modulus of 67 GPa and an interlaminar shear strength of 83 MPa [7]. These values are not guaranteed by Hexcel if storage time has expired, which it has in this case. The resin in the pre-preg is self-curing which results in a less viscous resin. Reduced resin viscosity yields lesser wetting and a lesser material.

The material has been tested by NTNU Revolve project and produced these results: 90/0/S tensile test: $E_1=E_2=42 \text{ GPa}$, Poisson 1-2=0.068, $\sigma_{\text{uts}}=800 \text{ MPa}$, 45/45/S tensile test: shear module 1-2= 1500 MPa, $\sigma_{\text{uts}}:40 \text{ MPa}$.

To achieve the best possible mechanical properties the manufacturer's guidelines have to be followed. This involves debulking, heat treatment and autoclave. Debulking is the process of removing air, in this case by applying vacuum. Debulking increases the density of the composite. Heat treatment is done to cure the matrix and this pre-preg does have a heat-up rate of $2^\circ\text{-}5^\circ \text{ C/ min.}$ and to be held for 2 hours at 175° C . The recommended pressure in the autoclave is 0.7 MPa. The cool-down rate is reverse to the heat up rate.

3.4.2. Manufacturing CFRP

Layup

The LV does not specify the orientation of the deployer. This uncertainty influences the choice of pre-preg and layup of the composite. To be best prepared a woven pre-preg with [0/90] orientation was chosen. The pre-preg is sold on rolls with the same orientation. If sheets are cut with a 45° angle it is the same as a [-45/45] orientation, see Figure 28. This is utilized in this layup. Four sheets are used in this stacking order [0/90, -45/45, -45/45, 0/90], see Figure 29. The machine utilized to manufacture the pre-preg has limitation on size of the mould, 310 x 310 mm. Each CFRP-panel has the dimension of 93 x 196 mm, width and height respectively. Each sheet cut is approximately 220 x 220 mm. This means the manufacture process has to be repeated in order to have four panels.

Primary structure

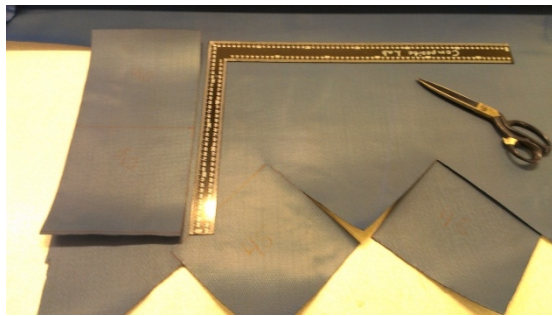


Figure 28: Cutting pre-preg

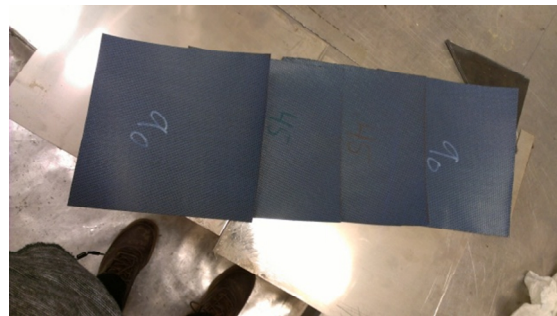


Figure 29: Pre-preg layup

The next step after cutting the pre-preg sheets is debulking. Debulking is a process to remove air between the sheets and thus increasing the density of the composite. Figure 30 show the lay-up schematized, and Figure 31 how it was done.

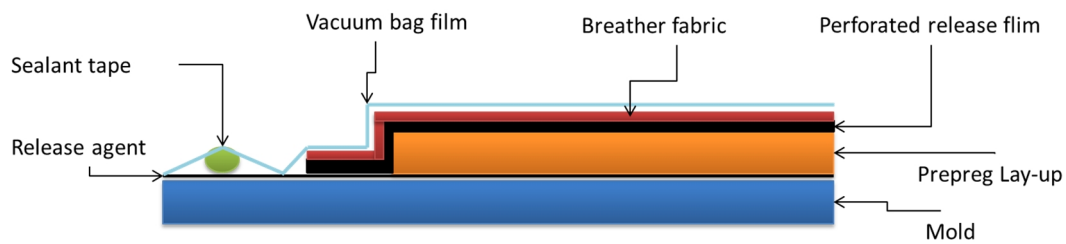
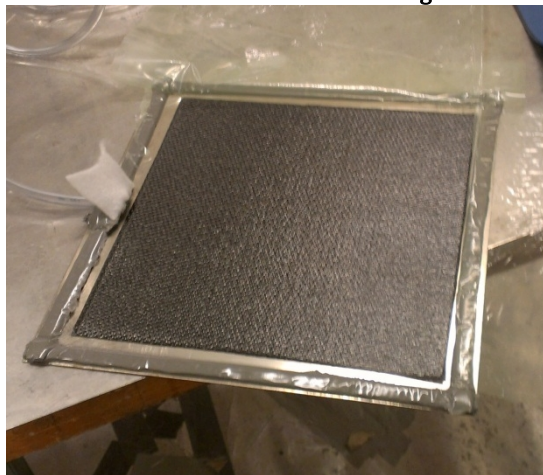
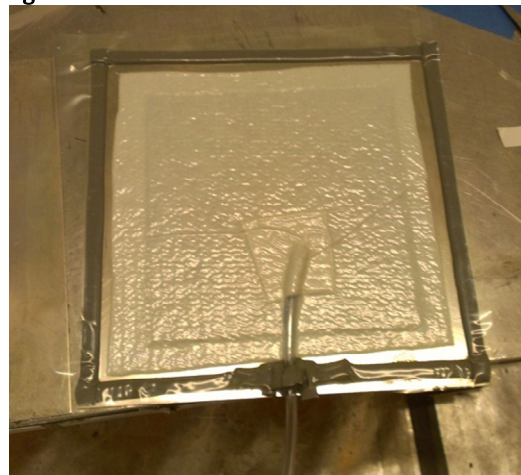


Figure 30: Debulking schematic



a)



b)

Figure 31: Debulking

Mould preparations

Before the release agent can be applied the moulds have to be cleansed with acetone. The whole process can be described as followed:

Primary structure

1. Thoroughly cleanse moulds with acetone
2. Apply release agent, 1 layer of Frekote 44-NC is sufficient
3. Apply sealant tape around edges of mould
4. Apply pre-preg in predefined order
5. Apply perforated film
6. Apply breather
7. Insert vacuum tube
8. Apply vacuum bag film
9. Turn on vacuum pump and seal
10. Leave under vacuum for minimum 15 minutes

Compression moulding

For the purpose of making the side panels compression moulding was used, see Figure 32. The machine consists of two planar faces which can be pressed together with a maximum force of 150 kN, and it also provide heating and cooling control. The space within is limited to approximately 310 x 310 mm, thus limiting the production to two panels per go. The reason for using this machine is because there is no suitable autoclave at NTNU, and compression moulding is. The compression mould could be seen as a substitute to an autoclave for plane sheets since it apply uniformly distributed pressure on two sides.

In a previous study the CFRP thickness was decided to be equal to the minimal thickness that could be milled in the slot of the rail, which was 1.0 mm. This was when the rail was designed to have a slot for the CFRP-panel. In order to not change the dimension of all internal components the thickness was maintained. The ply thickness of HexPly 6376C-905-36% is 0.281 mm with a resin content of 36% [7], and four plies results in a total thickness of 1.124 mm. Usually pre-preg is ordered to coincide with the design thickness or the designed according to the ply thickness. Compression moulding can be convenient when making panels with a certain thickness. The plies yield 1.124 mm and the goal is 1.00 mm thickness. To obtain the goal, shims are places around the plies. The pressure from the compression mould is applied instantly, but the thickness is not obtained before the temperature has increased the viscosity of the resin, thus squeezing it out of the laminate until the press meets the 1 mm shims.

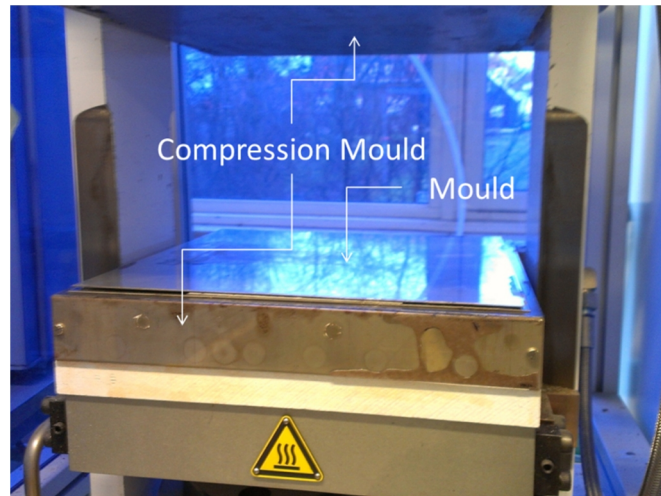


Figure 32: Compression mould and mould

The machine was set to a force of 100 kN and the temperature was manually adjusted with a heat-up rate of 5° C/min up to 175° C according to Hexcel. The maximum cycle time for the machine is on is 100 minutes. The curing time for the prepreg is 120 minutes. Therefore it is important to manually reset the timer before it powers down, and complete the last 20 minutes. The cooling was manually adjusted and with the lowest flow rate the temperature decreased twice the recommended 2-5° C per min. No visible twisting or other damages was observed due to the rapid cooling.

Machining pre-preg

The pre-preg sheets were 220 x 220 mm and thus needed to be machined to obtain wanted dimensions of 93 x 196 mm. IET has a computer numerical control, CNC, milling machine for milling PCB-cards, see Figure 32. The pre-preg sheet is unfit for the standard constraints which the mill provides. Therefore duct tape is utilized as constraint, with a good result. The mill was set with a spindle speed of 30 000 rpm with a feed rate of 2 mm/s. These operation parameters yield a fine cut where the rest material is turned to dust. To ensure the whole panel is milled with precision, cut-outs is programmed. The cut-outs needed to be cut off and grinded down after the milling operation.

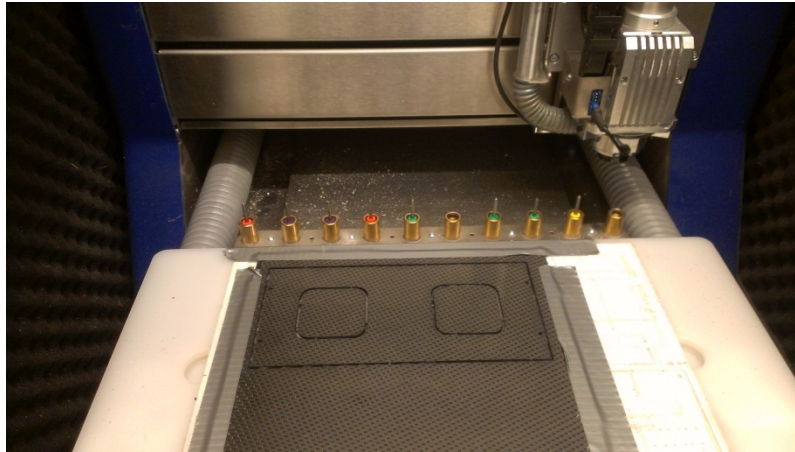


Figure 33: Machining CFRP-panel

3.4.3. Assembly procedure

Preparation

Below is a list of equipment needed for the assembly. This is important to have ready before the adhesive and hardener is mixed. The pot life, which is the time available after mixing the adhesive, is 35 minutes. After the adhesive was mixed, 30 minutes were used in the each of the four adhesive sessions.

- Ball hex keys, M4, M6, M8
- Wipes
- Acetone
- Syringes, one per side
- Marking vernier calliper
- Clamps, four
- Abrasive
- Mixing pot for the adhesive
- Mass
- Spatula
- Nitrile Gloves
- Safety glasses
- Adhesive and hardener

Pre-treatment is a necessity in order to achieve a good result, meaning a solid bond between the materials. First the inside of the two rails were grinded with abrasive-coated paper, see Figure 34 a). Then the panel was masked to ensure that only 5 mm

Primary structure

was grinded. 5 mm is the width of the contact area on the inside of the rail, see Figure 34 b).

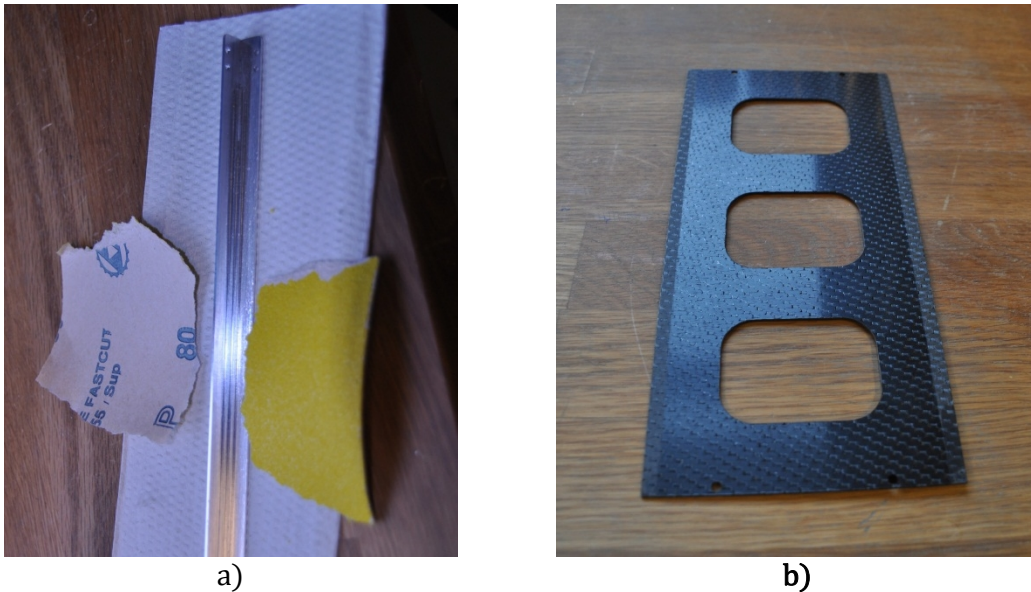


Figure 34: Abrasive pre-treatment

After grinding, the parts and the jig had to be thoroughly cleansed with acetone. To obtain the best surface, each wipe was used only once to not contaminate the surface. After changing gloves the rails were placed in the jig and the jig were partially assembled.

Adhesive procedure

The mix ratio in weight is 10 to 4 in resin and hardener content respectively, see Figure 35 and Figure 36. For the purpose of mixing them a new and cleansed flat head screw driver was used. This was easy to clean and reusable. When thoroughly mixed the adhesive were put in a syringe. A syringe was used in order to control the amount of adhesive. The recommended layer thickness is 0.05 – 0.10 mm and with an area of 5.0 x 196 mm, it yields a total of 98 mm³ which is 0.098 ml.

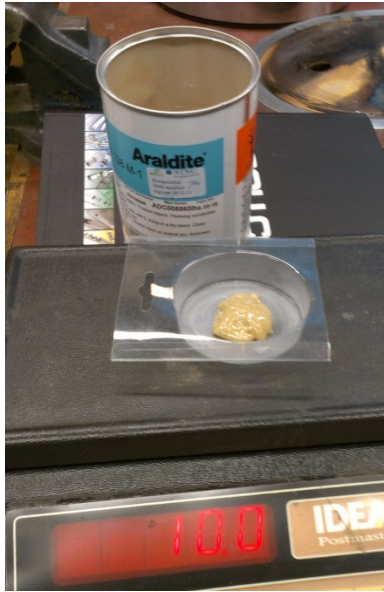


Figure 35: 10 g of resin

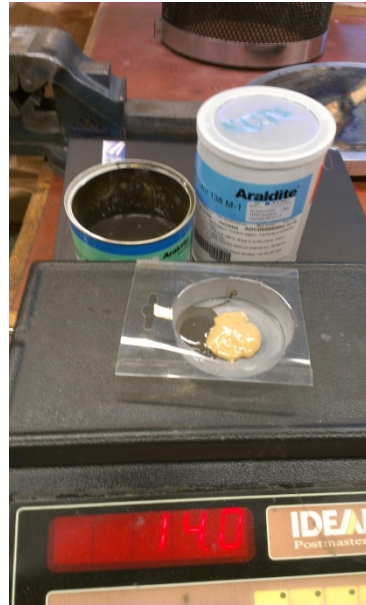


Figure 36: 4 g of hardener

When the adhesive were in the syringe the small needle made it hard to apply, but the high viscosity helped to not apply to much and also prevented spillage when moving the syringe. After the adhesive was applied, it was distributed as even as possible, see Figure 37. It is important to apply adhesive in all contact surfaces between CFRP and aluminium to obtain a galvanic barrier. After the adhesive were applied, the jig was assembled and left to cure for a minimum of 24 hours, see Figure 38.

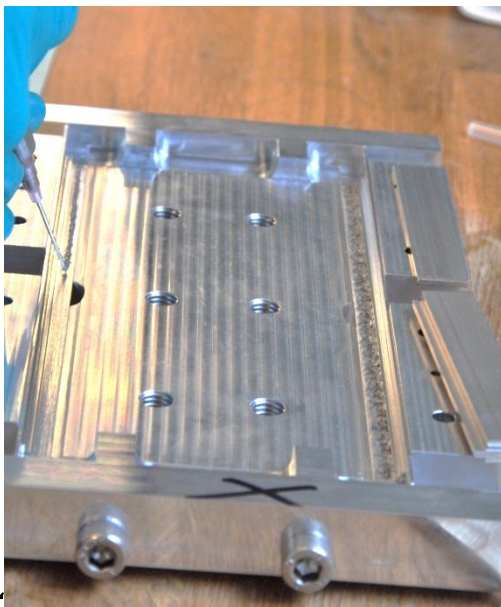


Figure 37: Applying adhesive

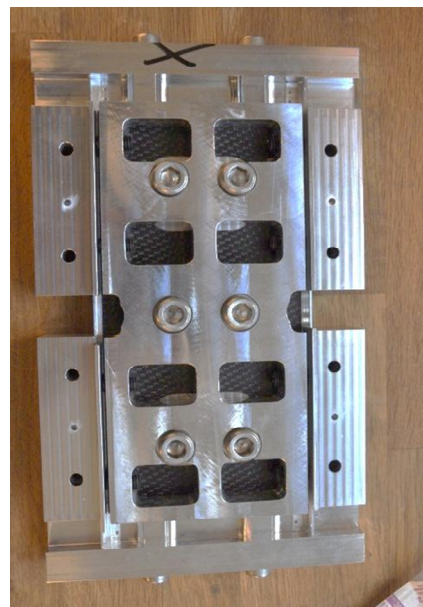


Figure 38: Jig assembled for 1 side

3.4.4. Evaluation of the Primary structure

The width of the satellite was measured on eight points, on top and bottom of each face. The results can be seen in Table 1 and Appendix 1

Table 1: X-Y dimensions

	Face 1 [mm]	Face 2 [mm]	Face 3 [mm]	Face 4 [mm]
Top	100.01	99.98	99.98	99.98
Bottom	99.99	99.98	99.98	99.98

The length of each rail was measured, see Table 2

Table 2: Z dimensions

	Rail 1 [mm]	Rail 2 [mm]	Rail 3 [mm]	Rail 4 [mm]
Z length	226.95	226.98	227.02	226.99

The dimensional requirements are 100.0 ± 0.1 mm in X-Y direction, and 227.0 ± 0.1 in the Z direction. With the results from the prototype it can be concluded that the jig and manufacture process can be utilized in the production for the flight model.

Chapter 4

4 ANTENNA MODULE ASSEMBLY

The antenna module assembly consists of radios, antenna elements and solar panels see Figure 39. This section will go in depth in the development of the antenna module, burn-off mechanism, prototyping, manufacturing and testing of different features.

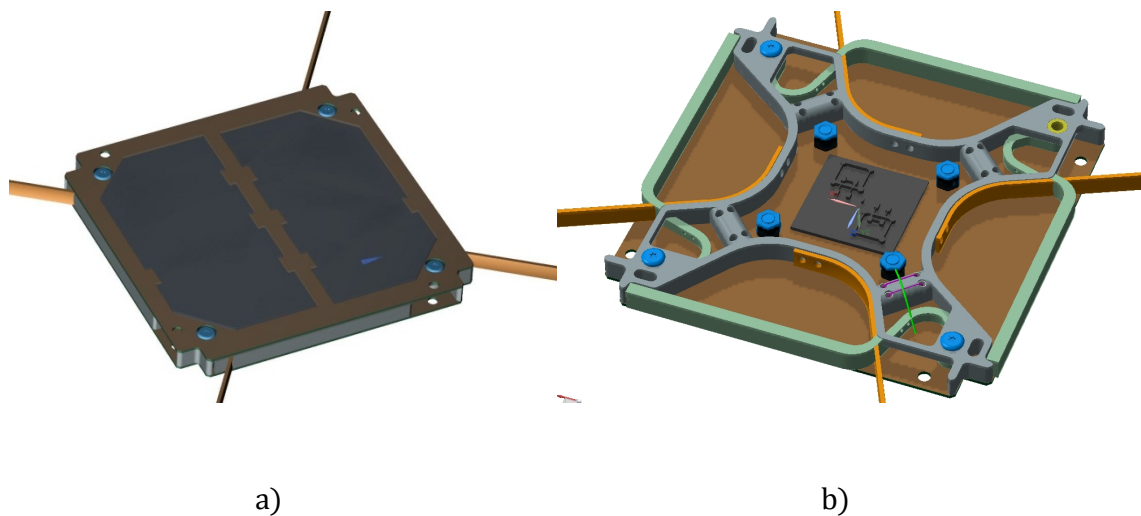


Figure 39: Antenna module assembly

4.1. Design of antenna module

The antenna elements for the radio are for most satellites longer than the satellites itself. Therefore there they have to be stored in or around the satellite during launch. This has yielded many different solutions in how to store and launch the antennas. Many satellites are inspired by the tape spring. Some have sent satellites into space with of the shelf tape spring such as PhoneSat by NASA[8]. The tape

Antenna module assembly

spring has characteristics which is very valuable for a designer. It is commonly made out of cold formed spring steel. This can be bent around small radiuses without plastic deformation, it has acceptable electrical properties, it will gain its original form and it can be bought in all hardware stores. For these reasons, the first prototypes of the antenna module for NUTS was made of tape spring, and later designs evolved from this spring.

In the next section an evaluation of previous antenna module designs in NUTS are presented. The evaluation is based on experience learned, the pilot project and a study by Max Rödelsperger on "*Lightweight design of subsystems for satellite application*" [9]. In Figure 40 the different ideas around coiling antennas are presented. The first design in NUTS were coiling around the height in X-Z and Y-Z plane, see Figure 40 a), and another where it was coiled around the sides in X-Y plane, Figure 40 b) [9].

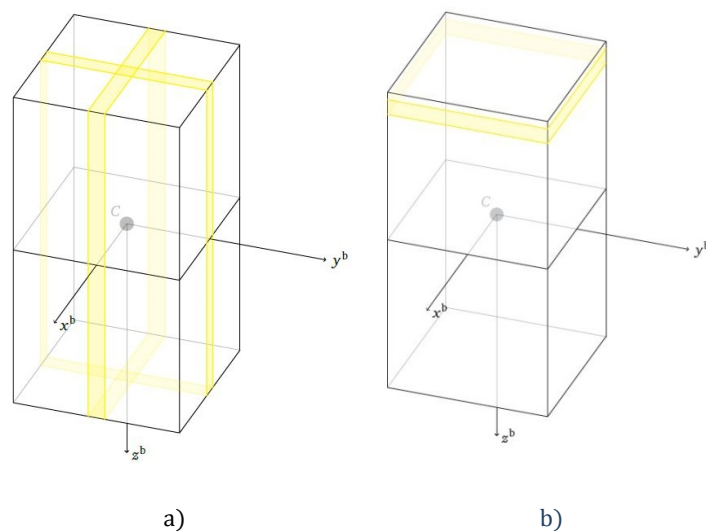


Figure 40: Antenna configurations

Evaluation of antenna configuration around X-Y plane

The idea was to attach the four antenna elements between two PCB-cars on the top of the satellite. The antenna should be bent around the edges between the rails. This resulted in a total height less than 3 mm and thus being a volume efficient solution see, Figure 41 [10]. To use the space between the rails does have its advantages and disadvantages. In the ISIPOD there are four envelopes between the rails with the depth of 9.5 mm and each satellite could utilize 9 mm of them [11]. The use this

Antenna module assembly

space is very volume efficient. Wrapping the antennas in this area also involves a significant risk of damaging the side solar panels under launch and transport. Any scratches on the solar panels would reduce their efficiency. Other concerns are constraining them, releasing them, and once attached it would inhibit access for maintenance. Special edges around the satellite would have to be made in order to increase the bending radius to prevent the antenna elements to exceed their yield strength[9]. If the edges were made, the volume efficiency would diminish since the edges would inevitably utilize the volume inside the satellite. Therefore this solution was not pursued further.

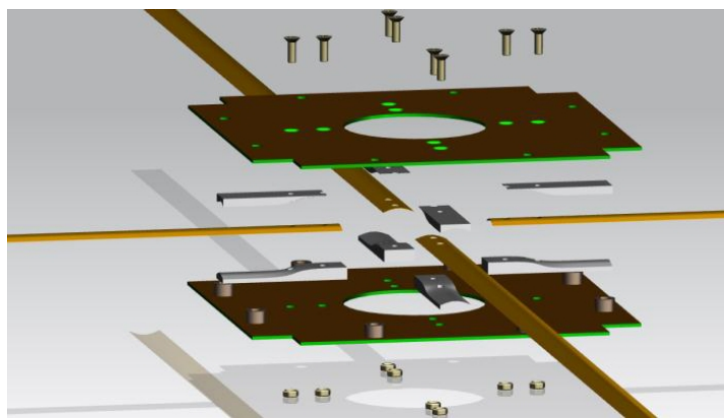


Figure 41: X-Y plane configuration

Evaluation of antenna configuration around Z-axis

The wrapping around the Z-axis would not inflict damage to the solar panels. This proposed solution had a total height of 5 mm. In order to wrap around the Z-axis there had to be an indentation in the rail or the standoff, in this case the standoff. The dimensional requirements of 100.0 ± 0.1 mm around the rail cannot be exceeded (since they would be in contact with rail in deployer). This was solved with a special standoff piece, see Figure 42 [10]. The more the standoff piece would need to be retracted, the less structural sound the solution be. Since the bearing structure is in the corners. This consists of the rails in the primary structure and the braces in the secondary structure. If the standoff piece were placed further away from the corner the PCB- card would need to be sufficiently solid to transfer forces. The proposed standoff pieces were not drawn in much and resulting in a small radius, R4.25.

Antenna module assembly

In this design, the width of the element was planned to be 3 mm where it is constrained and have a transition to 5 mm further away from the standoff, see Figure 42. This means the most vulnerable part of the antenna element would be the structural weakest. Two of the antenna elements have a length of 171.5 mm while two have a length of 517.5 mm. Wrapping these in the same direction would result in several layers of overlapping antennas. Constraining overlapping antennas proved difficult, even to wrap them before constraining them were difficult. Another challenge was that the antenna elements are very volatile and they won't be straight after being bent around the corner, they would bulk and needed to be drawn more toward the centre of the satellite. Still the main concern was how to attachment the antennas and how to release them.

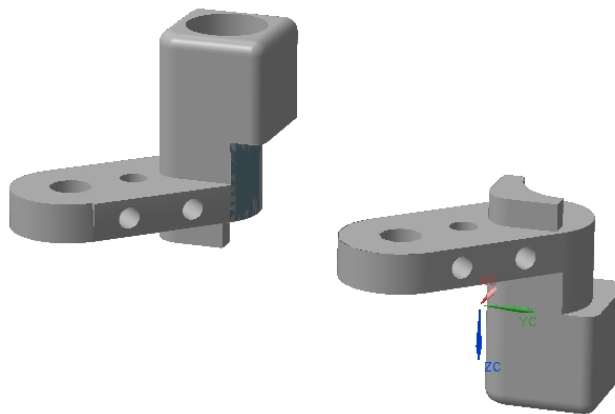


Figure 42: Standoff piece wrapping around Z-axis

The wrapping around Z axis was prototyped in a combination with a science fair. The evaluation and prototype of the antenna module designs yielded insight and experience. This was discussed with the NUTS team and a new solution was desired. The design process was started in the pilot project, and preliminary design requirements were put down. First the focus was on developing the idea, not to implement all components. It was not possible to implement all components since the radios and release mechanism was not developed. The design requirements evolved along with the project progression.

Design requirements

- Two sets of dipole antennas
- Not affect the rail and standoff design

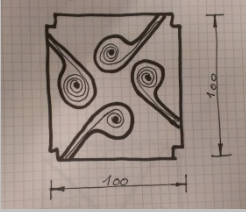
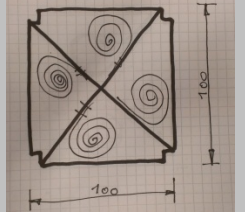
Antenna module assembly

- The antennas must be pairwise aligned through centre
- The antennas must be securely constrained
- Modular design
- Low mass and low volume
- Design for multiple tests
- Inclusion of a release mechanism
- Redundancy

Antenna module

A solution where the antenna elements where stored inside the satellite was desired in order to prevent any contact with POD. This resulted in coiled antenna elements. The stored potential energy would then be exploited to unfold the antenna elements. In Table 3 an evaluation of two solutions for coiled antennas are evaluated.

Table 3: Antenna module

Solution	Reverse tape measure	Unfolding of spring
Sketch		
How it works	Unlike a regular tape measure which rolls up, when released this would roll out, or deploy the antenna element.	The antenna element could be coiled up and hindered from unfolding by restricting the space it's in.
Constraint	The reverse tape measure solution would need a housing which would constrain translation in the X-Y plane and allow rotation around the Z-axis.	Spring/gate solution could be constrained by utilizing a screw connection through the antenna element into the antenna module
Release mechanism	A burn off thread could be burned off by electric resistance wire. This could be used in a friction /spring, gate, tie in.	Releasing the antenna element by opening a gate. The gate could be kept close by a burn off thread.
Advantages	-The area used could potentially be small -The housing would be all that would be needed	-Simple, yet reliable -Would not need many mechanisms
Disadvantages	-The height of the structure	-Does need a antenna mod-

Antenna module assembly

	would be taller -Strict friction demands inside the housing, and in the bearing in the rotating axis -Prevent it from coiling up in the housing and prevent uncoiling -Would need a housing release design	ule and gate -Antenna element could not unfold due to friction
Conclusion	More complex mechanisms and uncertainty around friction in a housing this solution was not chosen.	Easier mechanisms and less concern about friction, therefore this solution was chosen.

Design of unfolding of spring

To be able utilize the design presented as unfolding of spring, a hinge mechanism or similar needed to be implemented. Different hinges and gates were investigated while the assembly order was kept in mind. The antenna module together with top solar cell panel is planned to be placed on +Z face. The secondary structure has a ring truss on top and bottom to assemble the corner braces. The truss has holes for screw joints. The antenna module assembly utilize these holes for constraints. These screws are only used in the final assembly of antenna module assembly to the satellite. In order to wrap the antenna elements up and constrain them another screw was needed. This second screw, located behind the rail and standoff, see Figure 43 b), work as rotation point for the hinge mechanism. It fastens the antenna module to the bottom PCB-card and not to the secondary structure. This makes it possible to have an operational antenna module separate from the satellite and solar cell module.

To prevent axial from loading increasing the friction on the hinge a bushing is inserted. The bushing is designed to have a sliding clearance of g6/H7 for shaft and hole respectively. The hole can be between 5.00 and 5.12 and the shaft between 4.988 – 4.996 mm [12]. The antenna module works in pair with the gate to serve as a hinge. Therefore clearance was needed here as well. This is not critical as the bushing and is set to be 0.1 mm.

Antenna module assembly

These screws for assembly constraint inhibit free rotation of the gate. Therefore the gate has a curvature which allows it to rotate around the assembly fastening screw. In the curve there are two holes which are there to keep the gate closed. A thread is planned to be tied in the gate and when in orbit burnt off. Then the element will push open the gate. See chapter 4.2 for more details around burn off design.

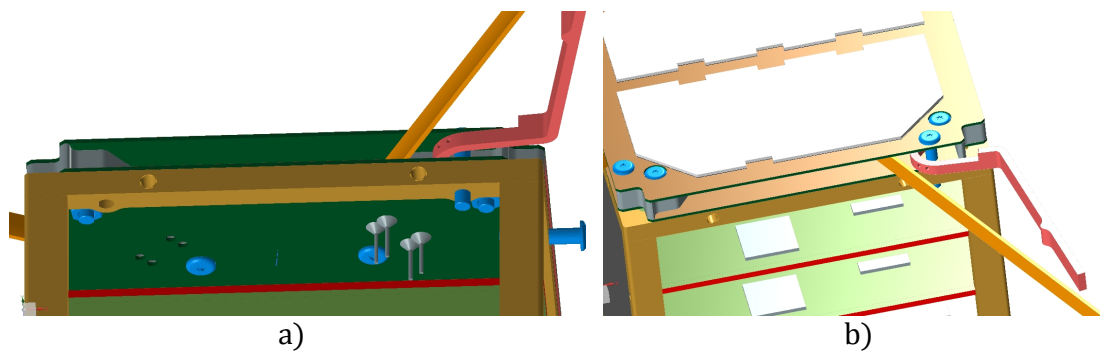


Figure 43: Antenna module fastened to secondary structure

The space available for the antenna element has been changed many times. First the space was too spacious since the dimensions of burn off and radio was unknown. It was also made large to prevent too many turns of coiling, since it was thought this could prevent a successful release of antenna element. The hypothesis proved to be not true. The shorter element proved to not open the gate as often when space was too large. Therefore different sizes have been tested.

The antenna module has been designed so the antenna element in pairs will be in a straight line through centre on both sides, see Figure 44. When the antenna module is loaded with antenna elements the solar panel can be laid on top and connected to the backplane and screwed to the secondary structure. This makes it a modular design.

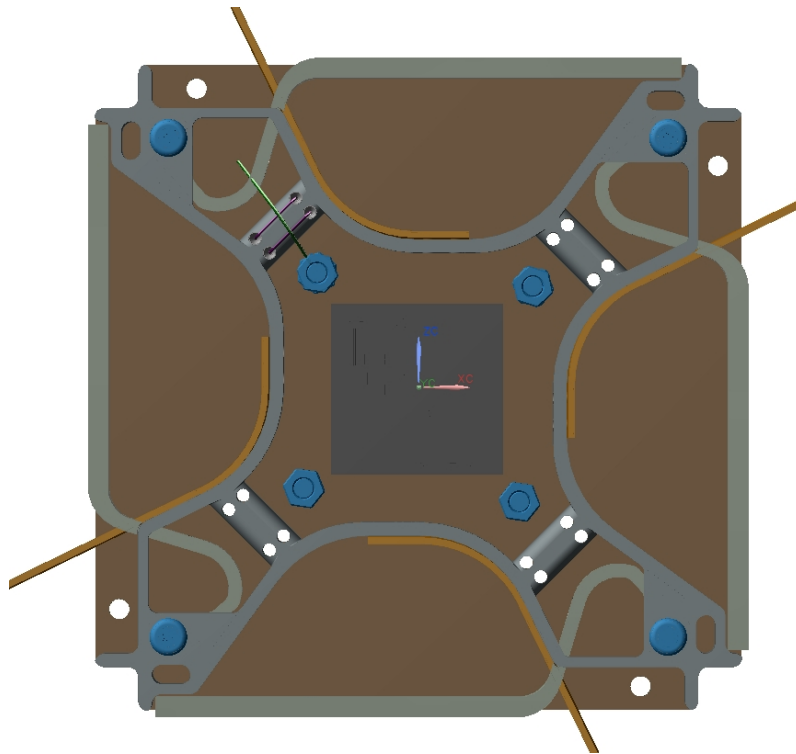


Figure 44: Antenna module v09 prototype

4.2. Design of antenna module release mechanism

The gate in the antenna module is designed to be kept closed with a thread. The thread is referred to as burn off thread. The release mechanism is a two-step process. First the burn off thread has to be burnt off. This allows the antenna elements to open the gates. Then the stored energy in the antenna element needs to open the gate. In this section the focus is on how the design of the burn of thread is, not how the antenna element opens the gate.

Electrical design requirements

- Voltage of 3.3 V
- Currents under 1.0 A

Design requirements

- Functional
- Implementable solution
- Redundant
- Easy to reset and retest

Antenna module assembly

The first decision is the number of burn off point. It can either be one burn off point for each gate, one for each antenna pair or one for all elements. The basic solutions are sketched, see Figure 45.

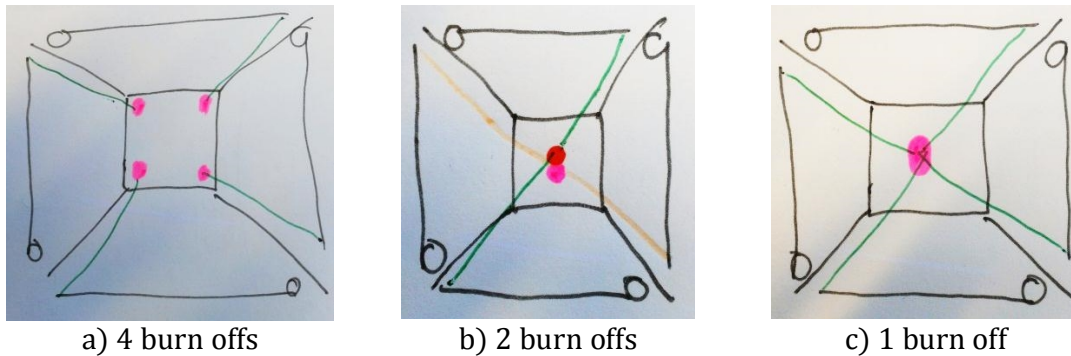


Figure 45: Burn off points

The solutions with one or two burn off points are placed in the centre. To allow a centric placement would limit the space for radios and radio components. The thread could also be tangled up in radio components. The burn off points could have been placed on other locations by the help of pulleys. This would make the system more complex and use more space. Therefore a redundancy calculation was done to see how the number of burn off points affected the chance to get contact with earth. Each burn off point had two burn offs. Three cases were examined. The burn off success rate is the ability for one burn off point to burn off the thread. They are set as independent events, since they have separate circuits. The VHF radio is dependent that its two antenna elements are unfolded to work, but independent to the UHF to get contact with earth. In Figure 46 the success of contact with earth is illustrated vs. the rate of burn off success, see Appendix 1. It can be seen that 2 burn off points will get contact with earth with lower burn off success rate.

It can also be seen that, for a burn off success rate above 80% the 2 and 4 burn off points yields the rate for contact with earth. A burn off success rate below 80 % is not considered a reliable solution. With this basis it was decided to develop the solution with four burn off points.

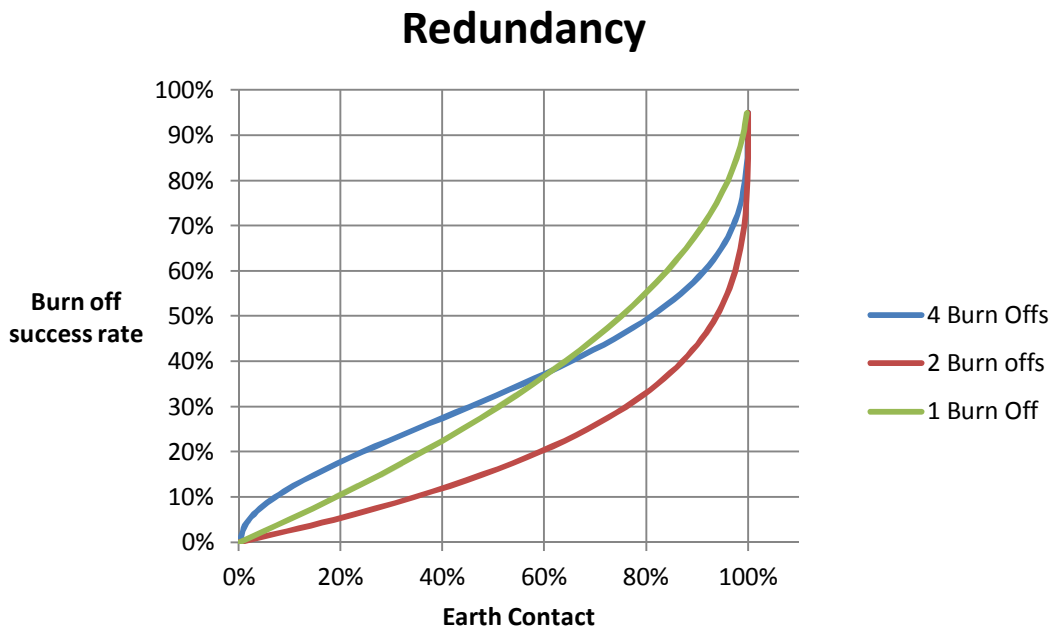


Figure 46: Probability of earth contact vs. burn off success rate

The burn off thread needs to come in contact with something that could elevate the temperature quickly, and also ensure contact between source of heat and burn of thread. Different solutions were drawn, see Figure 47. The solution needed to fit inside the antenna module assembly with height of 5.1 mm and two separate burn offs per point. In space there is almost 100% vacuum. This implies that convection is non-existing and heat can only be radiated away or by transferring heat in materials.

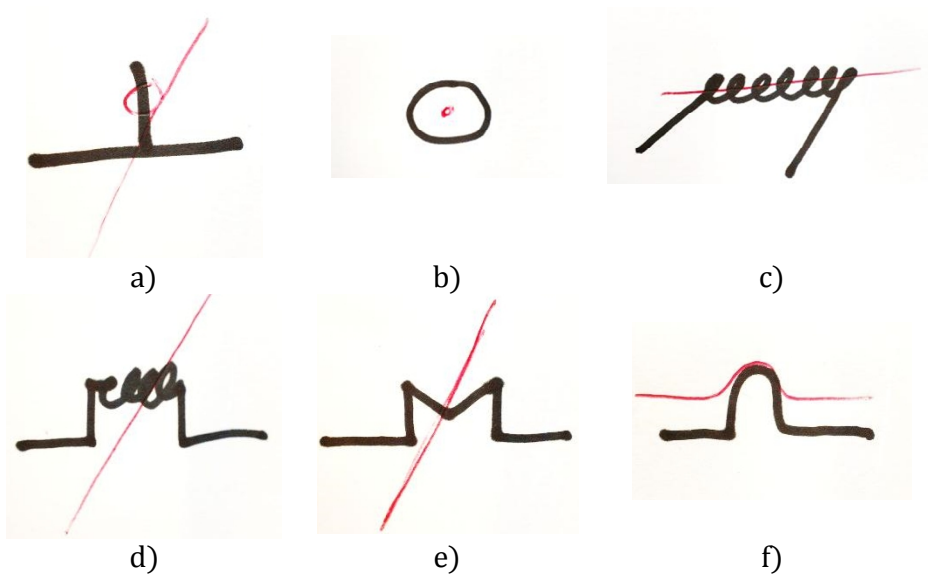


Figure 47: Burn of contact

Table 4: Evaluation of burn off mechanisms

Solution	Description	Review
a)	Treaded around a pole	Either the pole have to be the burn off, meaning it would require a lot of power, or it have to be large enough to implement another heat source.
b)	Thread pulled through a baking oven	This is solely based on radiated heat and thus require a lot of power
c)	The thread pulled through a coiled resistance wire	This solution is either based on radiated heat or that it will be in contact with one of the coils at some point.
d)	A coiled resistance wire drawn across the thread path.	Uncertainty about how it would withstand the vibration during launch. Could be made small and with two burn off points.
e)	The thread could be tightened over an M structure. In the M structure a resistance wire could be implemented	Could be made with two burn off points. Might experience rubbing between the thread and M structure during launch.
f)	Thread pulled over curved structure	Similar but opposite to M structure. Resistance wire would be in contact with the structure.
Conclusion	<ul style="list-style-type: none"> - Solution a) and b) draws too much current or too difficult to implement with regard to available space - Solution c) and d) has too much uncertainty regarding launch and contact between thread and resistance coil. Therefore it was not chosen. - Solution e) and f) are very similar, based on the same principle of forcing the thread to be in contact with the structure. It could be made small with two burn offs in one point. Solution f) is chosen since it won't require a strict angle of the wire over the structure. This can be beneficial when designing the gate. This solution might need heat isolation to prevent the structure to absorb the heat. 	

Since the antenna module has limited height and space available, every feature which can be imbedded in the antenna module is favoured. When built into the antenna module it can be milled out in one operation and prevent assembly of new components. The resistance wire is difficult to solder and was therefore put in a casing. There are four casings for each burn off point with two resistance wires. The

Antenna module assembly

thread is tied in the gate and over the burn off structure and fastened in the nut connection behind, see Figure 48 a). The resistance wires are illustrated with purple and the thread in green, see Figure 48 b). The need of a curved structure is to ensure that it will be in contact with both resistance wires.

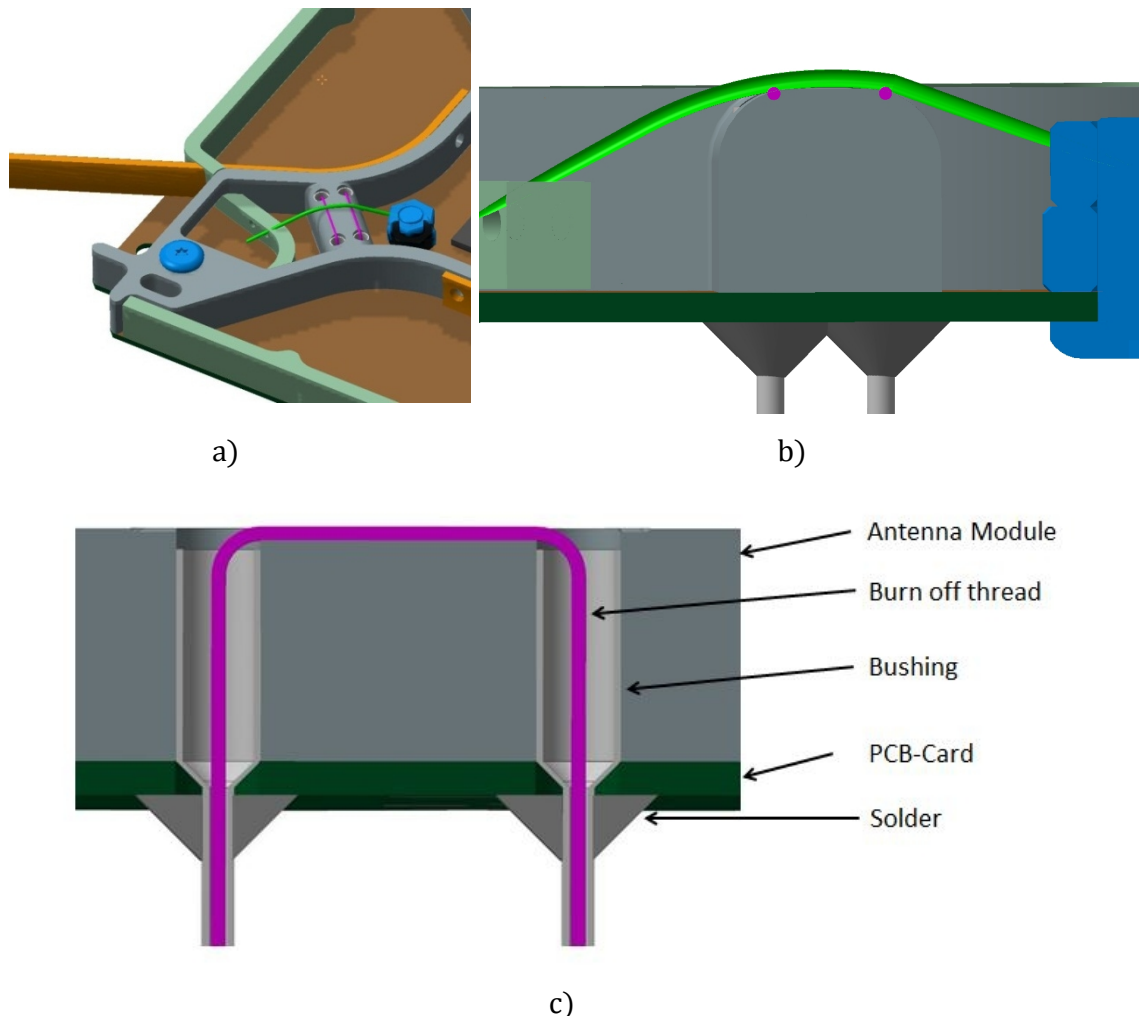


Figure 48: burn off mechanism

The thread which is used is a dyneema fishing line. It is multifilament thread with a thickness of 0.15 mm with 7.9 kg in tension strength. The antenna elements will not generate a force greater than 7.9 kg. The thread will experience vibration and rubbing against resistance wire. Therefore the strongest multifilament fishing line was chosen. The thread has been tested by filed down and an attempt to tear it apart was done without success. Human hand power is

4.3. Antenna element

The antenna element is a significant part of the antenna module assembly. Therefore a chapter has been devoted to this aspect.

Material

Materials for the antennae elements have been evaluated in a previous NUTS study. The materials looked upon were spring steel and beryllium copper. For a spring it is important to have a sufficiently high Young's Modulus to generate momentum for bending, high yield strength to avoid plastic deformation and high electric conductivity.

Table 5: Material properties

Material	Yield Strength [MPa]	Electrical Conductivity [S x 10 ⁶]	Density [g/cm ³]
Spring Steel - AISI 1097 annealed	525	6.9	7.8
BeCu	585	8.7 – 12.2	8.360
BeCu - Heat Treated	1169-1173	8.7 – 12.2	8.360

BeCu was selected because of the higher yield strength and better electrical properties. It has also been used in another satellite in Norway, which could provide material. The higher yield strength reduces the risk of plastic deformation and gives higher safety margins. BeCu can obtain very good mechanical properties with regards to spring mechanisms. This is done by age hardening or precipitation hardening. Age hardening can be done by underaging, overageing or “normal” see Figure 49 [13].

In the process of making BeCu, it is usually annealed and rapidly cooled down, and in this process the beryllium remains in supersaturated solid solution. A heat treatment in the temperature range between 200 and 400° C for over an hour or more will result in precipitation hardening. A beryllium phase called beryllides will precipitate out of solution [10, 14, 15]. For the purpose of antenna elements the heat treatment of minimum three hours at a temperature of 315 ° C would yield the highest yield strength, see Figure 50 [13].

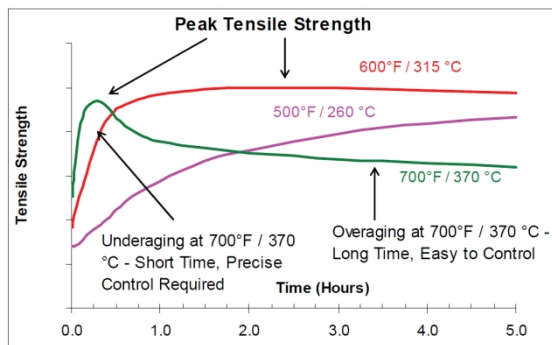


Figure 49: Heat treatment of BeCu, tensile strength

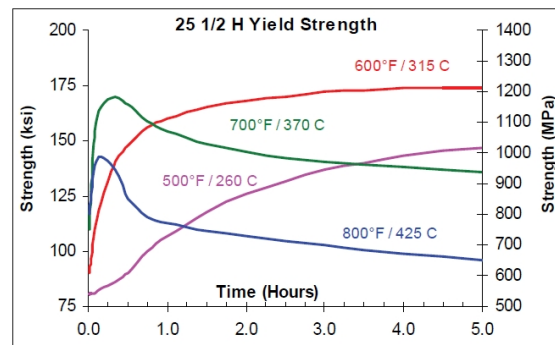


Figure 50: Heat treatment of BeCu, yield strength

Cold forming is a way to plastically form the material. This is done by inducing stress exceeding the yield strength of the material. From material science it is known that some of the deformation induced in the forming process will be elastic deformation. The elastic deformation will return to its original form and is called spring back. This means material going through a forming process with a forming tool with radius of R2 will not obtain this curvature after the process due to spring back.

After the deformation the element will be heat treated and during this process the material will be subjected to age distortion[16]. This is due to residual stresses after the cold forming operation. In this case there will be compressive stresses on the inside and tension on the outer side even though the material is in a state of equilibrium. Heat treatment of beryllium copper will result in a volume contraction which is increased density. According to Le Chatelier's principle the system in equilibrium subjected to change in concentration, in this case volume contraction, the equilibrium will be changed to reduce the effect of the change imposed[17-19]. This means the area in compressive stress will have a larger response to the ageing, meaning the contraction will be relatively larger and the radius will decrease. To sum up the material will first undergo cold forming and the material will experience spring back, increased radius, then it is heat-treated and the radius will decrease.

Theory

The antenna element is a curved rectangular strip of BeCu. The curve increases the spring effect of the strip due to changes of the section modulus. The spring utilizes the potential energy stored in it to uncoil. During testing and prototyping it has been discussed whether it should be coiled with a negative or positive smile. It was questioned if the potential energy stored was different in the two situations. It could eas-

Antenna module assembly

ily be seen the difference in the buckling force required for the two situations. The buckling with a positive smile has the highest buckling resistance. This was then brought to an associate professor at NTNU. He explained that the reasons for the buckling force to be higher one way or the other was due to which part was under compression and tension. When the section is a positive smile and the force is put downwards it is the centre section which is in compression and the outer flanges in tension. The centre is much stronger in compression than the flanges, see Figure 51. That is the explanation of the buckling. When the element is buckled, which it is in all corners, it has the same cross section. This does not increase the potential stored energy because the section is the same for both directions. This means it does not matter which way it is coiled up.

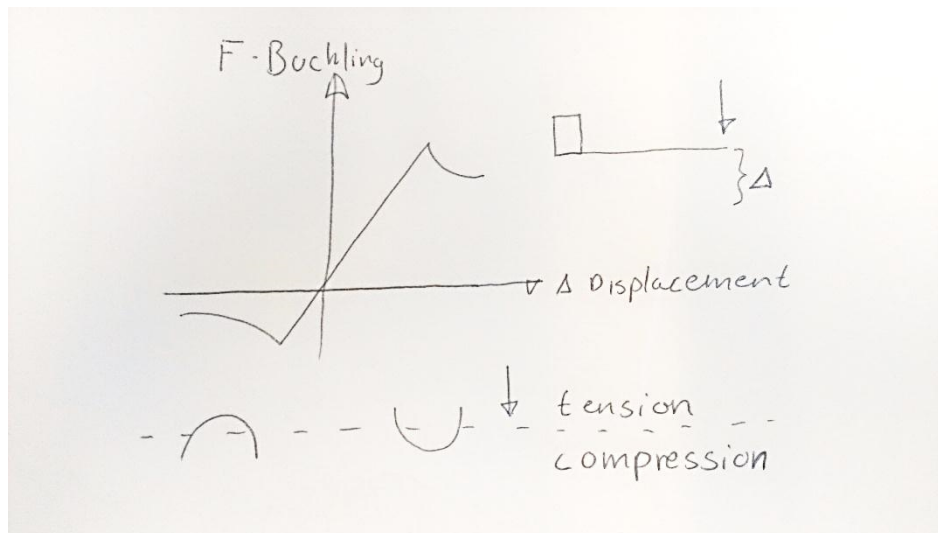


Figure 51: Buckling load in the different directions of the antenna element.

The application of the spring is to have enough stored energy to open the gate when deployed in space. The energy will be stored as the momentum created and the momentum is based on this formula:

Equation 1

$$M = \frac{\varphi EI}{L}$$

Equation 2

$$I_x = \frac{\pi}{8} (a_1 b_1^3 - a_2 b_2^3) = \frac{\pi}{8} (a_1 b_1^3 - (a_1 - 1)(b_1 - t)^3)$$

[20]

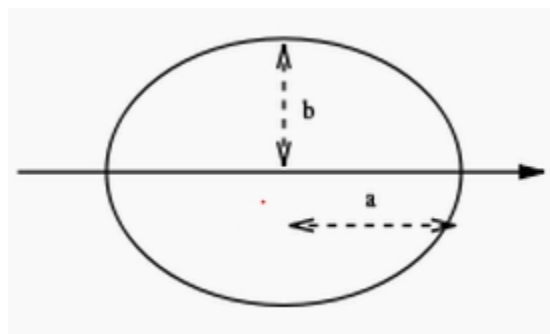


Figure 52: Inertia of an ellipse

Where E is the Young's modulus, φ is rotation, I is the inertia of half of an elliptic cylinder, a length in x - direction, b is length in the y - direction, t is the thickness and L the length. Equation 1 is based on the moment about deformation of beams, and Equation 2 is based on inertia of an ellipse, and the relationship between the inertia of half a circle and a full circle which is 0.5. This is an approximation since it's not an ellipse that is cut in half. The end result looks more like a "V" with radius at the bottom. But these equations describe what influences the momentum. The inertia is governed by the distance b, see Equation 2 and Figure 52, and a larger b is obtained by a smaller radius.

Beryllium has as all materials the ability to cause health problems, but don't have any health effect in solid state. It can cause health effects in 4% of the population, and to cause health issues the particles have to be smaller than 10 μm . This may happen in cases of oxidation, and should be considered for high temperature heat treatment, above 510° C. The heat treatment used in this case will be at 315° C.[13, 14, 21-23]

Cutting the antenna elements

Antenna module assembly

The antenna elements are cut out of a sheet of BeCu. The thickness of the sheet is 0.05 mm and the elements width is 5.0 mm. Because of the relative thinness of the sheet it has proven difficult to obtain the right dimensions over the length with cutting. Either the scissors at the mechanical workshops are designed to cut greater thicknesses or they have been slightly damaged. Four different scissors and one fabric roller scissor have been tested. The best result achieved was with a sheet cutter when the BeCu sheet was placed on top of a thicker aluminium sheet. But the width was not consistent over the length and therefore made the press operation more difficult. After consulting with the fine mechanical workshop at The Faculty of Natural Sciences and Technology, it was decided that their water jet cutter was their best option. The water jet made a rough edge due to a whipping effect of the water jet. This was expected and thought to be something that could be overcome. When a strip is cut it is very delicate and it is challenging not to damage it between operations. The strips are more exposed to damages than the sheet. After the strips have undergone plastic deformation and age hardening they are no longer vulnerable.

Machining forming tool FIKSE LOL

When the strips are cut they need to undergo plastic deformation. To be able apply this deformation a forming tool was made.

Antenna element specifications:

- Length: 117.5 – 517.5 mm
- Width: 5.0 mm
- Thickness: 0.05 mm

The forming tool made for applying a radius on the antenna element was made in the pre project. The end mill which was used broke before the whole length was cut. This meant the tool was not complete. The end result of that prototype did not have the expected quality of a finished product, even though the product worked well for prototyping purposes.

It was desired to make the forming tool in a stainless material which could be reused. The first forming tool was made in low grade aluminium and the grade of the material does affect the surface finish. It is often easier to obtain better surface fin-

Antenna module assembly

ish in high grade material compared to low grade. Therefore the second was made in high grade aluminium.

In the process of designing the forming tool, the forming process was evaluated. The first tool was made with a track depth of 2.5 mm, making a complete half circle. This meant that the arc length of the curvature was longer than the width of the antenna element, and twisting could occur. To account for the twisting a design was made where the arc length was equal to width of the antenna element, 5.0 mm, see Figure 53. This tool was made before the elements were chosen to be cut with a water jet. The rough edges on the antenna elements jammed itself in the forming tool, and the elements were damaged when it was taken out of the tool.

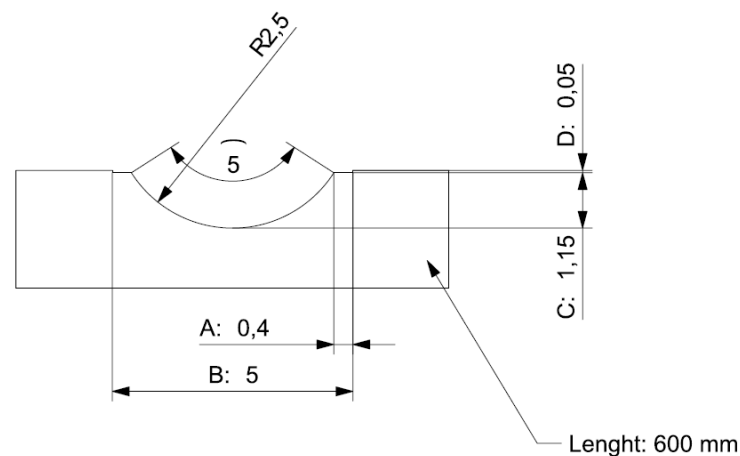


Figure 53: Antenna press machine drawing

To overcome the issues with the rough edges a tool very similar to the original was made. It was desired to have the arc length of the curvature tool shorter than the width of the element. This way the rough edges would not be in contact with the forming tool under the press operation, thus preventing jamming of the edges. The arc length is governed by the milling depth of the radius mill. By changing the radius on the female press from R2.5 – R2.0 a greater percentage of the half circle is kept. This helps to form as much as possible of the antenna element, since reducing the arc length effectively removes the flanges from being formed.

To obtain a good surface finish a lot of test runs were done to find the right feed rate and cut depth. If the cut depth was too deep or the feed rate too high, the chips fol-

Antenna module assembly

lowed the mill and ruined the surface. Also the angle and positioning of the coolant proved important. The mill rotation was clock wise with a rotation of 2200 rpm and moved from left to right. The rotation of the mill created a current in the coolant. This current has a tendency to pull chips back into the mill and yield a bad result. The coolant could be placed to counteract the current created by the mill and the chips were lead away, see Figure 54. Still with this adjustment of the coolant each cut could not be deeper than 0.4 mm with a feed rate of 75 mm/min. The flat end mill was not as dependent to cut depths and feed rates as the radius end mill. After the milling all edges were grinded by hand to smooth transitions and edges. This reduced the risk of jamming the antenna element.

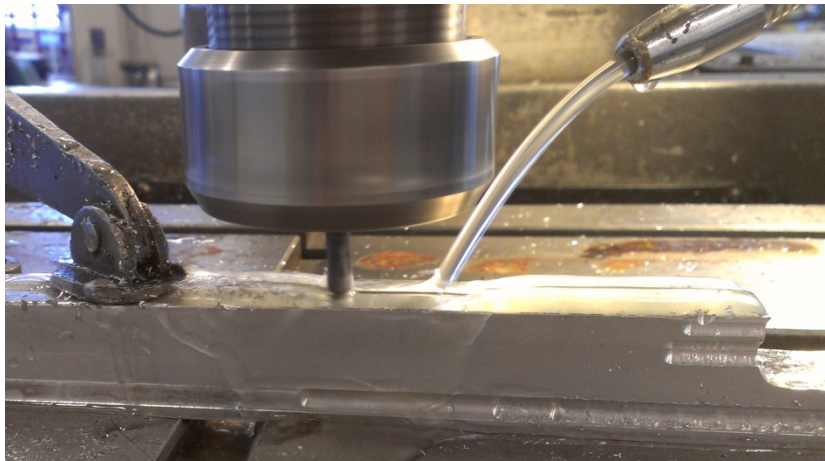


Figure 54: Milling antenna element press

Prototyping antenna element

After the antenna elements were cut with water jet the edges were grinded down with a 400 emery paper. This needs to be done carefully to prevent damages on the antenna elements. When put in the forming tool, see Figure 55, it was important to ensure the alignment and not press down on the whole length to prevent any twisting. If a antenna element has twisted counter actions can be made by forming around male press by hand.

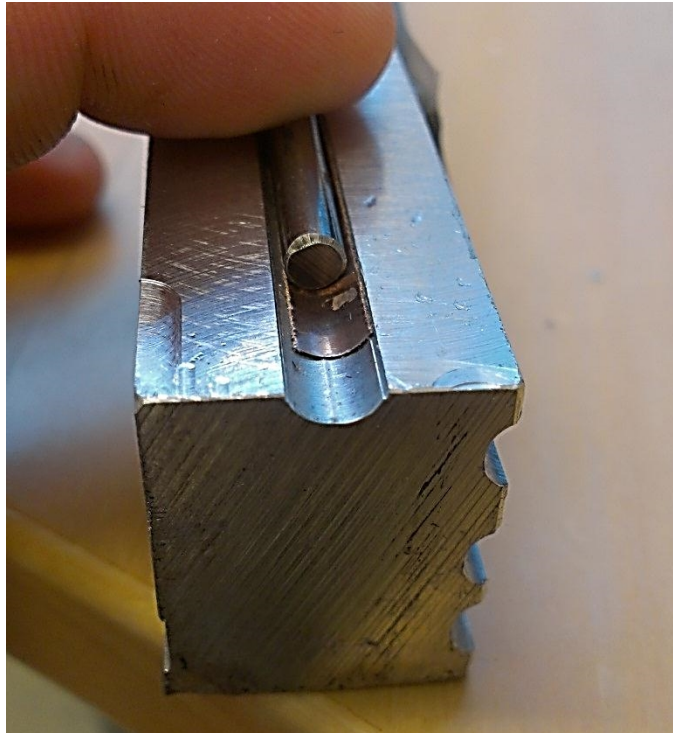


Figure 55: Forming tool

In the forming operation the material is put under stress exceeding the yield strength. The material is put under compression on one side of the material and tension on the other, in the cross section. The same stress state is seen in the length direction. This stress state curves the element along the length, see Figure 56 a). A reason for this to happen maybe that the press operation is not uniform. To account for this the element is put under tension in a heat treatment jig, see Figure 56 b). The jig also prevents the element to be in contact with other components than the air. After the heat treatment the antenna element was straight, see Figure 56 c).



a)



b)



c)

Figure 56: Antenna element

Learning points

The jig is made out of steel and the coefficient of thermal expansion is 13 to BeCu $17 \cdot 10^{-6} \text{ m/m K}$ [24]. Since the BeCu has less material the expansion is within seconds. This expansion made the antenna element to go from a tension to compression state and this making it curve. This effect is matched during the heat treatment and the straightness is regained.

The antenna elements are made from the prototype sheet. The reason for calling it prototype sheet is due to its dents and twists. These damages make a weak spot since it makes a low energy mode. It is very difficult to fix and a not damaged sheet should be used to prevent this.

The antenna element undergoes a press operation where it is pressed to a R2, after spring back it has R4, and after heat treatment it is between R4 - R4.5 mm.

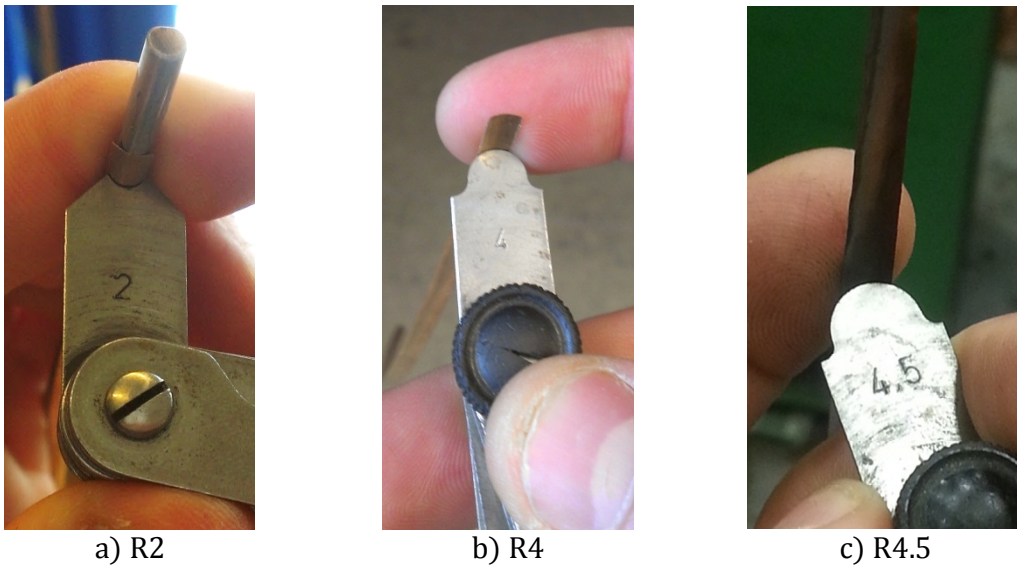


Figure 57: Change in radius under manufacturing

In Figure 58 two different antenna elements are shown, and the element with the largest displacement is the one with the largest radius. In Figure 59 a test was done to see how small a coil could be made. This coil was left for two days and no visible plastic deformation was found.

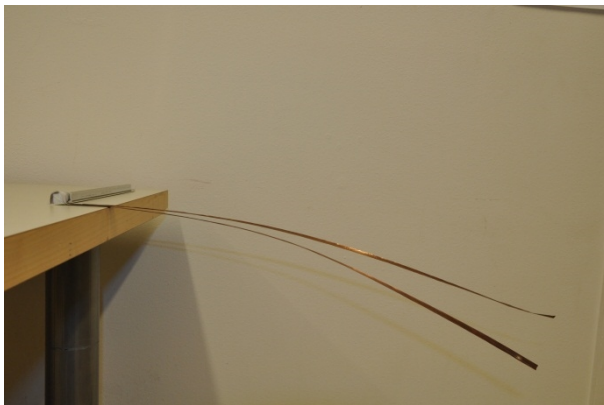


Figure 58: The radius effect on stiffness

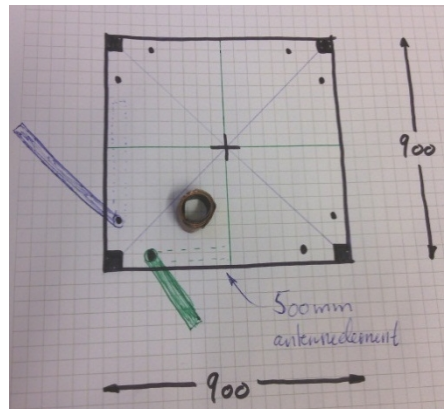


Figure 59: Coiled up with a radius of 1-2 mm



Figure 60: R5



Figure 61: R2



Figure 62: R1.5



Figure 63: R0.75



Figure 64: No visible plastic deformation



Figure 65: No visible plastic deformation



Figure 66: Plastic deformation

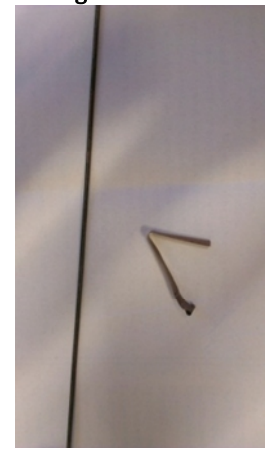


Figure 67: Plastic deformation

Preliminary test proved the antenna element did not show any visible plastic deformations when bent around object with R5, R2 but clear visible damage occurred when bent around R1.5 and R0.75, see Figure 60 through Figure 67. Kim Sandvik did FEA of an antenna element with the dimensions of 7.6 x 0.1 mm in width and thickness respectively and with a radius of approximately 4 -5 mm. When this was bent around a bar with radius of 2 mm in a 45 ° angle it experienced a stress of 1075 MPa, which close to the yield strength of 1169-1173 MPa [10]. Therefore it is suggested to prevent the antennas to be subjected to these radiuses.

As for the functionality it does prove to be very solid. It seems to be a material that can be relied on and will therefore most likely be used. The fact that it can withstand small bends and have a strong spring effect is important.

4.4. Prototyping electrical release mechanism

The release mechanism of the antenna module is based on tying up the gate with a thread. This thread is burned off by stretching it over two separate resistance wires which is powered. When powered, the temperature will rise and burn off the nylon thread, thus the gate is free to be opened.

The resistance wire needs to have the correct resistance. A too high resistance will reduce the current which would not sufficiently elevate the temperature. Too low resistance will increase the current and it will drain the batteries without providing the required temperature. The current can be drawn from different systems and modules. The EPS, have two separate systems where the designer can choose from either the 3.3 V or 5.0 V circuit. At 3.3 V the EPS can deliver 2.0 A to the entire satellite. Therefore it is expected that the radio module can deliver a minimum of 1 A to the burn off mechanism. Another solution could be drawing current straight from the batteries, but then it would bypass the safety systems build into the satellite and it could potentially drain the batteries and kill the satellite. With this in mind the prototyping was set up to be similar to the current and voltage of the radio module.

Prototyping burn off thread 1

At IET there were different resistance wires, but they were old with incomplete marking. Therefore the resistance of each wire was measured and also it was seen how easily the thread burnt off. The goal was to learn about what was required to burn of the thread instantly and within electrical limits.

Goals with prototype

- Find resistance of the resistance wires available
- Find a resistance wire which can be used
- Examine if the electrical properties proposed is sufficient

A test jig was set up to measure the resistance of each wire. The jig consisted of two clamps with a predefined distance, multimeter and a power supply, see Figure 68. The distance was set to be 25 mm which was the approximate length of resistance wire expected to be needed.

Antenna module assembly

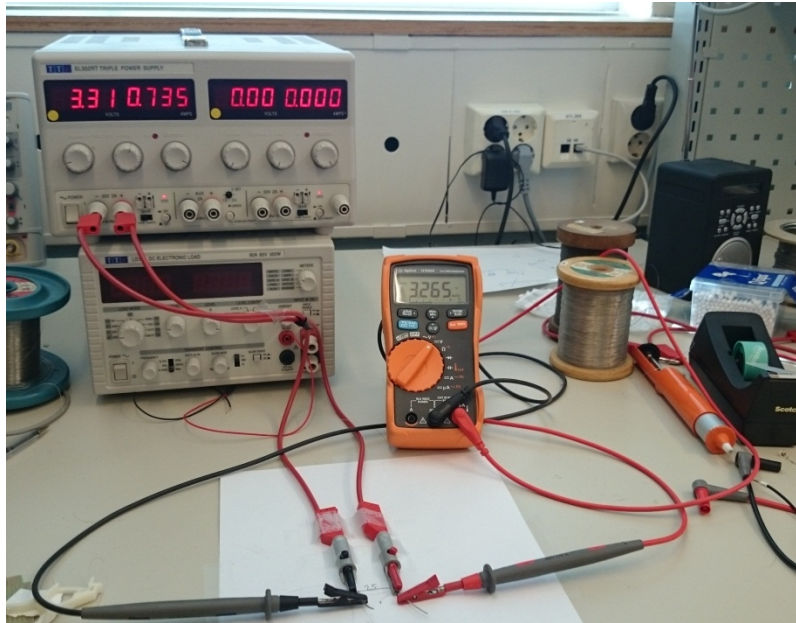


Figure 68: Burn of thread test jig 1

Six different resistance wires were measured. The different values are presented in Table 6. All but #2 burned off the nylon thread, but the most promising was #1 and #3. These two were selected for more extensive testing.

Table 6: Resistance wires

Wire	Ω
#1	4,1
#2	1
#3	4,3
#4	1,4
#5	1,85
#6	1,2

The resistance of wire #1 was measured a second time to be $4.7 \Omega / 25 \text{ mm}$ and $133.2 \Omega / \text{m}$. At full capacity it draws 724 mA at 3.3 V. This wire had a tendency to turn fiery red for a short period of time, but did not burn itself off, and worked after repeated test runs. This wire was also tested with a 5.0 V with a current draw of 1100 mA. With this current and voltage the wire turned fiery red instantly and also burned itself off after a gentle touch. It means the wire should not be exposed to these currents in order to be able to retest.

Antenna module assembly

Wire #3 was also retested to have a resistance of $4,3 \Omega / 25 \text{ mm}$ and $140.5 \Omega / \text{m}$. At full capacity it draws 740 mA at 3.3 V. This wire did not get fiery red but turned blue after a few tests.

After the testing of different wires a temperature probe was attached to the resistance wire #1. This was filmed in order to see how quickly the temperature rose. Two different wires were tested. The blue line in Figure 69 had undergone several tests before the heat rise was timed. The old wire did clearly need longer time to reach 200°C , but the red needed longer time to go from $270 - 300^\circ \text{C}$.

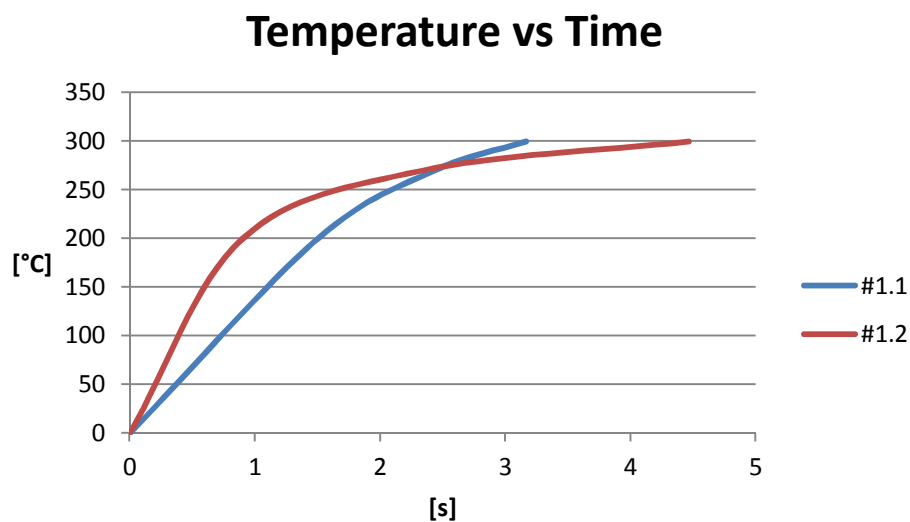


Figure 69: Temperature vs. time, prototype 1

Learning points

This prototype showed that the two wires with the highest resistance did burn off the thread instantly with currents below 1 A, with 3.3 V, showing that the power used is sufficient to elevate the temperature quickly enough to burn off the thread. When designing the circuit board a timer has to be put in before it switches through burn offs 1 through 8, each burn off point has two resistance wires. This input will be 2 seconds, which will elevate the temperature to 250°C .

Prototyping burn off thread 2

Antenna module assembly

In the second prototype the resistance wire was placed inside the casings to be used in order to check any affects to the burn off process.

Goals with prototype

- Find the resistance when the wire is placed in casings
- See how the casings affect the heat elevation

The distance between the centres of the holes in the casings are 8.5 mm, this and the test jig can be seen in Figure 70. The wire #3 was used in this prototype. It had a resistance of 4.3 Ω / 25 mm, and since the casings are considered to have much lower resistance than the resistance wire, the effective length of the wire is only 6.5 mm. The resistance wire still needs same current and voltage to obtain the equivalent power over the resistance wire, see Equation 4. Therefore a second resistance has to be put in series to obtain the same total resistance that will let Equation 3 be in equilibrium.

Equation 3

$$U = R I$$

Equation 4

$$P = U I = R I^2 = \frac{U^2}{R}$$

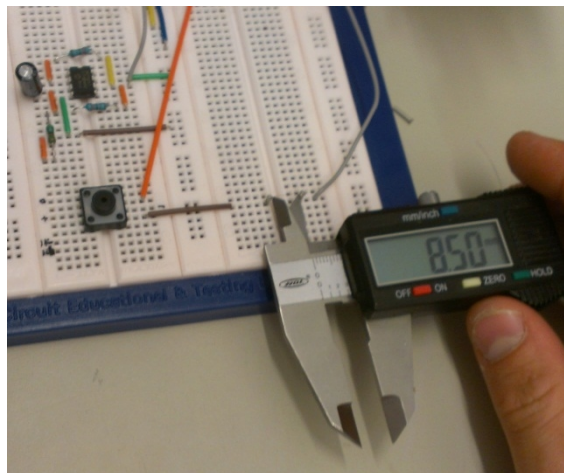


Figure 70:Burn of thread test jig 2

Antenna module assembly

This prototype was tested to see how quickly the temperature rose. As can be seen in Figure 71 the temperature did not rise as quickly nor to as high temperature as the longer wire did. This is thought to be due to the casings. The wire is a shorter and has less power, since the power is divided to both resistances, and thus can't elevate the temperature in the casings. The wire still burned off instantly with a current draw equal to 742 mA and with 3.3 V.

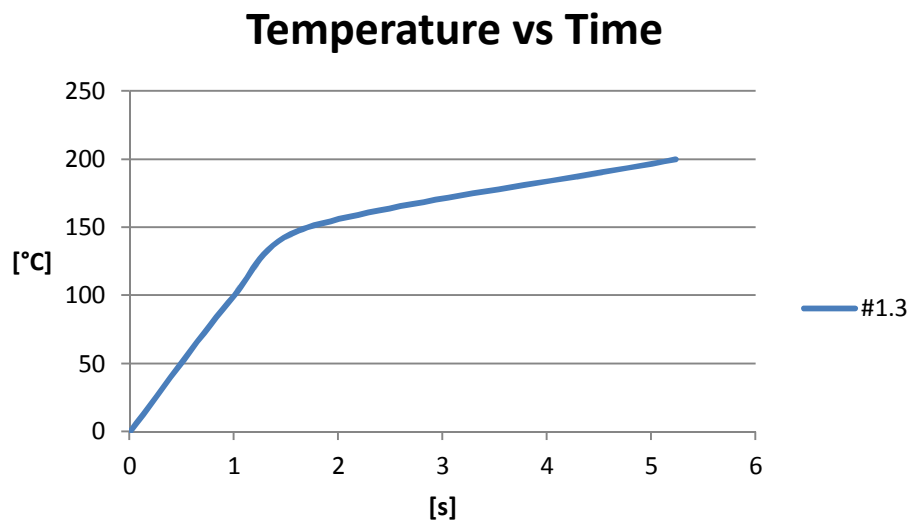


Figure 71: Temperature vs time, prototype 2

Learning points

With the electrical requirements of 3.3 V and the resistance wire #3 a satisfying burn off was observed. The resistance in the wire was measured to be 1.3 Ω . This slightly more than can be expected. The resistance of a wire is linear and thus should be 1.1 Ω . When the thread was in contact with the resistance wire it burned off instantly with a current of 740 mA. It is expected that the temperature in the wire will be higher in space due to vacuum, but the start temperature can also be -25 instead of 25 $^{\circ}\text{C}$. This needs to be tested further. The resistance wire was tested to burn off with 1.5 A. In conclusion this setup proved to be so reliant that it was chosen to pursue further.

4.5. Prototyping the mechanical release mechanism

The mechanical antenna release mechanism is the ability of the antenna element to open the gate closing it in. It is of utmost importance for the success of the satellite campaign that the antenna element will unfold properly. To learn what is happening under the opening of the gate and the unfolding of the antenna element it has been photographed and video recorded. The photos and videos have been analysed to see if any conclusion or tendencies could be observed.

Goals with prototype

- Test different antenna pocket configurations to find the most optimal one
- Learn what is going on during unfolding

Testing of the antenna release mechanism with UHF element

The parts in this test setup consist of prototyping parts. The antenna element is made out of BeCu with the manufacturing process described in 4.3, and is the same as will be used in the satellite. The gate and antenna module have been 3D-printed at the Department of Engineering Cybernetics. The material is acrylonitrile butadiene styrene, ABS. The bottom plate is a PCB-card milled at the Department of Electronics and Telecommunication and is the same as will be used in satellite. The antenna module and gate will later be made out of PEEK. This material was not used as it is more expensive, time consuming milling and 3D printing is optimal for rapid prototypes as this.

There were several different configurations and a variety of tests were done with each configuration. The different configurations are shown in Figure 72 through Figure 76. The column to left indicate failure and the right hand column indicates success.

Antenna module assembly

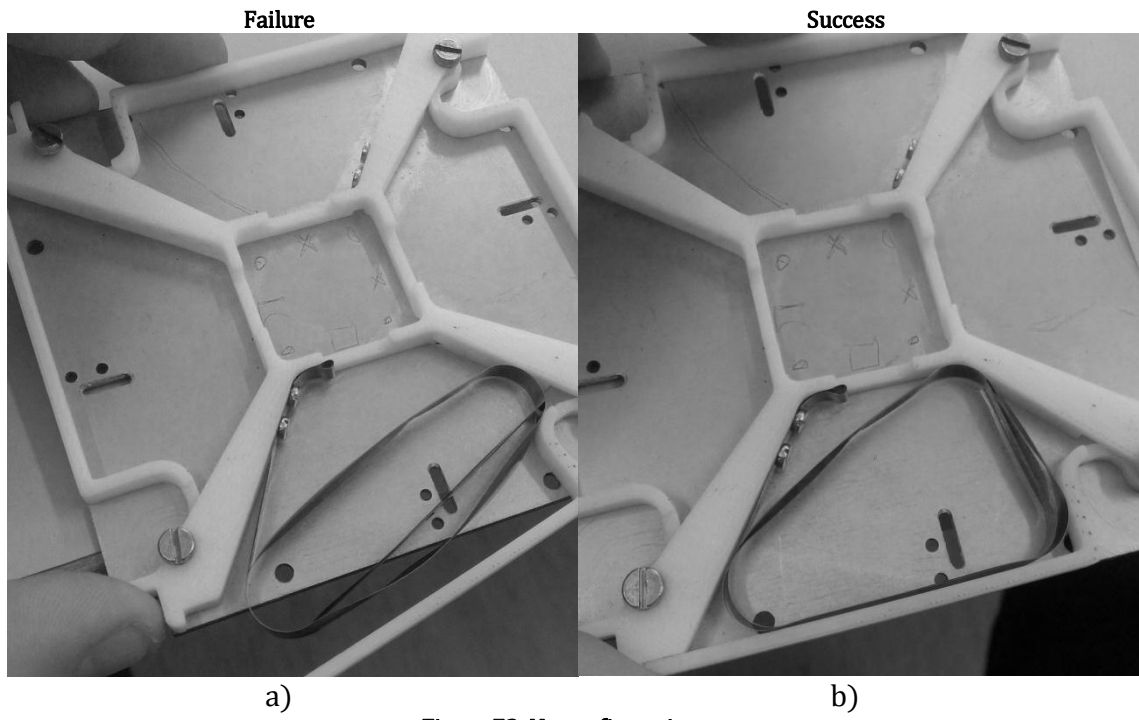


Figure 72: No configuration

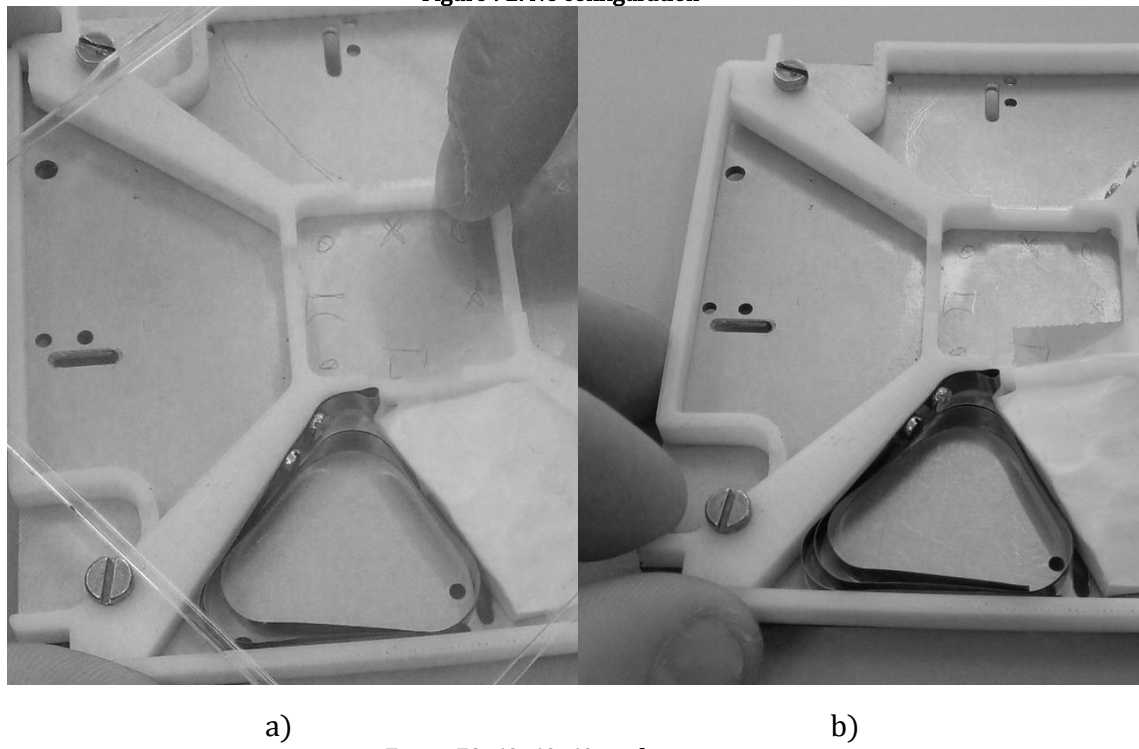


Figure 73: 60x60x60 configuration

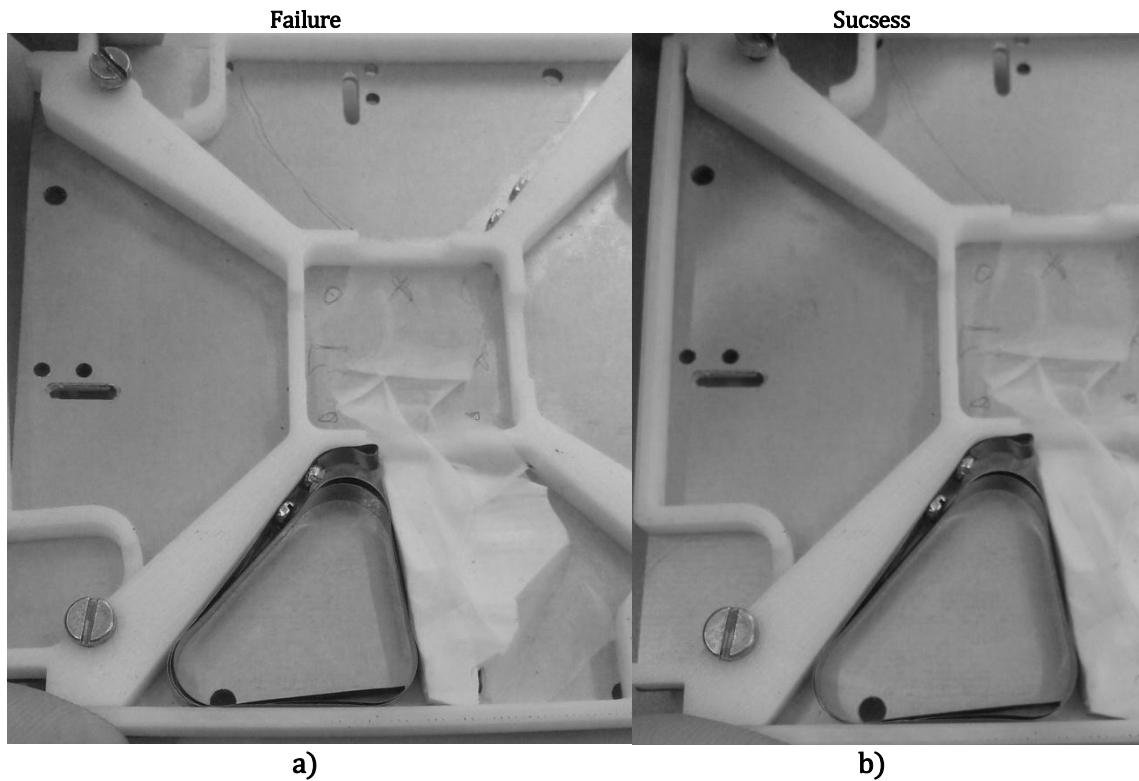


Figure 74: Sharp angle configuration

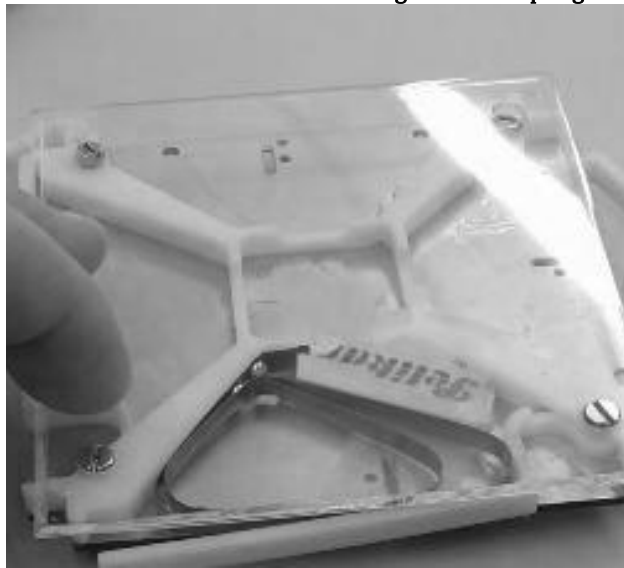


Figure 75: Wide angle configuration

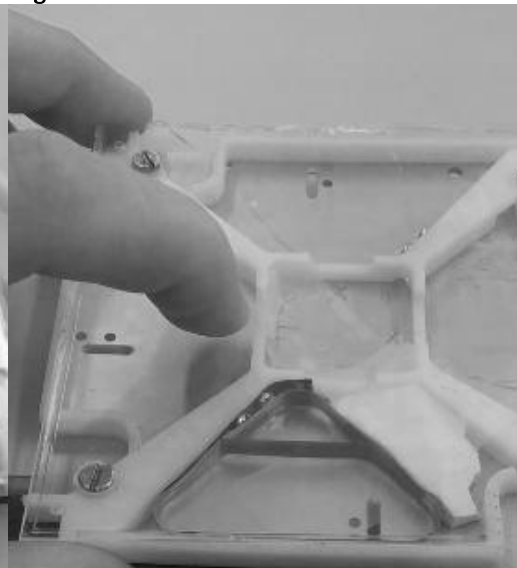


Figure 76: Medium angle configuration

Results from test and video analysis

The picture and video analysis provided a lot of insight. The most important job was to try and find factors or tendencies which were repeated. Therefore it was convenient to divide tendencies in reason for error or success.

Reasons for error

The potential energy in the antenna element is not utilized to open the gate. The direction of force is normal to bending orientation, see Figure 77. If the antenna element end was located just in front of a corner, the uncoiling stops. The success of the uncoiling was independent of which direction the end was up against as long as it had a free length, see Figure 78.

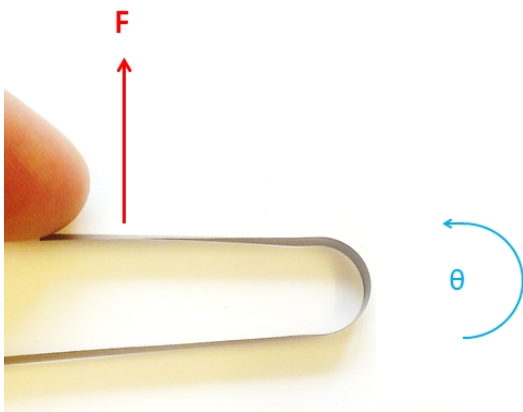


Figure 77: Direction of force in relationship to bending angle

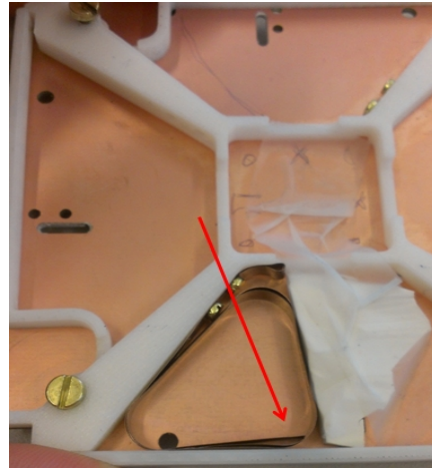


Figure 78: Antenna element end

There were also some configurations that that both worked and failed. This was most likely due to a twist at the end of the antenna element. The twist did in some incidents wedge itself under the antenna element. Before the effect of the twist was discovered the rate of failure was higher. The coiling of the antenna element is done by hand. With special care to the coiling the twist could be neglected, and the opening was successful. This is one of the reasons some of the configurations had success and failure. Too oblong configuration does not transfer the energy in the right direction, it applied force to keeping the gate closed, and results in failure. The hinge mechanism is rotating around a screw connection and this was sometimes too tight, resulting in failure.

Reasons for success

Antenna module assembly

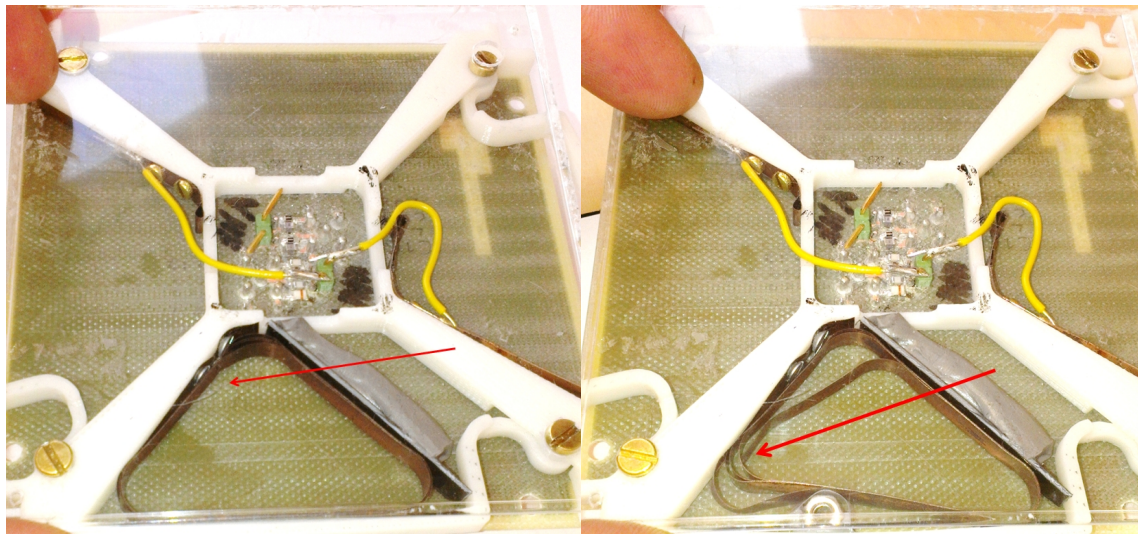
One thing was concurrent for all the success figurations. The end of the antenna element had nearly a whole length before it came to a corner. This is believed to be important for the gaining of momentum and the force necessary to open the gate. Positive angles, meaning that the force from the antenna elements pushes the antennas out of the pocket.

General observations

- The spring effect of the antenna element is strong enough to open the gate, if it is made right. It is more a question of directing the energy of the antenna element to open the gate.
- It will use all space available
- The hinge should be placed on the opposite side of the used in this prototype
- A better manufactured prototype will most likely yield more consistent results

Testing of the antenna release mechanism with VHF element

The VHF antenna element is in testing 500 mm long. It was of interest to see if it behaved in the same manner and using the shorter UHF antenna element. This time the configuration found to be the most applicable were used, see Figure 79. The antenna element ends are pointed out with a red arrow. One idea that was checked out was with a pressure point on the gate. The pressure point was a nut which would change the shape of the antenna element and the gate would be pushed open before the antenna element was being unfolded.



a) b)
Figure 79: UHF element release mechanism configuration

In this set of 15 tested, success was seen in 9. Four of the failures were related to the pressure point. For the pressure point to work it had to push in the antenna element. This made the gate open before the unfolding of the antenna had started, which was the purpose. It also disrupted the coiling of the antenna and on all occasions it caused wedging and failure. The pressure from the antenna element bent the gate to be outside the PCB-card. The reason of success was the same as for the UHF element.

Design requirements

- The confinement space shall be designed in a way so the spring energy only works in the opening direction.
- The antenna element shall only be in contact with the gate where it can be opened. See this picture
- The hinge is supposed to be fastened with screw and nut. Therefore an insert should be made to take up the axial forces. This insert should have as low friction as possible.

4.6. Redesign of antenna module

The hinge mechanism was in the first design iterations placed on the opposite side of the antenna element exit, see Figure 80 a). The idea was that this would yield the longest arm and thus the highest momentum. But after video analysis it was clear

Antenna module assembly

that the idea was based on a bad assumption. The antenna unfolds from the opposite side from where it is attached. The easiest way to change this was to attach the antenna element the opposite way. But the hinge is curved in the start in order to rotate around a fastener. This curve needed to be enlarged to widen the angle necessary to let the antenna element align in a straight line, see Figure 80 b).



Figure 80: Hinge mechanism opposite sides

The cross section of the antenna element change when it is coiled up. It changes from a half circle to a rectangular cross section. When it's a rectangular cross section the width is the same as the original width of 5 mm. Therefore the height of the antenna module needed to be changed from 5.0 – 5.1 mm

The gate is curved to be able to rotate around the assembly fastening screw. In the first design the gate was not built in, see Figure 81. This design in combination to antenna exit direction caused the antenna element of keep the gate closed. Therefore the curvature was later built in as seen in Figure 82.

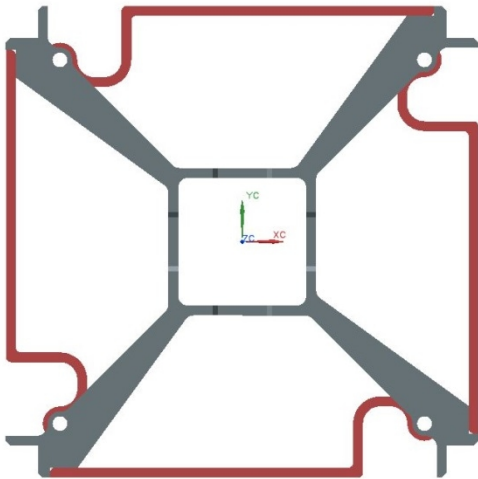


Figure 81: Antenna module v.01

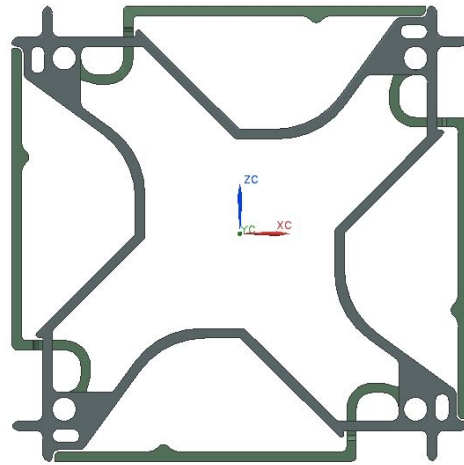


Figure 82: Antenna module v.05

One of the findings in the prototype in section 4.5 was that all with successes had one free length of travel inside the pocket of the antenna module. Therefore it was of interest to try to design the pocket in compliance with the length of the antenna element. In Figure 83 the lengths of each side in the pocket was measured in Siemens NX, and with a certain radius this was the end position of the 117.5 mm antenna element. This is a solution that could have worked.

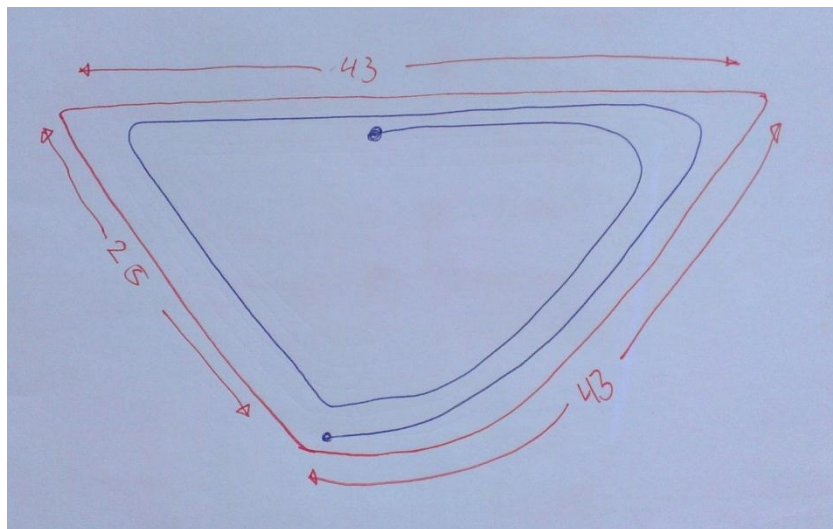


Figure 83: Antenna element start end position

Antenna module assembly

The length of the antenna element is initially found from Equation 5. This formula yields theoretic antenna element lengths of 171.62 mm and 517.24 mm for UHF and VHF respectively. The antennas work with current creating a field around the antenna somewhat like a magnetic field. The magnetic field of the earth is longer than the diameter of the earth. It is the same with the field around the antennas. The field is easily disturbed by any conductive parts or components, such as screws and orientation of radio components. All these aspects together determines the real length. Therefore it is impossible to design the pocket for the antenna element at this time.

Equation 5

$$c = f \cdot \lambda$$

4.7. Testing the antenna module

When all subcomponents were tested the antenna module assembly were going to be tested. For this purpose the antenna module was 3D-printed and holes were broached, pressure cylinders were made out of Teflon in a lathe, two UHF and VHF antenna elements were made, a special PCB-board was milled out for the purpose of burning off each burn off point, and a circuit was made on a bread board.

Assembly of prototype

First the casings were put in the antenna module and resistance wires were put through the casings before the casings were pressed around the wire, see Figure 84.

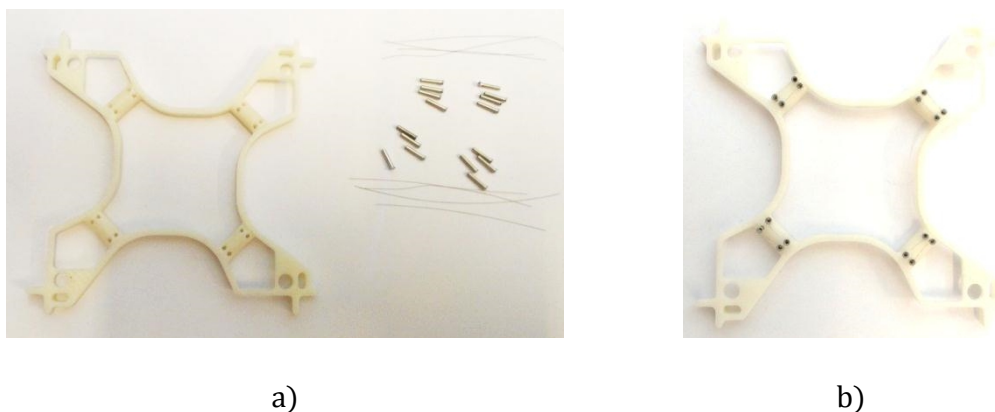


Figure 84: Antenna module assembly 1

Antenna module assembly

The casings were soldered to the PCB-board and wires were attached from the bread board to the PCB-board, see Figure 85.

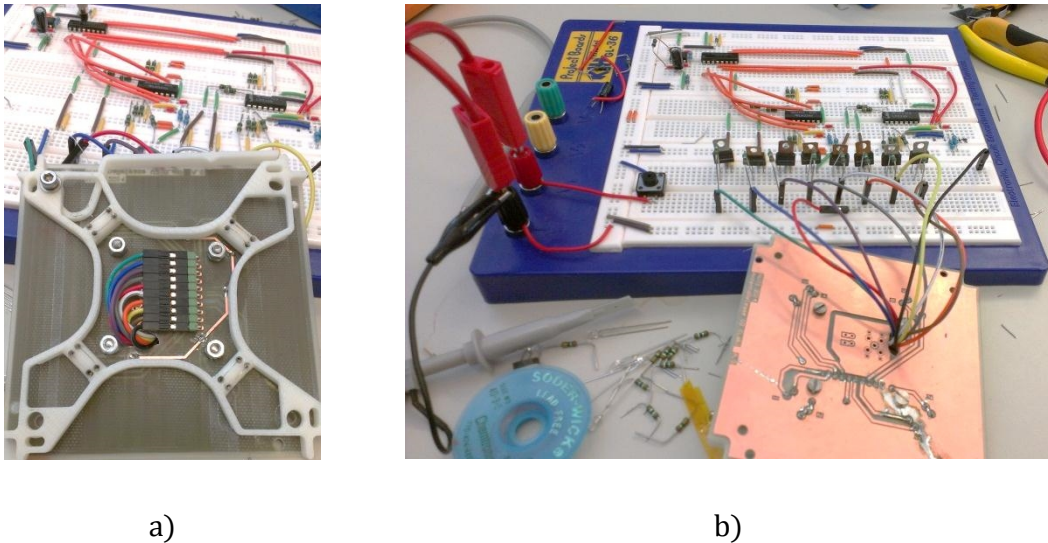


Figure 85: Assembly connected to bread board

The electrical circuit was built up with a counter, capacitor, and resistances. The capacitor was also used as a timer to work for two seconds. In the beginning the noting happened and the signal was tested, see Figure 86. It was first measured to be on for 160 ms and was initially set to be on for 2 s.

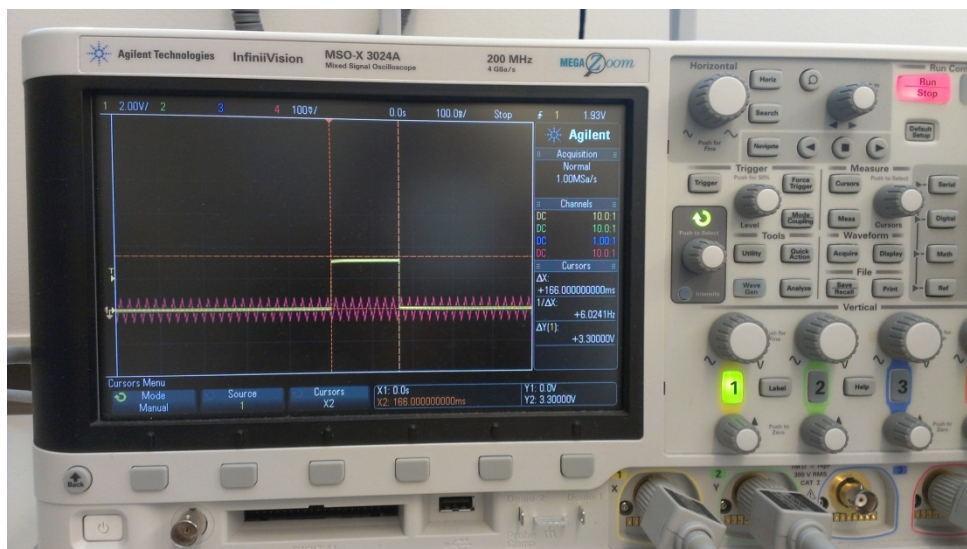


Figure 86: Signal processor

Antenna module assembly

When this was sorted out the system retested. A thread was tightened over the burn off wires and the circuit was set on. In one location the resistance wire melted into the antenna module instead of burning off the thread. This was considered an option, but it was assumed that the thread would burn off before melting into the module. The other did not burn off the thread. The material in the antenna module, ABS, is the same for the whole antenna module. Therefore the burning into the antenna module shows that the antenna module needed isolation. The fact that it only burnt into one of four locations indicates a fault in the electrical system. This was debugged and fixed.

The thermal conductivity of PEEK and ABS is very similar, 0.25 and 0.17 W / (mK) respectively [25, 26]. This means the material will absorb approximately the same amount of heat from the resistance wire. Therefore a non-conductive thermal film, Kapton Polyimide, was placed between the module and the resistance wire. The amount of current was also increased from 600-700 to 900-1000 mA. These measures made the antenna element to release properly. In Figure 87 a close-up of the thread, resistance wire and isolation film can be seen.



Figure 87: Antenna module release mechanism

4.8. Evaluation of antenna module

The antenna module assembly has been fully tested and with very promising results. The mechanical release mechanism is working and will be better when made in proper material. The electric release mechanism successfully burned of the constraining thread. Both mechanisms worked according to plan after a few improvements. This supported the proposed solution and strengthened the belief in it. It cannot be neglected that this was after the antenna module was isolated, nevertheless the rate of successful burn offs will rise when made in PEEK. This is based on improved electrical system and redesign of antenna module. The structure where the casings are put in will in next iteration have reduced thickness with less material, it will be made with more space for isolation and lower to reduce the angle the burn off thread. A damper to absorb the energy of motion of the antenna elements after unfolding has to be implemented. It can be as simple as a strip of rubber along the inside of the antenna module in space grade.

Chapter 5

5 TESTING

5.1. Lap shear test

Lap shear test is a commonly known method for testing adhesive bonds. ASTM standard test method described in D1002-10 "*Apparent shear strength of single-lap-joints adhesively bonded metal specimen by tension loading*" is widely used. This test method is shown in Figure 88 and is basis for most ASTM LSS standards. The test consists of two specimens made according to the standard chosen. This method is known to not be the best method to describe LSS of materials, but is widely used for its simplicity. With an increased thickness improved results can be expected. A too thin specimen will bend and the result will be a stress concentration test rather than measuring the LSS. Therefore the specimens need a certain thickness which can withstand the bending moment sufficiently so the effect of bending can be neglected. The thickness was made to be 2 mm after conferring with Kongsberg Aero Space which continuously conduct lap shear test on their pre-preg products, see Appendix 3. Lap shear test should be done to confirm the strength of the adhesive bond between the CFRP-panels. According to hand calculations in the pilot project the adhesive bond need a minimum strength of 6 MPa to withstand thermal cycling fatigue [6, 27]

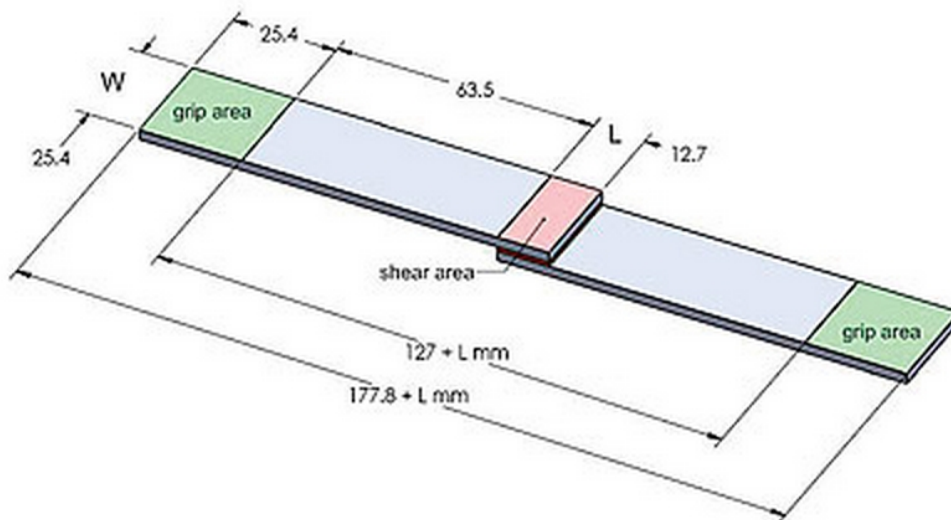


Figure 88: Single lap shear

5.1.1. Test procedure

The adhesive were used between the aluminium rail and CFRP-panel. The data sheet for the adhesive had values for aluminium – aluminium, thus the bond between CFRP – CFRP needed to be tested.

Test specimen

The specimens were made according to ASTM D5868. The dimension is based on inches. The length is 4" and the width, grip area and adhesive area is all 1". The thickness was 2.0 mm. The specimens were cut to dimension with a water jet. The panels were made with the same method and material as the panels for the satellite. The method is described in chapter 3.4.2.

Adhesive

The adhesive used in this test is the same adhesive which is going to be used in the satellite. It is two component epoxy adhesive from Huntsman, named Araldite Av 138 M-1 epoxy with HV 998 hardener. It has ident-number 001734908 and expiry date 16-10-18.

CFRP

Testing

The CFRP used is pre-preg from Hexcel named, HexPly 6376 with a resin content of 36 %. This is a $\pm 45^\circ$ weave with thickness of 0,281. Stacking orientation is [0/90, -45/45, 0/90, -45/45, 0/90, -45/45, 0/90]. This was made with the same method described in 3.4.2. The sheet was 250 x 250 mm and yielded 7 lap shear specimens. This was cut with a water jet and none specimens were discarded which is proposed in the ASTM D5858. In ASTM D5868 another cutting method is thought to be used. The specimen were then prepared with abrasive paper and thoroughly cleansed with acetone. First one spacer where adhered to each end and left to cure. Then two lengths were adhered together and left to cure. The curing time in 23° C is 24 hours for this adhesive [6]. It was all cured under pressure from clamps.

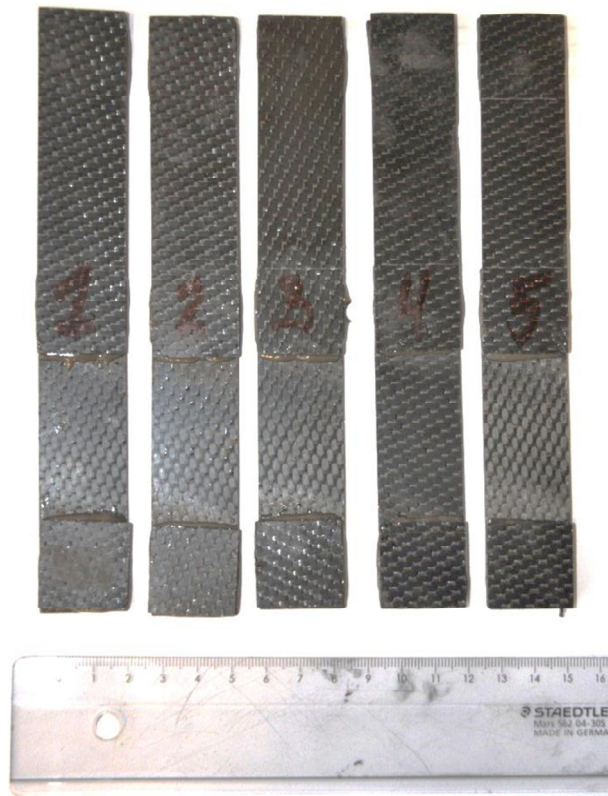


Figure 89: Lap shear test specimens

Laboratory and equipment

Testing

The test was conducted in the fatigue laboratory at Department of Engineering Design and Materials at NTNU. The machine used was a ± 100 kN Instron 8800 hydraulic machine. All tests were conducted under a temperature of 21.5° C and a humidity of 33 %.



Figure 90: Test specimen #2 in the machine

Results

All five test specimens experienced failure in the adhesive bond. The load rate was set to 13 mm/min according to ASTM 5868 [28]. In Table 7 the load at break and elongation at break can be seen. In Table 8 it can be read that the difference in the adhesive layer thickness does not impact on the strength of the adhesive. Table 9 is there to see how the LSS vary with the adhesive layer thickness.

Testing

Table 7: Shear stress and elongation at break

TEST	Force [N]	Shear area [mm ²]	Shear stress [MPa]	Elongation at break
2	5076	645.16	7.87	0.96 %
5	5504	645.16	8.53	1.38 %
3	5832	645.16	9.04	1.47 %
4	5852	645.16	9.07	1.46 %
1	6252	645.16	9.69	1.12 %
Mean:	5703,2	645.16	8.84	1.28 %
Max Shear Strength	6252	645.16	9.69	1.12 %
Min Shear Strength	5076	645.16	7.87	0.96 %

Table 8: Sorted by adhesive layer thickness

Test	Left [mm]	Right [mm]	Total [mm]	Adhesive Layer [mm]	Shear Stress [MPa]
4	2.21	2.09	4.33	0.03	9.07
2	2.11	2.07	4.27	0.09	7.87
1	2.07	2.09	4.29	0.13	9.69
5	2.11	2.08	4.33	0.14	8.53
3	2.10	2.10	4.41	0.21	9.04
Max adhesive layer:	2.10	2.10	4.41	0.21	9.04
Min adhesive layer:	2.21	2.09	4.33	0.03	9.07
Mean adhesive layer:	2.12	2.09	4.33	0.12	8.84

Table 9: Sorted by shear stress values

Test	Left [mm]	Right [mm]	Total [mm]	Adhesive Layer [mm]	Shear Stress [MPa]
2	2.11	2.07	4.27	0.09	7.87
5	2.11	2.08	4.33	0.14	8.53
3	2.1	2.1	4.41	0.21	9.04
4	2.21	2.09	4.33	0.03	9.07
1	2.07	2.09	4.29	0.13	9.69

Conclusion

Testing

The adhesive proved sufficiently strong for the purpose of fatigue in space. This was the main goal with the test. The mean elongation at break is 1.28 % which is higher than the 1.2 % from the datasheet. This is in contrast to the LSS which is lower than what is given in the datasheet.

All the specimens experiences failure in the adhesive, see **Error! Reference source not found.** This was also expected according to data sheets [6, 7]. The datasheet states the LSS of the adhesive range from 10 – 20 MPa according to surface and curing temp. The CFRP should according to datasheet have a tensile strength of 1006 MPa.

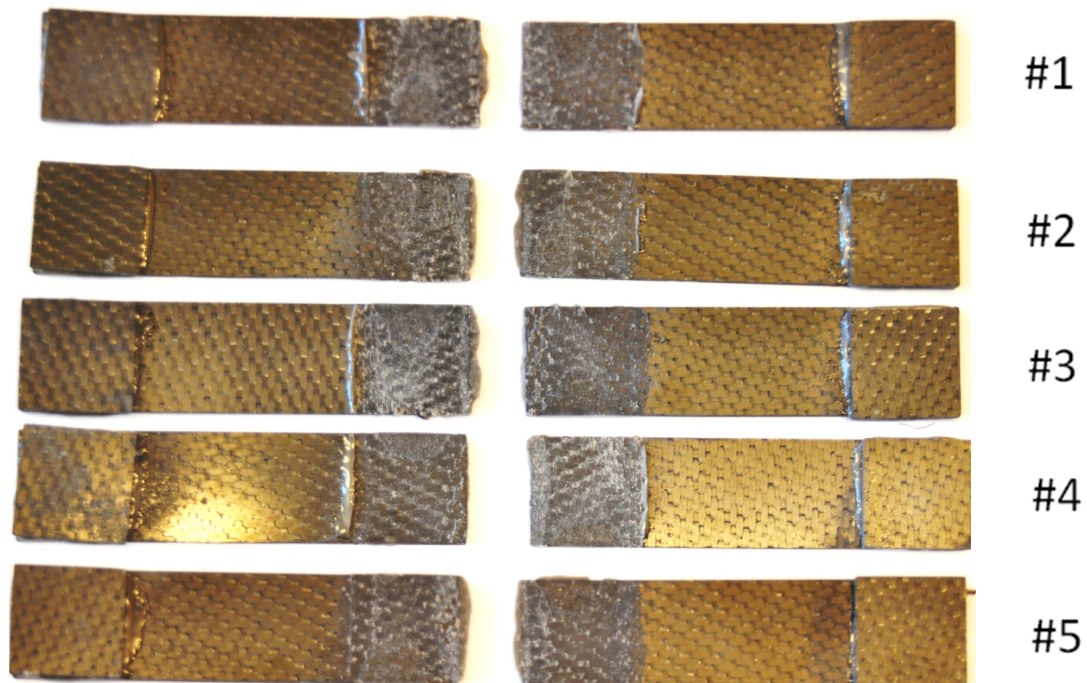


Figure 1: Test specimens post test

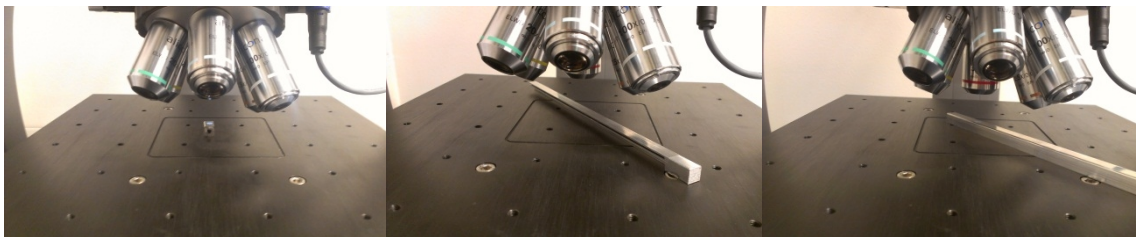
5.2. Surface roughness measurements

The CDS specifies that all faces in contact with deployer shall be hard anodized and have a surface roughness of no greater than $1.6 \mu\text{m}$ [5]. These requirements are made to prevent cold friction welding due to vibration during launch. It is important to achieve the right surface roughness before the parts undergo the anodizing treatment. Because the surface roughness will be approximately the same before and after surface treatment. Therefore it would be most convenient if the parts had the right roughness after the milling operation. This means the surface roughness measurements have two different agendas.

1. To determine what surface roughness can be achieved with this milling process.
2. To document the surface roughness if values are below threshold values.

The first measurements were conducted in preparation of the pilot study. Then measurements were conducted on one rail and one standoff piece. These measurements are presented in Table 10.

In the pilot project the first surface measurements was completed on rail and stand-off. The measurements were performed on the two contact faces of the rail, and on one side of the standoff. The rails and standoffs are milled out of blocks. It is used a three axis mill for the production of the different parts with an end mill. The two different sides of the rails have been milled different. One side has been milled from the side of the mill. The other side has been milled from the top of the mill. The standoff has been milled from the side on all sides, but this did encounter more vibration due to the shape of part and constraint on part. The measurement is done with the use of a 3D microscope. It produces pictures at different depths and layering to a 3D picture and then completes measurement. The measurement is done as shown in Figure 91, Figure 92 and Figure 93. On each location three measurements were done to obtain a better mean value.



Testing

Figure 91: Standoff measured

Figure 92: Rail measured in centre
side 1

Figure 93: Rail measured in end
side 2

Table 10: Result of surface roughness test

Test	Ra [μm]	Ra [μm]	Ra [μm]
1	1.4864	0.7310	1.1089
2	1.3580	0.7690	0.9640
3	1.1434	0.7550	-
Mean	1.3293	0.7517	1.0365

All measurements were below the limit of 1.6 μm and no additional surface treatment would be required before anodization. The variation in the test is thought to be due to interaction with mill and vibration as mentioned above.

For the master thesis the new rails were manufactured. In Figure 94 it is shown how the difference in milling position affect the surface. On the left it is milled from the top of the mill, and on the right it is milled from the side in. Figure 95 shows the difference between the two different production series, pilot project and master thesis. The rail in the pilot project had a mean value of max 1.329 vs It can also be seen that the last cut was done with two cuts.

Important factors to achieve a fine surface finish are milling speed, cut depth, constraint/vibration, mill interaction, mill type, pro milling or counter milling, material, temperature etc.



Figure 94: Left side milled from top, right side milled from side

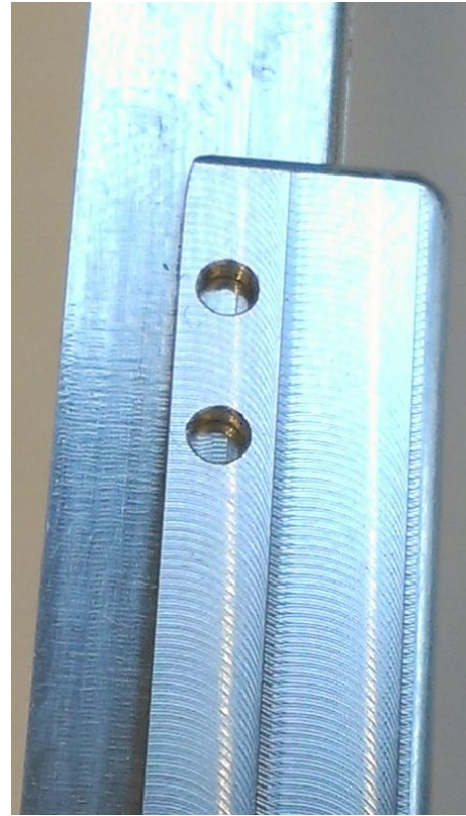
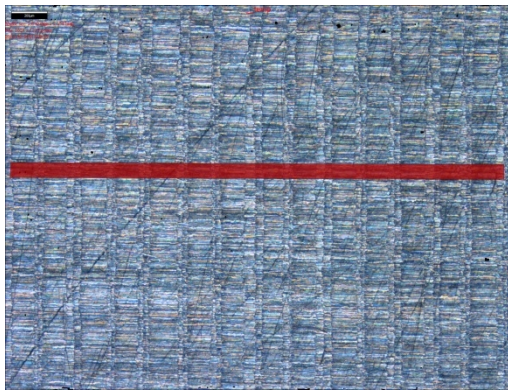
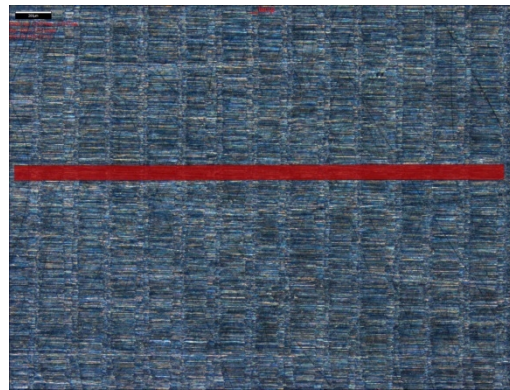


Figure 95: Difference between the two production series.

All four rails were milled with the same mill input and they looked the same. As the figures above shows it is possible to detect the surface roughness by the naked eye. The first measurements were completed on side of the rail milled from side in. The red line in Figure 96 is the area where the measurement is performed. The rail was the same overall and two measurements were sufficient to achieve reasonable results. The results are presented in Table 11. It can be seen that this side had a surface roughness less than the limit of $1.6 \mu\text{m}$. In the top left corner a black box can be seen, it has the length of $200 \mu\text{m}$.



a)



b)

Figure 96: Measurement 1 and 2

Table 11: Measurement of side in milling master thesis rail

Measure	Measurement 1	Measurement 2
Ra [μm]	1.189	0.711
Mean [μm] =	0.950	

The other side which was milled from the top of the mill had a coarser surface and more measurement was done to see how the surface roughness was affected by the different areas. There were generally three areas, fine, course and between. Measurement 1, Figure 97, is along the course area, measurement 2, Figure 98, is between the fine and course, and measurement 4, Figure 100, which is along the fine area. The result is presented in Table 12 and it can be seen that this rail does not meet the design requirements of 1.6 μm . The fine are is within specification but the rail as whole is not.

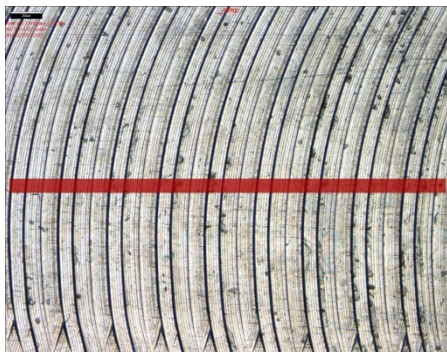


Figure 97: Measurement 1



Figure 98: Measurement 2

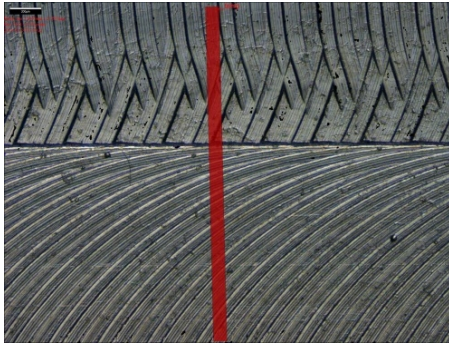


Figure 99: Measurement 3

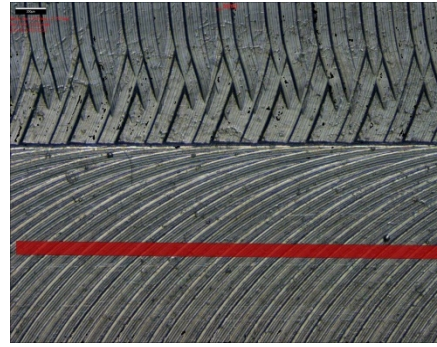


Figure 100: Measurement 4

Table 12: Measurement of top down milling on master thesis rail

Measurement	Measurement 1	Measurement 2	Measurement 3	Measurement 4
Ra [μm]	3.1653	3.2972	2.0496	1.1071
Mean [μm]	2.4298*			

The mean value is of no use since the real mean value will be governed by percentage of the different paths. As an approximation 55% of the top milled side is governed by the measurements with 3.2972 and 3.1653 and the rest 45 % by 1.1075. This would still yield a mean value above 1.6 μm . When there is significant difference between the two cuts it would be bad engineering to utilize the mean value. The roughness values, Ra, above are given as an average value from the peak and height of the valley, but that is more reasonable. A single peak can be worn down, but a large area will increase the friction significantly. This is still useful information for further production. The main difference in the roughness is thought to be the feed rate. This means polishing or a change in the manufacturing process would be required to achieve the goal of surface roughness less than 1.6 μm .

Chapter 6

6 DISCUSSION

The main outcome of the study is that NUTS has taken a major and important step forward towards launch. This has been made possible due the collective effort and development from the whole NUTS group. As each component is one step closer to its finished state, completion of more components can commence.

The primary structure has been manufactured and assembled. The prototype verifies the production of the structure in regard of quality and dimensions. The surface roughness of rails and standoff can be obtained with milling parameters set to appropriate values. The surface roughness can be visually controlled against rails with known surface roughness values. The jig for assembly of the structure worked according to plan and yielded results in accordance with the CDS. The LSS of the adhesive bond of CFRP has been tested and proved to be sufficiently strong for the application. This means the manufacturing of the test model can commence, and testing of the structure can be carried out in the near future.

All applications in the antenna module assembly have been through development and are tested separately in order to find improvements, and this gave valuable insight to the design process. By cutting the antenna elements with a water jet, the elements obtained the desired width throughout the length. The rough edges from the jet were overcome by redesigning the forming tool to have a shorter arc length than the width of the element. This made it possible to achieve better quality of the antenna elements, which implies higher rate of successful releases. Different configurations of the antenna module were prototyped to find the best design for the me-

chanical release mechanism. The latest solution was tested in the last prototype, with success. The electric release mechanism was through several prototypes and tests in order to find an applicable resistance wire in accordance with the electrical requirements. The chosen wire was put into the antenna module which was used in the antenna module test. The test verified the proposed solution for releasing of the antenna elements and strengthened the belief in it.

The secondary structure is designed and only awaits the final design of the backplane in order to set the distance between the PCB-cards. The distance governs the cuts needed in the braces of the secondary structure. The top trusses are ready to be milled out and to be made ready with helicoils. The inserts for the joints can be turned. The solar cell panel design is finished, thus the solar cells can be bought in and assembled onto PCB-cards. The ADCS module designs have been finalized and are ready for manufacturing.

6.1. Further work

In order to finish the NUTS satellite and get it ready for launch many components needs to be manufactured. The first thing which should be manufactured is the rail and standoffs. These are time consuming to mill and needs to be sent to Denmark for hard anodization. The manufacturing of the rails and standoff should be manufactured during the summer when the work load is low at the work shop. New CFRP-panels has to be made, and it has to be decided if material with TML less than 1% should be bought , or the material available shall undergo a thermal bake out test to verify the TML. A minimum of two sets of rail, standoffs and CFRP-panels should be made, one for test model and one for flight model.

The antenna module should be made in PEEK as soon as possible in order to run more test. The ADCS coils should be manufactured when cleared with the person in charge of the ADCS, the design is finished.

When all electrical components are chosen, it is possible to run a thermal analysis of the system and this should be completed. This has not been prioritized since the power usage and heat generated by each component has been unknown. If this is neglected the system has to trust its heat sensors and shut down the heat affected components.

Discussion

From vibration test real launch load can be obtained and the natural frequencies measured. This can then be utilized in analyses for further improvements of the mechanical design.

If the launch slot in 2015 is available all mechanical structure should be made as soon as possible and assembled in order to be tested. The wiring has been thought of but not tested and can become an issue.

Chapter 7

7 CONCLUSION

All parts in the CAD assembly are up to date with machine drawings for the components which can be produced. The adhesive lap shear strength has been tested, and according to calculations and Hexcel datasheet, should withstand thermal cycling due to different CTE values between aluminium and CFRP. A mechanical model has been made and the manufacturing methods of the primary structure are verified, can be copied for the test model. The antenna module assembly test worked as intended and should therefore be put into production for further testing with an improved test model. The NUTS project has moved one step closer to space.

8 REFERENCE

- [1] C. Nomme, "Mechanical Design," 2013.
- [2] N. gov, "Outgassing Data for Selecting Spacecraft Materials Online," 2008.
- [3] H. Hai, "Hårdaluksering."
- [4] S. Wernick, R. Pinner, and P. Sheasby, "The surface treatment and finishing of aluminium and its alloys," 1964.
- [5] D. Pignatelli, "CubeSat Design Specification Rev. 13 C," p. 41, 2013.
- [6] Huntsman, "Araldite® AV 138M-1 / Hardener HV 998," p. 4, 2009.
- [7] Hexcel, "HexPly® 6376C-905-36%," p. 4.
- [8] PhoneSat.
- [9] M. Rödelsperger, "Lightweight design of subsystem for satellite application," 2013.
- [10] K. Sandvik, "Develepment of Comosite and Polymere Material CubeSat Structure," 2012.
- [11] ISIS, "ISIPOD CubeSat Deployer."
- [12] J. Johannessen, *Tekniske tabeller*. [Oslo]: Cappelen, 2002.
- [13] Materion, "Heat Treating Copper Beryllium Parts."
- [14] C. D. Association. *Beryllium Copper*. Available: www.copperinfo.co.uk
- [15] C. D. A. Inc. *Beryllium Copper*. Available: http://www.copper.org/resources/properties/microstructure/be_cu.html
- [16] Materion, "Shape Distortion of High Strength Copper Beryllium during," Materion, Ed., ed.
- [17] J. Clark. (2002). *LE CHATELIER'S PRINCIPLE*. Available: <http://www.chemguide.co.uk/physical/equilibria/lechatelier.html>
- [18] Wikipedia. *Le Chateliers prinsipp*. Available: http://no.wikipedia.org/wiki/Le_Chateliers_prinsipp
- [19] Wikipedia. *Le Chatelier's principle*. Available: http://en.wikipedia.org/wiki/Le_Chatelier's_principle
- [20] F. Irgens, *Fomelsamling mekanikk*: Tapir, 1999.
- [21] Materion, "SAFETY PRACTICES FOR HEAT TREATING COPPER BERYLLIUM PARTS," 2008.
- [22] Materion, "Processing Copper Beryllium Alloys," 2011.
- [23] materion, "MATERIAL SAFETY DATA SHEET - NO. A29," 2011.
- [24] T. E. Toolbox. Available: http://www.engineeringtoolbox.com/linear-expansion-coefficients-d_95.html
- [25] Q. AG, "KETRON PEEK-100," vol. January 2003.
- [26] P. Plastics, "Thermal Properties of Plastic Materials."
- [27] A. Håland, "Development of mechanical structure for NUTS CubeSat," 2013.
- [28] ASTM, "Standard Test Method for Lap Shear Adhesion for Fiber Reinforced Plastic (FRP) Bonding," 2008.

Contents

1	Appendix 1	1
1.1.	Antenna Element Length.....	1
1.2.	Pre-preg density	2
1.3.	Burn off points redundancy	3
1.4.	Static hand calculation on truss in secondary structure	7
1.5.	CTE and fatigue	8
1.6.	Measurements of satellite.....	9
2	Appendix 2	19
2.1.	Primary structure.....	19
2.1.1.	Rail	20
2.1.2.	Standoff top	21
2.1.3.	Standoff separation spring.....	22
2.2.1.	CFRP-Panel	25
2.3.	Secondary structure.....	26
2.3.1.	Truss.....	27
2.3.2.	Brace.....	28
2.3.3.	Brace mirrored.....	29
2.3.4.	Insert.....	30
2.4.	Antenna module assembly	31
2.4.1.	Antenna module	31
2.4.2.	Gate	32
2.4.3.	Bushing.....	33
2.4.4.	PCB bottom	34
2.5.	Solar cell.....	35

Reference

2.5.1.	PCB solar cell interface	35
2.5.2.	Solar cell interface assembly	37
2.5.3.	PCB solar cell side	38
2.5.4.	Solar cell side assembly	39
2.5.5.	PCB solar cell top.....	40
2.5.6.	Solar cell top assembly.....	41
2.6.	Adhesive jig.....	42
2.6.1.	Bottom plate.....	42
2.6.2.	Top plate.....	43
2.6.3.	Wall.....	44
2.6.4.	Endplate.....	45
2.7.	ADCS	46
2.7.1.	ADCS top	47
2.7.2.	ADCS left side.....	48
2.7.3.	ADCS right side.....	49
3	Appendix 3	50
3.1.	Lap shear test thickness	50
3.2.	Adhesive.....	51
3.3.	CDS	55
3.4.	PEEK	92
3.5.	Pre-Preg	93
3.6.	ISIS.....	97
3.7.	BeCU	100
4	Appendix 4	109
4.1.	HMS.....	109

1 APPENDIX 1

1.1. Antenna Element Length

$$c=f \times \lambda$$

c = speed of light

f = frequency

λ = wave length = L

$$L1 = \text{Wave length 1 mm}$$

$$L2 = \text{Wave length 2 mm}$$

$$Le1 = \text{Element 1 length mm}$$

$$Le2 = \text{Element 2 length mm}$$

$$c = 300000000 \text{ m/s}$$

$$f1 = 437 \text{ MHz}$$

$$f2 = 145 \text{ MHz}$$

$$L1=c \times f1 = 686.50 \text{ mm}$$

$$L2=c \times f2 = 2,068.97 \text{ mm}$$

$$Le1=L1 / (2 \times 2) = 171.62 \text{ mm}$$

$$Le2=L2 / (2 \times 2) = 517.24 \text{ mm}$$

Appendix 1

1.2. Pre-preg density

Pre-preg mass and density

Fibre density	x	1.770 g/cm ³	
Resin density	y	1.330 g/cm ³	
Composite density	c1	1.612 g/cm ³	
Ply thickness		0.281 mm	
Thickness of 4 plies autoclave	t1	1.124 mm	
Thickness of 4 plies compression moulding	t2	0.970 mm	
fibre content	x1	64.00%	
Resin content	y1	36.00%	
Thickness fibre content	xt1	0.719 mm	
Thickness resin content	yt1	0.405 mm	
Thickness fibre content	xt1 equal to xt2	0.719 mm	Only loss in resin content
Thickness resin content	yt2	0.251 mm	
fibre content	xt2	74.16%	
Resin content	yt2	25.84%	
Composite density	c2	1.656 g/cm³	
Approximate volume of 1 CFRP-panel		13,228.000 mm ²	
Original mass		21.318 g	
Approximate mass of 1 CFRP-panel		21.910 g	
Density increase		2.77 %	
		pre	
CFRP-Panel two cut-outs	v01	13,371.41 mm ³	
Calculated mass of 1 panel		22.15 g	
CFRP-Panel three cut-outs	v01	12,957.25 mm ³	
Calculated mass of 1 panel		21.46 g	
Measured Mass of 1 panel		21.25 g	

1.3. Burn off points redundancy

4 burn off points with 2 burn offs

- Burn offs are independent
- An antenna element is dependent on at least one burn offs to function
- An radio is dependent on both antennas to be released
- To obtain radio contact with earth, at least one radio needs to function

$$P(\text{Antenna}) =$$

$$P(A1 \cup A2) = P(A1) + P(A2) - P(A1 \cap A2)$$

$$P(A1 \cap A2) = P(A1) * P(A2)$$

$$P(\text{Radio}) =$$

$$P(\text{AntennaA} \cap \text{AntennaB}) = P(\text{AntennaA}) * P(\text{AntennaB})$$

$$P(\text{Earth}) =$$

$$P(\text{Radio1} \cup \text{Radio2}) = P(\text{Radio1}) + P(\text{Radio2}) - P(\text{Radio1} \cap \text{Radio2})$$

$$P(\text{Radio1} \cap \text{Radio2}) = P(\text{Radio1}) * P(\text{Radio2})$$

2 burn off points with 2 burn offs

$$P(\text{Radio1}) =$$

$$P(A1 \cup A2) = P(A1) + P(A2) - P(A1 \cap A2)$$

$$P(A1 \cap A2) = P(A1) * P(A2)$$

$$P(\text{Earth}) =$$

$$P(\text{Radio1} \cup \text{Radio2}) = P(\text{Radio1}) + P(\text{Radio2}) - P(\text{Radio1} \cap \text{Radio2})$$

$$P(\text{Radio1} \cap \text{Radio2}) = P(\text{Radio1}) * P(\text{Radio2})$$

Appendix 1

1 burn off point with two burn off points

$$P(\text{Earth}) =$$

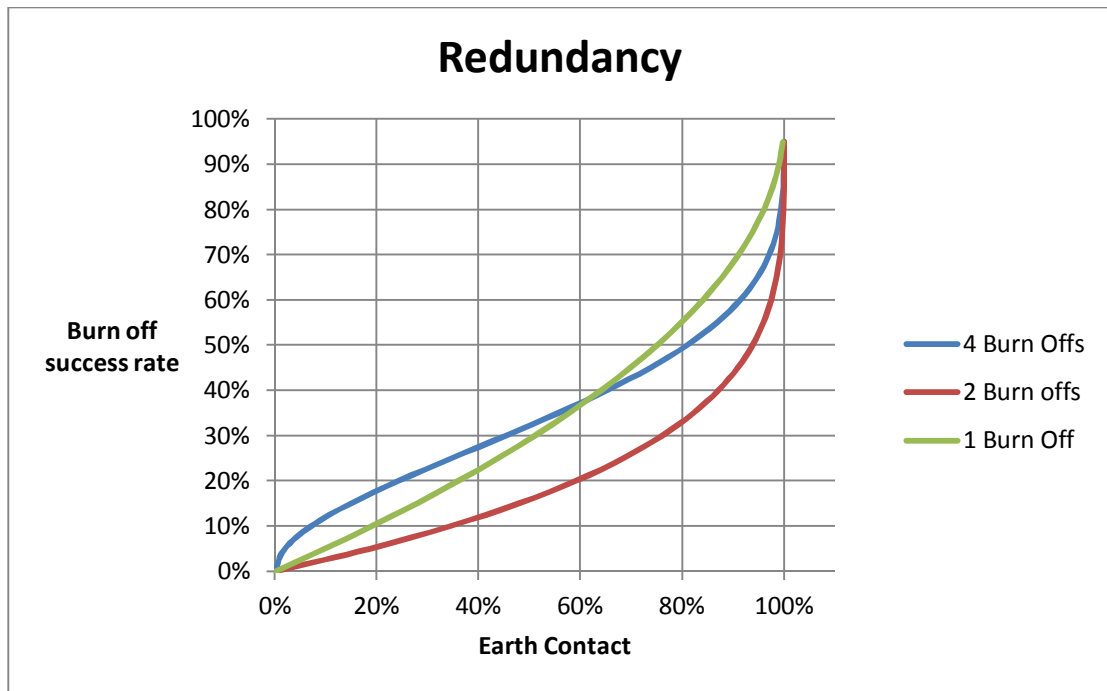
$$P(A1 \cup A2) = P(A1) + P(A2) - P(A1 \cap A2)$$

$$P(A1 \cap A2) = P(A1) * P(A2)$$

Burn off success	Antenna A	Radio 1	Earth contact 4 burn offs
0	0 %	0 %	0 %
0,05	10 %	1 %	2 %
0,1	19 %	4 %	7 %
0,15	28 %	8 %	15 %
0,2	36 %	13 %	24 %
0,25	44 %	19 %	35 %
0,3	51 %	26 %	45 %
0,35	58 %	33 %	56 %
0,4	64 %	41 %	65 %
0,45	70 %	49 %	74 %
0,5	75 %	56 %	81 %
0,55	80 %	64 %	87 %
0,6	84 %	71 %	91 %
0,65	88 %	77 %	95 %
0,7	91 %	83 %	97 %
0,75	94 %	88 %	99 %
0,8	96 %	92 %	99 %
0,85	98 %	96 %	100 %
0,9	99 %	98 %	100 %
0,95	100 %	100 %	100 %
1	100 %	100 %	100 %

Appendix 1

Burn off success	Radio 1	Earth contact 2 burn offs	Burn off success	Earth 1 burn off Contact
0	0 %	0 %	0	0 %
0,05	10 %	19 %	0,05	10 %
0,1	19 %	34 %	0,1	19 %
0,15	28 %	48 %	0,15	28 %
0,2	36 %	59 %	0,2	36 %
0,25	44 %	68 %	0,25	44 %
0,3	51 %	76 %	0,3	51 %
0,35	58 %	82 %	0,35	58 %
0,4	64 %	87 %	0,4	64 %
0,45	70 %	91 %	0,45	70 %
0,5	75 %	94 %	0,5	75 %
0,55	80 %	96 %	0,55	80 %
0,6	84 %	97 %	0,6	84 %
0,65	88 %	98 %	0,65	88 %
0,7	91 %	99 %	0,7	91 %
0,75	94 %	100 %	0,75	94 %
0,8	96 %	100 %	0,8	96 %
0,85	98 %	100 %	0,85	98 %
0,9	99 %	100 %	0,9	99 %
0,95	100 %	100 %	0,95	100 %
1	100 %	100 %	1	100 %

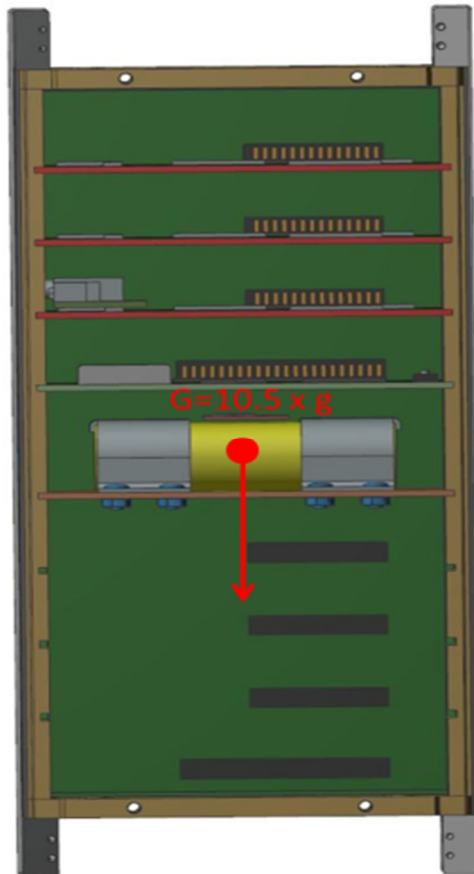


Appendix 1

1.4. Static hand calculation on truss in secondary structure

The truss is constrained by the standoff pieces in primary structure. The contact area between standoff and truss is 6.5 x 6.5 mm in each corner. The total mass of structure is 2.33 kg, this is the most mass the acceleration can expose onto the secondary structure, in reality it will be less. The most stress exposed situation is when the Z axis is parallel with LV

Compressive strength of PEEK	29		MPa
Design acceleration	10.5		g
Mass of structure	2.33		kg
Contact surface	6.5 x 6.5 mm	42.25	mm ²
A	4 x 625	169	mm ²
	g	9.81	m/s ²
Newton 1. law	F=ma		
Compressional stress	P=F/A		
Stress in truss from stand offs	$P = 2.33 \times 10.5 \times 9.81 / 169$	1.42012810650888	MPa



Appendix 1

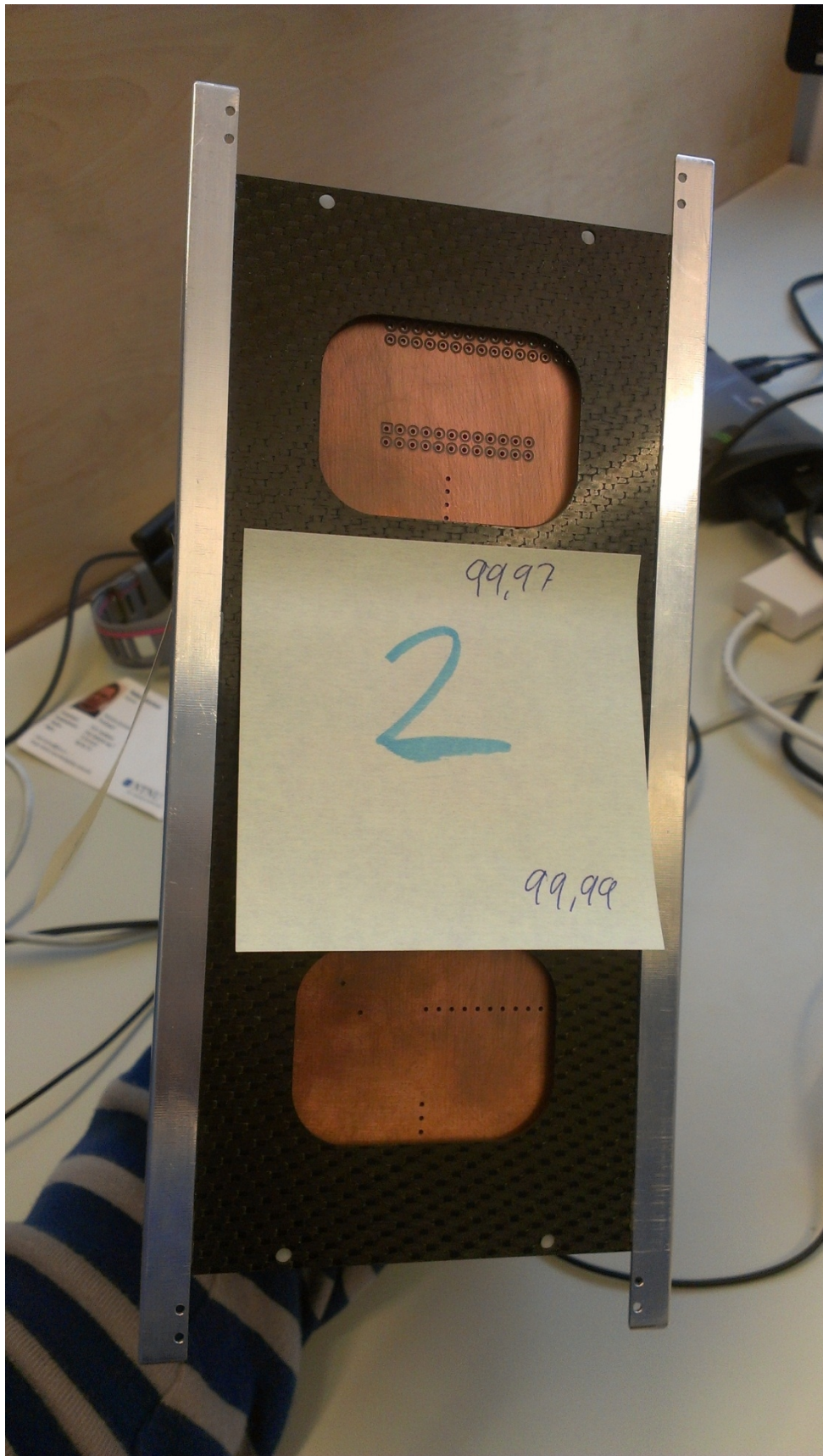
1.5. CTE and fatigue

The adhesives CTE value is higher than the one of CFRP. Therefore this is the most critical. The design temperature is 85° C, the start temperature is 22° C. The length is set to be half the adhesive joint length of 196mm. The shear modulus is given stated in the data sheet to be 400 MPa at 75° C and 100 MPa at 100° C. Therefore an estimated value has been found. The datasheet states the adhesive will withstand 10^7 cycles if the load is less than 25% of static fal

Material	CTE	Shear modulus	LO	T0	T85
CFRP	0		98	22	85
Adhesive	0,000067	E85* E75=400, E100=100	98	22	85
Displacement		$\Delta L=L0\alpha(T85-T0)$	0,413658	[mm]	
True strain		$e= \ln ((L0+\Delta L)/L0)$	0,004212		
E85*		$E75-E100((T85-T75)/(T100-T85))$	333,3333	[MPa]	
Shear stress		$Ss= e * E85^*$	1,404039	[MPa]	
25% of static load > 10^7 cycles to failure					
Required lap shear strength		$LSS=Ss / 0.25$	5,616155	[MPa]	
NUTS cycle/ year		$N_{cycle}=2*14*365$	10220	[cycle/year]	
Adhesive lifetime in years		$10^7 / 10\ 220$	978,4736	[year]	

1.6. Measurements of satellite

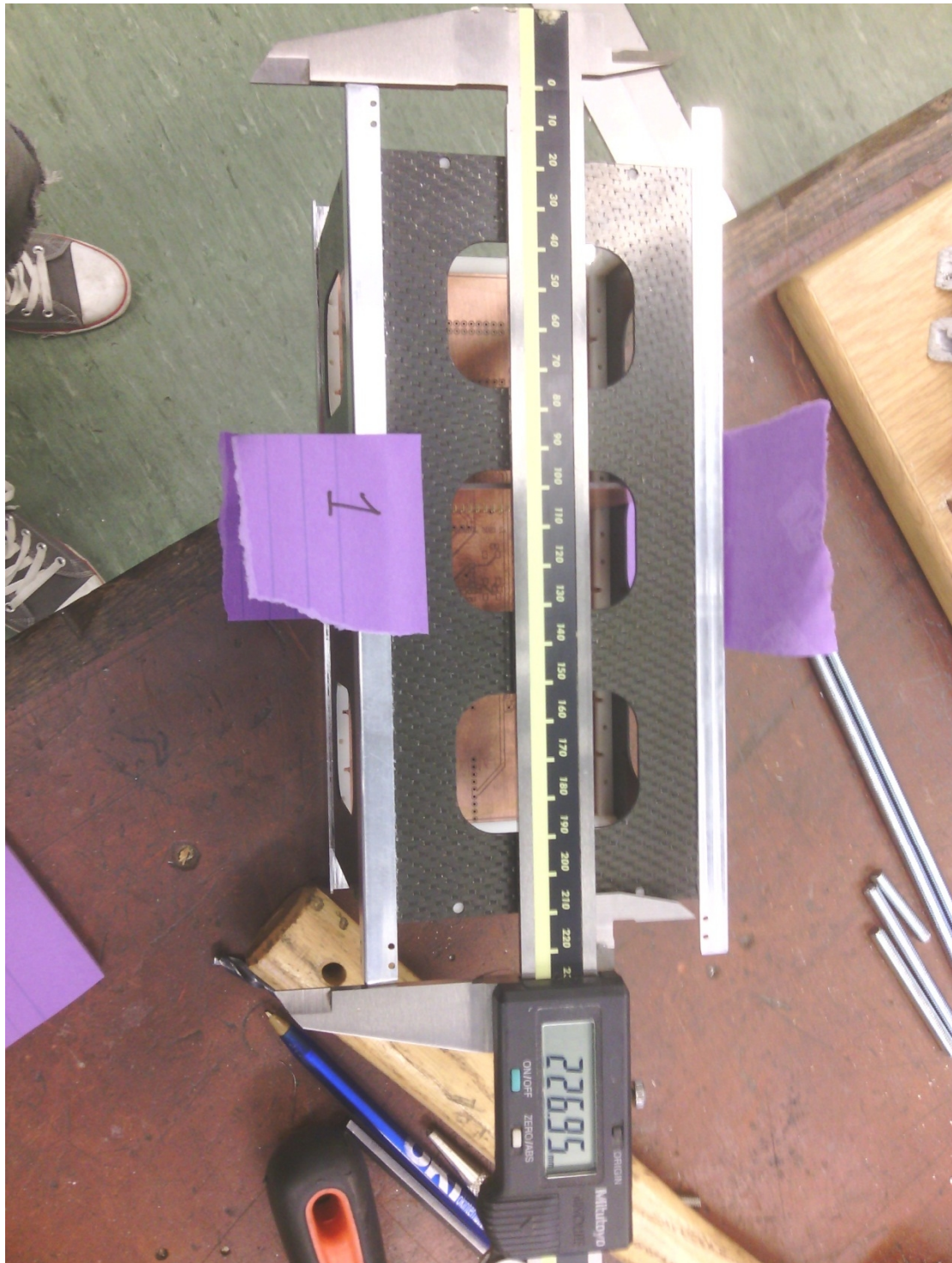








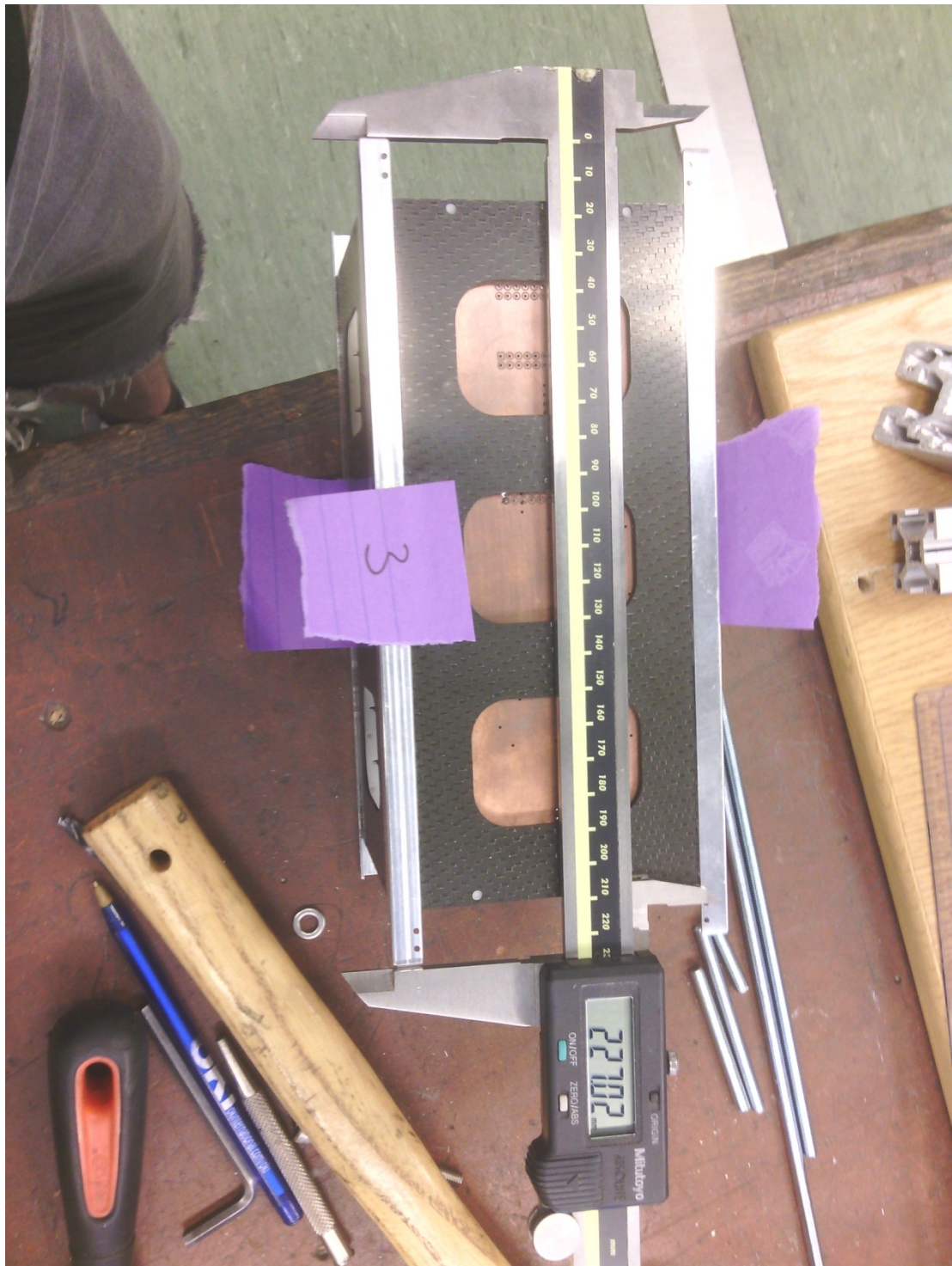
Appendix 1



Appendix 1



Appendix 1



Appendix 1

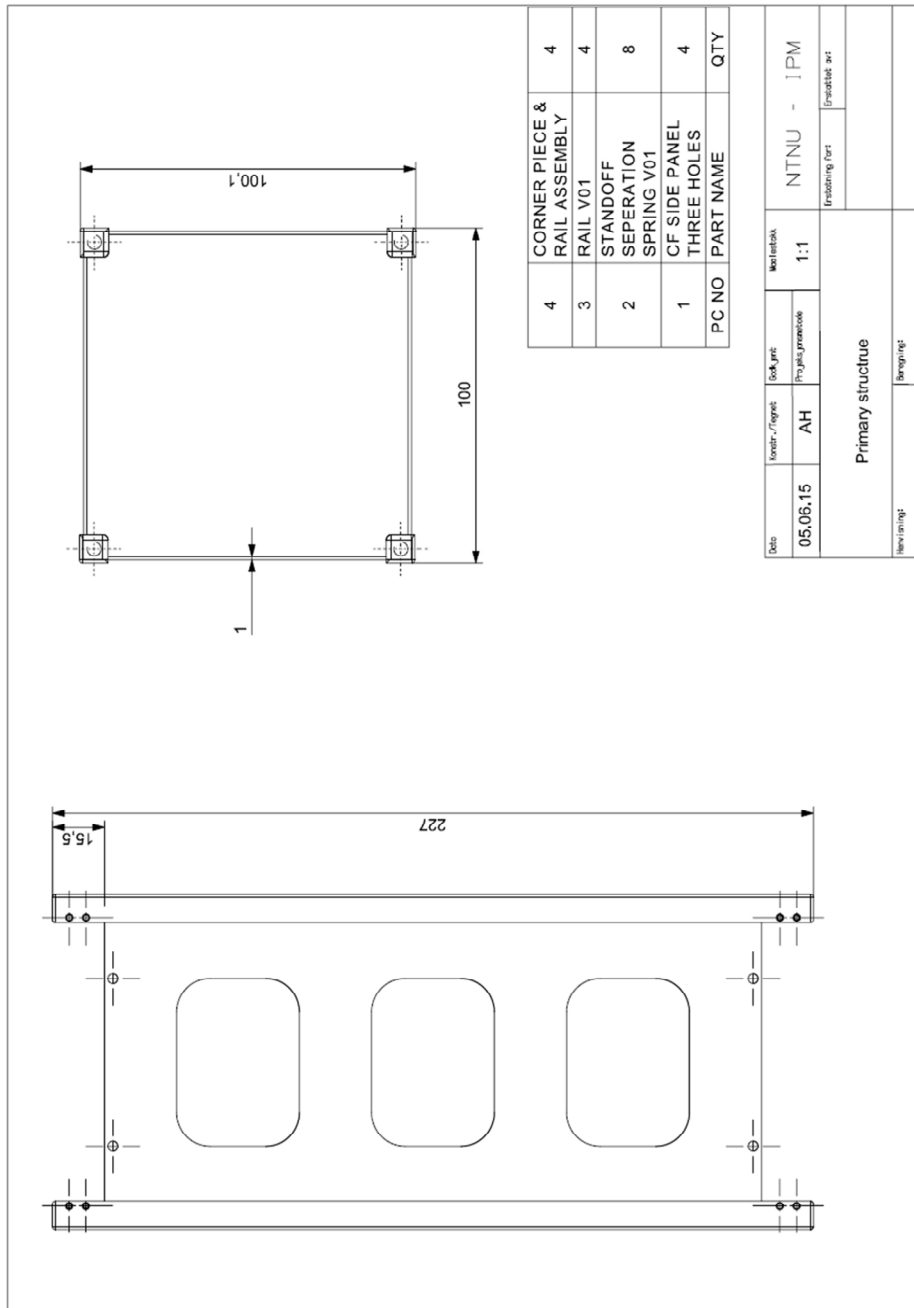






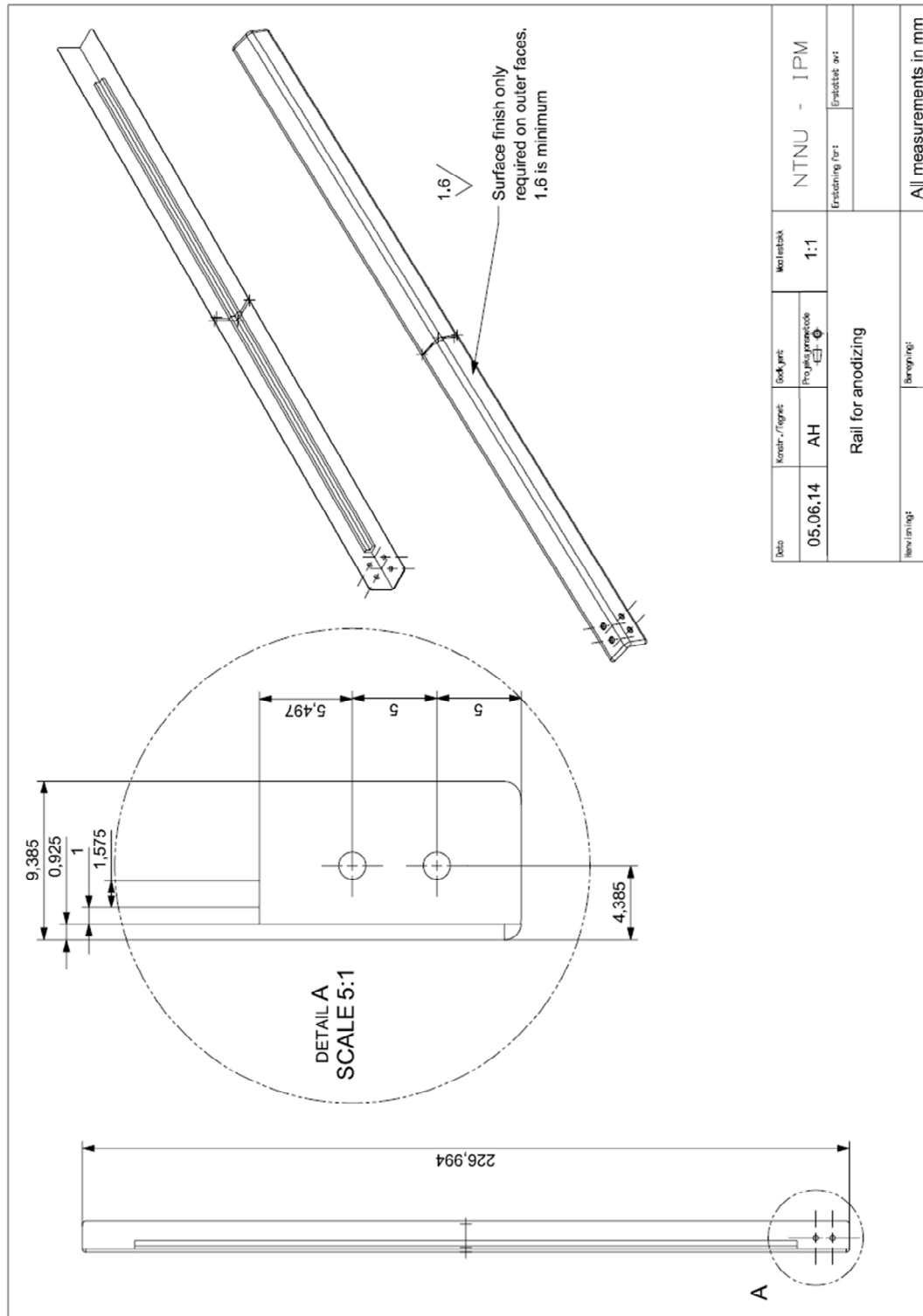
2 APPENDIX 2

2.1. Primary structure



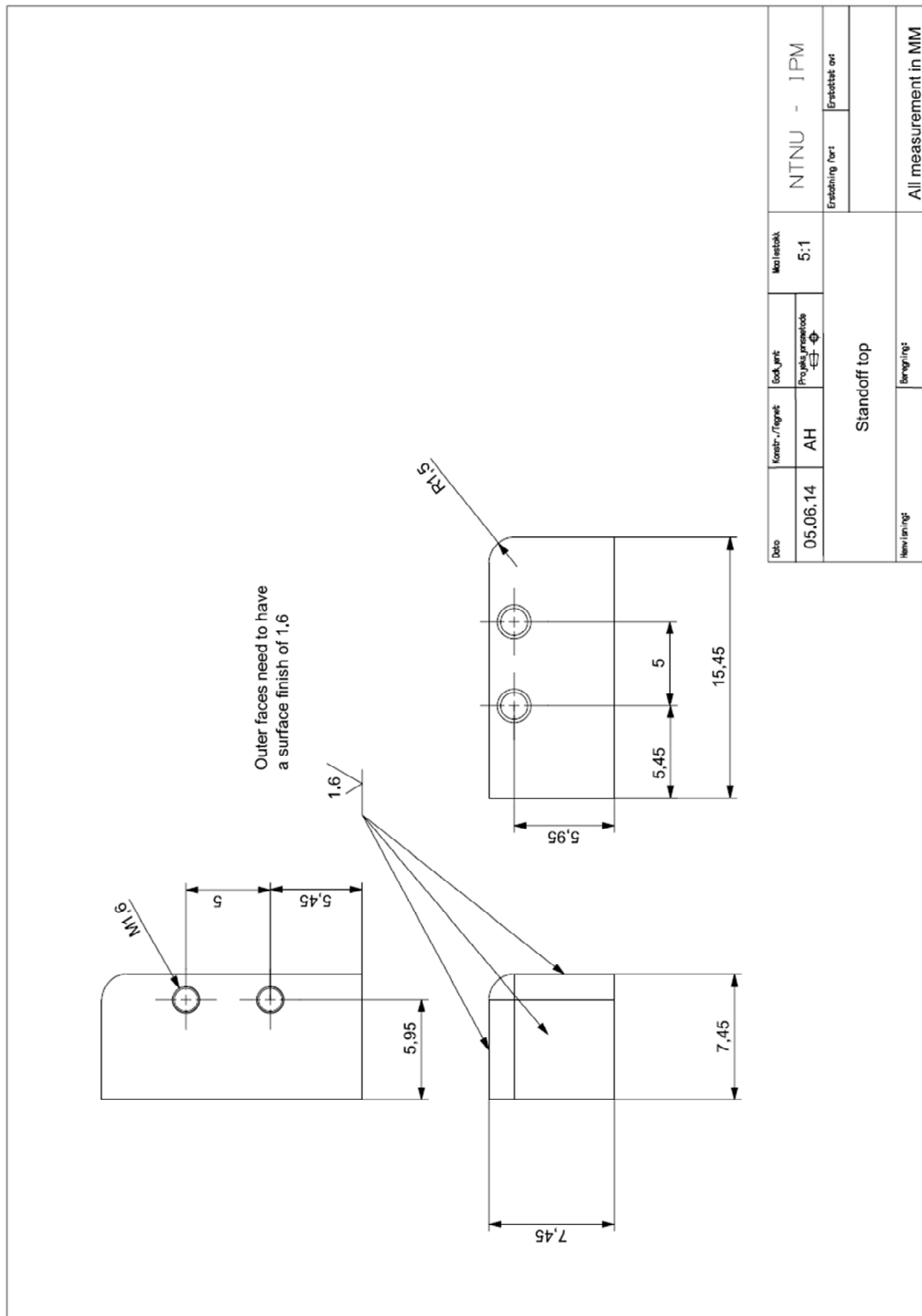
Appendix 2

2.1.1. Rail



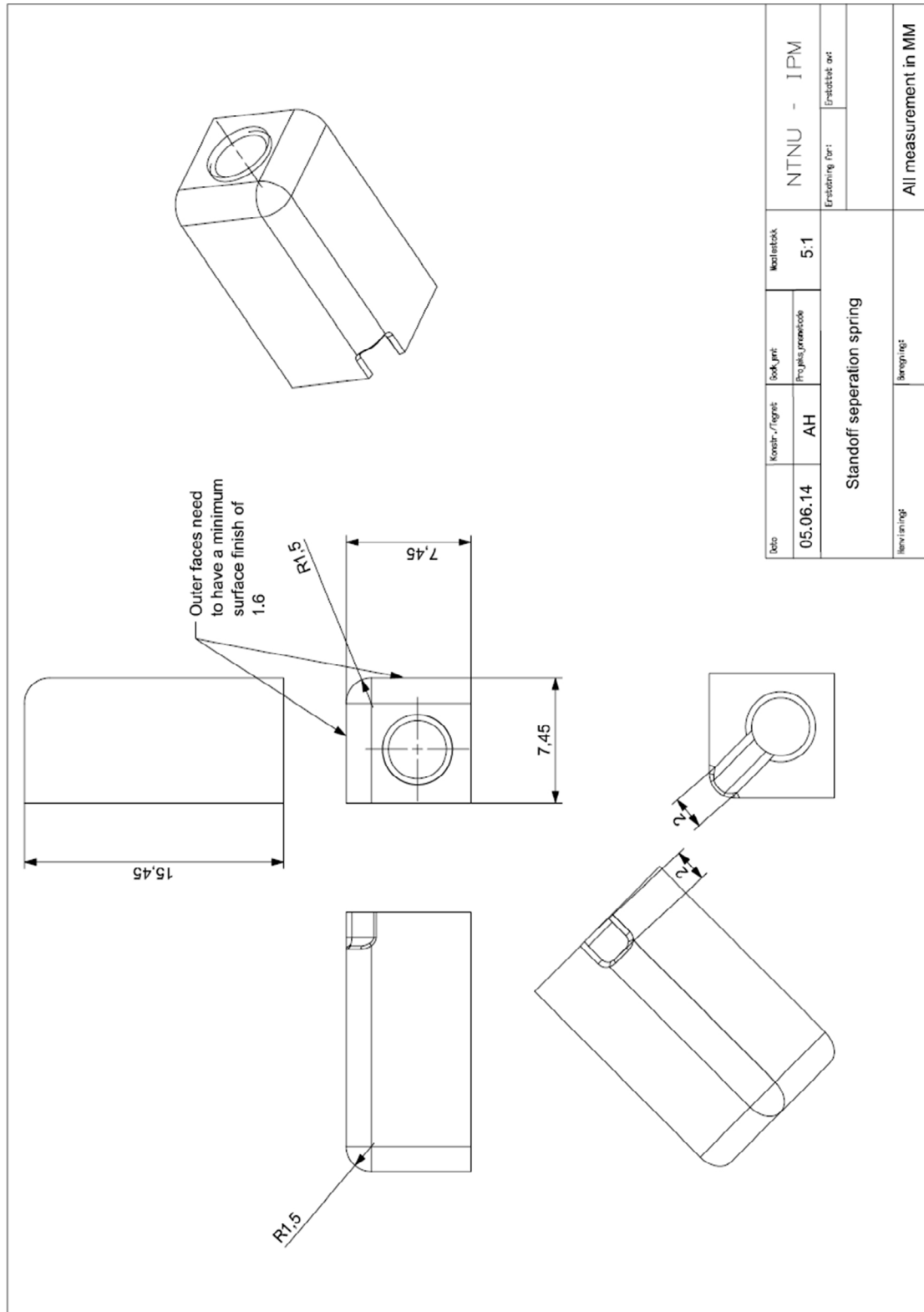
Appendix 2

2.1.2. Standoff top



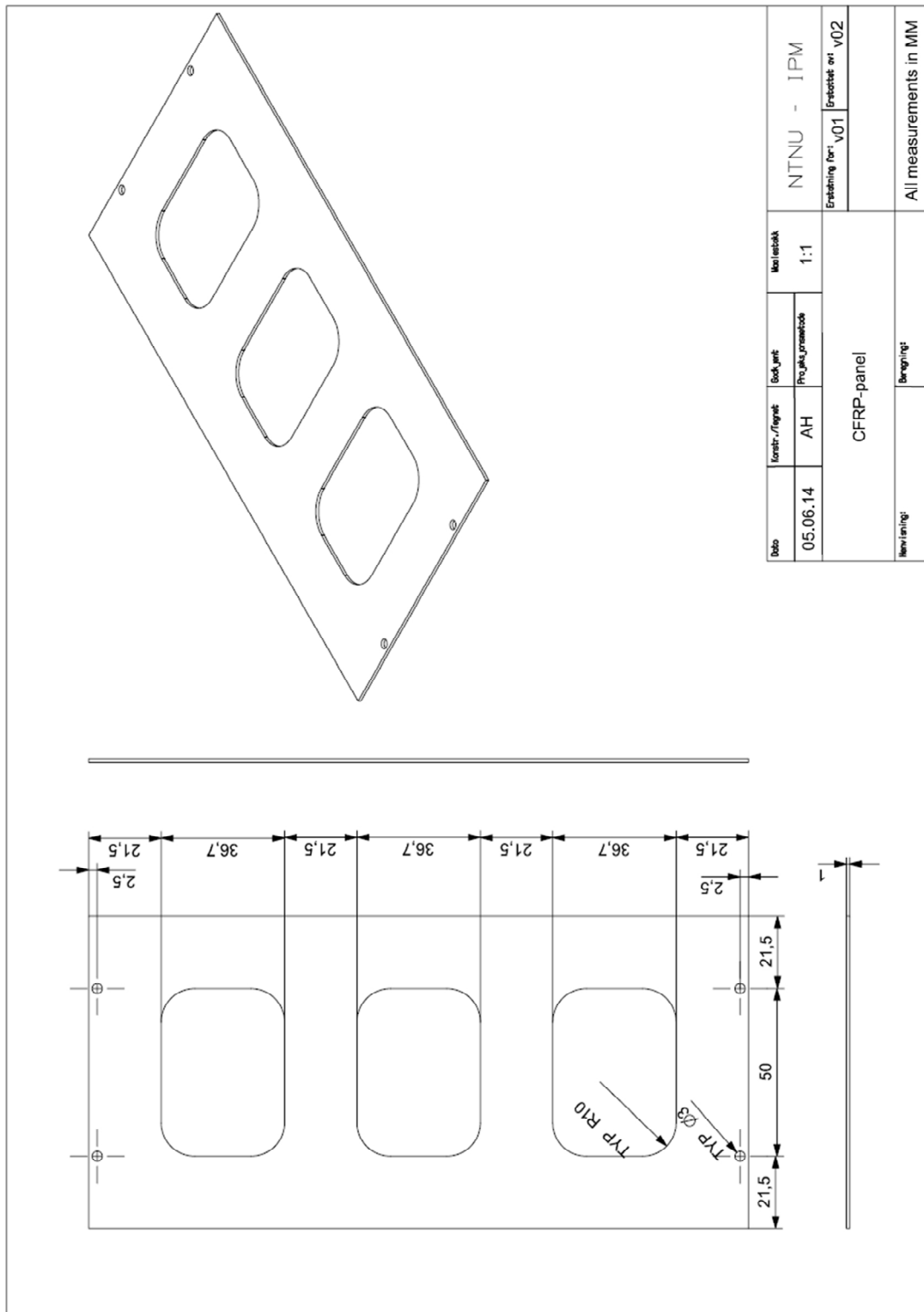
Appendix 2

2.1.3. Standoff separation spring

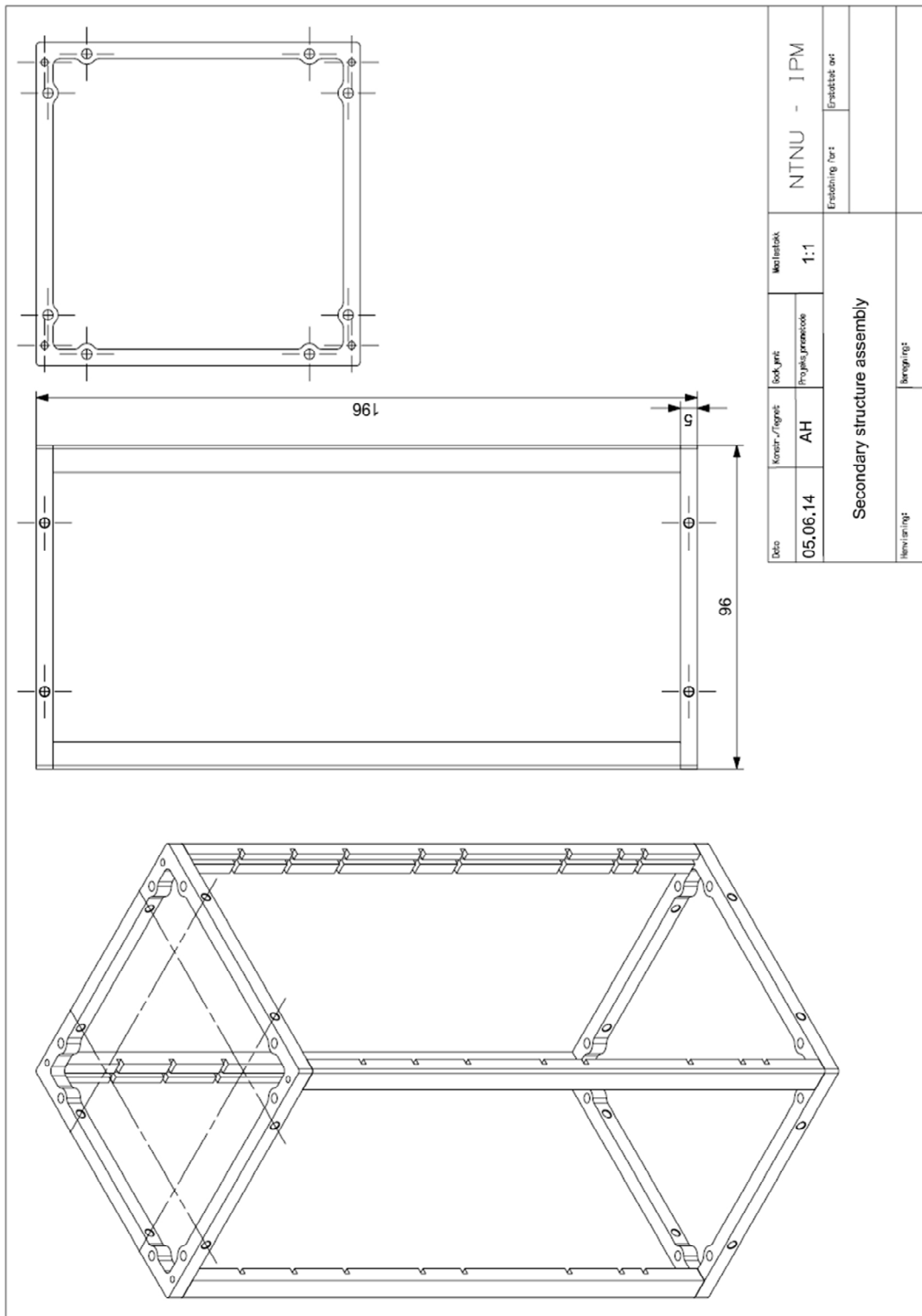


Appendix 2

2.2.1. CFRP-Panel

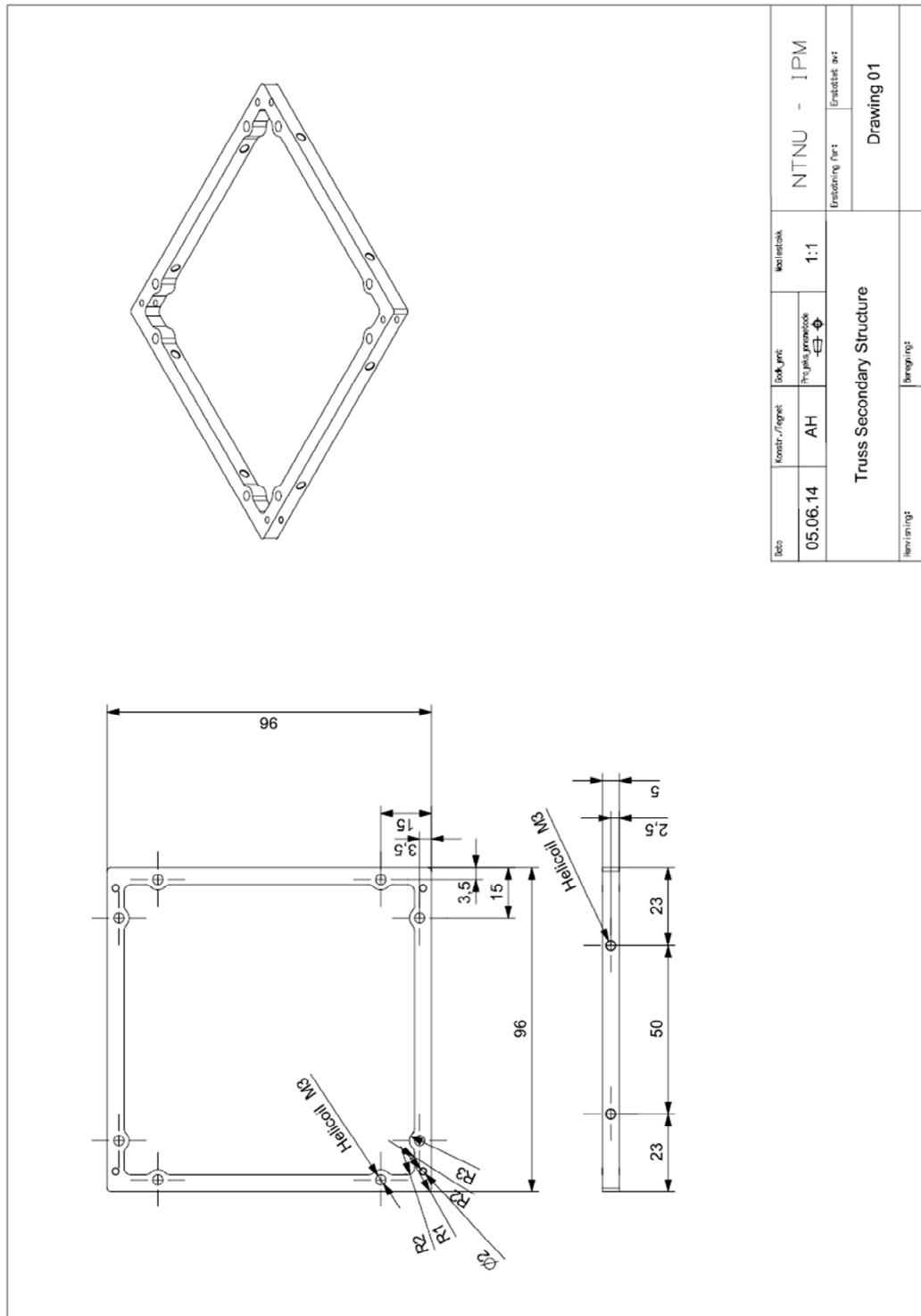


2.3. Secondary structure



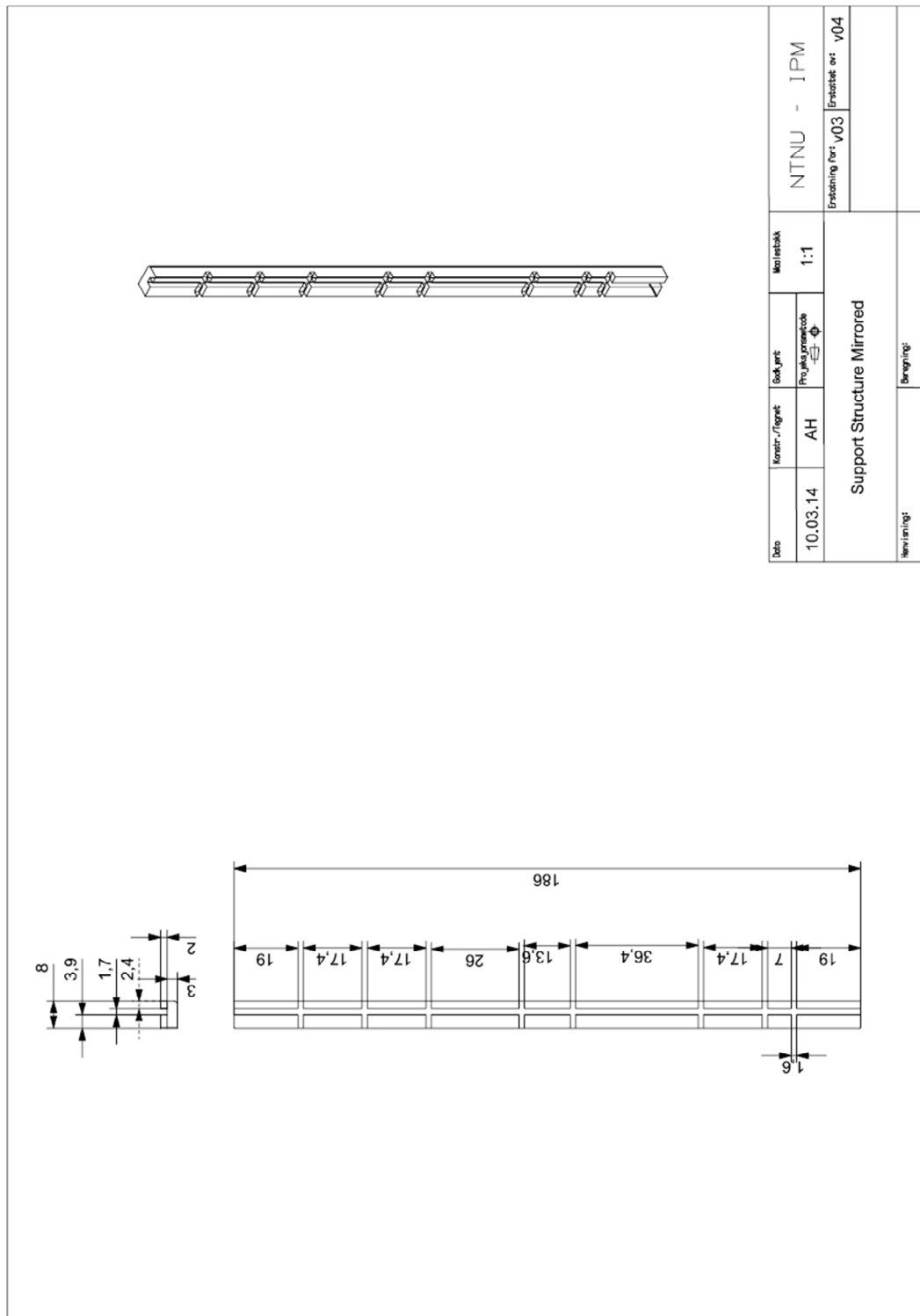
Appendix 2

2.3.1. Truss



Appendix 2

2.3.3. Brace mirrored



Appendix 2

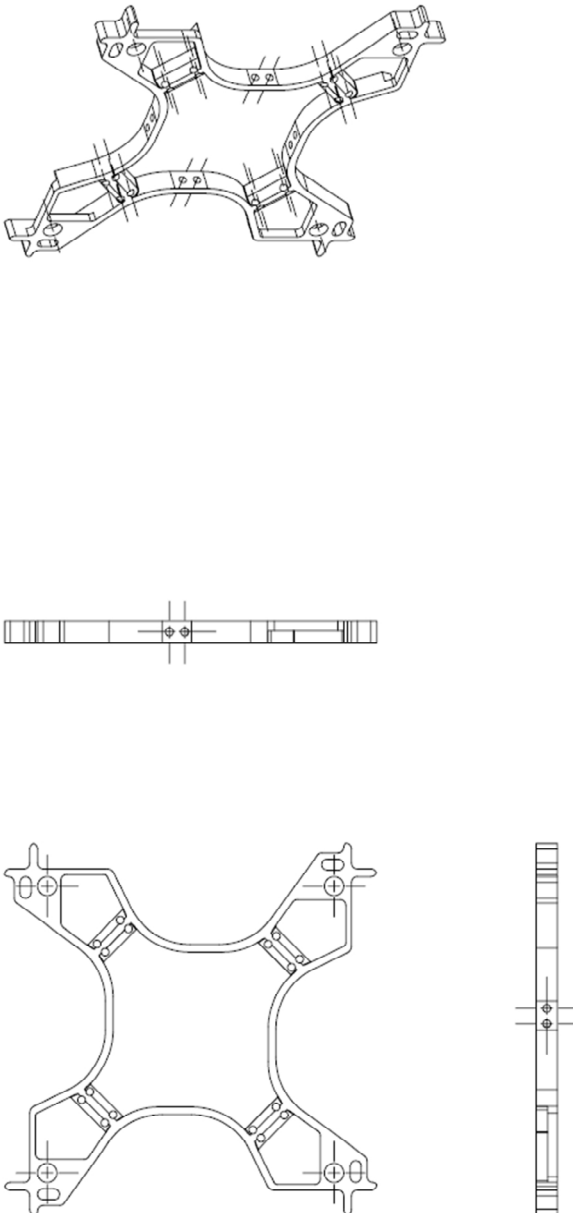
2.3.4. Insert

Date	Konstr./Tegnet	Isk. ynt.	Målestok	NTNU - IPM
0.5.06.14	AH	Projektnummer ϕ	1:1	Erstatning for: Erstatte av:
Insert for Secondary Structure				Drawing 01
Navn/ingr:			All measurements in MM	

Appendix 2

2.4. Antenna module assembly

2.4.1. Antenna module

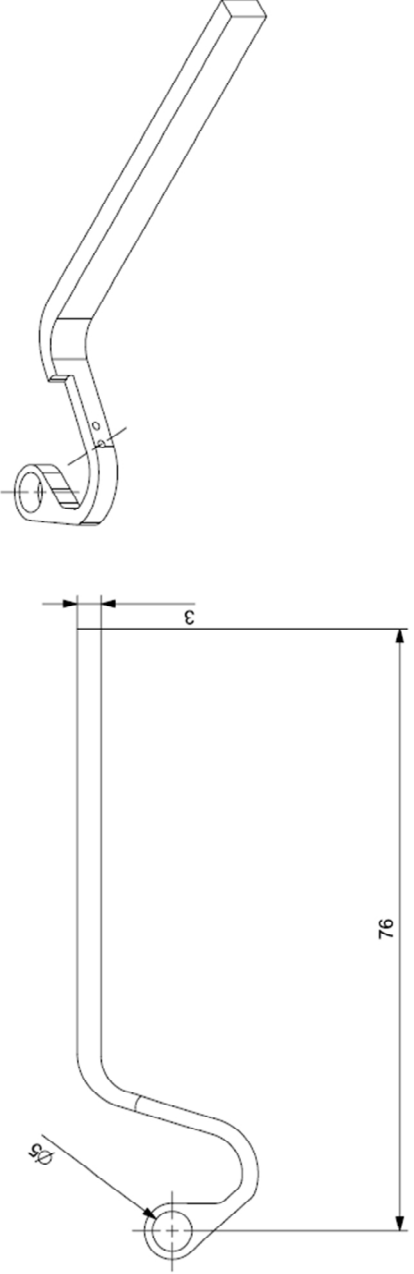


To be CNC milled from NX-file

Date	03.03.14	Kreier-/Figel	AH	Lock-ymt	Project name/code	Masterbak	1:1	NTNU - IPM
				Antenna Module v05		Erstatning for V03 Created: ant V05		NUTS
Benevning:				Benevning:				

Appendix 2

2.4.2. Gate

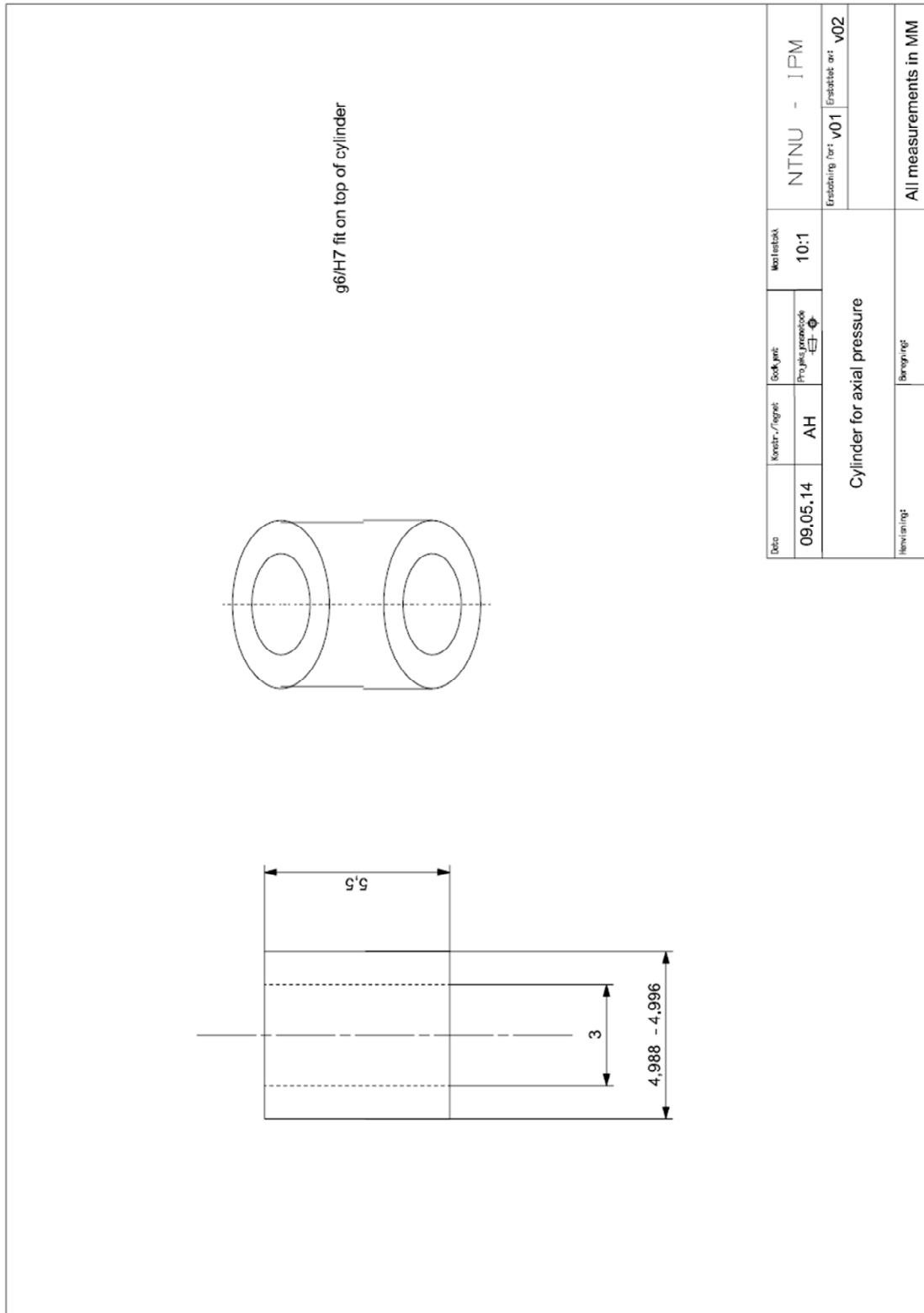


To be CNC milled from NX-file

Date	Konstr./revisj:	Skj. gr:	Ma. tittel	NTNU - IPM
05.06.14	AH	Prosjektpr. kode	1:1	Erstatning for: Erstatlet av:
Gate				
Rev. i anngi:	Beregning:			

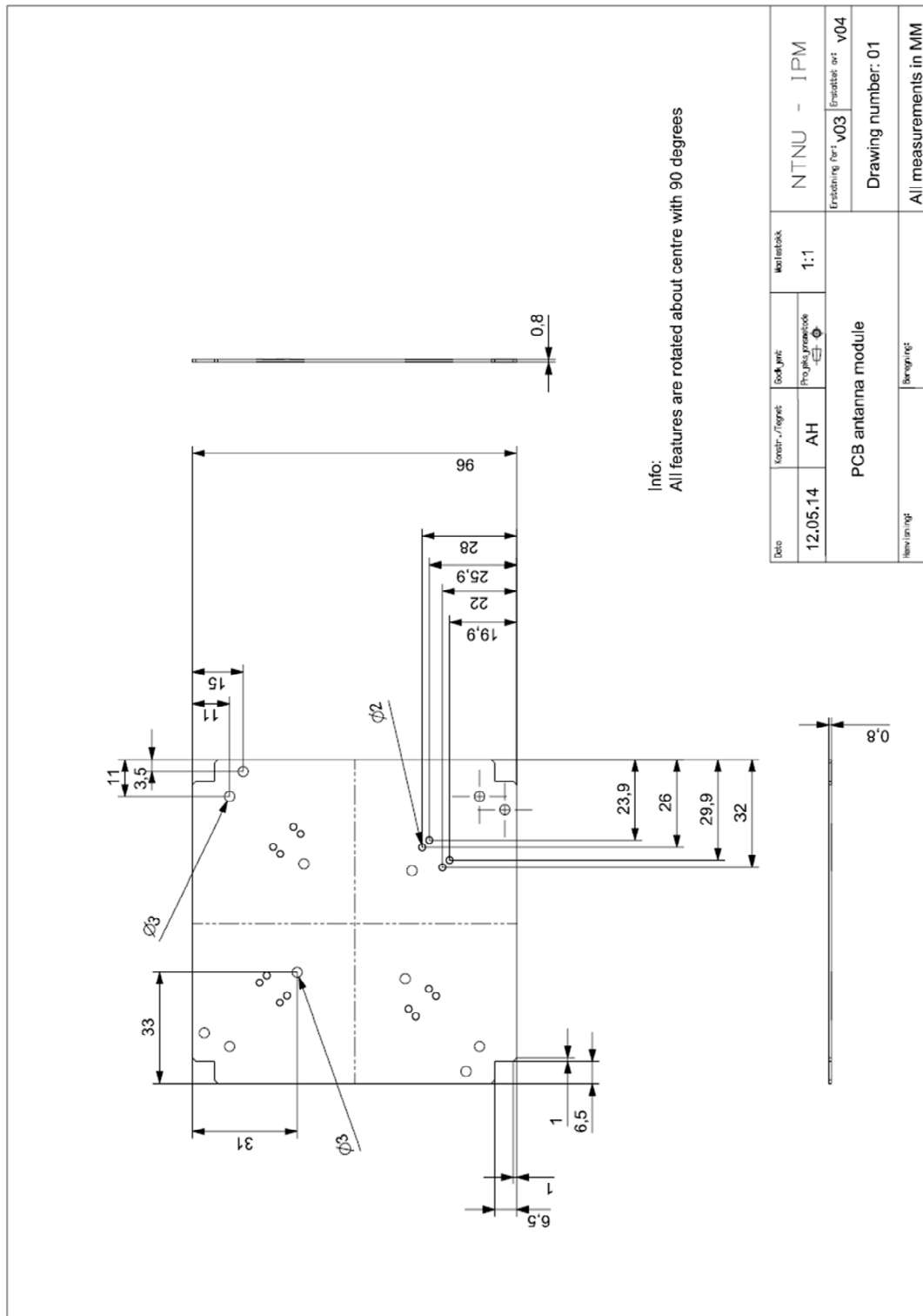
Appendix 2

2.4.3. Bushing



Appendix 2

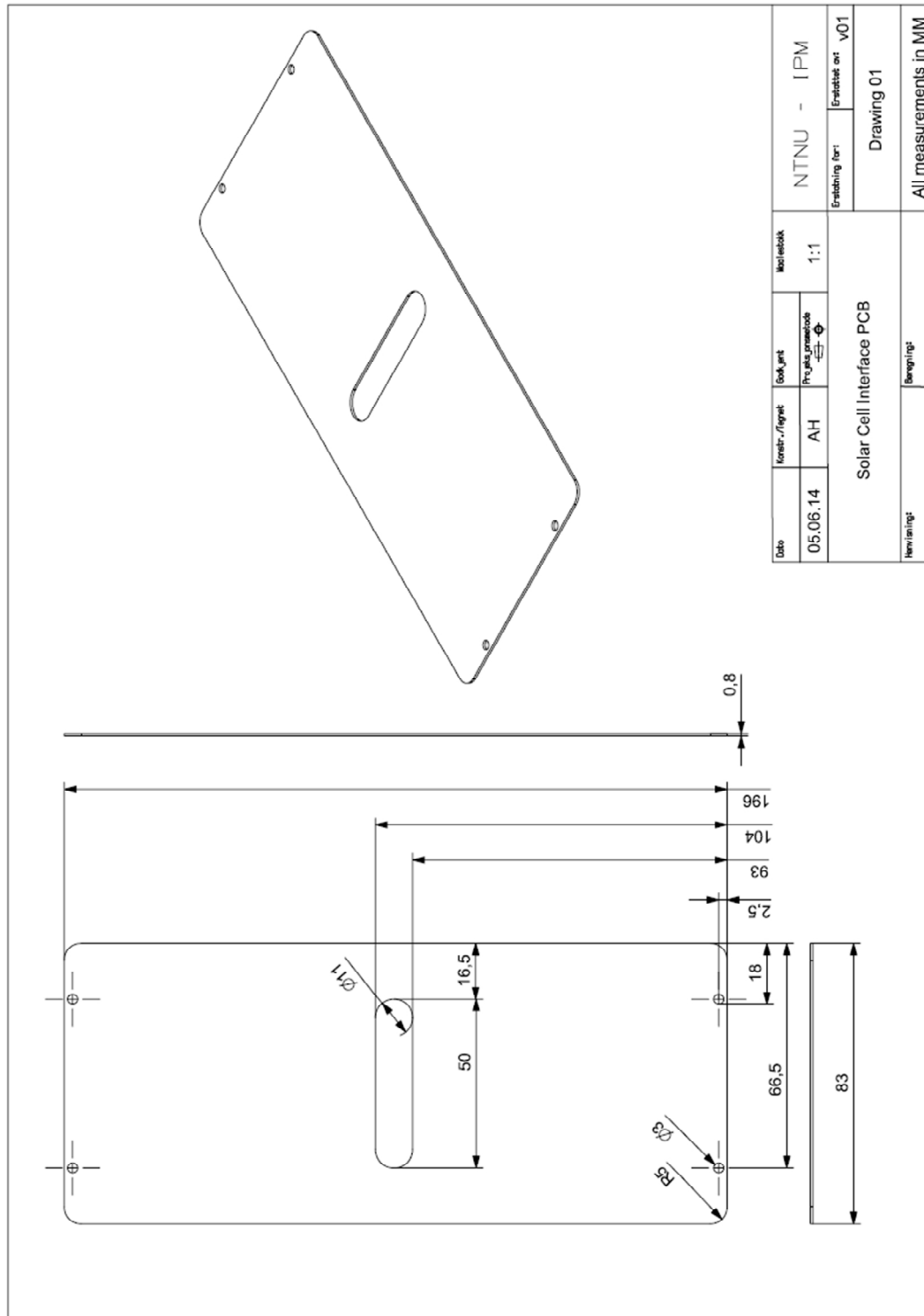
2.4.4. PCB bottom



Appendix 2

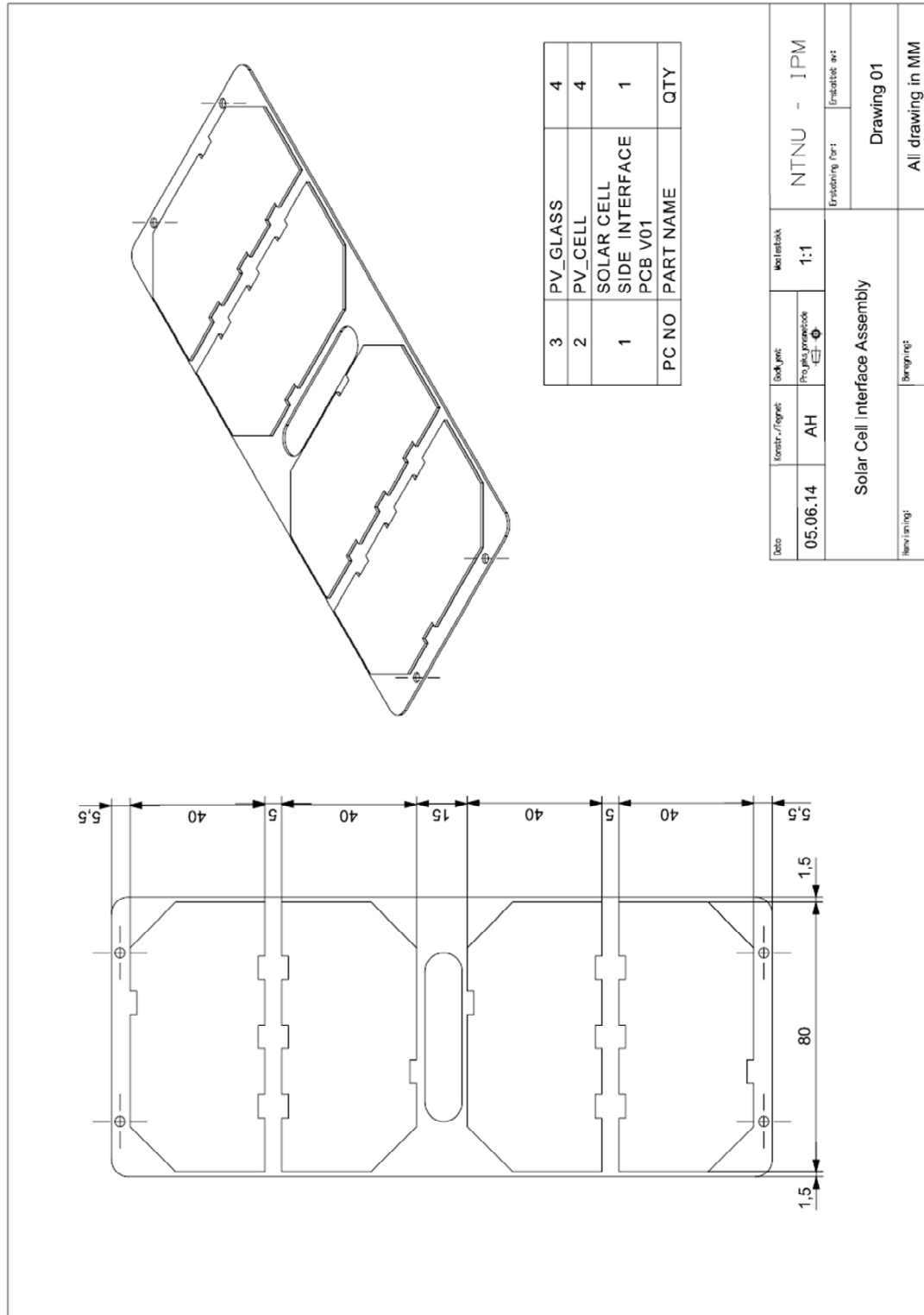
2.5. Solar cell

2.5.1. PCB solar cell interface



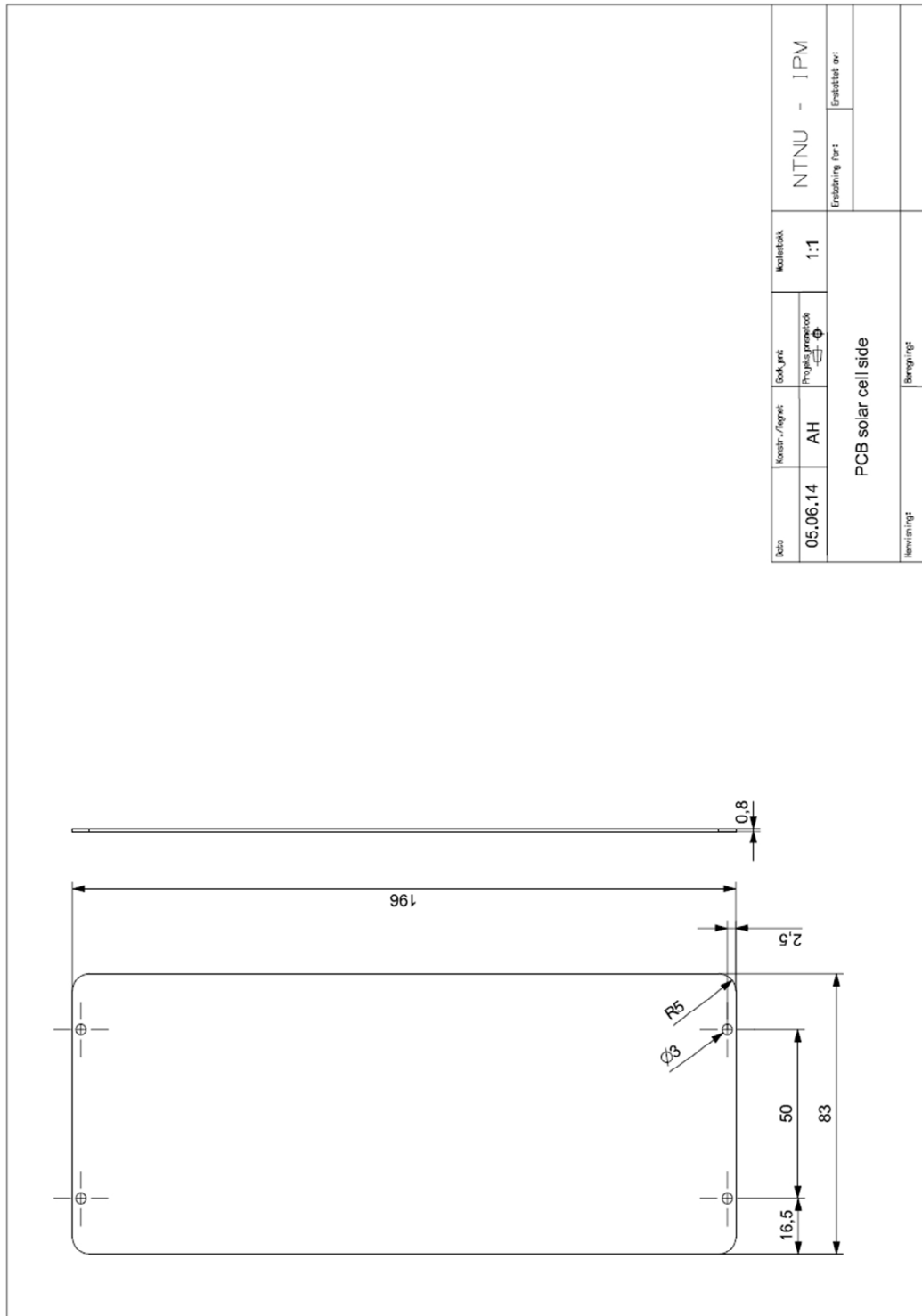
Appendix 2

2.5.2. Solar cell interface assembly

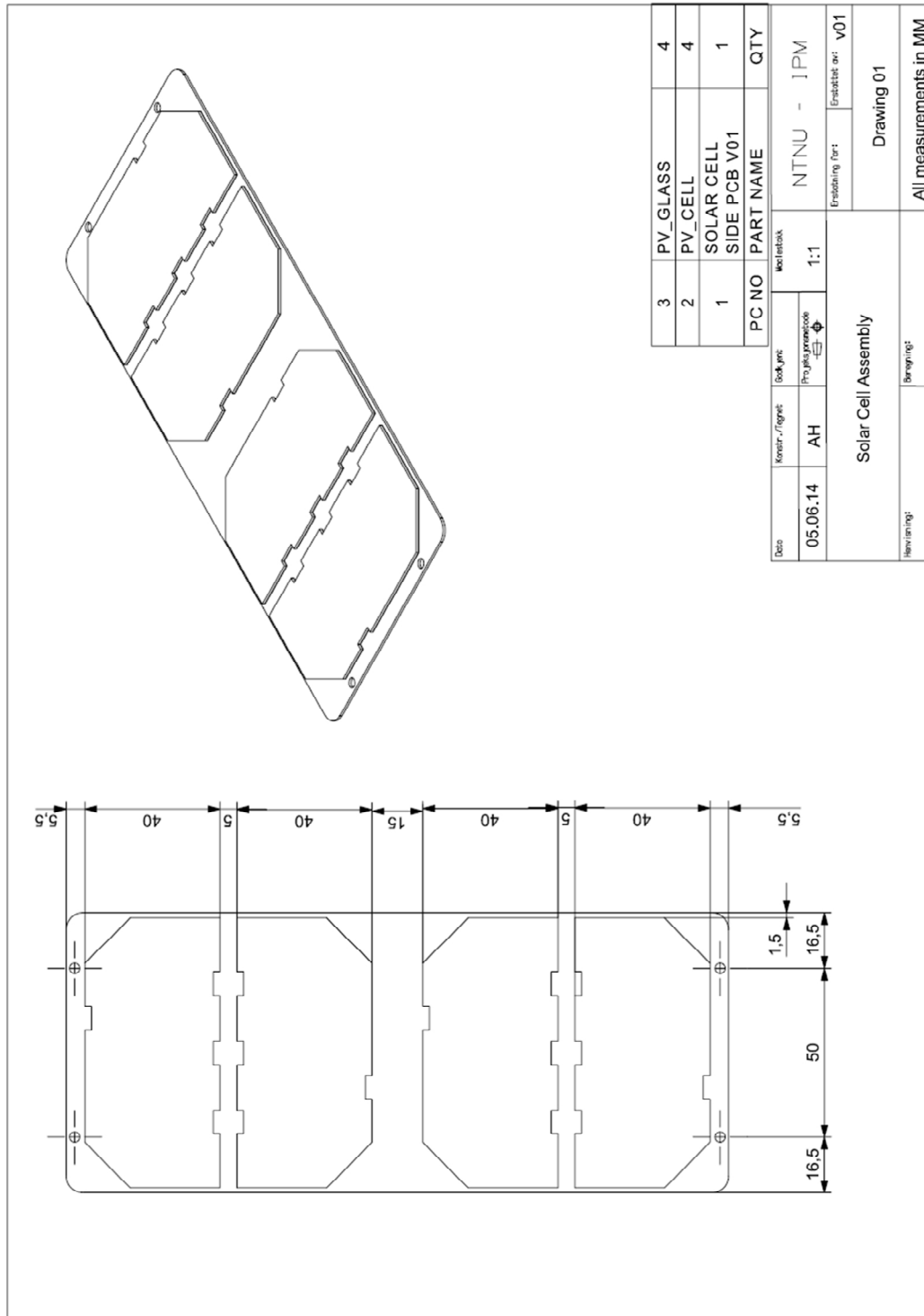


Appendix 2

2.5.3. PCB solar cell side

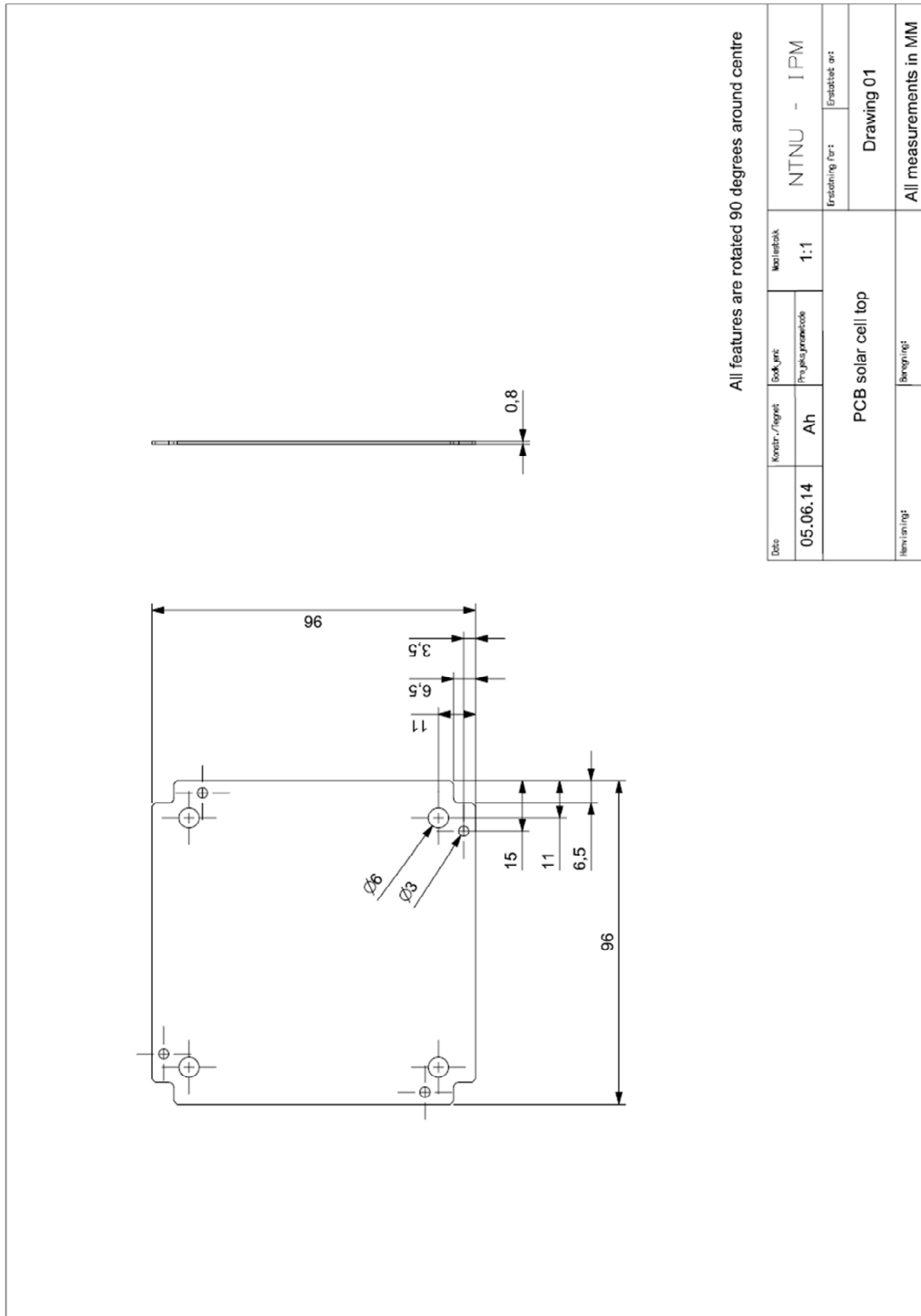


2.5.4. Solar cell side assembly



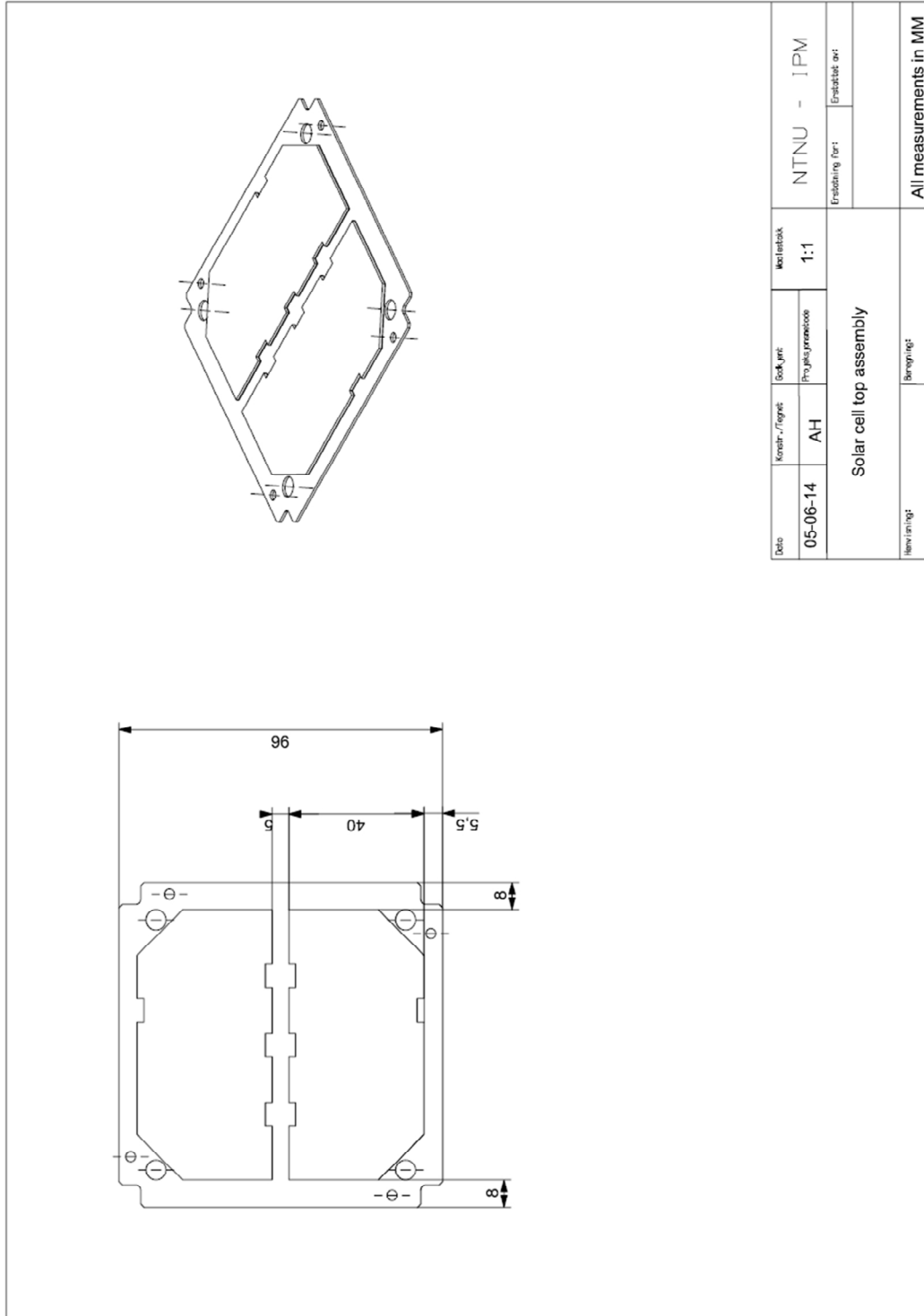
Appendix 2

2.5.5. PCB solar cell top



Appendix 2

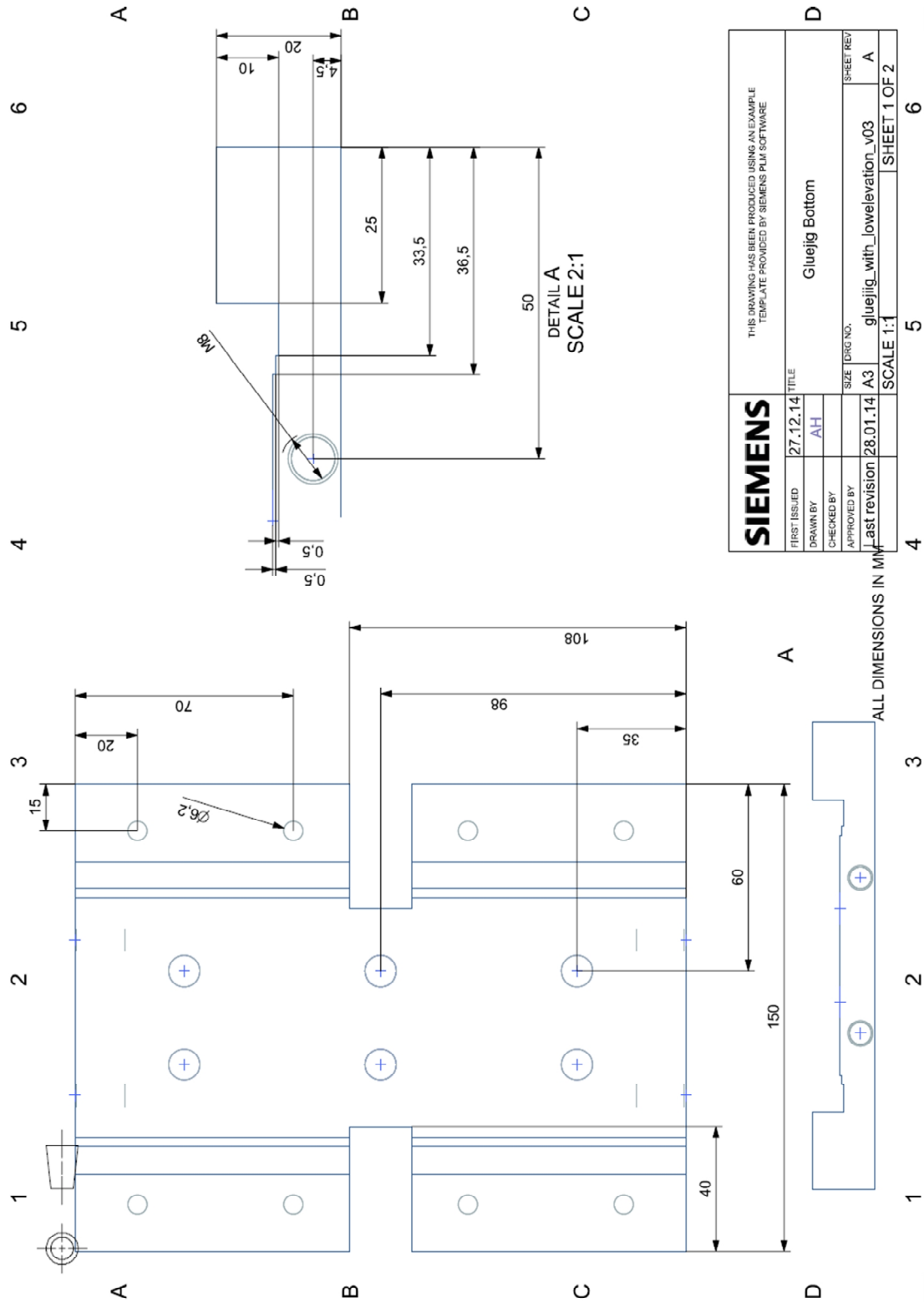
2.5.6. Solar cell top assembly



Appendix 2

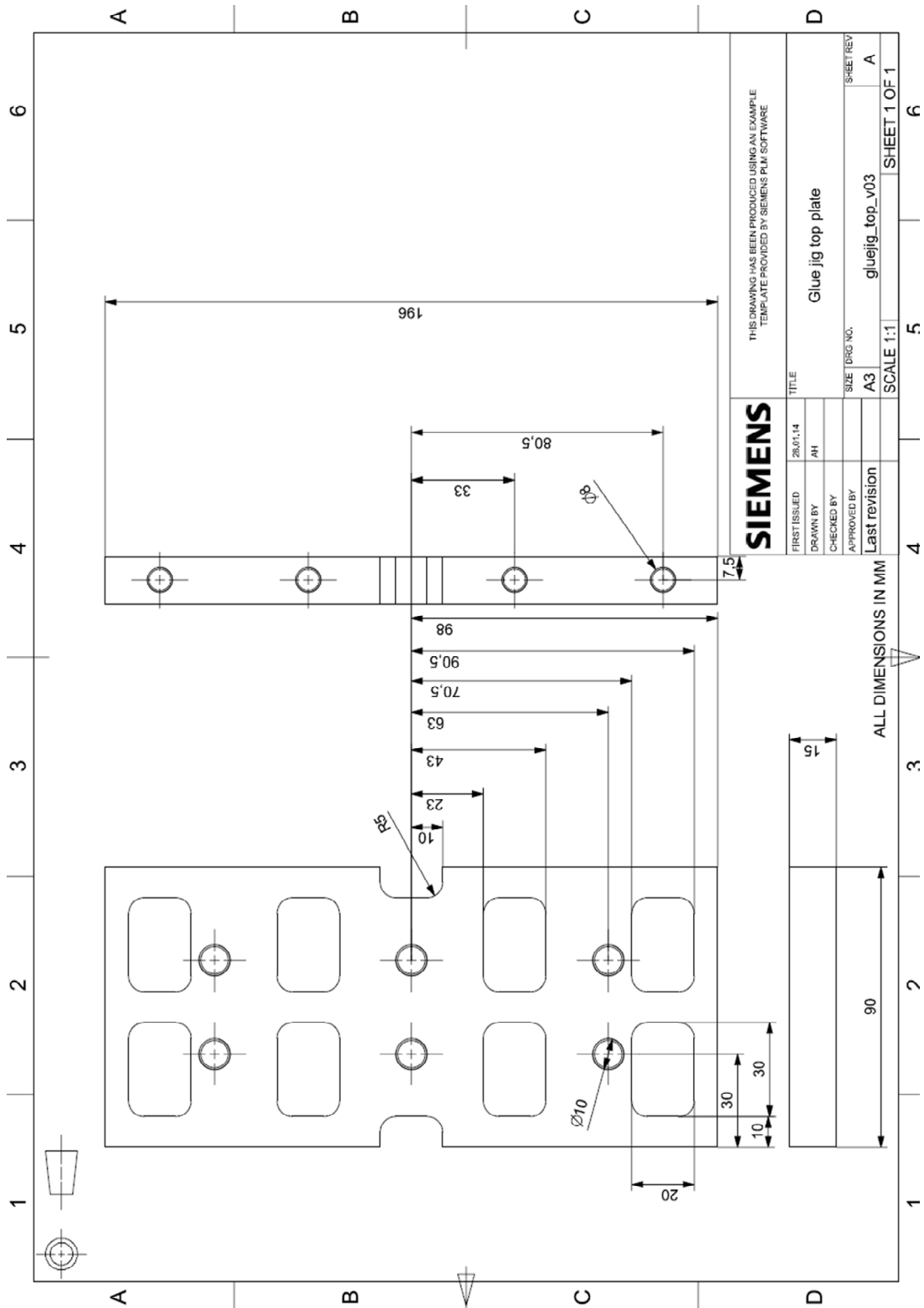
2.6. Adhesive jig

2.6.1. Bottom plate



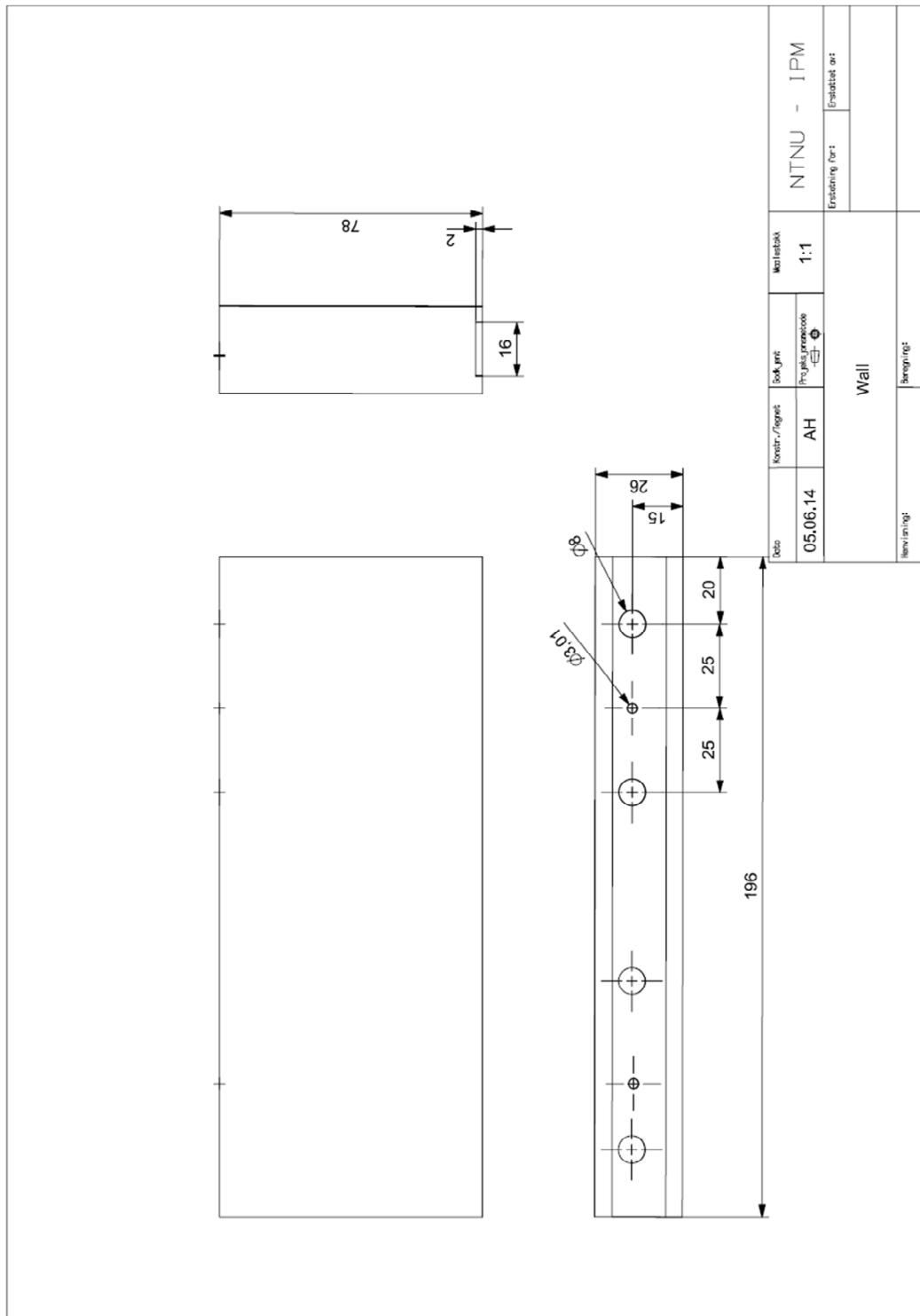
Appendix 2

2.6.2. Top plate

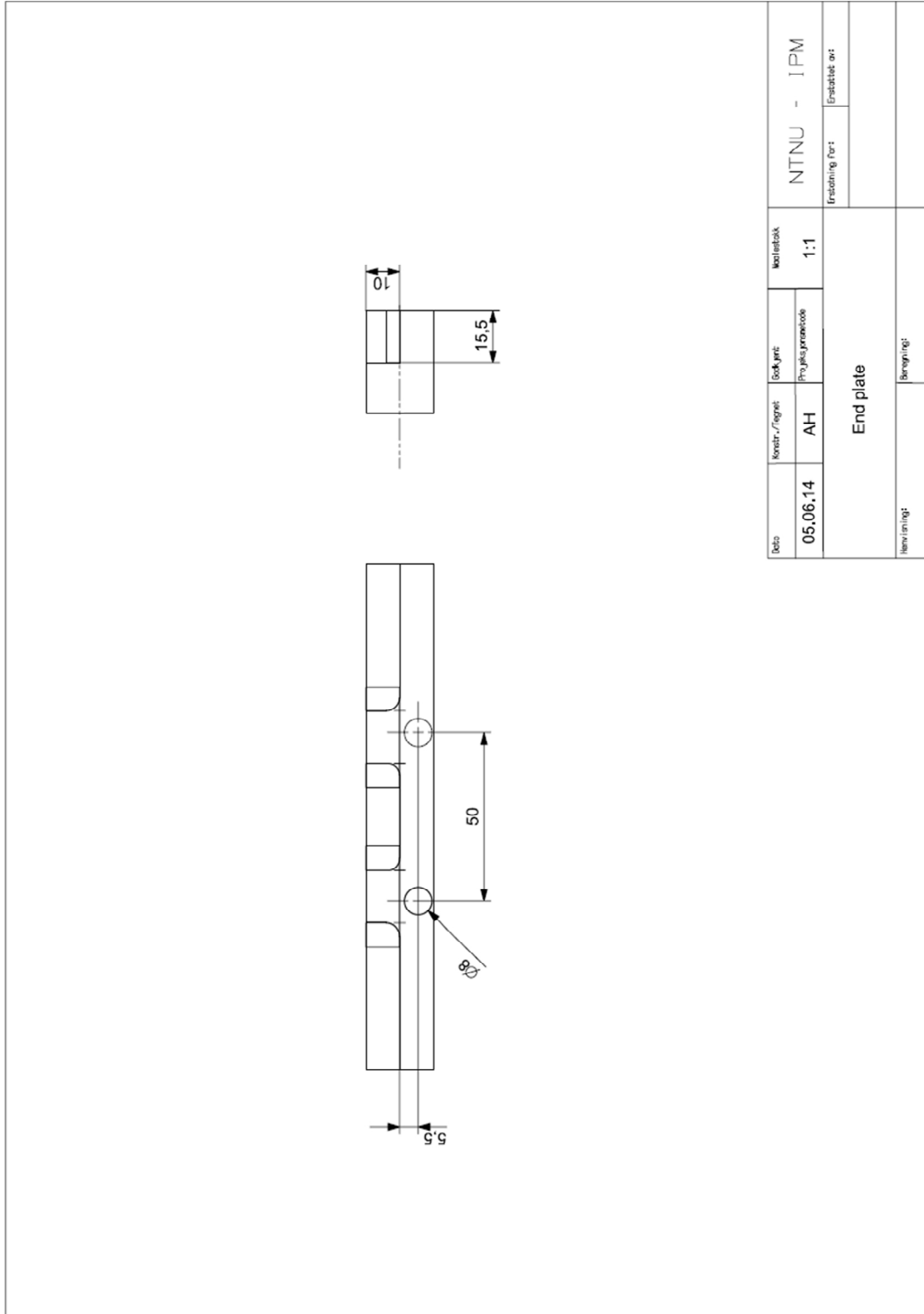


Appendix 2

2.6.3. Wall



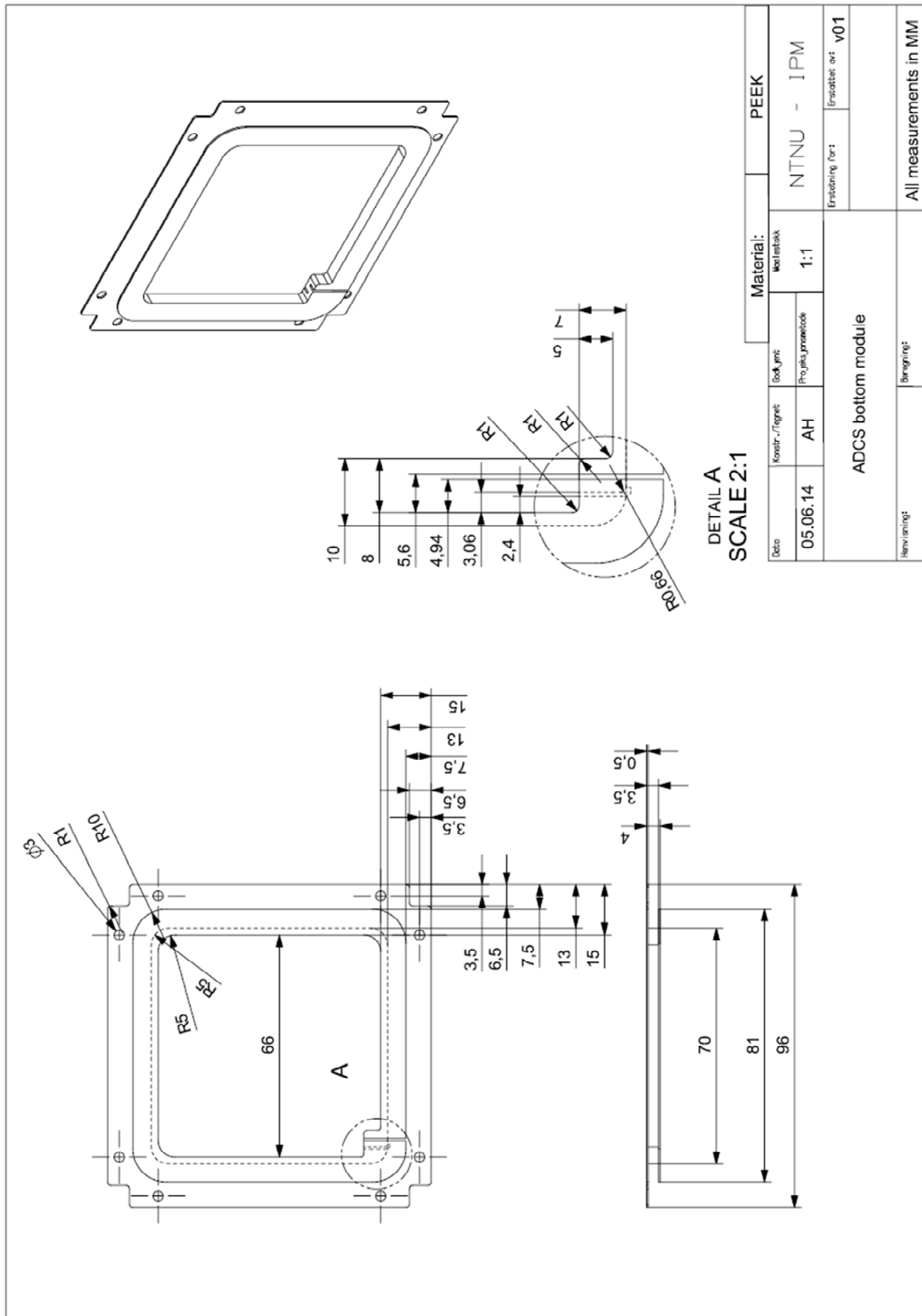
2.6.4. Endplate



2.7. ADCS

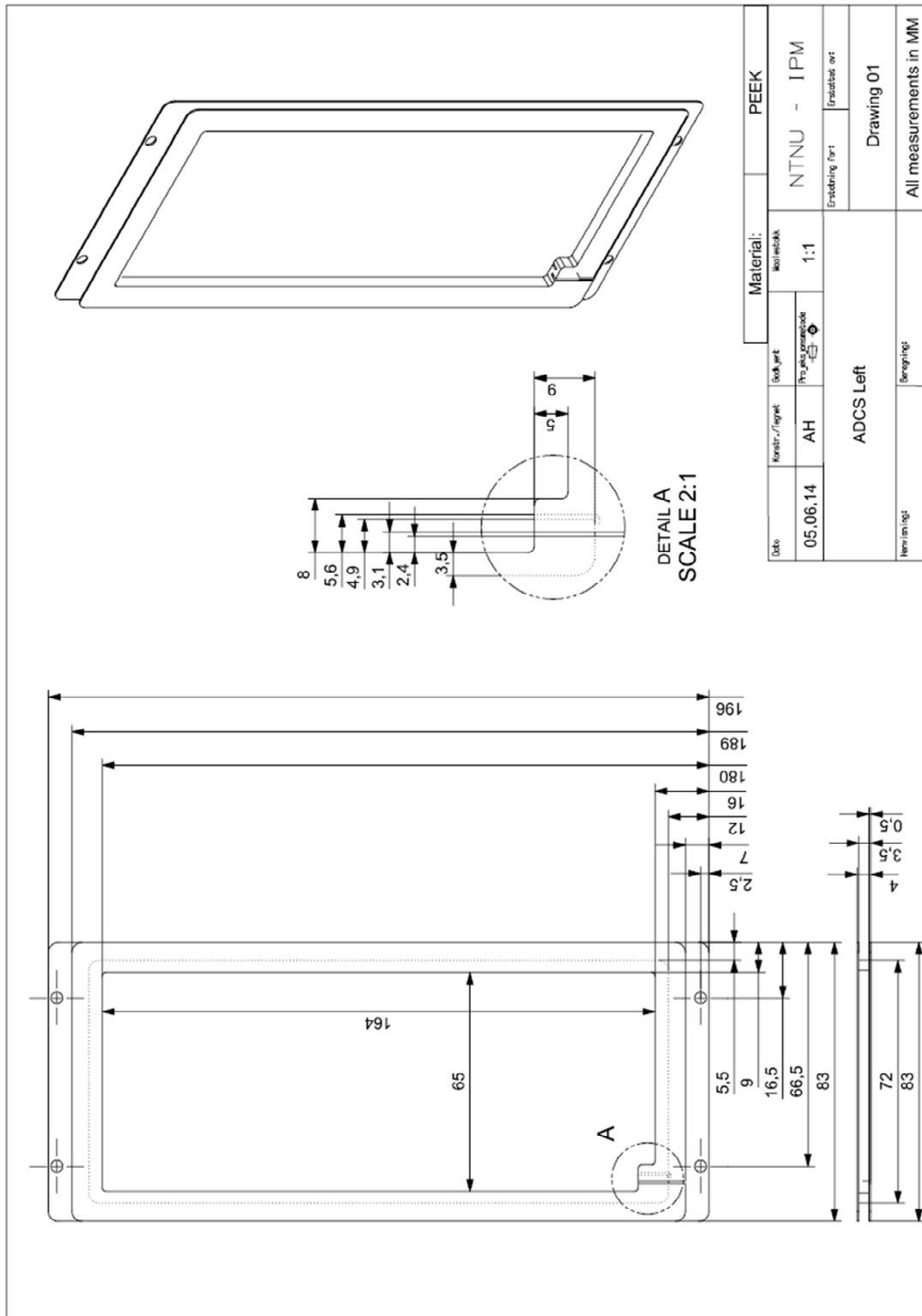
Appendix 2

2.7.1. ADCS top



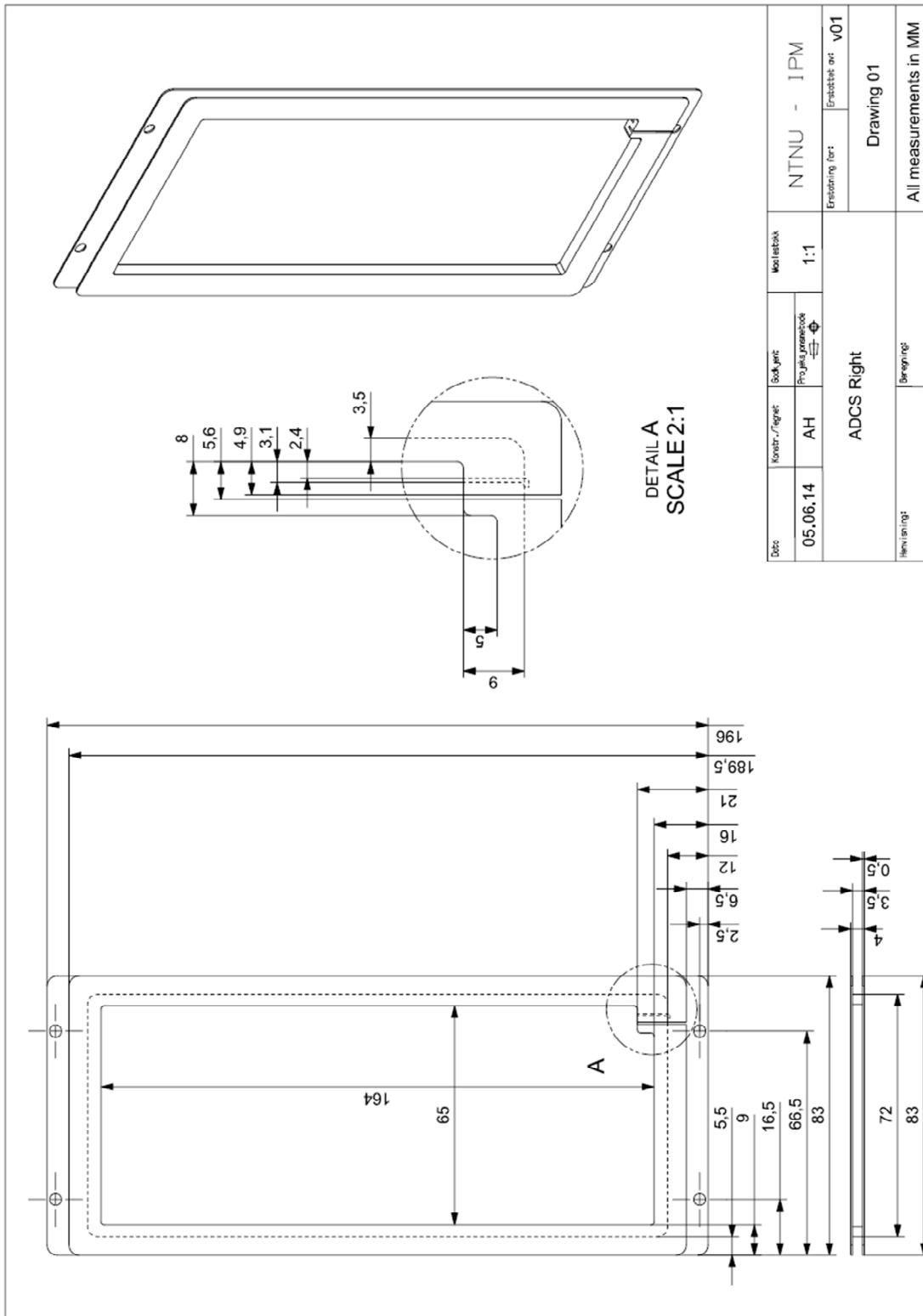
Appendix 2

2.7.2. ADCS left side



Appendix 2

2.7.3. ADCS right side



Appendix 3

3 APPENDIX 3

3.1. Lap shear test thickness

6/8/2014

Gmail - Lap shear test, tykkelse



Anders Haaland <anders.haaland@gmail.com>

Lap shear test, tykkelse

2 e-poster

Anders Håland <anders.haaland@gmail.com>
Til: Tor.S.Breivik@kongsberg.com

11. februar 2014 kl. 08.31

Hei

Hvordan er tykkelsen på prøvene til single lap shear test?

Hilsen
Anders Håland

Tor.S.Breivik@kongsberg.com <Tor.S.Breivik@kongsberg.com>
Til: anders.haaland@gmail.com

11. februar 2014 kl. 15.02

Hei, er på reise, men kjapt innpå:

Prøvestav: ca 2mm
Fuge: 0.1 - 0.2 mm optimalt

Tor s

Sendt fra min iPhone

Den 11. feb. 2014 kl. 08:31 skrev "Anders Håland" <anders.haaland@gmail.com>:

[Siteret tekst skjult]

CONFIDENTIALITY

This e-mail and any attachment contain KONGSBERG information which may be proprietary, confidential or subject to export regulations, and is only meant for the intended recipient(s). Any disclosure, copying, distribution or use is prohibited, if not otherwise explicitly agreed with KONGSBERG. If received in error, please delete it immediately from your system and notify the sender properly.

3.2. Adhesive



Structural Adhesives

Araldite® AV 138M with Hardener HV 998

Two component epoxy adhesive

- Key properties**
- Low out gassing / volatile loss
 - Excellent chemical resistance
 - Temperature resistant to 120°C
 - Cures at temperatures down to 5°C
 - Thixotropic, gap filling paste

Description

Araldite AV 138M with Hardener HV 998 is a two component, room temperature curing paste adhesive of high strength. When fully cured the adhesive will have excellent performance at elevated temperatures and has high chemical resistance. It is suitable for bonding a wide variety of metals, ceramics, glass, rubbers, rigid plastics and other materials, and is widely used in many industrial applications where resistance to aggressive or warm environments are required. The low out gassing makes this product suitable for specialist electronic telecommunication and aerospace applications.

Typical product data

Property	AV 138M	HV 998	Mixed adhesive
Colour (visual)	beige	grey	grey
Specific gravity	ca. 1.7	ca. 1.7	ca. 1.7
Viscosity (Pas)	thixotropic	thixotropic	thixotropic
Pot Life (100 gm at 25°C)	-	-	35 mins

Processing

Pretreatment

The strength and durability of a bonded joint are dependant on proper treatment of the surfaces to be bonded. At the very least, joint surfaces should be cleaned with a good degreasing agent such as acetone or other proprietary degreasing agents in order to remove all traces of oil, grease and dirt. Low grade alcohol, gasoline (petrol) or paint thinners should never be used. The strongest and most durable joints are obtained by either mechanically abrading or chemically etching ("pickling") the degreased surfaces. Abrading should be followed by a second degreasing treatment

Mix ratio	Parts by weight	Parts by volume
Araldite AV138M	100	100
Hardener HV 998	40	40

Resin and hardener should be blended until they form a homogeneous mix.

Application of adhesive

The resin/hardener mix is applied with a spatula, to the pretreated and dry joint surfaces. A layer of adhesive 0.05 to 0.10 mm thick will normally impart the greatest lap shear strength to the joint. The joint components should be assembled and clamped as soon as the adhesive has been applied. An even contact pressure throughout the joint area will ensure optimum cure.

Appendix 3

Mechanical processing

Specialist firms have developed metering, mixing and spreading equipment that enables the bulk processing of adhesive. We will be pleased to advise customers on the choice of equipment for their particular needs.

Equipment maintenance

All tools should be cleaned with hot water and soap before adhesives residues have had time to cure. The removal of cured residues is a difficult and time-consuming operation.

If solvents such as acetone are used for cleaning, operatives should take the appropriate precautions and, in addition, avoid skin and eye contact.

Curing times

Temperature	°C	10	15	23	40	60	80	100
Cure time	hours	48	36	24	16	1	-	-
	minutes	-	-	-	-	-	15	10
LSS at 23°C	N/mm ²	10	11	13	14	15	16	18

LSS = Lap shear strength.

Typical cured properties

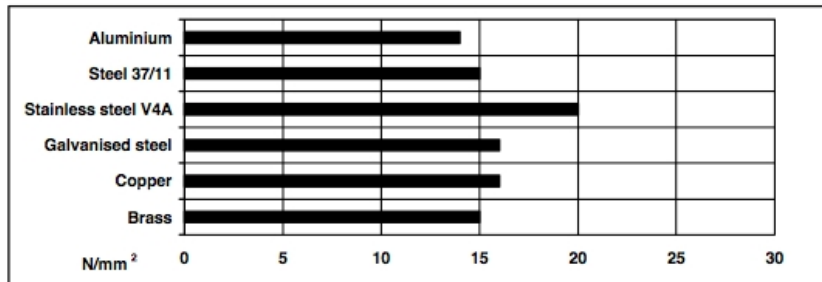
Unless otherwise stated, the figures given below were all determined by testing standard specimens made by lap-jointing 170 x 25 x 1.5 mm strips of aluminium alloy. The joint area was 12.5 x 25 mm in each case.

The figures were determined with typical production batches using standard testing methods. They are provided solely as technical information and do not constitute a product specification.

Average lap shear strengths of typical metal-to-metal joints (ISO 4587)

Cure: 16 hours at 40°C and tested at 23°C

Pretreatment - Sand blasting



Shear modulus (DIN 53445)

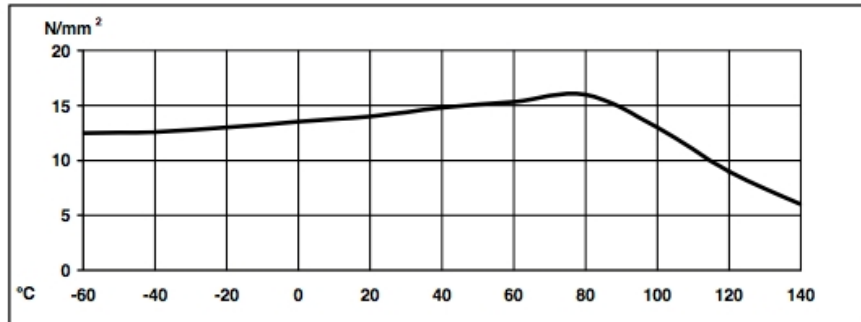
Cure: 16 hours at 40°C

- 25°C - 3GPa
- 50°C - 2GPa
- 75°C - 0.4GPa
- 100°C - 0.1GPa
- 125°C - 3MPa
- 150°C - 2MPa

Appendix 3

Lap shear strength versus temperature (ISO 4587) (typical average values)

Cure: 16 hours at 40°C



Roller peel test (ISO 4578)

Cure: 16 hours at 40°C

1.8 N/mm

Shore hardness

D84-86

Tensile strength

Cure: 16 hours at 40°C

43 MPa

Tensile modulus

4.7 GPa

Elongation at break

1.2%

Electrolytic corrosion (DIN 53489) - Cure: 16 hours at 40°C

Tested 4 days in 40°C/92% RH as specified in DIN 50015

Rated AN1

Coefficient of linear thermal expansion (VSM 77110)

Tested over range 18-93°C. Cure: 16 hours at 40°C

$67 \times 10^{-6} \text{K}^{-1}$

Volume resistivity (VSDE 0303) at 22°C

1.8×10^{17} ohm cm at 50 Hz

Electric strength (VSM 7710) at 22°C

45.8 kV (instantaneous value)

Fatigue test on simple lap joints (DIN 532852)

Cure: 16 hours at 40°C. Test frequency 90-130Hz

25% of static failing load

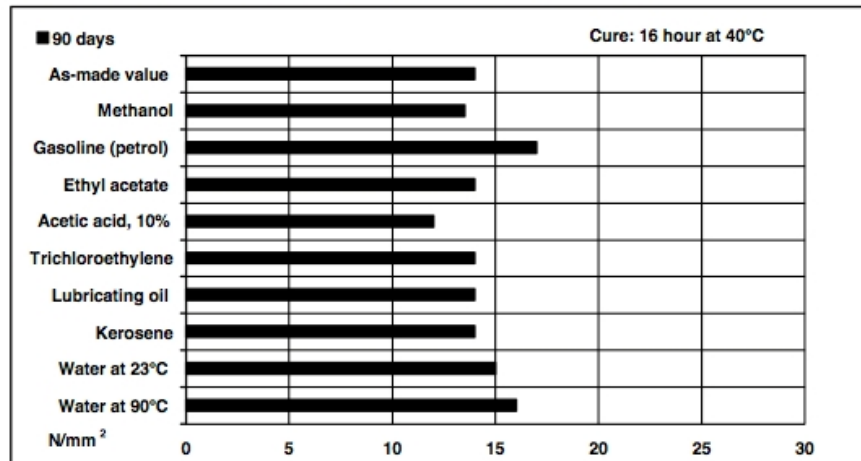
$> 10^7$ cycles to failure

30% of static failing load

10^5 - 10^6 cycles to failure

Lap shear strength versus immersion in various media (typical average values)

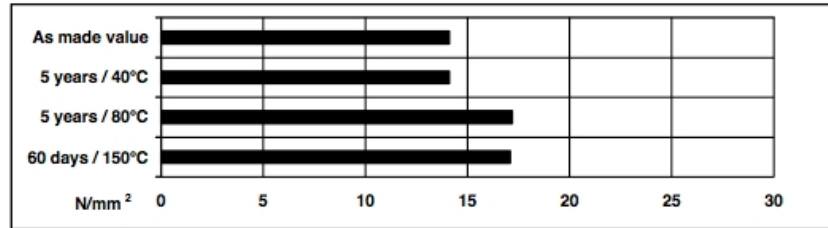
Unless otherwise stated, L.S.S. was determined after immersion for 90 days at 23°C



Appendix 3

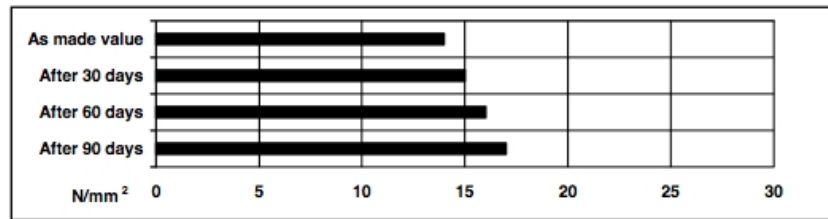
Lap shear strength versus heat ageing

Cure: 16 hours at 40°C



Lap shear strength versus tropical weathering

(40/92, DIN 50015; typical average values)
Test at 23°C



Storage

Araldite AV 138M and hardener HV 998 may be stored for up to 6 years and 3 years respectively at room temperature provided that the components are stored in sealed containers. The expiry date is indicated on the label.

Handling precautions

Caution

Our products are generally quite harmless to handle provided that certain precautions normally taken when handling chemicals are observed. The uncured materials must not, for instance, be allowed to come into contact with foodstuffs or food utensils, and measures should be taken to prevent the uncured materials from coming in contact with the skin, since people with particularly sensitive skin may be affected. The wearing of impervious rubber or plastic gloves will normally be necessary; likewise the use of eye protection. The skin should be thoroughly cleansed at the end of each working period by washing with soap and warm water. The use of solvents is to be avoided. Disposable paper - not cloth towels - should be used to dry the skin. Adequate ventilation of the working area is recommended. These precautions are described in greater detail in the Material Safety Data sheets for the individual products and should be referred to for fuller information.

Huntsman Advanced Materials

Duxford, Cambridge
England CB2 4QA

Tel: +44 (0) 1223 832121
Fax: +44 (0) 1223 493322
www.araldite.com

All recommendations for the use of our products, whether given by us in writing, verbally, or to be implied from the results of tests carried out by us, are based on the current state of our knowledge. Notwithstanding any such recommendations the Buyer shall remain responsible for satisfying himself that the products as supplied by us are suitable for his intended process or purpose. Since we cannot control the application, use or processing of the products, we cannot accept responsibility therefor. The Buyer shall ensure that the intended use of the products will not infringe any third party's intellectual property rights. We warrant that our products are free from defects in accordance with and subject to our general conditions of supply.

© Huntsman Advanced Materials (Switzerland) GmbH

© Araldite is a registered trademark of Huntsman LLC or an affiliate thereof in one or more, but not all, countries

Appendix 3

CubeSat Design Specification Rev. 13
The CubeSat Program, Cal Poly SLO

3.3. CDS

Document Classification	
X	Public Domain
	ITAR Controlled
	Internal Only

CubeSat Design Specification

(CDS)

REV 13 – PROVISIONAL

August 19, 2013

PROVISIONAL



CUBESAT
California Polytechnic State University

PRC

CHANGE HISTORY LOG

Effective Date	Revision	Author	Description of Changes
N/A	8	Simon Lee	N/A
5/26/05	8.1	Amy Hutputanasin	Formatting updated.
5/15/06	9	Armen Toorian	Information and presentation revised.
8/2/07	10	Wenschel Lan	Information updated.
10/02/08	11	Riki Munakata	1.1.1.1.1.1.1 Format Design specification and Mk.III P-POD compatibility update.
8/1/09	12	Riki Munakata	Requirements update, waiver form requirements, and 3U CubeSat Specification drawing.
3/30/12	1.1.1.1.	Justin Carnahan	Reformatted document to improve readability, updated to include 1.5U, 2U, and 3U+. Added and modified some req.
7/12/13	13	David Pignatelli	Added applicable documents section. Removed restrictions on propulsion, added guidance for propulsion systems and hazardous materials. Added magnetic field restrictions and suggestions. Cleaned Section 3.2. Added custom spring plunger specs and recommendation. Extended restrictions on inhibits. Added links to outside resources. Cleaned Section 4.

TABLE OF CONTENTS

1. INTRODUCTION.....7#

1.1! OVERVIEW#.....8!

1.2! PURPOSE#.....8!

1.3! WAIVER PROCESS#.....8!

2! POLY PICOSATELLITE ORBITAL DEPLOYER#.....8!

2.1! INTERFACE#.....8!

3! CUBESAT SPECIFICATION#.....8!

3.1! GENERAL REQUIREMENTS#.....8!

3.2! CUBESAT MECHANICAL REQUIREMENTS#.....9!

3.3! ELECTRICAL REQUIREMENTS#.....#1!

3.4! OPERATIONAL REQUIREMENTS#.....#2!

4! TESTING REQUIREMENTS#.....#3!

4.1! RANDOM VIBRATION#.....#3!

4.2! THERMAL VACUUM BAKEOUT#.....#3!

4.3! SHOCK TESTING#.....#3!

4.4! VISUAL INSPECTION#.....#3!

4.5! CUBESAT TESTING PHILOSOPHY#.....#3!

5! CONTACTS#.....#5!

APPENDIX

A. WAIVER FORM 14

B. CUBESAT SPECIFICATION DRAWINGS..... 17

C. CUBESAT ACCEPTANCE CHECKLISTS..... 19

PROVISIONAL

List of Acronyms

AFSPCMAN	Air Force Space Command Manual
CAC	CubeSat Acceptance Checklist
Cal Poly	California Polytechnic State University, San Luis Obispo
CDS	CubeSat Design Specification
cm	Centimeters
CVCM	Collected Volatile Condensable Mass
DAR	Deviation Waiver Approval Request
FCC	Federal Communication Commission
GSFC	Goddard Space Flight Center
IARU	International Amateur Radio Union
kg	Kilogram
LSP	Launch Services Program
LV	Launch Vehicle
MIL	Military
mm	Millimeters
NASA	National Aeronautics and Space Administration
NPR	NASA Procedural Requirements
P-POD	Poly Picosatellite Orbital Deployer
RBF	Remove Before Flight
Rev.	Revision
RF	Radio Frequency
RTC	Real-Time Clock
SLO	San Luis Obispo
SSDL	Space Systems Development Lab
STD	Standard
TML	Total Mass Loss
µm	Micrometer

Applicable Documents

The following documents form a part of this document to the extent specified herein. In the event of conflict between the documents referenced herein and the contents of this document, the contents of this document shall take precedence.

Launch Services Program Program Level P-POD and CubeSat Requirements Document (LSP-REQ-317.01)

General Environmental Verification Standard for GSFC Flight Programs and Projects (GSFC-STD-7000)

Military Standard Test Requirements for Launch, Upper-stage, and Space Vehicles (MIL-STD-1540)

Air Force Space Command Manual 91-710, Range Safety User Requirements Manual (AFSPCMAN 91-710)

Metallic Material Properties (MIL-HDBK-5)

Standard Materials and Processes Requirements for Spacecraft (NASA-STD-6016)

NASA Procedural Requirements for Limiting Orbital Debris (NPR 8715.6)

between CubeSat developers, P-POD integrators, range safety personnel, and launch vehicle providers. This will help to better identify and address any issues that may arise prior to integration and launch. The DARJ can be found at <http://www.cubesat.org> and Prof. Bob Twiggs should be contacted at btwiggs@stanford.edu. The purpose of the project is to provide a standard for P-POD integrators to review the request, develop any questions and address them, create any additional tests, analyses, or presentations to support the project. If so, the Developer, with inputs from the P-POD Integrator, will write a test plan and perform the tests before the waiver is conditionally accepted by the P-POD Integrator. Waivers can only be conditionally accepted by the P-POD Integrator until a launch has been identified for the CubeSat. Once a launch has been identified, the waiver becomes mission specific and passes to the launch vehicle Mission Manager for review. The launch vehicle Mission Manager has the final say on acceptance of the waiver, and the Mission Manager may require more corrections and/or testing to be performed before approving the waiver. Developers should realize that each waiver submitted reduces the chances of finding a suitable launch opportunity.

CubeSat Standard Deviation Waiver Process

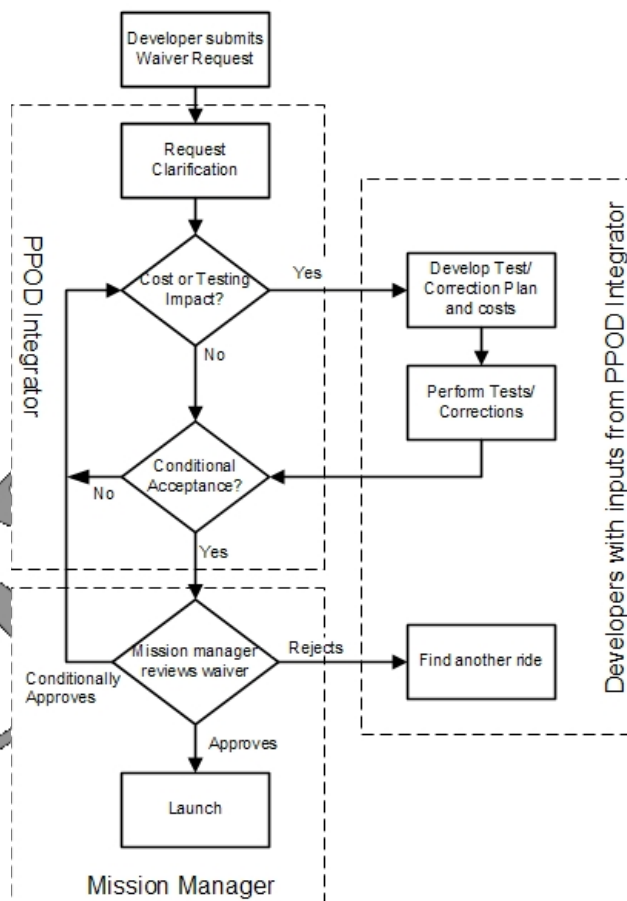


Figure 2: CubeSat Standard Deviation Wavier Process Flow Diagram

Waiver is in violation of any requirements in sections 2 or 3. The waiver process is intended to be quick and easy. The intent is to help facilitate communication and explicit documentation

2. Poly Picosatellite Orbital Deployer

2.1 Interface

The Poly Picosatellite Orbital Deployer (P-POD) is Cal Poly's standardized CubeSat deployment system. It is capable of carrying three standard CubeSats and serves as the interface between the CubeSats and LV. The P-POD is a rectangular box with a door and a spring mechanism. Once the release mechanism of the P-POD is actuated by a deployment signal sent from the LV, a set of torsion springs at the door hinge force the door open and the CubeSats are deployed by the main spring gliding on its rails and the P-PODs rails (P-POD rails are shown in Figure 3b). The P-POD is made up of anodized aluminum. CubeSats slide along a series of rails during ejection into orbit. CubeSats will be compatible with the P-POD to ensure safety and success of the mission by meeting the requirements outlined in this document. The P-POD is backward compatible, and any CubeSat developed within the design specification of CDS rev. 9 and later will not have compatibility issues. Developers are encouraged to design to the most current CDS to take full advantage of the P-POD features.

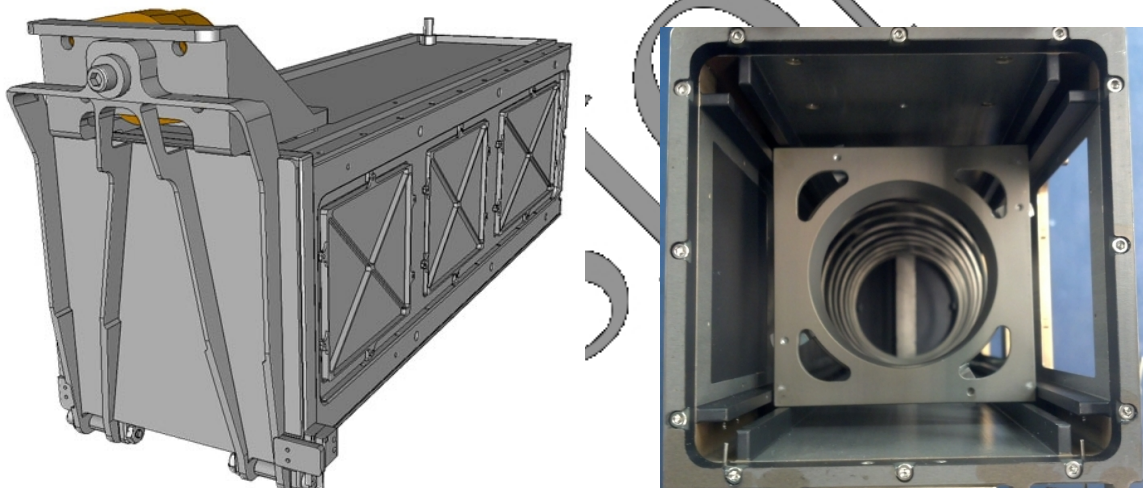


Figure 3a and 3b: Poly Picosatellite Orbital Deployer (P-POD) and cross section

3. CubeSat Specification

3.1 General Requirements

- 3.1.1 CubeSats which incorporate any deviation from the CDS will submit a DAR and adhere to the waiver process (see Section 1.3 and Appendix A).
- 3.1.2 All parts shall remain attached to the CubeSats during launch, ejection and operation. No additional space debris will be created.
- 3.1.3 No pyrotechnics shall be permitted.
- 3.1.4 Any propulsion systems shall be designed, integrated, and tested in accordance with AFSPCMAN 91-710 Volume 3.
- 3.1.5 Propulsion systems shall have at least 3 inhibits to activation.
- 3.1.6 Total stored chemical energy will not exceed 100 Watt-Hours.

- 3.1.6.1 Note: Higher capacities may be permitted, but could potentially limit launch opportunities.
- 3.1.7 CubeSat hazardous materials shall conform to AFSPCMAN 91-710, Volume 3.
- 3.1.8 CubeSat materials shall satisfy the following low out-gassing criterion to prevent contamination of other spacecraft during integration, testing, and launch. A list of NASA approved low out-gassing materials can be found at: <http://outgassing.nasa.gov>
- 3.1.8.1 CubeSats materials shall have a Total Mass Loss (TML) $\leq 1.0\%$
- 3.1.8.2 CubeSat materials shall have a Collected Volatile Condensable Material (CVCM) $\leq 0.1\%$
- 3.1.9 The latest revision of the CubeSat Design Specification will be the official version which all CubeSat developers will adhere to. The latest revision is available at <http://www.cubesat.org>.
- 3.1.9.1 Cal Poly will send updates to the CubeSat mailing list upon any changes to the specification. You can sign-up for the CubeSat mailing list here: www.cubesat.org/index.php/about-us/how-to-join
- 3.1.10 Note: Some launch vehicles hold requirements on magnetic field strength. Additionally, strong magnets can interfere with the separation between CubeSat spacecraft in the same P-POD. As a general guideline, it is advised to limit magnetic field outside the CubeSat static envelope to 0.5 Gauss above Earth's magnetic field.
- 3.1.11 The CubeSat shall be designed to accommodate ascent venting per ventable volume/area < 2000 inches.

3.2 CubeSat Mechanical Requirements

CubeSats are cube shaped picosatellites with dimensions and features outlined in the CubeSat Specification Drawing (Appendix B). The P-POD coordinate system is shown below in Figure 4 for reference. General features of all CubeSats include:

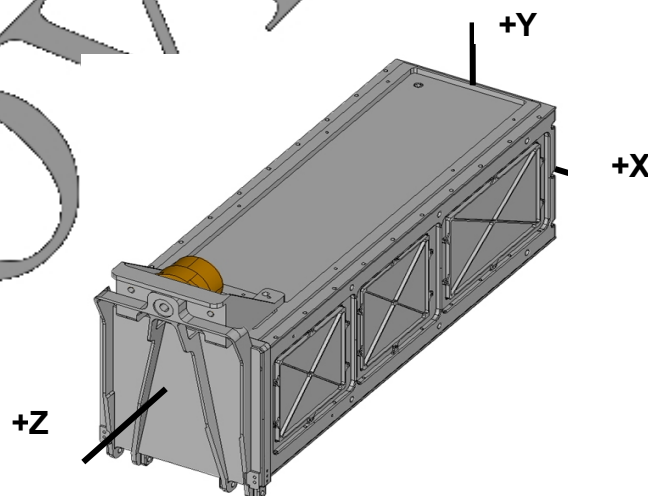


Figure 4: P-POD Coordinate System

- 3.2.1 The CubeSat shall use the coordinate system as defined in Appendix B for the appropriate size. The CubeSat coordinate system will match the P-POD coordinate system while integrated into the P-POD. The origin of the CubeSat coordinate system is located at the geometric center of the CubeSat.
- 3.2.1.1 The CubeSat configuration and physical dimensions shall be per the appropriate section of Appendix B.
- 3.2.1.2 The extra volume available for 3U+ CubeSats is shown in Figure 6.
- 3.2.2 The $-Z$ face of the CubeSat will be inserted first into the P-POD.
- 3.2.3 No components on the green and yellow shaded sides shall exceed 6.5 mm normal to the surface.
- 3.2.3.1 When completing a CubeSat Acceptance Checklist (CAC), protrusions will be measured from the plane of the rails.
- 3.2.4 Deployables shall be constrained by the CubeSat, not the P-POD.
- 3.2.5 Rails shall have a minimum width of 8.5mm.
- 3.2.6 Rails will have a surface roughness less than 1.6 μm .
- 3.2.7 The edges of the rails will be rounded to a radius of at least 1mm
- 3.2.8 The ends of the rails on the $\pm Z$ face shall have a minimum surface area of 6.5 mm x 6.5 mm contact area for neighboring CubeSat rails (as per Figure 6).
- 3.2.9 At least 75% of the rail will be in contact with the P-POD rails. 25% of the rails may be recessed and no part of the rails will exceed the specification.
- 3.2.10 The maximum mass of a 1U CubeSat shall be 1.33 kg.
- 3.2.10.1 Note: Larger masses may be evaluated on a mission to mission basis.
- 3.2.11 The maximum mass of a 1.5U CubeSat shall be 2.00 kg.
- 3.2.11.1 Note: Larger masses may be evaluated on a mission to mission basis.
- 3.2.12 The maximum mass of a 2U CubeSat shall be 2.66 kg.
- 3.2.12.1 Note: Larger masses may be evaluated on a mission to mission basis.
- 3.2.13 The maximum mass of a 3U CubeSat shall be 4.00 kg.
- 3.2.13.1 Note: Larger masses may be evaluated on a mission to mission basis.
- 3.2.14 The CubeSat center of gravity shall be located within 2 cm from its geometric center in the X and Y direction.
- 3.2.14.1 The 1U CubeSat center of gravity shall be located within 2 cm from its geometric center in the Z direction.
- 3.2.14.2 The 1.5U CubeSat center of gravity shall be located within 3 cm from its geometric center in the Z direction.
- 3.2.14.3 The 2U CubeSat center of gravity shall be located within 4.5 cm from its geometric center in the Z direction.
- 3.2.14.4 3U and 3U+ CubeSats' center of gravity shall be located within 7 cm from its geometric center in the Z direction.
- 3.2.15 Aluminum 7075, 6061, 5005, and/or 5052 will be used for both the main CubeSat structure and the rails.
- 3.2.15.1 If other materials are used the developer will submit a DAR and adhere to the waiver process.
- 3.2.16 The CubeSat rails and standoff, which contact the P-POD rails and adjacent CubeSat standoffs, shall be hard anodized aluminum to prevent any cold welding within the P-POD.

- 3.2.17 The 1U, 1.5U, and 2U CubeSats shall use separation springs to ensure adequate separation unless adjacent CubeSats are part of the same mission and built by the same CubeSat developer. The developer will present the design to the mission integrator and receive concurrence that the approach is acceptable before proceeding.
- 3.2.17.1 Note: Recommended separation spring specifications are shown below in Table 1. Contact cubesat@gmail.com in order to obtain these separation springs.
- 3.2.17.2 The compressed separation springs shall be at or below the level of the standoff.
- 3.2.17.3 The 1U, 1.5U, and 2U CubeSat separation spring will be centered on the end of the standoff on the CubeSat's -Z face as per Figure 7.
- 3.2.17.4 Separation springs are not required for 3U CubeSats.

Table 1: CubeSat Separation Spring Characteristics

Characteristics	Value
Plunger Material	<i>Stainless Steel</i>
End Force Initial/Final	<i>0.14lbs / 0.91lbs</i>
Throw Length	<i>0.16 inches minimum above the standoff surface</i>
1.1.1.1.1.1.3 Thread Pitch	1.1.1.1.1.1.4 6-36 UNF-2B

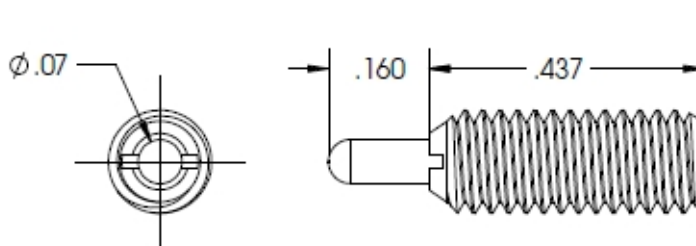
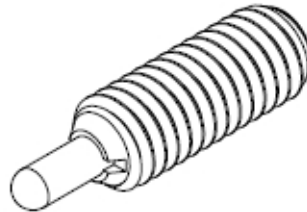


Figure 5: Custom Spec Spring Plunger (Separation Spring)

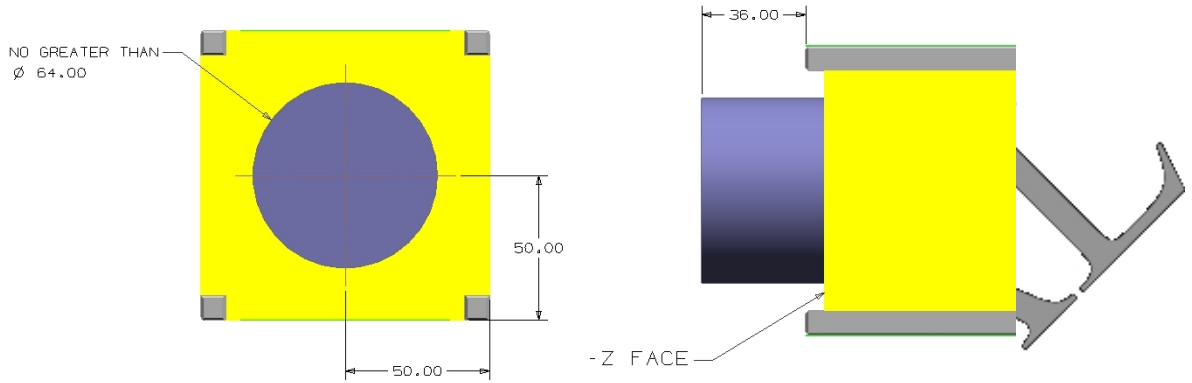


Figure 6: 3U+ Extra Volume ("Tuna Can")

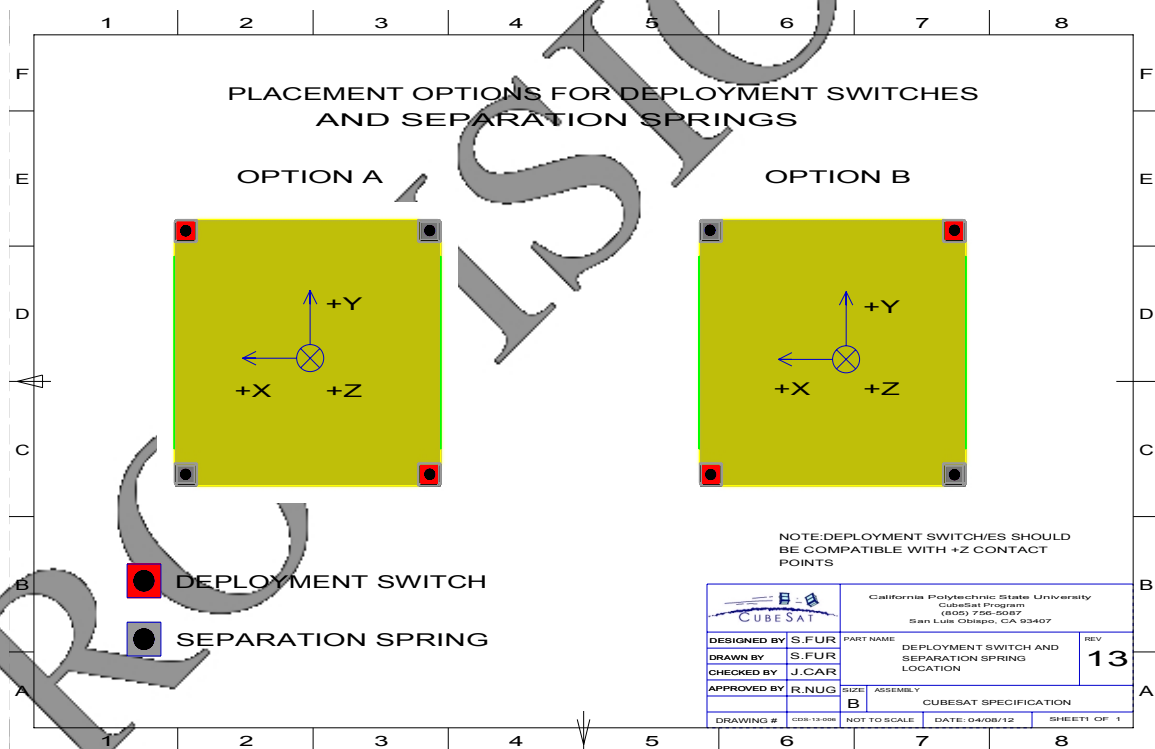


Figure 7: Deployment Switches and Separation Spring Locations

3.3 Electrical Requirements

Electronic systems will be designed with the following safety features.

- 3.3.1 The CubeSat power system shall be at a power off state to prevent CubeSat from activating any powered functions while integrated in the P-POD from the time of delivery to the LV through on-orbit deployment. CubeSat powered function include the variety of subsystems such as Command and Data Handling (C&DH), RF Communication, Attitude Determine and Control (ADC), deployable mechanism actuation. CubeSat power systems include all battery assemblies, solar cells, and coin cell batteries.
- 3.3.2 The CubeSat shall have, at a minimum, one deployment switch on a rail standoff, per Figure 7.
- 3.3.3 In the actuated state, the CubeSat deployment switch shall electrically disconnect the power system from the powered functions.
- 3.3.3.1 Note: Real time clocks (RTC) may be permitted, but could potentially limit launch opportunities.
- 3.3.4 The deployment switch shall be in the actuated state at all times while integrated in the P-POD.
- 3.3.4.1 In the actuated state, the CubeSat deployment switch will be at or below the level of the standoff.
- 3.3.5 If the CubeSat deployment switch toggles from the actuated state and back, the satellite shall reset to a pre-launch state, including reset of transmission and deployable timers.
- 3.3.6 The RBF pin and all CubeSat umbilical connectors shall be within the designated Access Port locations, green shaded areas shown in Appendix B.
- 3.3.6.1 Note: All diagnostics and battery charging within the P-POD will be done while the deployment switch is depressed.
- 3.3.7 The CubeSat shall include an RBF pin.
- 3.3.7.1 The RBF pin shall cut all power to the satellite once it is inserted into the satellite.
- 3.3.7.2 The RBF pin shall be removed from the CubeSat after integration into the P-POD.
- 3.3.7.3 The RBF pin shall protrude no more than 6.5 mm from the rails when it is fully inserted into the satellite.
- 3.3.8 CubeSats shall incorporate battery charge/discharge protection to avoid hazardous cell conditions. Additional manufacturer documentation and/or testing will be required for modified, customized, or non-UL-listed cells.
- 3.3.9 The CubeSat shall be designed to meet at least one of the following requirements to prohibit inadvertent radio frequency (RF) transmission. The use of three independent inhibits is highly recommended and can reduce required documentation and analysis. An inhibit is a physical device between a power source and a hazard. A timer is not considered an independent inhibit.
- 3.3.9.1 The CubeSat will have one RF inhibit and RF power output of no greater than 1.5W at the transmitting antenna's RF input.
- 3.3.9.2 The CubeSat will have two independent RF inhibits.

5. Contacts

Cal Poly - San Luis Obispo

Prof. Jordi Puig-Suari
Aerospace Engineering Dept.
(805) 756-5087
(805) 756-2376 fax
jpuigsua@calpoly.edu

Cal Poly Program Manager

Roland Coelho
(805) 756-5087
rcoelho@calpoly.edu

SRI International

Dr. Scott Williams, Program Manager
Engineering Systems Division
(650) 859-5057
(650) 859-3919 fax
scott.williams@sri.com

Cal Poly Student Contacts

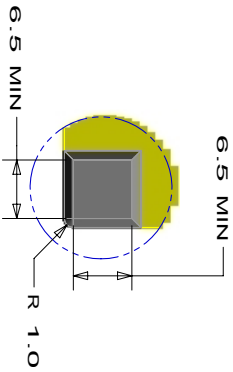
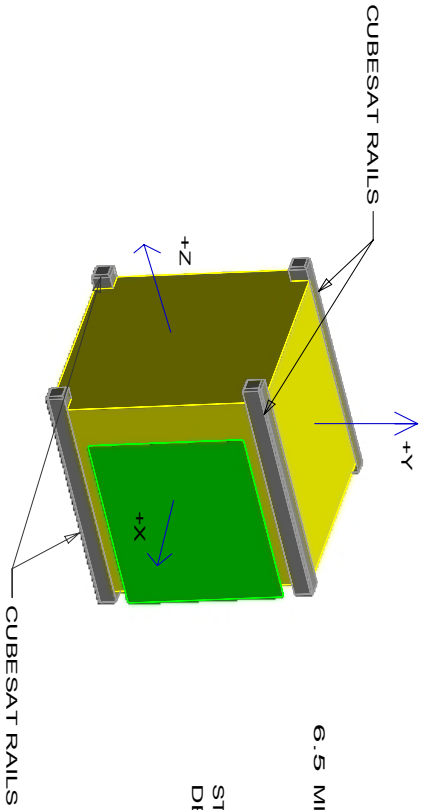
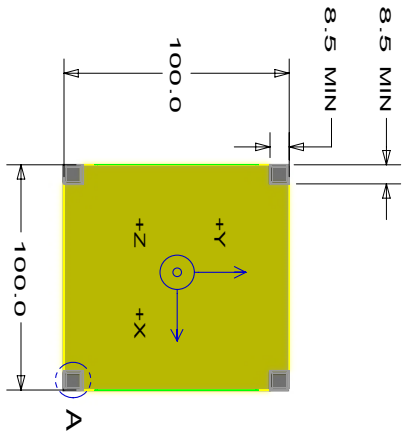
(805) 756-5087
cubesat@gmail.com

PROVISIONAL

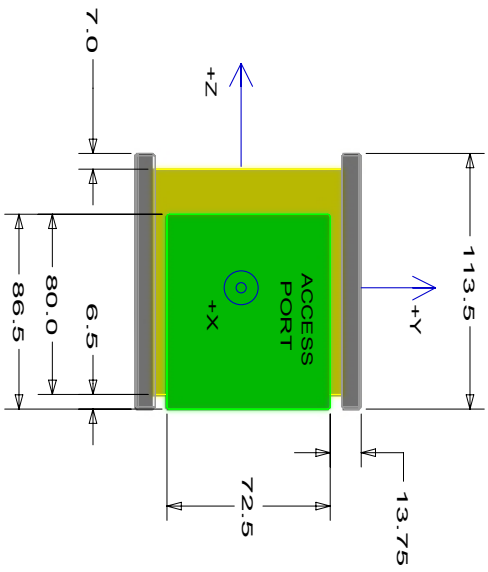
**Appendix A:
Waiver Form**

PROVISIONAL

Section 1
1U CubeSat Design Specification Drawing



DETAIL A
STANDOFF CONTACT
DETAIL FOR +Z



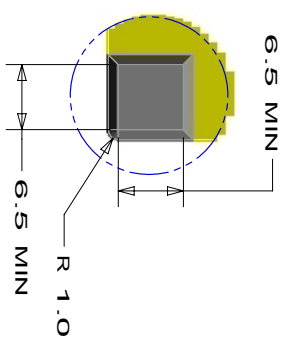
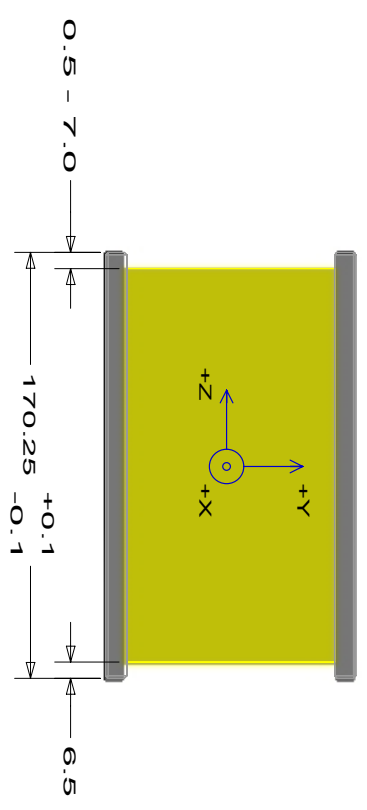
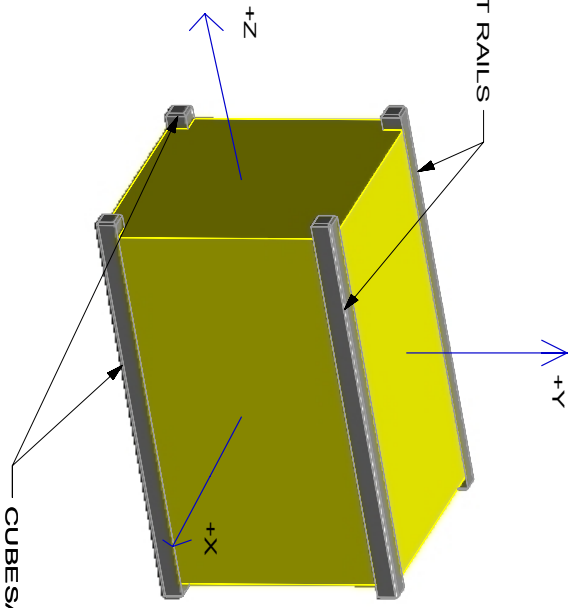
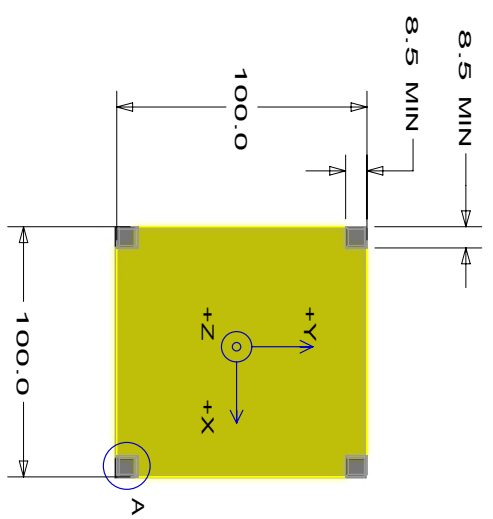
ADDITIONAL NOTES:

- CubeSat coordinate system located in the geometric center of the CubeSat.
- No external components other than the rails shall touch the inside of the P-POD.
- At least one (1) deployment switch must be incorporated on all CubeSats on -Z face.

ALL DIMENSIONS IN MILLIMETERS		DESIGNED BY S.FUR		PART NAME	
TOLERANCE X ± 0.1		DRAWN BY S.FUR		1U CUBESAT	
ROUND ALL EDGES AND CORNERS		CHECKED BY J.CAR		ASSEMBLY	
DRAWING #		APPROVED BY R.NUG		CUBESAT SPECIFICATION	
CDS-13-001		NOT TO SCALE		DATE: 04/05/12	
SHEET 1 OF 1		REV		13	
California Polytechnic State University CubeSat Program (805) 756-5087 San Luis Obispo, CA 93407		CUBESAT			

Section 2
1.5U CubeSat Design Specification Drawing

Appendix 3



DETAIL A
STANDOFF CONTACT
DETAIL FOR +Z

ADDITIONAL NOTES:

- CubeSat coordinate system located in the geometric center of the CubeSat.
- No external components other than the rails shall touch the inside of the P-POD.
- At least one (1) deployment switch must be incorporated on all CubeSats on -Z face.

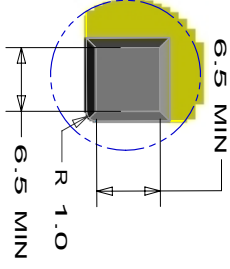
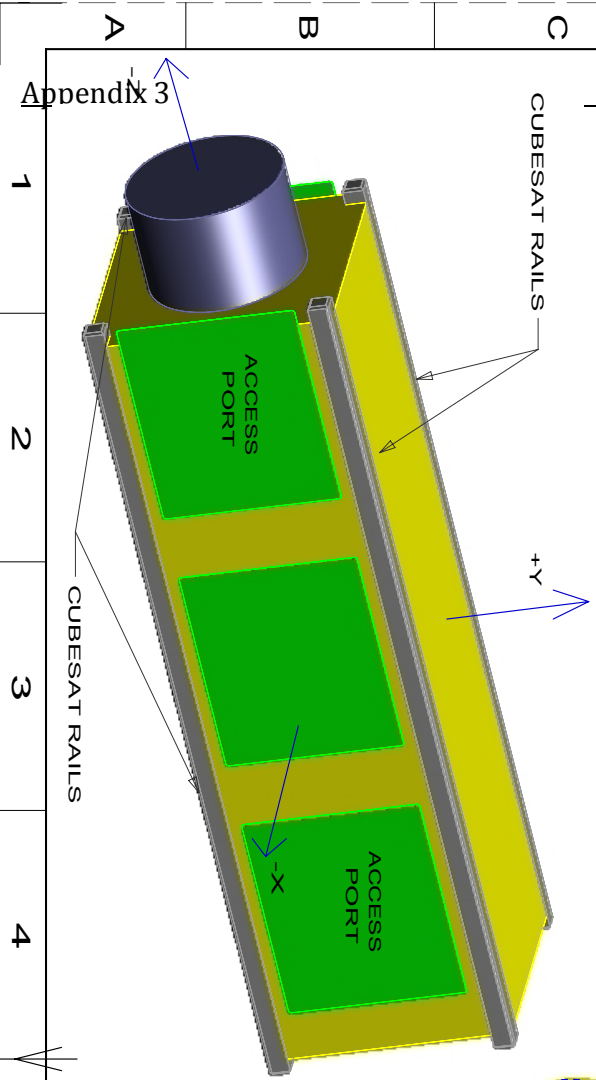
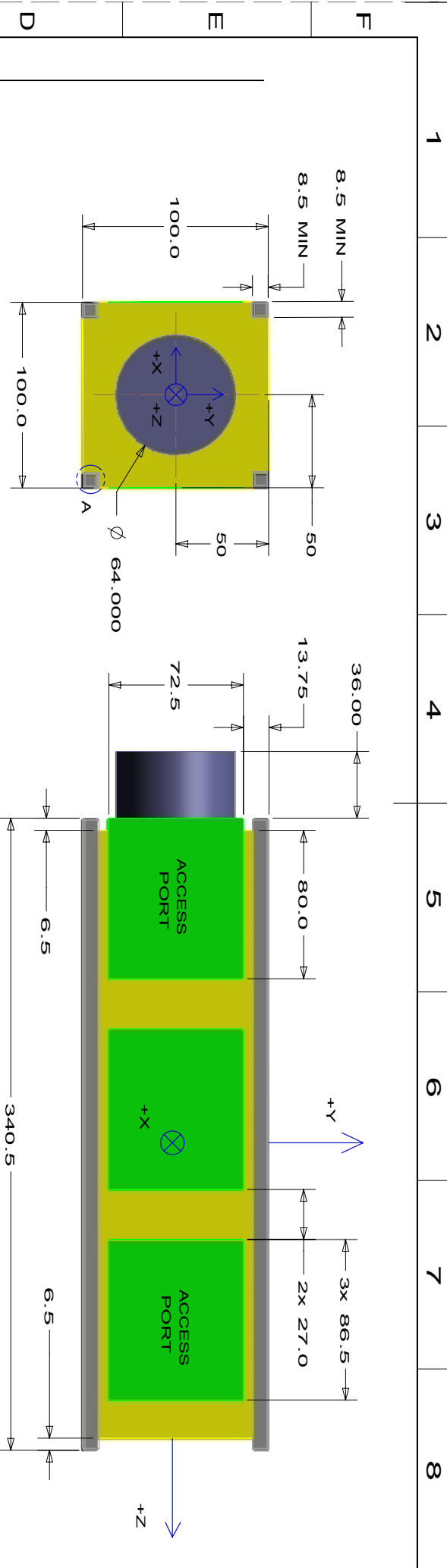
ALL DIMENSIONS IN MILLIMETERS		DESIGNED BY S.FUR		PART NAME		REV	
TOLERANCE ± 0.1		DRAWN BY S.FUR		California Polytechnic State University CubeSat Program (805) 756-5087 San Luis Obispo, CA 93407		13	
ROUND ALL EDGES AND CORNERS		CHECKED BY J.CAR		SIZE ASSEMBLY		CUBESAT SPECIFICATION	
DRAWING # GDS-13-002		APPROVED BY R.NUG		B		NOT TO SCALE	
		DATE: 04/03/12		DATE: 04/03/12		SHEET 1 OF 2	

1.5U CUBESAT

REV 13

Section 3
2U CubeSat Design Specification Drawing

Section 5
3U+ CubeSat Design Specification Drawing



DETAIL A
STANDOFF CONTACT
DETAIL FOR -Z

ADDITIONAL NOTES:

- Cubesat coordinate system located in the geometric center of the Cubesat.
- No external components other than the rails shall touch the inside of the P-POD.
- At least one (1) deployment switch must be incorporated on all Cubesats on the -Z face.

		California Polytechnic State University Polytechnic Department (805) 756-5087 San Luis Obispo, CA 93407	
DESIGNED BY	S.F.FUR	PART NAME	3U+ CUBESAT
DRAWN BY	S.F.FUR	REV	13
CHECKED BY	J.CAR	SIZE	ASSEMBLY
APPROVED BY	R.NUG	DATE	04/05/11
DRAWING #	GPS-13-002	NOT TO SCALE	
ALL DIMENSIONS IN MILLIMETERS TOLERANCE ± 0.1		CUBESAT SPECIFICATION SHEET 1 OF 1	
ROUND ALL EDGES AND CORNERS			

1 2 3 4 5 6 7 8

A B C D E F

**Appendix C:
1U, 1.5U, 2U, 3U, and 3U+
CubeSat Acceptance Checklist**

PROVISIONAL

Section 1
1U CubeSat Acceptance Checklist

1U CubeSat Acceptance Checklist

Appendix 3

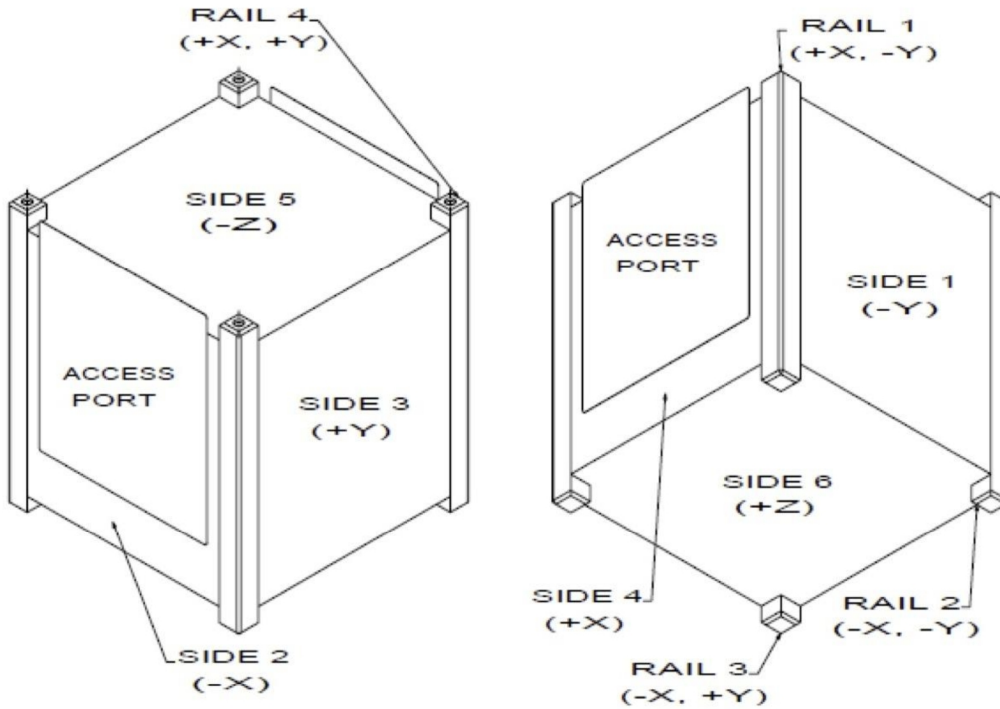
Project: _____ Date/Time: _____ Engineers: _____

Organization: _____ Location: _____

Satellite Name: _____ Satellite S/N: _____

Mass ($1.0^{+0.5}_{-0.2}$ kg)	_____	RBF Pin (≤ 6.5 mm)	_____
Spring Plungers (Depressed)	Functional Y / N Flush with Standoff Y / N	Rails Anodized	Y / N
Deployment Switches (Depressed)	Functional Y / N Flush with Standoff Y / N	Deployables Constrained	Y / N

Mark on the diagram the locations of the RBF pin, connectors, deployables, and any envelope violations.



Authorized By: _____

IT #1: _____

IT #2: _____

Passed: Y / N

List Item	As Measured						Required
Width [x-y]	Side 1 (-Y)	Side 2 (-X)	Side 3 (+Y)	Side 4 (+X)			
+Z	_____	_____	_____	_____			$100.0^{+0.1}_{-0.1}$ mm
Middle	_____	_____	_____	_____			$100.0^{+0.1}_{-0.1}$ mm
-Z	_____	_____	_____	_____			$100.0^{+0.1}_{-0.1}$ mm
Height [x-y]	Rail 1 (+X, -Y)	Rail 2 (-X, -Y)	Rail 3 (-X, +Y)	Rail 4 (+X, +Y)			113.5 ± 0.5 mm
	_____	_____	_____	_____			
+Z Standoffs	Rail 1 (+X, -Y) length x width	Rail 2 (-X, -Y) length x width	Rail 3 (-X, +Y) length x width	Rail 4 (+X, +Y) length x width			≥ 6.5 mm
	____ x ____	____ x ____	____ x ____	____ x ____			
-Z Standoffs	_____	_____	_____	_____			≥ 6.5 mm
	____ x ____	____ x ____	____ x ____	____ x ____			
Protrusions	Side 1 (-Y)	Side 2 (-X)	Side 3 (+Y)	Side 4 (+X)	Side 5 (-Z)	Side 6 (+Z)	≤ 6.5 mm
	_____	_____	_____	_____	_____	_____	

Section 2
1.5U CubeSat Acceptance Checklist

1.5U CubeSat Acceptance Checklist

Appendix 3

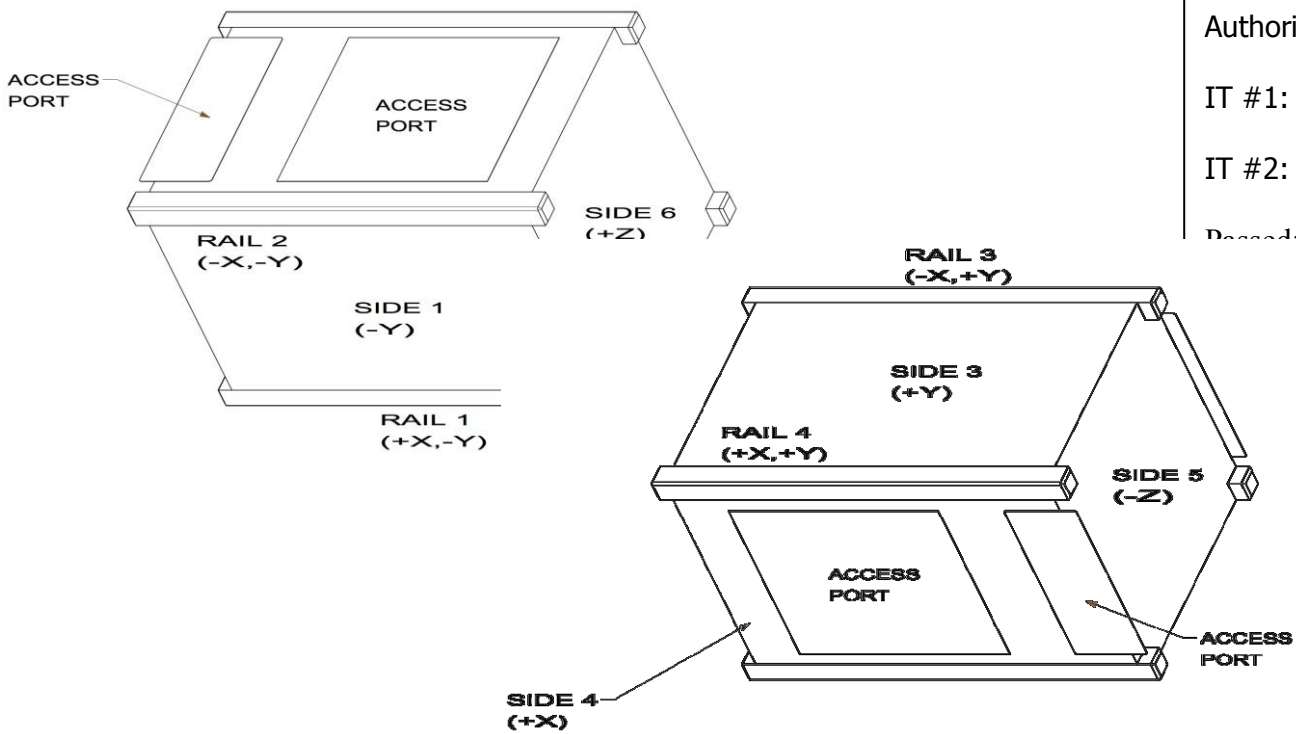
Project: _____ Date/Time: _____ Engineers: _____

Organization: _____ Location: _____

Satellite Name: _____ Satellite S/N: _____

Mass ($1.5^{+0.7}_{-0.3}$ kg)	_____	RBF Pin ($\leq \text{Ø} 8.00$)	_____
Spring Plungers (Depressed)	Functional Y / N Flush with Standoff Y / N	Rails Anodized	Y / N
Deployment Switches (Depressed)	Functional Y / N Flush with Standoff Y / N	Deployables Constrained	Y / N

Mark on the diagram the locations of the RBF pin, connectors, deployables, and any envelope violations.



List Item	As Measured					Required
Width [x-y]	Side 1 (-Y)	Side 2 (-X)	Side 3 (+Y)	Side 4 (+X)		
+Z	_____	_____	_____	_____		$100.0^{+0.1}_{-0.1}$ mm
Middle	_____	_____	_____	_____		$100.0^{+0.1}_{-0.1}$ mm
-Z	_____	_____	_____	_____		$100.0^{+0.1}_{-0.1}$ mm
Height [x-y]	Rail 1 (+X, -Y)	Rail 2 (-X, -Y)	Rail 3 (-X, +Y)	Rail 4 (+X, +Y)		170.2 ± 0.7 mm
	_____	_____	_____	_____		
	Rail 1 (+X, -Y) length x width	Rail 2 (-X, -Y) length x width	Rail 3 (-X, +Y) length x width	Rail 4 (+X, +Y) length x width		
+ Z Standoffs	____ x ____	____ x ____	____ x ____	____ x ____		≥ 6.5 mm
-Z Standoffs	____ x ____	____ x ____	____ x ____	____ x ____		≥ 6.5 mm
Protrusions	Side 1 (-Y)	Side 2 (-X)	Side 3 (+Y)	Side 4 (+X)	Side 5 (-Z)	Side 6 (+Z)
	_____	_____	_____	_____	_____	_____
						≤ 6.5 mm

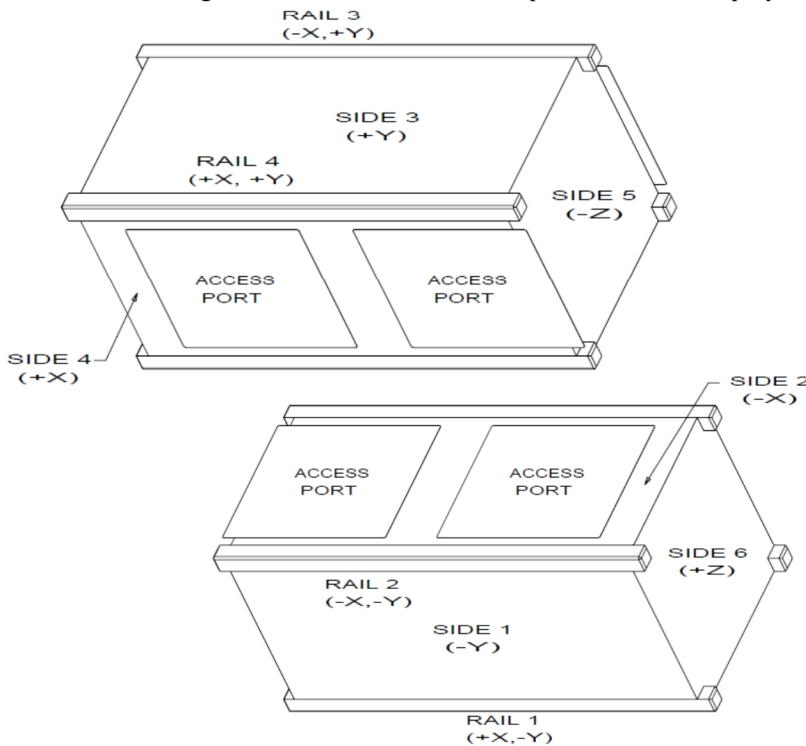
Section 3
2U CubeSat Acceptance Checklist

2U CubeSat Acceptance Checklist

Project: _____ Date/Time: _____ Engineers: _____
 Organization: _____ Location: _____
 Satellite Name: _____ Satellite S/N: _____

Mass ($2.0^{+0.7}_{-0.4} kg$)	_____	RBF Pin ($\leq 6.5mm$)	_____
Spring Plungers (Depressed)	Functional Y / N Flush with Standoff Y / N	Rails Anodized	Y / N
Deployment Switches (Depressed)	Functional Y / N Flush with Standoff Y / N	Deployables Constrained	Y / N

Mark on the diagram the locations of the RBF pin, connectors, deployables, and any envelope violations.



Authorized By: _____
 IT #1: _____
 IT #2: _____
 Passed: **Y / N**

List Item	As Measured					Required
Width [x-y]	Side 1 (-Y)	Side 2 (-X)	Side 3 (+Y)	Side 4 (+X)		
	+Z	_____	_____	_____	_____	$100.0^{+0.1}_{-0.1} mm$
	Middle	_____	_____	_____	_____	$100.0^{+0.1}_{-0.1} mm$
	-Z	_____	_____	_____	_____	$100.0^{+0.1}_{-0.1} mm$
Height [x-y]	Rail 1 (+X, -Y)	Rail 2 (-X, -Y)	Rail 3 (-X, +Y)	Rail 4 (+X,+Y)		
	_____	_____	_____	_____		$227.0 \pm 1.0mm$
+Z Standoffs	Rail 1 (+X, -Y) length x width	Rail 2 (-X, -Y) length x width	Rail 3 (-X, +Y) length x width	Rail 4 (+X, +Y) length x width		
	_____ x _____	_____ x _____	_____ x _____	_____ x _____		$\geq 6.5mm$
-Z Standoffs	_____ x _____	_____ x _____	_____ x _____	_____ x _____		$\geq 6.5mm$
Protrusions	Side 1 (-Y)	Side 2 (-X)	Side 3 (+Y)	Side 4 (+X)	Side 5 (-Z)	Side 6 (+Z)
	_____	_____	_____	_____	_____	_____

Section 4
3U CubeSat Acceptance Checklist

3U CubeSat Acceptance Checklist

Appendix 3

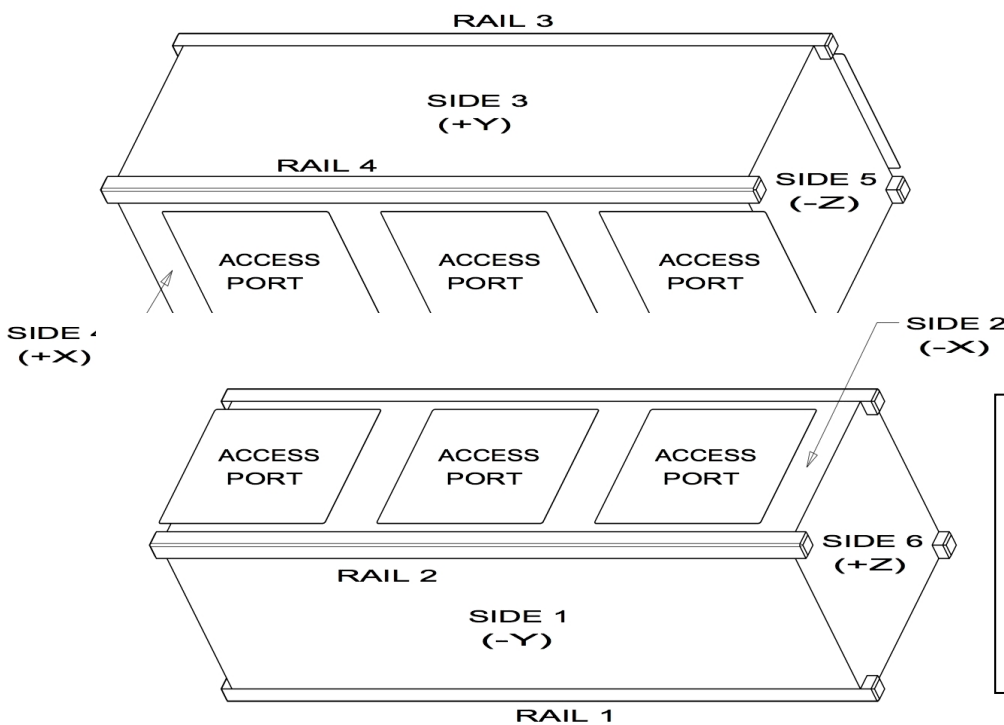
Project: _____ Date/Time: _____ Engineers: _____

Organization: _____ Location: _____

Satellite Name: _____ Satellite S/N: _____

Mass (< 4 kg)	_____	RBF Pin ($\leq \frac{8}{1000} \text{mm}$)	_____
Spring Plungers (Depressed)	Functional Y / N Flush with Standoff Y / N	Rails Anodized	Y / N
Deployment Switches (Depressed)	Functional Y / N Flush with Standoff Y / N	Deployables Constrained	Y / N

Mark on the diagram the locations of the RBF pin, connectors, deployables, 3U+ Protrusion, and any envelope violations.



Authorized By: _____
 IT #1: _____
 IT #2: _____
 Passed: **Y / N**

3U+ Volume
Length (Z): _____ $\leq 36\text{mm}$
Diameter: _____ $\leq 64\text{mm}$
3U+ Centered: Y / N

List Item	As Measured						Required
Width [x-y]	Side 1 (-Y)	Side 2 (-X)	Side 3 (+Y)	Side 4 (+X)			
+Z	_____	_____	_____	_____			100.0 ^{+0.1} _{-0.1} mm
Middle	_____	_____	_____	_____			100.0 ^{+0.1} _{-0.1} mm
-Z	_____	_____	_____	_____			100.0 ^{+0.1} _{-0.1} mm
Height [x-y]	Rail 1 (+X, -Y)	Rail 2 (-X, -Y)	Rail 3 (-X, +Y)	Rail 4 (+X, +Y)			340.5±1.5mm
	Rail 1 (+X, -Y) length x width	Rail 2 (-X, -Y) length x width	Rail 3 (-X, +Y) length x width	Rail 4 (+X, +Y) length x width			
+ Z Standoffs	_____ x _____	_____ x _____	_____ x _____	_____ x _____			≥ 6.5mm
-Z Standoffs	_____ x _____	_____ x _____	_____ x _____	_____ x _____			≥ 6.5mm
Protrusions	Side 1 (-Y)	Side 2 (-X)	Side 3 (+Y)	Side 4 (+X)	Side 5 (-Z)	Side 6 (+Z)	
	_____	_____	_____ 89	_____	_____	_____	≤ 6.5mm

Section 5
3U+ CubeSat Acceptance Checklist

3U+ CubeSat Acceptance Checklist

Appendix 3

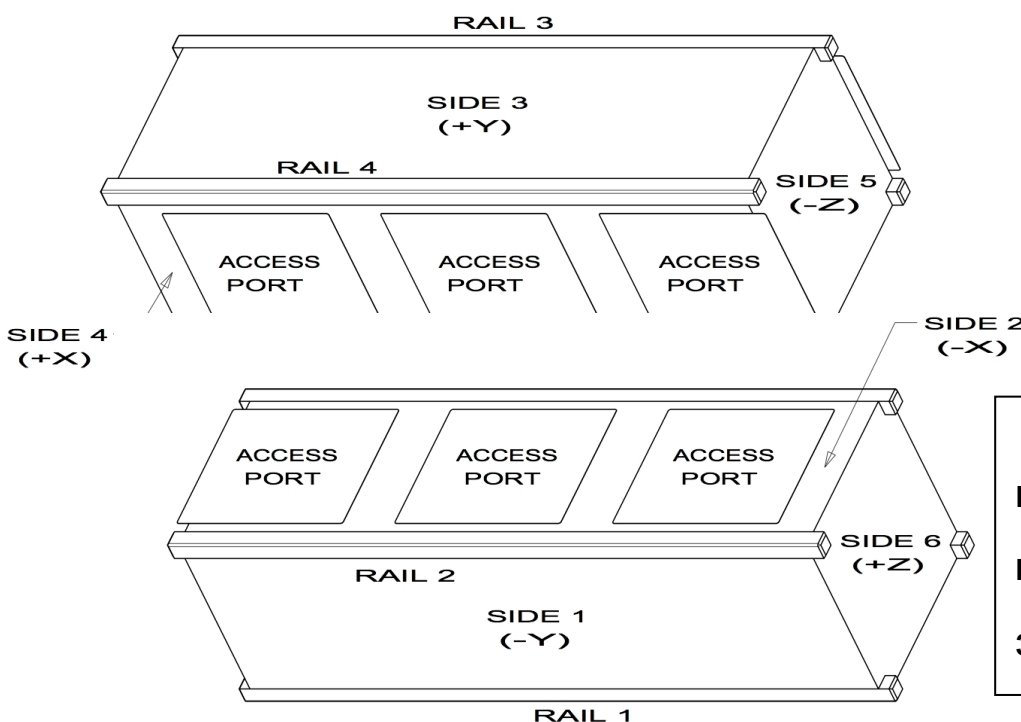
Project: _____ Date/Time: _____ Engineers: _____

Organization: _____ Location: _____

Satellite Name: _____ Satellite S/N: _____

Mass (< 4 kg)	_____	RBF Pin ($\leq \frac{8}{1000} \text{mm}$)	_____
Spring Plungers (Depressed)	Functional Y / N Flush with Standoff Y / N	Rails Anodized	Y / N
Deployment Switches (Depressed)	Functional Y / N Flush with Standoff Y / N	Deployables Constrained	Y / N

Mark on the diagram the locations of the RBF pin, connectors, deployables, and any envelope violations.



Authorized By: _____
IT #1: _____
IT #2: _____
Passed: **Y / N**

3U+ Volume
Length (Z): _____ $\leq 36\text{mm}$
Diameter: _____ $\leq 64\text{mm}$
3U+ Centered: Y / N


List Item	As Measured					Required
Width [x-y]	Side 1 (-Y)	Side 2 (-X)	Side 3 (+Y)	Side 4 (+X)		
+Z	_____	_____	_____	_____		100.0 ^{+0.1} _{-0.1} mm
Middle	_____	_____	_____	_____		100.0 ^{+0.1} _{-0.1} mm
-Z	_____	_____	_____	_____		100.0 ^{+0.1} _{-0.1} mm
Height [x-y]	Rail 1 (+X, -Y)	Rail 2 (-X, -Y)	Rail 3 (-X, +Y)	Rail 4 (+X, +Y)		340.5±1.5mm
	Rail 1 (+X, -Y) length x width	Rail 2 (-X, -Y) length x width	Rail 3 (-X, +Y) length x width	Rail 4 (+X, +Y) length x width		
+ Z Standoffs	_____ x _____	_____ x _____	_____ x _____	_____ x _____		≥ 6.5mm
-Z Standoffs	_____ x _____	_____ x _____	_____ x _____	_____ x _____		≥ 6.5mm
Protrusions	Side 1 (-Y)	Side 2 (-X)	Side 3 (+Y)	Side 4 (+X)	Side 5 (-Z)	Side 6 (+Z)
	_____	_____	_____	_____	_____	_____
			91			
						≤ 6.5mm

3.4. PEEK

PRODUCT DATA SHEET

» POLYETHERETHERKETONE [PEEK-GF30]

KETRON® PEEK-CA30



This 30% carbon fibre reinforced grade combines even higher stiffness, mechanical strength and creep resistance than KETRON PEEK-GF30 with an optimum wear resistance. Moreover, the carbon fibres provide 3.5 times higher thermal conductivity than virgin PEEK, dissipating heat from the bearing surface faster.

Physical properties (indicative values*)

PROPERTIES	Test methods ISO / (IEC)	Units	VALUES
Colour	—	—	black
Density	1183	g/cm ³	1.41
Water absorption:			
- at saturation in air of 23°C / 50% RH	—	%	0.14
- at saturation in water of 23°C	—	%	0.30
Thermal Properties			
Melting temperature	—	°C	340
Thermal conductivity at 23°C	—	W/(K·m)	0.92
Coefficient of linear thermal expansion:			
- average value between 23 and 100°C	—	m/(m·K)	25 · 10 ⁻⁶
- average value between 23 and 150°C	—	m/(m·K)	25 · 10 ⁻⁶
- average value above 150°C	—	m/(m·K)	55 · 10 ⁻⁶
Temperature of deflection under load:			
- method A: 1.8 MPa	75	°C	230
Max. allowable service temperature in air:			
- for short periods (1)	—	°C	310
- continuously: for min. 20,000h (2)	—	°C	250
Flammability (3):			
- "Oxygen Index"	45/89	%	40
- according to UL 94 (1.5/3 mm thickness)	—	—	0/V-0
Mechanical Properties at 23°C			
Tension test (4):			
- tensile stress at break (5)	527	MPa	830
- tensile strain at break (5)	527	%	10
- tensile modulus of elasticity (6)	527	MPa	1,100
Compression test (7):			
- compressive stress at 1% nominal strain (6)	604	MPa	60
- compressive stress at 2% nominal strain (6)	604	MPa	97
Charpy impact strength - linnotched (8)	179/1eJ	kJ/m ²	35
Charpy impact strength - Notched	379/1eA	kJ/m ²	4
Ball indentation hardness (9)	2039-1	Widupis	325
Rockwell hardness (9)	2039-2	M 102	
Electrical Properties at 23°C			
Volume resistivity	(60893)	Ω·cm	< 10 ¹

Legend

- (1) Only for short-time exposure (a few hours) in applications where no or only a very low load is applied to the material.
- (2) Temperature resistance over a period of min. 20,000 hours. After this period of time, there is a decrease of tensile strength of about 50% as compared with the original value. The temperature value given here is thus based on the thermal-oxidative degradation which takes place and causes a reduction in properties. Note, however, that the maximum allowable service temperature depends in many cases essentially on the location and the magnitude of the mechanical stresses to which the material is subjected.
- (3) These mostly experimental ratings, derived from raw material supplier data, are not intended to reflect hazards presented by the materials under actual fire conditions. There is no UL-yellow card available for KETRON PEEK-CA30 stock shapes.
- (4) Test specimens: type 1 B.
- (5) Test speed: 5 mm/min.
- (6) Test speed: 1 mm/min.
- (7) Test specimens: cylinders Ø 12 x 30 mm.
- (8) Indentor used: 4 J.
- (9) 10 mm thick test specimens.

This table is a valuable help in the choice of a material. The data listed here fall within the normal range of product properties of dry material. However, they are not guaranteed and they should not be used to establish material specification limits nor used alone as the basis of design. It has to be noted that KETRON PEEK-CA30 is a fibre reinforced, and consequently anisotropic material (properties differ when measured parallel and perpendicular to the extrusion direction).

Availability

Round Rods: Ø 6-80 mm - **Plates:** Thicknesses 5-60 mm - **Tubes:** O.D. 50-200 mm

All information supplied by or on behalf of Quadrant Engineering Plastic Products in relation to its products, whether in the nature of data, recommendations or otherwise, is supported by research and believed reliable, but Quadrant Engineering Plastic Products assumes no liability whatsoever in respect of application, processing or use made of the aforementioned information or products, or any consequence thereof. The buyer undertakes all liability in respect of the application, processing or use of the aforementioned information or product, whose quality and other properties he shall verify, or any consequence thereof. No liability whatsoever shall attach to Quadrant Engineering Plastic Products for any infringement of the rights owned or controlled by a third party in intellectual, industrial or other property by reason of the application, processing or use of the aforementioned information or products by the buyer.

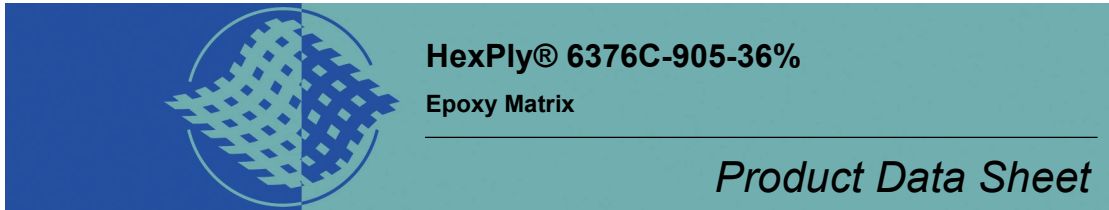
Quadrant Engineering Plastic Products

global leader in engineering plastics for machining

www.quadrantplastics.com

KETRON® is a registered trade mark of Quadrant AG - PEEK® is a trade mark of Wirtec plc. © 2003 Copyright Quadrant AG - Edition January 2003

3.5. Pre-Preg



Description

HexPly® 6376C-905-36% is a Epoxy High Strength Carbon Woven prepreg, whereby 6376 is the resin type; 36% is the resin content by weight; 905 is the reinforcement reference and C represents High Strength Carbon fibre. This data sheet is complementary to the 6376 resin data sheet, which should be consulted for additional information.

Reinforcement Data

			0°	90°
Nominal Area Weight	g/m ²	280	140	140
Composition		5H satin		
Fibre Type		High Strength Carbon 3K		
Nominal Fibre Density	g/cm ³	1,77		

Matrix Properties

Glass transition temperature of laminate (Cure cycle: 120min @ 175°C)	°C	196 (DMA onset, 5°C/min, 1Hz, 30µm),
Nominal Resin Density	g/cm ³	1,31

Prepreg Data

Nominal Area Weight	g/m ²	438
Nominal Resin Content	weight %	36
Tack Level		Medium

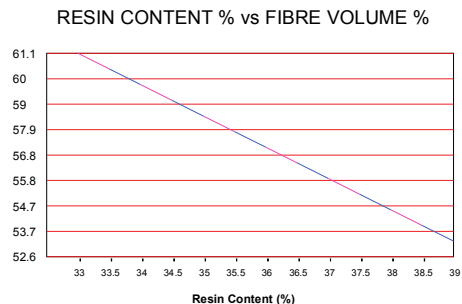
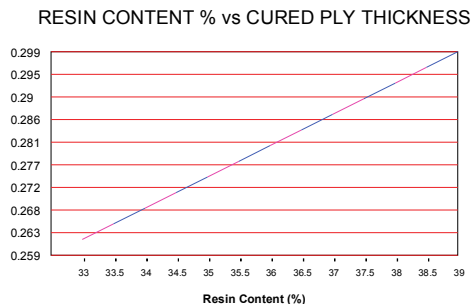
Processing

Cure Cycle	@ 175 °C	120 min
Recommended heat up rate	°C/min	2 - 5°C/min
Pressure gauge	bar	7

The optimum cure cycle, heat up rate and dwell period depend on part size, laminate construction, oven capacity and thermal mass of tool. (See prepreg technology brochure on our website for more information),

Cured Laminate Properties

(nominal composite density 1,57 g/cm³)



The above graphs enable the fibre volume content of a laminate to be estimated using the measured cured ply thickness. The calculation assumes no resin loss.



HexPly® 6376C-905-36%

Mechanical Properties

(Normalised to 60% fibre volume, except for ILSS)

Mechanical Properties are based on 175 °C cure for 120 min, at 7 bar pressure and 0,9 bar vacuum.

Data is the result from several tests on Autoclave cured laminates. Some of the values achieved will have been higher, and some lower, than the figure quoted. These are nominal values.

Warp (RT / Dry)	Tensile	Flexural	ILSS	Compression
Strength (MPa)	1006	-	83	920
Modulus (GPa)	67	-	.	-
Test Method	EN 2561		EN 2563	EN 2850

Prepreg Storage Life

Shelf Life¹: 6 months at -18°C/0°F (from date of manufacture).

¹ Shelf Life: the maximum storage life for HexPly® prepreg, when stored continuously, in a sealed moisture-proof bag, at -18°C/0°F or 5°C/41°F. To accurately establish the exact expiry date, consult the box label.

Out Life²: 21 days at Room Temperature.

² Out Life: the maximum accumulated time allowed at room temperature between removal from the freezer and cure.

Tack Life³: 10 days at Room Temperature.

³ Tack Life: the time, at room temperature, during which prepreg retains enough tack for easy component lay-up.

Prepreg should be stored as received in a cool dry place or in a refrigerator. After removal from refrigerator storage, prepreg should be allowed to reach room temperature before opening the polyethylene bag, thus preventing condensation. (A full reel in its packing can take up to 48 hours).

Precautions for Use

The usual precautions when handling uncured synthetic resins and fine fibrous materials should be observed, and a Safety Data Sheet is available for this product. The use of clean disposable inert gloves provides protection for the operator and avoids contamination of material and components.

Important

All information is believed to be accurate but is given without acceptance of liability. All users should make their own assessment of the suitability of any product for the purposes required. All sales are made subject to our standard terms of sale which include limitations on liability and other terms

® Copyright Hexcel Corporation
HexPly® | 6376C-905-36% | 12/2005 | version : a



HexPly® 6376

175°C curing epoxy matrix

Product Data

Description

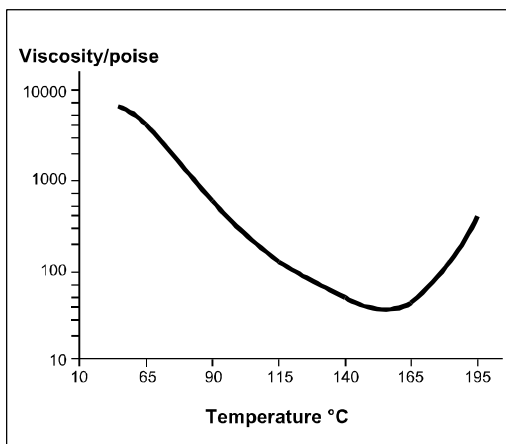
HexPly 6376 is a high performance tough matrix formulated for the fabrication of primary aircraft structures. It offers high impact resistance and damage tolerance for a wide range of high temperature applications.

Benefits and Features

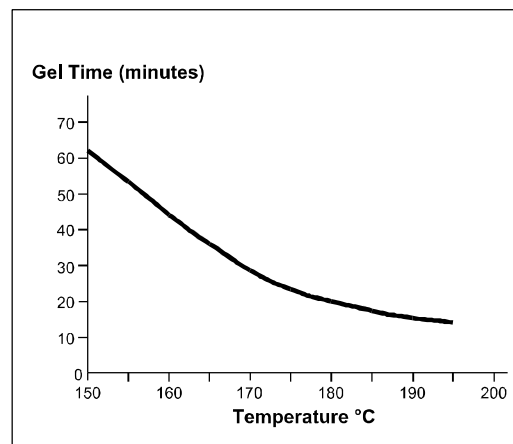
- Excellent toughness and damage tolerance
- Simple straight-up cure cycle
- Controlled matrix flow for ease of processing
- Effective translation of fibre properties
- Good hot/wet properties up to 150°C

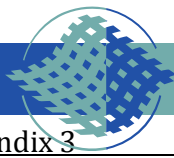
Resin Matrix Properties

Rheology



Gel Time





Cured Matrix Properties (cured at 175°C)

		Method
Tensile strength	105 MPa	ISO R527 type 1
Tensile modulus	3,60 GPa	ISO R527 type 1
Tensile strain	3,1%	ISO R527 type 1
Flexural strength	144 MPa	ISO 178
Flexural modulus	4,4 GPa	ISO 178
Toughness G _{1c}	432 J/m ²	Tested in accordance with EGF Task Group on Polymers and Composites protocol.
Cured density	1.31 g/cm ³	

Prepreg Curing Conditions

2 hours at 175°C and 700kN/m² (7 bar) pressure.

Heat up rate 2°C to 5°C.

Components up to 30 mm thick can be cured without a dwell in the schedule provided that the heat-up rate is not more than 3°C/minute. There is no deterioration in performance after 3 times the recommended cure schedule (verified by interlaminar shear strength tests).

Prepreg Storage Life

- Tack Life @ 23°C 10 days (still processable for up to 21 days).
- Guaranteed Shelf Life @ -18°C 6 months (minimum)
- Storage conditions.

HexPly 6376 prepregs should be stored as received in a cool dry place or in a refrigerator. After removal from refrigerator storage, prepreg should be allowed to reach room temperature before opening the polythene bag, thus preventing condensation. (A full reel in its packaging can take up to 48 hours).

Precautions for Use

The usual precautions when handling uncured synthetic resins and fine fibrous materials should be observed, and a Safety Data Sheet is available for this product. The use of clean disposable inert gloves provides protection for the operator and avoids contamination of material and components.

Important

All information is believed to be accurate but is given without acceptance of liability. Users should make their own assessment of the suitability of any product for the purposes required. All sales are made subject to our standard terms of sale which include limitations on liability and other important terms.

©Copyright Hexcel Corporation
Publication FTA051b (March 2007)

For More Information

Hexcel is a leading worldwide supplier of composite materials to aerospace and other demanding industries. Our comprehensive product range includes:

- Carbon Fibre
- RTM Materials
- Honeycomb Cores
- Continuous Fibre Reinforced Thermoplastics
- Carbon, glass, aramid and hybrid prepregs
- Reinforcement Fabrics
- Structural Film Adhesives
- Honeycomb Sandwich Panels
- Special Process Honeycombs

For US quotes, orders and product information call toll-free 1-800-688-7734

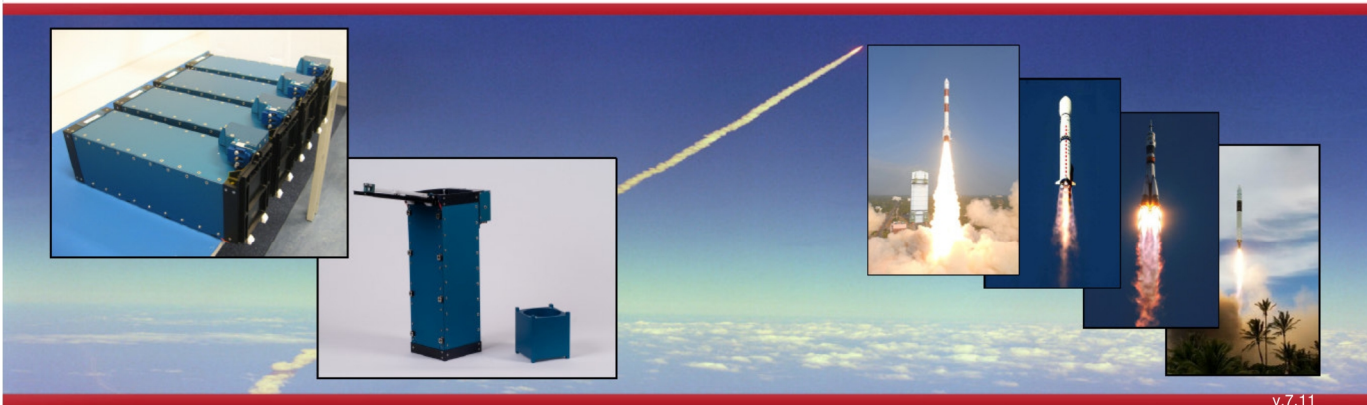
For other worldwide sales office telephone numbers and a full address list please go to:

<http://www.hexcel.com/contact/salesoffices>

3.6. ISIS



ISIPOD CubeSat Deployer



v7.11

Overview

The ISIPOD is an affordable European launch adapter developed by ISIS for use with its ISILaunch Services to accommodate CubeSats onboard a large variety of launch vehicles. Yet it can also be purchased separately in case a CubeSat developer has arranged a launch independently.

By design the ISIPOD provides simple, well defined interfaces with the CubeSats internally and with the launch vehicle externally. During launch, the CubeSats are fully enclosed by the ISIPOD and are only dispensed upon signal by the launch vehicle.

Features

- Provides deployment status signal
- No battery ('unlimited shelf life')
- No pyrotechnics
- No export restrictions
- Protects the CubeSats from external environment
- ISIPOD activated by Launch Vehicle
- More envelope for deployables than other CubeSat launch adapters

Compatibility

- Mechanically interfaces with CubeSats by means of guiderails
- Mechanically interfaces with Launch vehicle by means of standard fasteners
- Electrically interfaces with Launch vehicle for telemetry
- Adheres to latest CubeSat standards

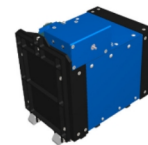
Included in shipment

- ISIPOD
- Documentation

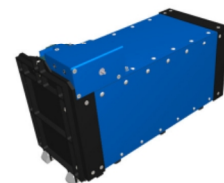
Available Configurations

- 1U ISIPOD
- 2U ISIPOD
- 3U ISIPOD
- Shared configuration possible
- Custom size on request (from 0,5 U to 5U in length)
- Other sizes under development (such as the '6 Pack')

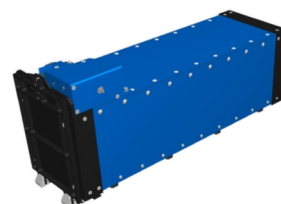
1 U



2 U

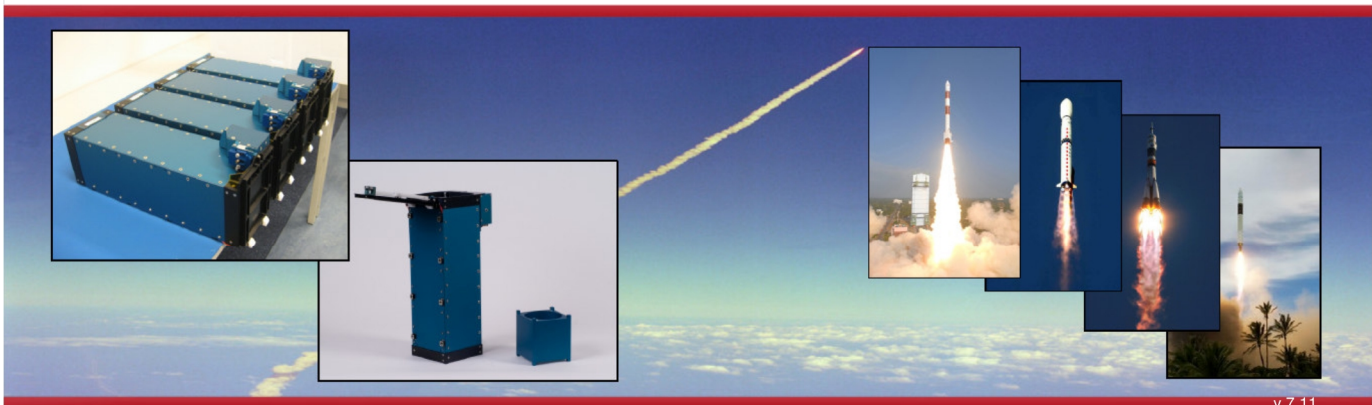


3 U





ISIPOD CubeSat Deployer



v.7.11

Overview

The ISIPOD is an affordable European launch adapter developed by ISIS for use with its ISILaunch Services to accommodate CubeSats onboard a large variety of launch vehicles. Yet it can also be purchased separately in case a CubeSat developer has arranged a launch independently.

By design the ISIPOD provides simple, well defined interfaces with the CubeSats internally and with the launch vehicle externally. During launch, the CubeSats are fully enclosed by the ISIPOD and are only dispensed upon signal by the launch vehicle.

Features

- Provides deployment status signal
- No battery ('unlimited shelf life')
- No pyrotechnics
- No export restrictions
- Protects the CubeSats from external environment
- ISIPOD activated by Launch Vehicle
- More envelope for deployables than other CubeSat launch adapters

Compatibility

- Mechanically interfaces with CubeSats by means of guiderails
- Mechanically interfaces with Launch vehicle by means of standard fasteners
- Electrically interfaces with Launch vehicle for telemetry
- Adheres to latest CubeSat standards

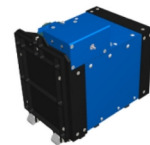
Included in shipment

- ISIPOD
- Documentation

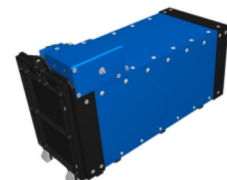
Available Configurations

- 1U ISIPOD
- 2U ISIPOD
- 3U ISIPOD
- Shared configuration possible
- Custom size on request (from 0,5 U to 5U in length)
- Other sizes under development (such as the '6 Pack')

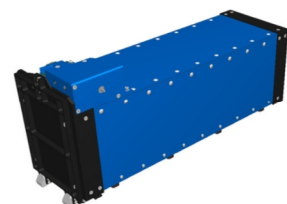
1 U



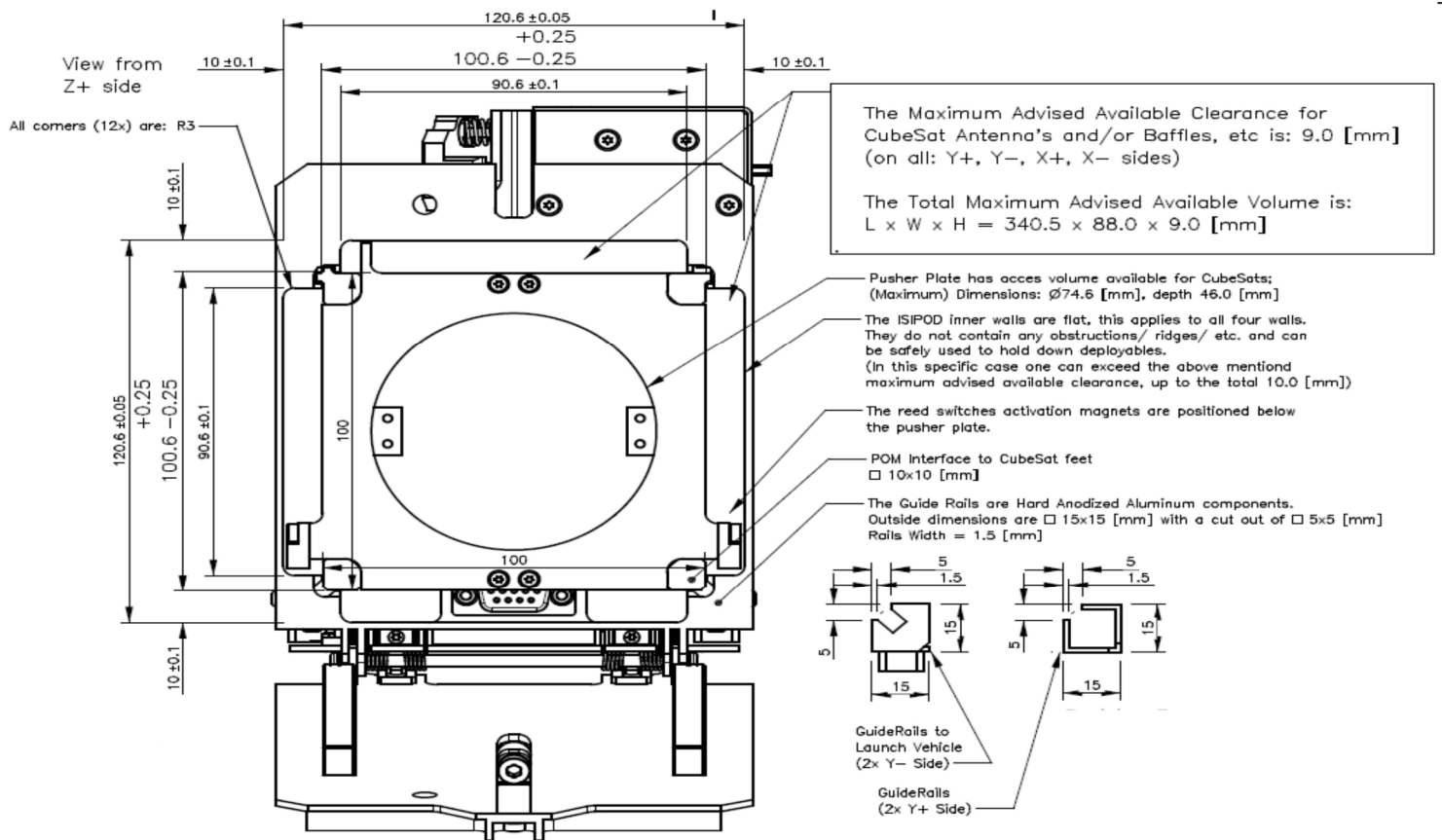
2 U



3 U



ISIPOD CubeSat Deployer

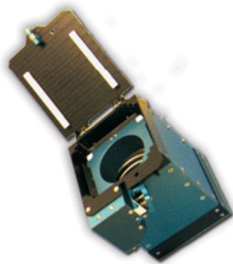


Specifications

	1U	2U	3U
ISIPOD mass	1.5 kg	1.75 kg	2.0 kg
Payload mass [typical]	1.0 kg	2.0 kg	3.0 kg
Payload mass [maximum]	2.0 kg	4.0 kg	6.0 kg
Envelope [H x W x L] (mm ³)	~ 182 x 127 x 186	~ 182 x 127 x 300	~ 182 x 127 x 414

Qualification

- Qualified for multitude of launch vehicles
- Qualified for heavier CubeSat payloads (up to 6.0 kg for a 3U ISIPOD)
- Qualified temperature range: -40 °C to +90 °C



Qualification and Acceptance Testing

Test	QT	AT
Functional	✓	✓
Vibration	✓	✓
Mechanical Shock	✓	-
Thermal Cycling	✓	✓
Thermal Vacuum	✓	-
Total Ionizing Dose	-	-

QT is performed on the design/qualification model

AT is performed on the unit to be shipped

This document is subject to change without notice. The latest technical information and price information is available on www.cubesatshop.com

ISIS - Innovative Solutions In Space

Molengraaffsingel 12-14, 2629 JD, Delft, The Netherlands • T +31152569018 • F +31152573969 • info@isispace.nl • www.isispace.nl

3.7. BeCU

Heat Treating Copper Beryllium Parts

Heat treating is key to the versatility of the copper beryllium alloy system. Unlike other copper base alloys which acquire their strength through cold work alone, wrought copper beryllium obtains its high strength, conductivity, and hardness through a combination of cold work and a thermal process called age hardening. Age hardening is often referred to as precipitation hardening or heat treating. The ability of these alloys to accept this heat treatment results in forming and mechanical property advantages not available in other alloys. For example, intricate shapes can be fabricated when the material is in its ductile, as rolled state and subsequently age hardened to the highest strength and hardness levels of any copper base alloy.

Heat treating the copper beryllium alloys is a two step process which consists of solution annealing and age hardening. Because Materion Brush Performance Alloys performs the required solution anneal on all wrought products prior to shipping, most fabricators' primary concern is the age hardening process. The following text details this process and overviews the available copper beryllium alloys. Specific heat treating procedures for Wrought and Cast products, recommended heat treating equipment, surface oxidation information, and general solution annealing practices are also included.

COPPER BERYLLIUM ALLOYS

Copper beryllium alloys are available in two basic classes (Table 1): *High Strength Copper Beryllium* offers high strength with moderate to good conductivity; and *High Conductivity Copper Beryllium* features maximum conductivity and slightly lower strength levels.

High Strength Copper Beryllium		High Conductivity Copper Beryllium	
Wrought	Cast	Wrought	Cast
25 (C17200) 190 (C17200)* 290 (C17200) M25 (C17300) 165 (C17000)	275C (C82800) 20C (C82500) 21C (C82510) 165C (C82400)	3 (C17510) 10 (C17500) 174 (C17410)* Brush 60 (C17460)* 390 (C17460)*	3C (C82200)

* These alloys are supplied only in the mill hardened condition and require no further heat treatment.

Table 1. Copper Beryllium Alloys, Materion Brush Performance Alloys Designations and UNS Numbers

Both the *High Strength* and *High Conductivity* Copper Beryllium are available as strip in the heat treatable and mill

hardened tempers. Mill hardened tempers are supplied in the heat treated condition and require no further heat treatment.

Copper beryllium is produced in tempers ranging from solution annealed (A) to an as rolled condition (H). Heat treating maximizes the strength and conductivity of these alloys. The temper designations of the standard age hardenable copper beryllium tempers are shown in Table 2.

Materion Brush Performance Alloys Designation	ASTM Designation	Description
A	TB00	Solution annealed
1/4 H	TD01	Cold worked, Quarter hard
1/2 H	TD02	Cold worked, Half hard
3/4 H	TD03	Cold worked, Three-quarter hard
H	TD04	Cold worked, hard
AT	TF00	The suffix "T" added to Materion
1/4 HT	TH01	Brush Performance Alloys temper
1/2 HT	TH02	designations indicates that the
3/4 HT	TH03	material has been age hardened by the
HT	TH04	standard heat treatment.

Table 2. Temper Designations, Alloys 25 strip and wire

AGE HARDENING COPPER BERYLLIUM ALLOYS

Copper beryllium achieves its maximum levels of strength, hardness, and conductivity through age hardening. During the age hardening process, microscopic, beryllium rich particles are formed in the metal matrix. This is a diffusion controlled reaction, and the strength will vary with aging time and temperature.

Appendix 3

Recommended or standard age hardening time and temperature combinations have been determined for each copper beryllium alloy. These standard times and temperatures allow parts to reach peak strength in two to three hours, without the risk of strength decrease due to extended temperature exposure. As an example, the Alloy 25 response curves in Figure 1 indicate how low, standard, and high aging temperatures affect both peak properties and the time required for the alloy to reach peak strength.

In Figure 1, at the low temperature of 550°F (290°C), the strength of Alloy 25 increases slowly, and peak strength is not reached until approximately 30 hours. At the standard temperature of 600°F (315°C), Brush Alloy 25 exhibits virtually no change in strength after three hours of exposure. At 700°F (370°C), peak strength is reached in 30 minutes and declines almost immediately. In short, as aging temperature increases, the time necessary to reach peak strength decreases, as does maximum obtainable strength. This response is similar for all copper beryllium alloys, but at different standard temperatures.

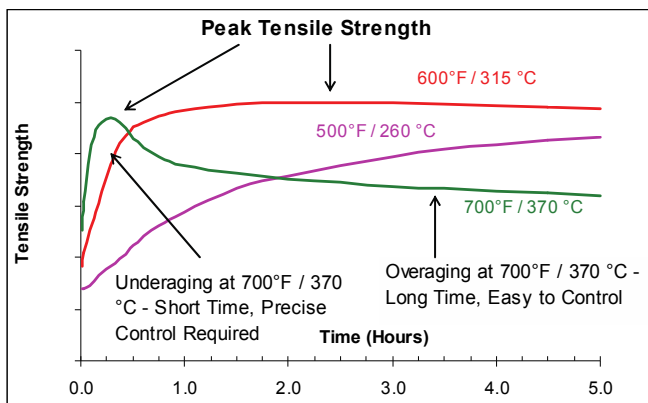


Figure 1. Alloy 25 – Response to Age Hardening Heat Treatment for three temperatures

Copper beryllium can be age hardened to varying degrees of strength. The term peak aged refers to copper beryllium aged to maximum strength. Alloys not aged to maximum strength are underaged, and alloys aged beyond maximum strength are overaged. Underaging copper beryllium increases toughness, uniform elongation, and fatigue strength. Overaging increases the alloy's electrical and thermal conductivity's and dimensional stability. Copper beryllium never ages at room temperature, even if material

is stored for significant lengths of time.

Allowable variances in age hardening time are dependent on furnace temperature and final property requirements. To peak age at the standard temperature, furnace time is typically controlled to ± 30 minutes. For high temperature aging, however, more precise time control is required to avoid overaging. For example, the aging time of Alloy 25 at 700°F (370°C) must be controlled to ± 3 minutes to hold peak properties. Similarly, underaging requires tight control of the process variables because of the sharp initial increase of the aging response curve. In the standard age hardening cycle, heating and cooling rates are not critical.

However, to assure that aging time does not begin until parts reach temperature, a thermocouple can be placed on the parts to determine when desired temperature has been achieved.

Standard age hardening times and temperatures for the High Strength Copper Beryllium alloys and the High Conductivity Copper Beryllium alloys are detailed in the following sections.

HIGH STRENGTH WROUGHT COPPER BERYLLIUM (ALLOYS 25, M25, AND 165)

Age hardening temperatures for high strength wrought copper beryllium varies from 500°F (260°C) to 700°F (370°C). The time required to reach peak properties at the lower temperature is longer than at the higher temperature. The standard age hardening treatment is 600°F (315°C) for two to three hours; two hours for cold worked alloys and three hours for annealed alloys. Figure 2 shows the effect of time and temperature on the mechanical properties of Alloy 25 1/2H temper.

Contact the Technical Service Department at Materion Brush Performance Alloys for a complete set of detailed aging response curves.

HIGH STRENGTH CAST BERYLLIUM COPPER ALLOYS (ALLOYS 275C, 20C, 21C, AND 165C)

The standard age hardening cycle for the high strength casting alloys, both annealed and as cast, is three hours at 625-650°F (320-340°C). However, to develop the highest strength for the as cast products, a separate solution anneal should precede the age hardening.

HIGH CONDUCTIVITY WROUGHT ALLOYS (ALLOYS 3 AND 10) AND HIGH CONDUCTIVITY CAST ALLOY 3C

The standard age hardening cycle for both the wrought and cast high conductivity alloys is 900°F (480°C) for two to three hours; two hours for the cold rolled alloys and three hours for the cast and annealed wrought alloys. The high conductivity alloys are noted for their excellent electrical and thermal conductivity's. They obtain their moderate strength through age hardening, but at a higher temperature than the high strength alloys.

Because their mechanical properties change only slightly with time, few high conductivity applications benefit from either underaging or overaging. As an example, the heat treating curves for Alloy 3 demonstrate the affects of aging on the mechanical properties (see Figure 3).

AGE HARDENING EQUIPMENT

Recirculating Air Furnaces

Recirculating air furnaces, with temperature controlled to $\pm 15^{\circ}\text{F}$ ($\pm 10^{\circ}\text{C}$), are recommended for the standard age hardening of copper beryllium parts. These furnaces are designed to accommodate both large and small batches of parts, and are ideal for reels of stamped parts aged on carrier strips. However, care must be exercised when aging large batches of parts. Because of their sheer thermal mass, large batches of parts will not have all parts at temperature for the same length of time. As a result, underaging or short aging cycles of large batches of parts should be avoided.

Strand Aging Furnaces

Strand aging furnaces, using a protective atmosphere as the heating medium, are suitable for processing large quantities of material in coil form. This process is generally used by metal producers, and performed in long furnaces where material can be uncoiled into the furnace, passed through heating and cooling zones, and upcoiled upon exiting the furnace. The advantages of this type of furnace include good time and temperature control, better part to part uniformity and the ability to control special cycles for underaging or high temperature/short time aging and selectively hardening a portion of a part.

Salt Baths

Also recommended for age hardening wrought products are salt baths. Salt baths offer rapid and uniform heating, and are recommended at any temperature in the hardening

range. They are particularly advantageous for short time, high temperature aging.

Vacuum Furnaces

Vacuum aging of copper beryllium parts can be done successfully, but caution must be exercised. Because vacuum furnace heating is by radiation only, it is difficult to uniformly heat large loads of parts. Parts on the outside of the load are subject to more direct radiation than those on the inside, as a result, the temperature gradient produces a variation in properties after heat treatment. To assure uniform heating, load size should be limited and parts must be shielded from the heating coils.

Alternatively, vacuum furnaces, backfilled with an inert gas such as argon or nitrogen, can be used. Again, parts must be shielded unless the furnace is equipped with a recirculating fan.

SURFACE OXIDE

During aging, the copper beryllium alloys develop a surface oxide composed of beryllium and, depending on the alloy and furnace atmosphere, copper oxides. These oxide films vary in thickness and composition and are often transparent.

Surface oxidation of beryllium during age hardening cannot be suppressed, even in a pure hydrogen atmosphere or a hard vacuum. However, some atmospheres can minimize the copper oxidation. For instance, a low dew point ($-40^{\circ}\text{F}/-40^{\circ}\text{C}$) atmosphere of approximately 5 percent hydrogen in nitrogen will minimize oxidation and economically aid in heat transfer. Air atmospheres contribute the most to surface oxide and reducing atmospheres the least.

Although oxide films are not detrimental to the base alloy, they should be removed if parts are to be plated, brazed, or soldered. For specific information on cleaning copper beryllium, consult the Materion Brush Performance Alloys TechBrief, "Cleaning Copper Beryllium".

SOLUTION ANNEALING

To elicit an effective age hardening response, copper beryllium must be solution annealed and quenched prior to aging. In addition to preparing the alloy for age hardening, annealing softens the alloy for further cold work and regulates grain size. Materion Brush Performance Alloys performs this required anneal on all wrought products at the mill. Therefore, customers usually do not need to anneal

Appendix 3

prior to age hardening. Furthermore, solution annealing will cause expansion and distortion of machined parts, and can cause generation of hazardous oxides on the surface.

If solution annealing is required, it is a high temperature soak: 1450°F (790°C) for the high strength alloys and 1650°F (900°C) for the high conductivity alloys. Annealing must be carefully controlled as excess time or temperature may cause grain growth. Solution annealing should be immediately followed by a water quench. As a precaution, large quantities of metal should not be annealed without first conducting a furnace simulation test. Thin sections, such as fine wire, require an annealing time of about 3-5 minutes. Fifteen minutes to one hour is required for thin walled tube and small castings. Heavy sections (above about one inch) usually require 1-3 hours. A heat up time of one hour per inch of thickness must be added to the soak time. If you need assistance in establishing an annealing cycle, call Materion Brush Performance Alloys' Customer Technical Service Department.

Because most salts will attack copper beryllium at temperatures in the solution annealing range, solution annealing should not be performed in a salt bath.

When peak aging copper beryllium castings and weldments, the customer must always solution anneal prior to age hardening. However, if peak properties are not required, castings can be age hardened from the as cast condition without the solution anneal.

MILL HARDENED ALLOYS

In applications not requiring severe forming, fabricators can eliminate the heat treating and cleaning of the heat treatable alloys by specifying mill hardened copper beryllium. Materion Brush Performance Alloys performs a special heat treatment on mill hardened product which delivers maximum formability at desired strength levels.

High Strength Mill Hardened Alloys

The high strength copper beryllium mill hardened alloys are Brush Alloy 190 and 290. Both alloys fall within the C17200 designation and are available in several tempers. Alloy 290 provides improved formability at a given strength level.

High Conductivity Mill Hardened Alloys

The high conductivity mill hardened copper beryllium alloys are Brush Alloys 3, 10, 174, Brush 60[®], BrushForm[®] 47, 390[®], and 390E. The mechanical properties of mill hardened Alloys 3 and 10 are equivalent to the peak aged properties of the AT or HT age hardenable tempers. High conductivity Alloys 174, Brush 60, BrushForm 47, 390 and 390E are available only in mill hardened tempers. Consult the "Guide to Materion Brush High Performance Alloys" for additional data on all mill hardened tempers.

SAFE HANDLING OF COPPER BERYLLIUM

Please refer to the Materion Corporation publications "Safety Facts 6 - Safety Practices for Heat Treating Copper Beryllium Parts", and "Safety Facts 105 - Processing Copper Beryllium Alloys."

Handling copper beryllium in solid form poses no special health risk. Like many industrial materials, beryllium-containing materials may pose a health risk if recommended safe handling practices are not followed. Inhalation of airborne beryllium may cause a serious lung disorder in susceptible individuals. The Occupational Safety and Health Administration (OSHA) has set mandatory limits on occupational respiratory exposures. Read and follow the guidance in the Material Safety Data Sheet (MSDS) before working with this material. For additional information on safe handling practices or technical data on copper beryllium, contact Materion Brush Performance Alloys, Technical Service Department at 1-800-375-4205.

BrushForm[®], Brush 60[®], and Alloy 390[®] are registered trademarks of Materion Brush Inc.

Annendix 3

Alloy 25 1/2 H

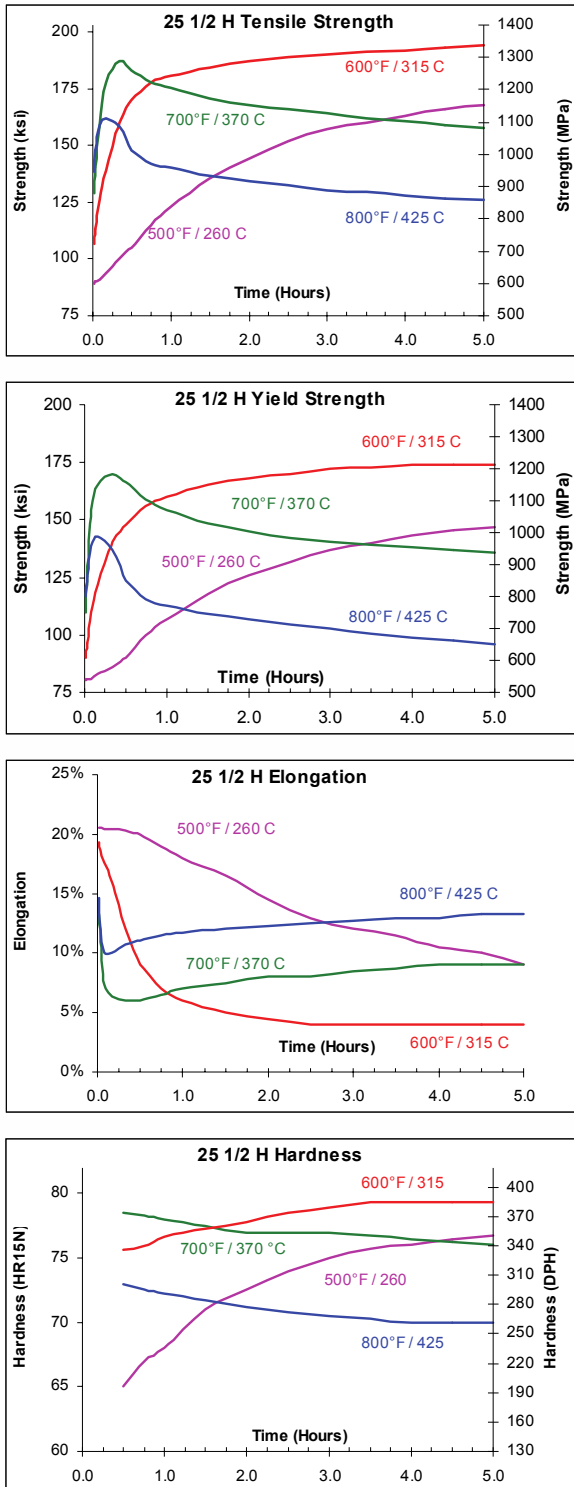


Figure 2. Alloy 25 1/2 H Aging Response Curves

Alloys 3 A and 10 A

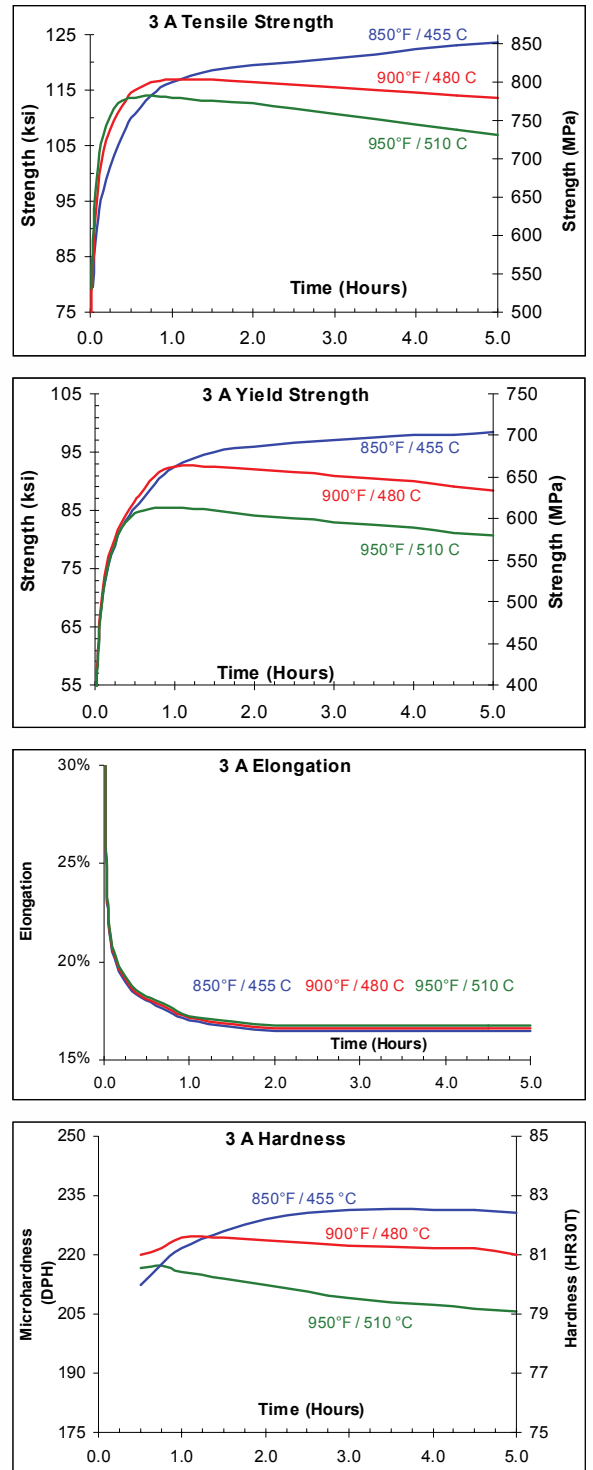


Figure 3. Alloys 3 A and 10 A Aging Response Curves



Processing Copper Beryllium Alloys

SF105 - Version 2, March, 2011

Copper beryllium (CuBe), in solid form and as contained in finished products, presents no special health risks. Most manufacturing operations conducted properly on well-maintained equipment are capable of safely processing copper beryllium containing materials. However, like many industrial materials, copper beryllium may present a health risk if handled improperly. The inhalation of dust, mist or fume containing beryllium can cause a serious lung condition in some individuals. The degree of hazard varies, depending on the form of the product, how it is processed and handled, as well as the amount of beryllium in the product. Read the product specific Material Safety Data Sheet (MSDS) for additional environmental, health, and safety information before working with copper beryllium alloys.

Potential for exposure to beryllium-containing particulate should be determined by conducting a workplace exposure characterization which includes air sampling in the worker's breathing zone, work area and throughout the department. Use an industrial hygienist or other qualified professional to establish the frequency and type of air sampling necessary. Develop and implement a sampling approach that identifies the extent of potential exposure variation and provides statistical confidence in the results. Make air sample results available to workers.

Facilities handling beryllium-containing materials in ways which generate particulate are encouraged to use engineering and work practice controls, including personal protective equipment, to control potential worker exposure. Use exposure controls to keep beryllium work areas clean and keep beryllium particulate out of the lungs, off the skin, off of clothing, in the work process, in the work area and on the plant site. It remains the best practice to maintain levels of all forms of beryllium exposure as low as reasonably achievable, and continue to work to improve exposure control practices and procedures.

SOURCES OF EXPOSURE

The following table provides a summary of those copper beryllium processes that typically present low inhalation concern (green).

Low Inhalation Concern Operations			
Adhesive Bonding	Drawing	Milling	Shipping
Age Hardening (<950°F)	Drilling	Packaging	Sizing
Assembly	Dry Tumbling	Painting	Skiving
Bending	Electroless Plating	Physical Testing	Slitting
Blanking	Electroplating	Piercing	Stamping
Bonding	Extrusion	Pilger	Straightening
Boring	Filing by Hand	Plating	Stretch Bend Leveling
Broaching	Gun Drilling	Pressing	Stretcher Leveling
CNC Machining	Hand Solvent Cleaning	Radiography/X-ray	Tapping
Cold Forging	Handling	Reaming	Tensile Testing
Cold Heading	Heading	Ring Forging	Thread Rolling
Cold Pilger	Heat Treating (inert atmosphere)	Ring Rolling	Trepanning
Cold Rolling	Inspection	Roll Bonding	Tumbling
Cutting	Machining	Rotary forging	Turning
Deburring (non-grinding)	Metallography	Sawing (tooth blade)	Ultrasonic Cleaning
Deep Hole Drilling		Shearing	Ultrasonic Testing
			Upsetting

Notes:

- Operations in the "Low Inhalation Concern" category represent operations that typically release non-respirable (>10 micrometer) particles, are not expected to generate significant ultra-fine particulate, and/or are not expected to result in exposures in excess of the Occupational Safety and Health Administration (OSHA) Permissible Exposure Limit (PEL).
- This list is not all-inclusive and variation can exist within specific processes. To verify the adequacy of engineering and work practice controls, conduct an exposure characterization of all copper beryllium processing operations.
- Age hardening, as included in this table, is a heat treatment process conducted at <950°F.
- When evaluating operations, consideration must be given to potential exposures from activities in support of these operations such as setup, preparation, cleanup and maintenance.

Appendix 3

The following table provides a summary of those copper beryllium processes that may present a likely inhalation hazard (yellow).

Likely Inhalation Hazard Operations			
Abrasive Blasting	Dross Handling	Laser Cutting	Sanding
Abrasive Processing	Electrical Chemical Machining (ECM)	Laser Machining	Scrap Management (Clean)
Abrasive Sawing	Electrical Discharge Machining (EDM)	Laser Scribing	Sectioning
Annealing	Electron Beam Welding (EBW)	Laser Marking	Slab Milling
Brazing	Forging	Laser Welding	Soldering
Bright Cleaning	Grinding	Laundering	Solution Management
Brushing	Heat Treating (in air)	Melting	Spot Welding
Buffing	High Speed Machining (>10,000 rpm)	Photo-Etching	Sputtering
Burnishing	Honing	Pickling	Swaging
Casting	Hot Forging	Point and Chamfer	Torch cutting (i.e., oxy-acetylene)
Centerless Grinding	Hot Rolling	Polishing	Water-jet Cutting
Chemical Cleaning	Investment Casting	Process Ventilation	Welding (ARC, TIG, MIG, etc.)
Chemical Etching	Lapping	Maintenance	Wire Electrical Discharge Machining (WEDM)
Chemical Milling		Resistance Welding	
Coolant Management		Roller Burnishing	
Deburring (grinding)		Sand Blasting	
Destructive Testing		Sand Casting	

Notes:

- Operations in the "Likely Inhalation Hazard" category represent those operations which may release respirable (<10 micrometer) particles, may generate ultra-fine particulate, may generate beryllium oxide and/or may result in exposures in excess of the OSHA PEL.
- This list is not all-inclusive and variation can exist within specific processes. Determine, then verify, the adequacy of engineering and work practice controls by conducting an exposure characterization of all copper beryllium processing operations.
- Effective ventilation, work practices and personal protective equipment use can control a "Likely Inhalation Hazard".
- When evaluating operations, consideration must be given to potential exposures from activities in support of these operations such as setup, preparation, cleanup and maintenance.
- High temperature annealing (>1000°F) conducted in air can generate a loose beryllium-containing oxide scale that can flake off during processing and become airborne. Annealing in an inert or reducing atmosphere can minimize the formation of surface metal oxides.
- Pickling, as included in this table, involves the use of strong acid and/or caustic solutions to remove metal oxides from the surface of beryllium-containing alloys. Other chemical cleaning or surface preparation operations should be characterized to determine potential exposure risk.
- The use of the term "may generate ultra-fine particulate" to categorize the hazard of particular operations addresses the hypothesis that exposure to a large number of beryllium-containing particles with low mass and an aerodynamic diameter of 1 micrometer or less increases the risk of developing CBD.

ADDITIONAL INFORMATION

The information contained in this Safety Facts applies only to the subject referenced in the title. Read the MSDS specific to the products in use at your facility for more detailed environmental, health and safety guidance. MSDSs can be obtained by contacting the Materion Brush Inc. Product Safety Hotline at (800) 862-4118 or website at www.materion.com.

Additional information can also be obtained by contacting a Materion Brush Inc. Sales Representative or:

Product Stewardship Department
Materion Brush Inc.
6070 Parkland Boulevard
Mayfield Heights, Ohio 44124
(800) 862-4118



SAFETY FACTS

SAFETY PRACTICES FOR HEAT TREATING COPPER BERYLLIUM PARTS

SF6 - Version 1.3, December 2008

Copper beryllium (CuBe), in solid form and as contained in finished products, presents no special health risks. Most manufacturing operations, conducted properly on well-maintained equipment, are capable of safely processing copper beryllium-containing materials. However, like many industrial materials, copper beryllium may present a health risk if handled improperly. The inhalation of dust, mist or fume containing beryllium can cause a serious lung condition in some individuals. The degree of hazard varies, depending on the form of the product, how it is processed and handled, as well as the amount of beryllium in the product. Read the product specific Material Safety Data Sheet (MSDS) for additional environmental, health and safety information before working with copper beryllium alloys.

Heat treating of copper beryllium parts presents minimal environmental hazards. However, as with all heat treating operations, certain safety precautions are required. Before heat treating, the parts should be cleaned to remove the stamping or machining lubricant, which, if not removed, can cause staining when exposed to elevated temperatures. While copper beryllium heat treating operations do not generate any beryllium-containing fume, spalling of the surface oxide during subsequent machining or handling steps can cause potential exposure.

High temperature annealing operations in air produce a thick oxide that is easily dislodged from the surface. Although the scale is composed mostly of copper oxides, it contains beryllium oxide in proportion to the beryllium content of the alloy. It is best if the furnace atmosphere is controlled to minimize oxide formation. An inert or reducing furnace atmosphere in the lower temperature precipitation aging step produces a thin, adherent oxide that usually presents no handling problems.

The oxidized surface of heat-treated copper beryllium parts should be cleaned before further processing, particularly if they will be plated, soldered, brazed or welded. Chemical cleaning in an acid solution is preferred to minimize the potential for exposure to fine particulate. Mechanical surface conditioning, such as grinding or grit blasting, must be done in a safe manner to prevent generation of airborne particulate. Keeping the oxide moist will control generation of airborne particulate during handling and disposal; however, ventilation is the preferred method to control airborne generation of particulate.



ADDITIONAL INFORMATION


The information contained in this Safety Facts applies only to the subject referenced in the title. Read the MSDS specific to the products in use at your facility for more detailed environmental, health and safety guidance. MSDSs can be obtained by contacting the Brush Materion Inc. Product Safety Hotline at (800) 862-4118 or visit our website at www.materion.com.

Additional information can also be obtained by contacting a Brush Materion Inc. Sales Representative or:

Product Stewardship Department
Brush Materion Inc.
6070 Parkland Boulevard
Mayfield Heights, Ohio 44124
(800) 862-4118

4 APPENDIX 4

4.1. HMS

NTNU	Risikovurdering				Utarbeidet av	Nummer	Dato
					Anders Håland	HMSRV002	07.02.2014
HMS					Godkjent av Jan M. G. Farstad		Erstatter 09.09.2013

Enhet:

Linjeleder:

Deltakere ved kartleggingen (m/ funksjon):

Velleder: Jan Magnus G. Farstad, Student Tech: Anders Håland

Risikovurderingen gjelder hovedaktivitet: Masteroppgave for Anders Håland, Ferdigstilling og testing av mekanisk struktur for NUTS CubeSat

Signaturer:

Ansvarlig veileder: Student: 

Dato: 10.02.14

ID nr	Aktivitet fra kartleggings-skjemaet	Mulig uønsket hendelse/ belastning	Vurdering av sannsynlighet (1-5)	Vurdering av konsekvens:				Risikoverdi (monneske)	Kommentarer/status Forslag til tiltak
				Menneske (A-E)	Ytre miljø (A-E)	Øk/ materiell (A-E)	Om- domme (A-E)		
1	Skrive oppgave på kontor, dvs sitte for mye i ro	- Belastningsskader, nakke, rygg, - "musesyke" osv	4	B				B4	-Ny og bedre stol ønskes. -Benytte pauser -Ungå for lange 3D-modieringsøker
2	Maskinering ved bruk av fres, dreiebenk, søylebormaskin	- Kuttiskader - Avrivning av lem.	4 2	A C		A C	A D	A4 C3	Følge generelle regler i verktødet, Gjennomført aktuell opplæring. Høre på erfarent personell, og tenke godt igjennom operasjoner før de igangsettes. Aldri hastearbeide. Bruke vernebriller.
3	Gjennomføre lap shear tester	- Inhalering av uønskede gasser - Irritert hud - Brannfare - Klemfare ved utstyr	3 4 2 2	A A E C	A - C		C A E	A/C3 A4 C/E2	Les datablad for å forstå konsekvenser og forhindre uønskede hendelser. Bruke avsgv hvis det kreves, bruke relevant personlig sikkerhetsstyr. Hvis

NTNU	Risikovurdering			Utarbeidet av	Nummer	Dato
				Anders Håland	HMSRV002	07.02.2014
HMS				Godkjent av	Erstatler	
				Jan M. G. Farstad		08.09.2013




	Alvorlig personskade.	Mindre skade og lang restitusjonstid	Drifts- eller aktivitetstans < 1 mnd	Troverdighet og respekt svekket
C Moderat				
B Liten	Skade som krever medisinsk behandling	Mindre skade og kort restitusjonstid	Drifts- eller aktivitetstans < 1 uke	Negativ påvirkning på troverdighet og respekt
A Svært liten	Skade som krever førstehjelp	Ubetydelig skade og kort restitusjonstid	Drifts- eller aktivitetstans < 1 dag	Liten påvirkning på troverdighet og respekt

Risikoverdi = Sannsynlighet x Konsekvens

Beregn risikoverdi for Menneske. Enheten vurderer selv om de i tillegg vil beregne risikoverdi for Ytre miljø, Økonomi/materiell og Omdømme. I så fall beregnes disse hver for seg.

Til kolonnen "Kommentarer/status, forslag til forebyggende og korrigerende tiltak":

Tiltak kan påvirke både sannsynlighet og konsekvens. Prioriter tiltak som kan forhindre at hendelsen inntreffer, dvs. sannsynlighetsreducerende tiltak foran skjerpet beredskap, dvs. konsekvensreducerende tiltak.

NTNU		Risikomatrise		Dato	
				07.02.2014	
HMS/KS				Ersatter	
		utarbeidet av		Nummer	
		Anders Håland		HMSRV002	
		Godkjent av		Ersatter	
		Jan M. G. Farstad		09.09.2013	



MATRISE FOR RISIKOVURDERINGER ved NTNU

KONSEKVENSENS						
Svært alvorlig	E1	E2	E3	E4	E5	
Alvorlig	D1	D2	D3	D4	D5	
Moderat	C1	C2	C3	C4	C5	
Liten	B1	B2	B3	B4	B5	
Svært liten	A1	A2	A3	A4	A5	
	Svært liten	Liten	Middels	Stor	Svært stor	
SANNSYNLIGHET						

Prinsipp over akseptkriterium. Forklaring av fargene som er brukt i risikomatrisen.

Farge	Beskrivelse
Rød	Uakseptabel risiko. Tiltak skal gjennomføres for å redusere risikoen.
Gul	Vurderingsområde. Tiltak skal vurderes.
Grønn	Akseptabel risiko. Tiltak kan vurderes ut fra andre hensyn.

